LBNL/PUB-5464

Laboratory Directed Research and Development Program FY 2000

February 2001

DISCLAIMER

PUB-5464

Report on
Ernest Orlando Lawrence
Berkeley National Laboratory

Laboratory Directed Research and Development Program

FY 2000

BERKELEY LAB

Ernest Orlando Lawrence
Berkeley National Laboratory
Berkeley, California 94720

Office of Science
U.S. Department of Energy

Prepared for the U.S. Department of Energy under Contract No. DE-AC03-76SF00098

Table of Contents

Introduction

The Ernest Orlando Lawrence Berkeley National Laboratory (Berkeley Lab or LBNL) is a multi-program national research facility operated by the University of California for the Department of Energy (DOE). As an integral element of DOE's National Laboratory System, Berkeley Lab supports DOE's missions in fundamental science, energy resources, and environmental quality. Berkeley Lab programs advance four distinct goals for DOE and the nation:

- To perform leading multidisciplinary research in the energy sciences, general sciences, biosciences, and computing sciences in a manner that ensures employee and public safety and protection of the environment.

- To develop and operate unique national experimental facilities for qualified investigators.

- To educate and train future generations of scientists and engineers to promote national science and education goals.

- To transfer knowledge and technological innovations and to foster productive relationships among Berkeley Lab's research programs, universities, and industry in order to promote national economic competitiveness.

Berkeley Lab's programs, all unclassified, support DOE's mission for "a secure and reliable energy system that is environmentally and economically sustainable" and for "continued United States leadership in science and technology," as enunciated in DOE's Strategic Plan. These efforts support the Comprehensive National Energy Strategy to "work internationally on global issues," to "improve the efficiency of the energy system," and to "expand future energy choices through wise investments in basic science and new technologies."

The *Berkeley Lab Laboratory Directed Research and Development Program FY 2000* report is compiled from annual reports submitted by principal investigators following the close of the fiscal year. This report describes the supported projects and summarizes their accomplishments. It constitutes a part of the Laboratory Directed Research and Development (LDRD) program planning and documentation process that includes an annual planning cycle, projection selection, implementation, and review.

The Berkeley Lab LDRD program is a critical tool for directing the Laboratory's forefront scientific research capabilities toward vital, excellent, and emerging scientific challenges. The program provides the resources for Berkeley Lab scientists to make rapid and significant contributions to critical national science and technology problems. The LDRD program also advances Berkeley Lab's core competencies, foundations, and scientific capability, and permits exploration of exciting new opportunities. All projects are work in forefront areas of science and technology. Areas eligible for support include the following:

- Advanced study of hypotheses, concepts, or innovative approaches to scientific or technical problems;

- Experiments and analyses directed toward "proof of principle" or early determination of the utility of new scientific ideas, technical concepts, or devices; and

- Conception and preliminary technical analyses of experimental facilities or devices.

The LDRD program supports Berkeley Lab's mission in many ways. First, because LDRD funds can be allocated within a relatively short time frame, Berkeley Lab researchers can support the mission of the Department of Energy (DOE) and serve the needs of the nation by quickly responding to forefront scientific problems. Second, LDRD enables Berkeley Lab to attract and retain highly qualified scientists and supports their efforts to carry out world-leading research. In addition, the LDRD program also supports new projects that involve graduate students and postdoctoral fellows, thus contributing to the education mission of Berkeley Lab.

Berkeley Lab has a formal process for allocating funds for the LDRD program. The process relies on individual scientific investigators and the scientific leadership of Berkeley Lab to identify opportunities that will contribute to scientific and institutional goals. The process is also designed to maintain compliance with DOE Orders, in particular DOE Order 413.2 dated March 5, 1997, and 413.2A, dated January 8, 2001. From year to year, the distribution of funds among the scientific program areas changes. This flexibility optimizes Berkeley Lab's ability to respond to opportunities.

Berkeley Lab LDRD policy and program decisions are the responsibility of the Laboratory Director. The Director has assigned general programmatic oversight responsibility to the Deputy Director for Research. Administration and reporting on the LDRD program is supported by the Directorate's Office for Planning and Communications. LDRD accounting procedures and financial management are consistent with the Laboratory's accounting principles and stipulations under the contract between the University of California and the Department of Energy, with accounting maintained through the Laboratory's Chief Financial Officer.

In FY00, Berkeley Lab was authorized by DOE to establish a funding ceiling for the LDRD program of \$14.1 M, which equates to about 3.3% of Berkeley Lab's FY00 projected operating and capital equipment budgets. This funding level was provided to develop new scientific ideas and opportunities and allow the Berkeley Lab Director an opportunity to initiate new directions. Budget constraints limited available resources, however, so only \$9.5 M was expended for operating and \$0.5 M for capital equipment.

In FY00, scientists submitted 149 proposals, requesting over \$22.4 M in operating funding. Sixty-eight projects were funded, with awards ranging from \$30 K to \$380 K. These projects are summarized in Table 1.

Innovative Source Technologies for the Generation of Femtosecond-Scale Pulses of X-Rays

Principal Investigators: Swapan Chattopadhyay, Alexander Zholents, and Max Zolotorev

Project No.: 00001

Project Description

Time- and space-resolved studies of ultrafast phenomena in physics, chemistry, and life sciences on femtosecond time scales and at a spatial resolution of atomic scales (angstroms) require radiation sources of x-ray wavelengths and very short-pulse duration of tens to hundreds of femtoseconds. Coherent phonon dynamics, phase transition on the two-dimensional surface of a solid, photo-initiated chemical reaction of molecules such as rhodopsin, chemical reaction pathways in a solution, etc., can all be studied with proper short-pulse x-rays.

The techniques of short-pulse x-ray generation via orthogonal Thomson scattering of short-pulse, visible laser light off a relativistic electron beam and via laser femto-slicing of picosecond long electron bunches have both been demonstrated at Berkeley Lab's Advanced Light Source (ALS). The eventual utility of these sources is currently being evaluated based on the pulse characteristics of such sources, e.g. pulse duration, flux of photons, repetition rate, etc. The overall flux is about a million photons per second, a good three orders-of-magnitude away from the target figure of a billion photons per second.

The purpose of this investigation was to explore pushing the performance characteristics of short-pulse x-ray sources either via drastic upgrades of the above techniques or by innovative new concepts and techniques that promise a thousand-fold enhancement in flux.

Accomplishments

Several ideas have been advanced and explored to improve upon the fluxes of femtosecond x-rays obtained to date at the ALS storage ring and the Beamline Test Facility (BTF) at Berkeley Lab. These ideas and subsequent status are:

(a) Optimally Designed Thomson Source: This is similar to the BTF set-up at the ALS, but with a custom-designed laser and a linac with a high repetition rate, intensity, and beam quality to raise fluxes to a hundred million to a billion photons per second. This can be done quite readily, but requires a dedicated Thomson source facility separate from the ALS. Innovative experimentation techniques combining multiple scatterings and images to perform time-resolved crystallography, etc., are future directions.

(b) Femto-ring: This involves a dedicated storage ring with transversely deflecting and anti-deflecting cavities in conjunction with x-ray pulse compression via asymmetrically-cut crystals to reduce the effective source sizes to femtoseconds and simultaneously enhancing the intensity thousand-fold. This idea is extremely promising and is currently being pursued actively.

(c) Recirculating Linac with Energy Recovery: This idea is a variation of (b) above. In this case, however, the storage ring is replaced by a continuous wave (cw) superconducting linac of, say, 500 MeV energy with a few recirculating passes through it at proper phases to get the electron beam energy up to 2 to 3 GeV. All the transverse deflection gymnastics takes place followed by a few recirculating passes down through the same linac in opposite phase to recover 80% of the energy back from the electron beam into the radio frequency fields. This method has the advantage over (b) in that it allows for tapping various parts of the x-ray spectrum based on radiation from the electron beam at 0.5, 1.0, 1.5, 2.0, 2.5 and 3.0 GeV energies and it has an effective amplification factor of about a million for photon fluxes based on the cw operation with energy recovery. This idea is actively pursued not only at Berkeley Lab, but also at Cornell University, Brookhaven National Laboratory, and Thomas Jefferson National Accelerator Facility.

(d) Brehmsstrahlung: This approach involving a thin target brehmsstrahlung from a femtosecond linac pulse was demonstrated as far inferior in quality to the above three and has been dropped from the investigation.

(e) Laser-plasma Source: We are exploring the direct use of femtosecond pulses of electrons and synchrotron radiation from such electrons produced in the interaction of high-intensity lasers with gas jets under various conditions. This is a promising technique with the potential of being a compact source. However, the physics of the electron production and their quality need further investigation before studies of a radiation source configuration can be worked out. Active research is being carried out to understand the electron production from the laser-plasma source.

(f) Terahertz Sources: This method involves electromagnetic power stored in various inter-digitated capacitive arrays and switched on an ultrafast time-scale by a femtosecond laser pulse, which leads to far-field radiation of short pulses of terahertz radiation that can be properly used by various self amplification of spontaneous emission (SASE) schemes to generate femtosecond x-rays. This scheme is now being experimentally tested.

Publications

S. Chattopadhyay, A. Zholents, and M. Zolotorev, "A Material with a High Threshold for Breakdown under Electric Field and with an Optically Switched Permittivity," *CBP Tech Note*-347, (December 1999, internal note).

A. Zholents, "On a Possibility of a Source of Femtosecond X-ray Pulses based on a Racetrack Microtron," draft for *CBP Tech Note*, (November 2000).

Dynamics of Low-Emittance Electron Rings with Applications to High Energy Physics Colliders

Principal Investigators: John Corlett

Project No.: 99001

Project Description

This proposal represents a collaboration between the Accelerator and Fusion Research and Physics Divisions in the conceptualization of future high energy physics colliders. Consistent with the goals set by the recent High Energy Physics Advisory Panel (HEPAP) subpanel report "Planning for the Future of U.S. High Energy Physics" the project will develop and apply our existing and significant experience in low-emittance storage ring accelerator physics and engineering, and radiation-hardened electronics and novel controls systems for large accelerators.

We propose to develop an understanding of and key technologies for low-emittance storage ring systems. This work will include optimizing lattice schemes for low-emittance and rapidly damped beams, studies of impedance minimization and collective effects, and feedback systems to control residual beam motion. In collaboration with the Physics Division, we propose to utilize the existing expertise in radiation-hardened electronics to develop novel concepts in control system design, integrating radiation-hardened electronics located near the accelerator and incorporating complex algorithm's to allow efficient accelerator physics studies and manipulation of the beams in feedback and feedforward loops.

Accomplishments

This year we have developed parametric models to allow low-emittance lattice designs for a variety of beam energies and damping rates, and have continued studies of minimal impedance components for storage rings. We have developed models for the design and optimization of low-emittance storage-ring lattices, required to produce the very compact charged-particle beams necessary for high-luminosity colliding beam accelerators for high-energy-physics studies. These computer codes allow calculation of particle beam behavior in considerable detail, and are essential in design of modern accelerators. After comparison of different arrangements of magnetic elements, we have selected the "theoretical minimum emittance" lattice design, which produces a low-emittance beam with minimal magnetic elements, and produces a compact and cost-effective solution. Several iterations in lattice details have been required to optimize performance for each case. The dynamic aperture of such lattices—a measure of the efficiency of a storage ring in capturing and containing particles—has been studied and is now well understood in term of the phase advance between elements. We have developed compensation schemes that produce a large dynamic aperture while using higher-order magnetic fields that are necessary for stabilizing the particles within a bunch. Dynamic aperture has a direct impact on the operational integrity high-repetition rate storage rings, in that beam losses from high-power injectors (tens of kilowatts) result in substantial activation of accelerator components if the aperture is too small.

To take full advantage of low-emittance beams, it is important to operate below instability thresholds. Instabilities may be driven by electromagnetic fields coupling between particles within a single bunch, or by coupling through fields generated by a leading bunch and experienced by following bunches. In both cases, the dominant mechanism is wakefields produced in the vacuum chamber. Other instability mechanisms include coupling through ion or electron clouds in the residual gas. The strength of the interaction between the beam and its environment is characterized by the beam impedance (or equivalently the wakefield in time-domain analysis). Instabilities generally have a threshold current or impedance below which the natural damping mechanisms suppress the motion induced by the beam self-fields. Above threshold, the growth rate of the self-induced motion exceeds the damping rate, and beam quality degrades. Feedback and feedforward systems may help avoid instabilities by adding to the natural damping rate.

3-D electromagnetic simulation computer codes have been used to design radio frequency (rf) cavities that have minimal beam impedance, while maintaining operating efficiency. The cavity design uses waveguides to reduce higher-order-mode impedance by several orders of magnitude. RF cavities offer a very inviting geometry for accumulation of rf power and are the dominant impedance in many storage rings. The cavity design we have developed utilizes an efficient means of absorbing the power deposited in higher-order-modes of the cavity, by using waveguides attached to the cavity to absorb the rf power in resistive material inside the waveguide. The bandwidth over which cavity power must be dissipated is large, typically one to several gigahertz.

We have continued beam impedance measurements using microwave measurement techniques in the Lambertson Beam Electrodynamics Laboratory at Berkeley Lab. This year, using time-domain-reflectometry, we have analyzed low-impedance hardware for particle accelerators, and developed improved microwave matching techniques to better transfer high-frequency power through structures.

In conjunction with estimated impedance derived from 3-D computer modeling of other components, this work has allowed us to produce an impedance budget for a future low-emittance storage ring. Analysis of this data has to date focused on single-bunch effects, wherein the particles at the head of a bunch introduce fields which perturb the motion of particles following within the same bunch. Instabilities driven in this manner have in the past caused severe problems in storage rings, and our understanding of these is critical to successful design of future high intensity machines.

Publications

J. Corlett, "Parameters of Future Rings," submitted to Broadband Impedance Measurements and Modeling Workshop, SLAC (February 28 - March 2, 2000) *www-project.slac.stanford.edu/lc/wkshp/talks/Param_JC.pdf*

J. Corlett, "Mastering Beam Instabilities in Synchrotron Light Sources," submitted to Beam Instability Workshop, ESRF, Grenoble, France (March 13 - 15, 2000) *www.esrf.fr/machine/myweb/machine/Workshop/BIW/PROC/Corlett.pdf*

J. Corlett, K. Bane, J. Byrd, M. Furman, S. Heifets, K. Ko, C. Ng, T. Raubenheimer, G. Stupakov, and F. Zimmerman, "Damping Rings Impedance and Collective Effects," submitted to Beam Instability Workshop, ESRF, Grenoble, France (Mar. 13 - 15, 2000) *www.esrf.fr/machine/myweb/machine/Workshop/BIW/PROC/wg_single/NLCcollect_corlett.pdf*

J. Corlett, "Suppression of Beam Instabilities," submitted to Superconducting RF Workshop, Chester, England (April 14-16, 2000) *http://pmipc1.dl.ac.uk/scrf/corlett.htm*

J. Corlett, C. Ng, T. Raubenheimer, P. Emma, Y. Wu, H. Nishimura, D. Robin, R. Rimmer, and A. Novokatski, "Damping Ring Aperture and Impedance Studies" submitted to NLC Collaboration meeting (May 2000).

A. Wolski, "Damping Ring Design for NLC at 180 Hz Repetition Rate," CBP Tech Note **216**, LCC-0048, (October 2000).

J. Corlett, "Damping Rings Status and Plans," submitted to NLC Collaboration meeting (October, 2000).

R.A. Rimmer, J. Corlett, N. Hartman, D. Li, G. Koehler, D. Atkinson, T. Saleh, and R. Wiedenbach, "RF Cavity R&D at LBNL for the NLC Damping Rings, FY 2000," in preparation for *CBP Technical Note*, (December 2000).

J. Corlett, N. Hartman, K. Kennedy, G. Koehler, S. Marks, D. Atkinson, T. Saleh, and R. LaFever, "NLC Damping Rings Wiggler Studies, FY 2000," in preparation for *CBP Technical Note*, (December 2000).

Computational Studies of Atomic Medium Interactions with Attosecond Electron Bunches

Principal Investigators: Wim Leemans, Eric Esarey, Alexander Zholents, Max Zolotorev, and Swapan Chattopadhyay

Project No.: 00028

Project Description

This project is aimed at calculating the interaction of attosecond electron bunches with atomic medium. In this new regime, the duration of the electron bunches is on the order of, or shorter than the period associated with vibrational or electronic transitions in atomic media. This results in a very different behavior compared to interaction of long electron or laser beam pulses with media. In the case of long pulses, we deal with the adiabatic modification of atomic potential by the laser electric field or by the collective fields of the electron beam. This leads to, for example, electron tunneling ionization. Another known type of ionization in the laser field occurs due to multi-photon absorption. These two regimes have been explored elsewhere. Experiments have been done with CO_2-lasers, with Nd:glass lasers, and with electron beams.

In the case of the attosecond electron bunches, the expected processes of atomic excitation are completely different. They are non-adiabatic because the probability, W, of a transition between two atomic states is proportional to $| d E(\omega) |^2$, where $E(\omega)$ is the Fourier component of the excitation field and d is a dipole moment of the transition. For an electric field of the electron beam with Gaussian distribution, the electron density W is proportional to $exp(-\omega^2\tau^2)$ where τ is the root mean square of the longitudinal beam distribution and ω is a transition frequency. We propose to investigate the regime where the duration of the electric field is comparable to the atomic transition period, $\omega\,\tau < 1$. In this case, the attosecond electron bunch excites the atomic electrons in a superposition of quantum states—a class of final atomic states that is unreachable with long pulses. Studies of the time evolution of these excited states with pump-probe techniques can bring a new insight on the collapse of wave function and decoherence of the quantum state.

Accomplishments

Methods and their limitations for production of attosecond electron bunches are being explored. Ponderomotive acceleration in vacuum using high intensity laser beams with specially tailored radial profiles was proposed as a potential method for generating attosecond electron bunches.

When a powerful laser beam is focused on a free electron in vacuum, the ponderomotive force of the laser light pushes electrons in the direction opposite to the gradient of the light intensity and can accelerate them to relativistic energies. Significant progress has been made on laser-based particle acceleration in vacuum in recent years, both theoretically and experimentally. Despite these advances, many challenges remain. Because the ponderomotive force is proportional to the energy flux of the light, laser acceleration requires a tightly focused high-power beam. A small radial size of the beam, however, results in the large transverse gradient, which makes the electron motion unstable in the radial direction. Also, the amplitude of electron oscillations along the polarization direction (so called quiver motion) increases with the magnitude of the electric field, and for a small focal spot can easily exceed the beam size, causing the electrons to be scattered in the transverse direction. As a result, the electron leaves the acceleration zone prematurely and the phase volume of the accelerated electron beam turns out to be relatively large. This regime of acceleration has been intensively studied theoretically and was also observed in the experiment. We proposed a novel approach to the laser acceleration. This approach avoids the transverse scattering during acceleration and allows us to achieve extremely small phase volume for the electron beam. We also determined the maximum electron energy that can be obtained in such acceleration and showed how it scales with the laser parameters.

Averaged equations of motion for a relativistic electron were used to study the laser acceleration in vacuum in the regime that avoids radial scattering of accelerating electrons. A simple analytical formula for the electron energy was found, and it was shown that both effective acceleration and focusing can be achieved with the use of the radial profiling of the laser beam. The resulting electron beam is characterized by extremely small longitudinal and transverse emittances.

We performed computer simulations for the two-mode acceleration scheme assuming that the modes have the same frequency, equal Rayleigh lengths and ˙z, with energy E_0 = 1J (Gaussian beam), E_1 = 1:3J (second mode), λ = 0:8 μm, and $˙\sigma_z/c$ = 21 fs (50 fs full-width half-maximum). The resulting electron beam had a mean energy of 6 MeV, a duration of 100 attoseconds, an energy spread of 3 %, a normalized emittance of 8 nm-rad, with a bunch containing 10^5 to10^6 electrons. This work has been submitted for publication to *Phys. Rev. Lett.* (G. Stupakov and M. Zolotorev).

The second part of the work considered space charge effects on ultra-short, ultra-dense electron beams. Space charge effects can be important when these relatively low energy bunches propagate in vacuum, in the absence of external fields. The main focus of this work was to study longitudinal and transverse effects of space charge forces, for a variety of electron beam parameters. The evolution of the bunch sizes was modeled under the assumptions that the beam shape remains ellipsoidal in its spatial coordinates and that the density distribution is uniform. Electron beams with characteristics similar to beams produced in the laser wakefield accelerators as well as by direct ponderomotive acceleration were studied. As expected, space charge effects on longitudinal and transverse beam sizes have a very strong energy dependence, with higher energy beams becoming less susceptible to phase space increase due to space charge effects. Electron beams containing multi-picocoulomb (pC) charge with energies in excess of 40 MeV were found to be minimally affected by space charge forces. However, the longitudinal phase space area of low energy beams (e.g. < 10 MeV), containing pC/bunch was found to significantly increase. The results of this work will appear in the *American Institute of Physics Proceedings of the Advanced Accelerator Concept Workshop* (June 2000) and was also presented at the American Physical Society, Division of Plasma Physics 2000 meeting.

Publications

G.V. Stupakov and M.S. Zolotorev, "Ponderomotive Laser Acceleration and Focusing in Vacuum Application for

Attosecond Electron Bunches," submitted to *Phys. Rev. Lett.*

G. Fubiani, W.P. Leemans, and E. Esarey, "Studies of Space Charge Effects in Ultra-short Bunches," *Advanced Accelerator Concept Workshop Proceedings, AIP*, (September 2000).

G. Fubiani, W.P. Leemans, E. Esarey, and B.A. Shadwick, "Particle Trapping and Beam Transport Issues in Laser Driven Accelerators," presented at American Physical Society, Division of Plasma Physics Meeting, Quebec City, Canada (October 23-27, 2000).

Compact D-D or D-T Neutron Generator for Moderator Design and Biological Research

Principal Investigators: Ka-Ngo Leung, Gordon Wozniak, and Eleanor Blakely

Project No.: 00002

Project Description

Several areas of basic research and applied neutron research require an intense source that is compact, inexpensive, and safe to operate. The current options for neutron sources are reactors and high-energy accelerators. The plasma and ion source technology group of the Accelerator and Fusion Research Division has developed a unique technology that provides a sealed neutron tube producing a neutron flux that is about four orders of magnitude higher than current commercially-available sources. The advantages of the D-D or D-T neutron generator are multiple: it only requires a low-energy accelerator; and it is portable, compact, and cheaper than other neutron sources. The availability of a high-intensity neutron source would open up new and exciting research possibilities, including medical and biological applications, material research, airport security, mine detection, non-proliferation technologies, and other radiographic applications.

The goal of this LDRD is to advance the developed concepts for a compact neutron generator to the final design, fabrication, and testing stage. We expect that with the two years of funding requested, we would be able to build a modest-sized neutron generator capable of producing D-D neutrons at 10^{12}neutrons/second (n/s), and achieve several milestones in basic and applied testing.

Accomplishments

Sealed-Tube Neutron Generator

The final integrated sealed-tube neutron-generator system is illustrated in the attached figure. In principle, this type of neutron tube can be operated either in continuous wave (CW) or pulse mode. For CW operation, a 150 kV, 1.5 A beam will provide a neutron yield of 7×10^{11} n/s for D-D and 1×10^{14} n/s for D-T operation. For pulsed operation, the instantaneous neutron yield can be much higher. For example, if the tube is operated at a 25 A peak pulsed beam at 150 kV with a duty factor of 4%, the peak neutron yield is 2×10^{13} n/s for D-D and 1.3×10^{15} n/s for D-T. The time averaged neutron yield will be the same as the case for CW operation. We have designed and constructed a prototype system based on the attached figure. The individual components are described as followed.

Accelerator Column

The multi-hole design of the prototype accelerator column allows for crossover and increased expansion of the ion beam. Currently, the accelerator is composed of seven holes, adding up to an area of approximately 1 cm^2, but eventually it will contain an entire hemisphere of holes similar to the IGUN simulation model. The figure attached illustrates the accelerator column design showing the four electrodes and ion beam trajectories. The target is biased at a potential of -150 kV. Both the plasma and extractor electrodes in this system contain the holes, which aid in focusing the many beams down to a small area. Once this has been achieved, the space charge dominates the beam behavior, expanding the beam towards the target. Expansion of this beam is controlled to distribute ion current uniformly at the target electrode. Uniform beam distribution leads to uniform neutron flux and increased lifetime of the target material.

Target

The target is a copper substrate coated with a thin film of titanium. It contains water channels for cooling and thermodynamic stability of the target material. The target is machined from a solid copper block.

Moderator

Moderators were developed in order to produce different energies of neutrons for Boron Neutron Capture Therapy (BNCT). Monte-Carlo codes MCNP and BNCT_RTPE were used to compute the dose distribution in the patient under different moderated neutron spectra. Different combinations of materials are used to produce intense, broad-energy neutron beams. It is estimated that an epithermal neutron flux of 4×10^8 n/cm^{2}s and a thermal neutron flux of 5×10^8 n/cm^{2}s can be generated at the exit aperture of the moderator when the D-T tube is operated with a 150 kV, 1.5 A beam.

System Testing

The completed prototype system has been constructed in Test Stand 3 of Building 16. Initial testing began in August 2000, with the eventual production of a proton beam. The completed ion source and accelerator system can now be operated at 120 kV and 15 mA of H^+ beam current. These values are currently limited by the high voltage power supply. Deuteron beam operation is scheduled to take place in December 2000.

EH&S / Safety

A review of the safety aspects of the neutron tube design was performed with staff from the Nuclear Science (NSD) and Environment, Health & Safety (EH&S) Divisions. As a result of this review, the design was modified to minimize the associated hazards and allow ready operation. In preparation for neutron operation in FY 2001, the configuration of the neutron detection system was finalized. Al Smith and Dick McDonald from NSD have agreed to provide a neutron detector for the initial measurements.

Radiobiology

With the successful completion of the prototype source and production of an ion beam during the past year, we are preparing for the next milestone: neutron production. The biological lab, near the planned neutron exposure area in Building 16, is being prepared with a carbon dioxide incubator to provide adequate temperature and buffered gas control during the time before and after exposures. The primary tissue culture lab for this work is the Blakely Laboratory in Building 70A.

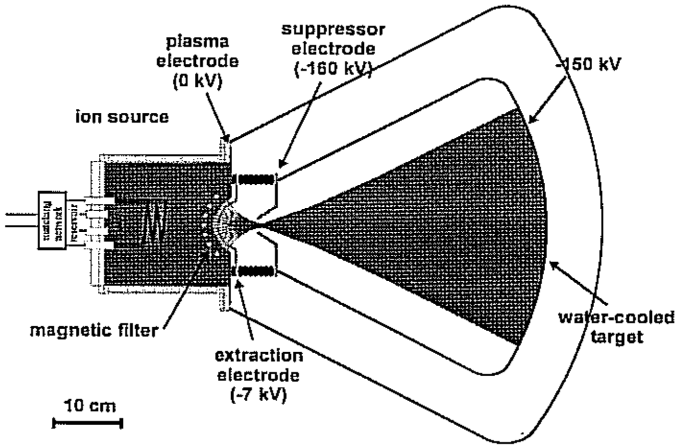

Figure 1: Prototype system currently being tested in Test Stand 3 of Building 16.

Publications

J.M. Verbeke, A.S. Chen, K.N. Leung, and J.L. Vujic, "Production of In-Phantom Dose Distribution Using In-Air Neutron Beam Characteristics for Boron Neutron Capture Synovectomy," *Nuclear Technology* (August, 2000).

K.N. Leung, A.S. Chen, J. Reijonen, B.W. Tolmachoff, J.M. Verbeke, and J. L. Vujic, "Development of a Compact Neutron Tube for BNCT Application," *Proceedings of The Ninth International Symposium on Neutron Capture Therapy for Cancer* (October 2-6, 2000).

B.W. Tolmachoff, A.S. Chen, K.N. Leung, J. Reijonen, J.M. Verbeke, and J.L. Vujic, "Development of a Compact Neutron Tube for BNCT Application," presented at DOE On-Site Review Student Poster Session, (October 12, 2000).

Next Generation Superconducting Magnets

Principal Investigators: GianLuca Sabbi

Project No.: 00003

Project Description

High-field accelerator magnets for use in future high-energy colliders are currently under development at many institutions. These superconducting magnets need to provide fields well above 10 T using high-performance conductors. Currently, the most advanced conductor available for such magnets is Nb3Sn. One of the challenges of utilizing Nb3Sn is that it is mechanically brittle. In order to use this material effectively, new design approaches are necessary. The goal is to develop a magnet that is cost-effective, simple to manufacture, and at the same time delivers good training performance and field-quality. While traditional magnets have been built using shell-type coils, our recent studies have focused on a racetrack geometry that has the virtues of simplicity and conductor compatibility. However, this new paradigm requires a different coil support approach, and new tools for field quality optimization. Furthermore, in order to overcome the difficulties in handling Nb3Sn, coil winding takes place before the composite material is reacted to form the superconducting Nb3Sn compound. Since reaction takes place at high temperature, it is difficult to predict precisely the final position of the superconducting strands, which determines the field quality. This LDRD addresses those issues associated with field-quality magnet design, and the efficacy of these designs, through comparison with measurements made on actual high-field superconducting magnets.

Accomplishments

A practical reference for the field errors in accelerator quality magnets is one part in 10000 ("unit") at 2/3 of the bore radius, with typical specifications ranging from a few units to fractions of a unit. It has been shown that in small-aperture, moderate field (10-11 T) racetrack dipoles, adequate field quality can be obtained using solely the main coils. However, for a high-field racetrack magnet with 40 mm clear bore, conductor efficiency dictates that "auxiliary" turns be placed in the vicinity of the bore to minimize the geometric harmonics. Resulting mechanical issues are the need to provide vertical support for the auxiliary turns and the need to return these conductors at the magnet ends without interfering with the beam tube.

A novel coil support system has been developed by the Berkeley Lab Accelerator and Fusion Research Division Superconducting Magnet Program. Structural calculations were performed to investigate the efficacy of this approach regarding coil separation, and therefore on the impact of field quality. Measurements conducted on a one-third scale model confirmed that the coil support is structurally sound. Unfortunately, the full size magnet (RD-3) failed under test, at a field of about 8 T (compared with the short sample limit of ~14 T), due to an electrical short, so the comparison of expected and predicted behavior could not be completed. This magnet is currently being rebuilt with improvements learned from the first test.

Subsequent to the RD-3 tests, the next step in the LDRD project involved comparison of the RD-4 magnet (which has all the physical elements associated with a true "field-quality" magnet with auxiliary coils), with that expected from simulations. The candidate coil configurations for RD-4 can provide geometric harmonics within a fraction of a unit at a reference radius of 10 mm. This will allow precise comparison of predicted vs. measured harmonics. In addition, we will take advantage of magnets currently being built at our sister laboratories in order to understand the differences between the measured and anticipated behavior of these magnets.

End design and optimization, together with saturation effects in racetrack coils, is also an issue for accelerator-quality magnets. It is anticipated that improvements in design, determined as a result of this study, will be incorporated in future developments of the RD series of magnets at Berkeley Lab, and in the designs of similar magnets being pursued at other institutions.

Publications

G. Sabbi, *et al.*, "Design of Racetrack Coils for High-Field Dipole Magnets," accepted for publication in *Proceedings of IEEE Trans. Appl. Superconductivity* (September 17-22, 2000).

Advanced Light Source Division

Ultrafast X-Ray Spectroscopy via Optical Gating

Principal Investigators: Thornton Glover, Philip Heimann, and Howard Padmore

Project No.: 98032

Project Description

Synchrotrons have provided valuable information about the static properties of materials important to the physical and life sciences. Their role in studying material dynamics, however, has been limited due to inadequate time-resolution. The ability to perform x-ray spectroscopy with sufficient time resolution to observe the fast (picosecond and femtosecond) primary events which drive many interesting chemical reactions, phase-transitions, etc., will have an important impact on a number of fields in physics, chemistry, and biology.

The goal of our research is to expand capabilities at the Advanced Light Source (ALS) for performing ultrafast x-ray spectroscopy by developing fast (picosecond and femtosecond) x-ray detectors based on two-color (x-ray + laser) interactions. Such two-color experiments represent an interesting direction for synchrotron-based research. From a fundamental perspective, x-ray/laser two-color experiments offer a means of studying novel structure and dynamics of matter exposed to intense, coherent (laser) radiation. From an applications perspective, x-ray/laser multiphoton processes can serve as the basis for a high time-resolution x-ray detector.

Specifically, in the current research, we study combined x-ray/laser interactions with a silicon target by observing laser-induced perturbations to x-ray photoelectron spectra (XPS). One can imagine two-types of laser-induced perturbations that are of interest: first, laser-induced material modifications that persist beyond the laser pulse and, second, laser-induced material modifications that are present only during the laser pulse. We have studied the x-ray/laser interaction at laser fluences both below (mJ/cm^2) and above (100 J/cm^2) the melting and ablation fluences for Si (~100 mJ/cm^2 and 1J/cm^2 respectively) and find evidence for both categories of material modification.

Accomplishments

Experiments have been performed at the micro-XPS endstation at beamline 7.3.1.2. X-rays (typically ranging from 400-800 eV) photo-emit Si 2p core-shell electrons. The electron spectrum indicates an isolated 2p photoemission peak. An 800 nm, femtosecond (or picosecond) laser pulse is then used to modify the XPS. Spatio-temporal overlap between the x-ray and laser pulses at the Si target is crucial and diagnostics have been developed to ensure this overlap.

The manner in which the laser modifies the XPS depends upon the laser fluence. At moderate laser fluence (~1 mJ/cm^2), we see indications of optical scattering. In this process, an x-ray photoelectron scatters (absorbs and/or emits) laser photons while in the vicinity of the nucleus. The observables are additional peaks in the XPS separated from the Si 2p peak by the laser photon energy (1.55 eV), and this 'material modification' occurs only during the laser pulse.

We describe two (related) pieces of data which suggest that we have observed optical scattering: first, (Figure 1, left inset), an x-ray/laser cross-correlation curve and, second, (Figure 1, right inset), a laser-perturbed Si XPS. The data are obtained by measuring the Si photoelectron spectrum as a function of laser arrival time at the sample (for fixed x-ray arrival time). The left inset to Figure 1 shows that the electron counts (in the vicinity of 730.5+1.55 = 732 eV) are 4-5% above the baseline for a time-interval corresponding to ~100ps. This curve amounts to an x-ray/laser cross-correlation measurement of the x-ray pulse indicating an x-ray pulse duration of ~100ps. The right inset to Figure 1 shows the laser-perturbed XPS. The spectrum is obtained by taking a Si spectrum corresponding to coincident x-ray/laser arrival at the sample (-50 ps on Figure 1, left inset) and subtracting the spectrum corresponding to non-coincident arrival (-150 ps). The spectrum shows a peak at 732 eV, corresponding to the primary x-ray peak (730.5 eV) plus one optical photon (1.55 eV).

As a second effect observed at moderate laser intensity, we observe (Figure 1, main figure) an overall shift in the Si 2p photoemission line to higher kinetic energy (by between 0 and 500 meV, depending on Si surface conditions). This shift is due to transient surface photovoltages induced by the laser. In brief, the laser generates photocarriers that move to offset band bending at the surface of this doped semi-conductor. This transient surface photovoltage provides information about both the Si surface quality and the surface carrier dynamics. This material modification persists beyond the laser duration (for several tens of nanoseconds) but exhibits a rapid (picosecond) rise time, which has permitted a 'step-function' measurement of the ALS (x-ray) pulse duration.

Finally, at high laser fluence (10-100 J/cm^2), we observe a fast and rapidly recoverable modification to the XPS. The Si 2p photoemission peak is shifted (~ 1 eV) to higher energy and returns to its initial (unperturbed) position in less than 100 ps. We interpret this to be a signature of a rapid laser-induced phase transition in Si when excited at very high laser fluence. This phenomenon permits a direct measure of the ALS pulse duration (not a step function measurement). Efforts to model this rapid and recoverable phase transition are in progress.

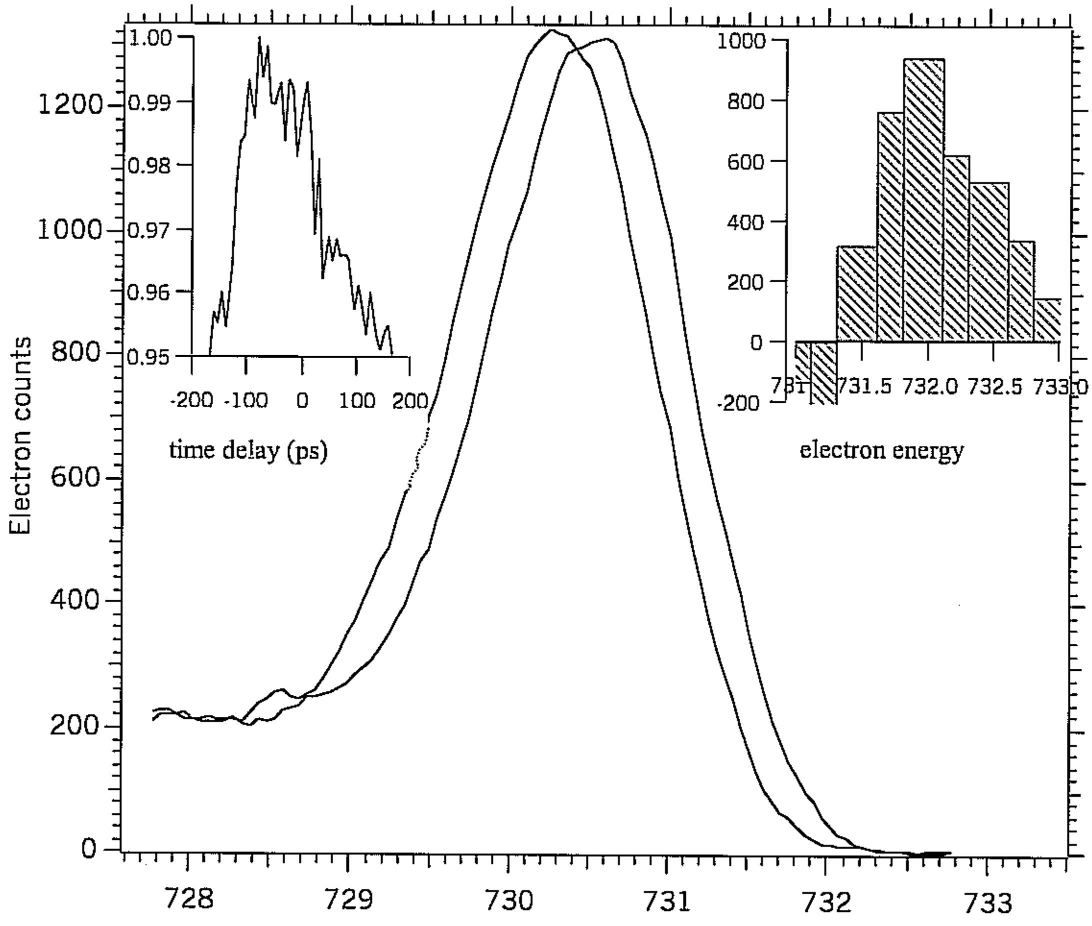

Figure 1: Main Figure- Si 2p photoemission spectra with laser off (dashed line) and on (solid line). Left inset: Electron counts (arbitrary) units) in the vicinity of 732 eV as a function of laser x-ray time delay. Right inset: Si 2p spectrum at 0 ps minus the Si 2p spectrum at –160 ps.

Publications

T.E. Glover, G.D. Ackermann, A. Belkacem, B. Feinberg, P.A. Heimann, Z. Hussain, H.A. Padmore, C. Ray, R.W. Schoenlein, and W.F. Steele, "Measurement of Synchrotron Pulse Durations Using Surface Photovoltage Transients," accepted for publication *in Nuclear Instruments and Methods A* (2000).

T.E. Glover, "X-ray/Laser Two-Color Processes: Novel Detectors For Future Light Sources," in preparation for *Journal of Synchrotron Research* (2000).

T.E. Glover, G.D. Ackermann, A. Belkacem, C. Ray, and W.F. Steele, "Ultrafast Phase Transition in Femtosecond-Laser-Heated Silicon," in preparation for *Physical Review Letter* (2001).

T.E. Glover, G.D. Ackermann, A. Belkacem, C. Ray, and W.F. Steele, "Picosecond Resolved Surface Photovoltage

Transients in Silicon," in preparation for *Applied Physics Letter*, (2001).

Phase- and Amplitude-Contrast Tomography using Intermediate-Energy X-Rays

Principal Investigators: Malcolm Howells, Alastair MacDowell, Howard Padmore, Robert Ritchie, and Wenbing Yun

Project No.: 99003

Project Description

X-ray tomography is opening up the study of the three-dimensional structure of complex solids, for example technologically important materials such as structural composites and bioceramics. However, current methods have a resolution that is restricted to a few microns, severely limiting potential applications. We have developed a new scheme that is theoretically capable of extremely high spatial resolution, as well as the imaging of weakly scattering objects—specifically, micro-cracks, which are the origin of structural failure in many of these materials. This proposal is to support demonstration experiments and the conceptual design of an optimized superbend tomography capability at the Advanced Light Source (ALS).

The resolution limitation of plane-wave phase-contrast tomography is caused by its lack of magnification combined with the poor resolution of existing x-ray detectors. This can be overcome by using optical schemes with the same existing detectors but with sufficient magnification. The critical technologies are then production of hard x-ray zone plates and pinholes (waveguides), efficient microfocusing onto the pinhole, and fast tomographic reconstruction. A resolution of less than 100 nanometers should be possible, opening up areas of study as diverse as crack propagation in strained monolithic and composite metallic and ceramic materials and imaging of interconnect structures in integrated circuits (ICs) under thermal strain.

Accomplishments

This is the second year of LDRD funding for the ALS tomography project and the following accomplishments can be listed.

- Research was launched at the ALS, including a new state-of-the-art beamline for tomography, and to gather a group of first class participating investigators. The participating groups and lead scientists are now: Martz, Haupt (Lawrence Livermore National Laboratory, Materials, NIF targets), Ritchie (University of California, Berkeley, Fracture mechanics), Breunig (University of California, San Francisco, Dentistry), Kinney (University of California, San Francisco, Medicine), Tomutsa (Lawrence Berkeley National Laboratory, Earth Sciences Division, Rock porosity), and Lucatorto and Devine (National Institute of Standards and Technology Micro-circuits).
- The technical design of a beamline has been developed with a number of unique features. In particular, it focused on two experimental stations: (1) a classical tomography station with an ultra large illuminated area and (2) an imaging microscope station with ultra high tomographic resolution.
  - The ALS superbend is the state-of-the-art source for radiographic microtomography. It has high brightness and can be made to have a large illuminated area. This, together with the high energy of an ALS superbend, allows large objects, such as a human vertebra, to be illuminated and projections to be made with detector-limited resolution.
  - At the other end of the size/resolution scale, the superbend source provides high-brightness illumination for a zone-plate imaging x-ray microscope which, in the hard x-ray regime, has been shown (via our first year LDRD efforts) to be capable of 0.15 μm resolution in two dimensions. When this system is used to produce three-dimensional images, it will be about an order-of-magnitude higher in resolution than existing tomography beamlines.
- Considerable effort has been devoted to developing a mirror system that can act as a condenser "lens" for the microscope and a beam expander for the classical tomography experiment. In fact, the system will provide a Kirpatrick-Baez pair of adjustable-focus mirrors, which will allow the light to be focused anywhere in the microscope, while one of the mirrors will also act as a convex (diverging) lens to fill large objects with illumination.
- Phase contrast will be available in various ways: Zernike and Nugent-style in the microscope and refractive and Nugent style in the classical tomography station.

The LDRD support has had a "seeding" effect, and commitments for funding in the form of either money or other material resources have been made by all of the user groups listed above. By this means, the construction costs of the beamline will be covered. In addition, several follow-on proposals that would advance this capability are also in various stages of preparation or submission.

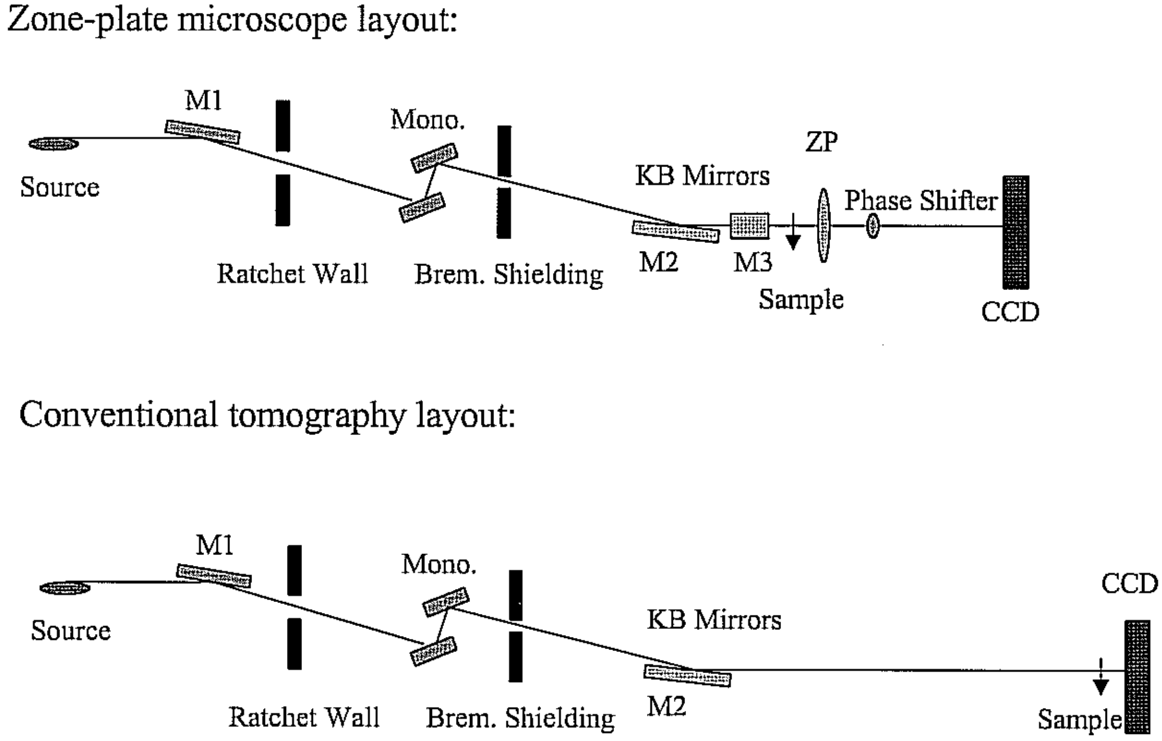

Figure 2: Beamline layout for the two experimental stations described in the text.

Micro X-Ray Absorption Spectroscopy at the Advanced Light Source

Principal Investigators: Howard Padmore, Alastair MacDowell, Geraldine Lamble, Richard Celestre, and Albert Thompson

Project No.: 00004

Project Description

We propose to instrument the Advanced Light Source (ALS) beamline 10.3.2 for x-ray absorption spectroscopy (XAS) at micron spatial resolution (μ-XAS). Initial tests of the concept have revealed that it should be possible to build a system that delivers high intensities into a few micron spot size, and perform scanning hard x-ray absorption spectroscopy. This will enable a new generation of chemical science on the micron scale. With a preliminary test system, we have shown that there is a huge user community from Materials to Life to Geo-scientists waiting to use such capabilities, if they can be demonstrated as robust and reliable. As about one-third of all synchrotron radiation research has used the technique of XAS, and most of it has been on model systems, the use of μ-XAS will have a huge impact in the study of chemical speciation in heterogeneous systems. The combination of a bright synchrotron with forefront x-ray optics will be unique.

A demonstration test station showed that viable μ-XAS experiments could be performed using small aperture beams focused to sub-micron spot sizes in combination with a four-crystal monochromator. Although a worthwhile test, all the users (~70 in total) who have tested this system need 100 to 1000 times the flux to do forefront science. This LDRD is to allow the fabrication of a system capable of such high performance. This will be done by using much higher aperture optics, and will therefore be substantially more difficult. The schematic layout of the proposed upgraded beamline is shown in Figure 3. The concept of the beamline is to have the 1:1 toroidal mirror relay the source to the adjustable slits, which then act as an adjustable-sized source for the following optics. In this way, the source is effectively much closer to the sample, with a consequent increase in flux. The spot size is dictated by the size of the adjustable slits, thus allowing spot size to be traded for flux. This will allow for rapid scanning over a large area of sample with a large beam (~10 microns) to find areas of interest, followed by a fine scan with a smaller beam (down to ~0.25 micron). The additional parabolic mirror after the slits is to allow illumination of the monochromator with parallel light. This will allow the full vertical acceptance (0.2 mrad) of the beamline rather than in the current situation where the test setup restricts the vertical acceptance to the angular acceptance of the four-crystal monochromator (~<0.05 mrad). The increased flux requires an improved detector and the scanning stages. A new multi-element detector is required with a five-time increase in solid angle of collection and with a fast processing electronic package. A new backlash-free XY scanning stage will also be required to allow for rapid scanning. The detector and stage need to be integrated with the existing developmental software to produce a robust user-friendly package. Elemental mapping scan times will drop from 10 hours with the current-test setup to less than 10 minutes with the upgraded beamline.

Accomplishments

All the hardware and instrumentation for this μ-XAS capability has been designed and built, or purchased and installed. This includes:

- Optical and engineering design work
- Fabrication, installation, and preliminary testing of the figure of the main toroidal mirror M1
- Fabrication, installation, and testing of the slit assembly
- Fabrication, installation, and preliminary testing of the endstation, which includes the monochromator, focusing mirrors, and vacuum housing
- Commissioning of the new seven-element germanium solid-state detector
- Commissioning of the new, fast XY scanning stages.

The experimental software control code is currently being modified from the previous existing code. This code will link all the above hardware devices together to produce a user-friendly capability. With follow-on support, the μ-XAS station is expected to turn on in February 2001 and to undergo commissioning with help from the outside community. Twelve outside user groups are scheduled to use this station in 2001. Five of these groups (University of Delaware, University of South Carolina, University of California at Berkeley, State University of New York at Stony Brook, Daresbury Lab, UK, and University of Grenoble, France) wish to help with the commissioning. This widespread, diverse, and enthusiastic participation demonstrates the size of the scientific community to be served. This investment has seeded an extensive user program at the ALS, which will become self sustaining in 2001 when the commissioning is complete.

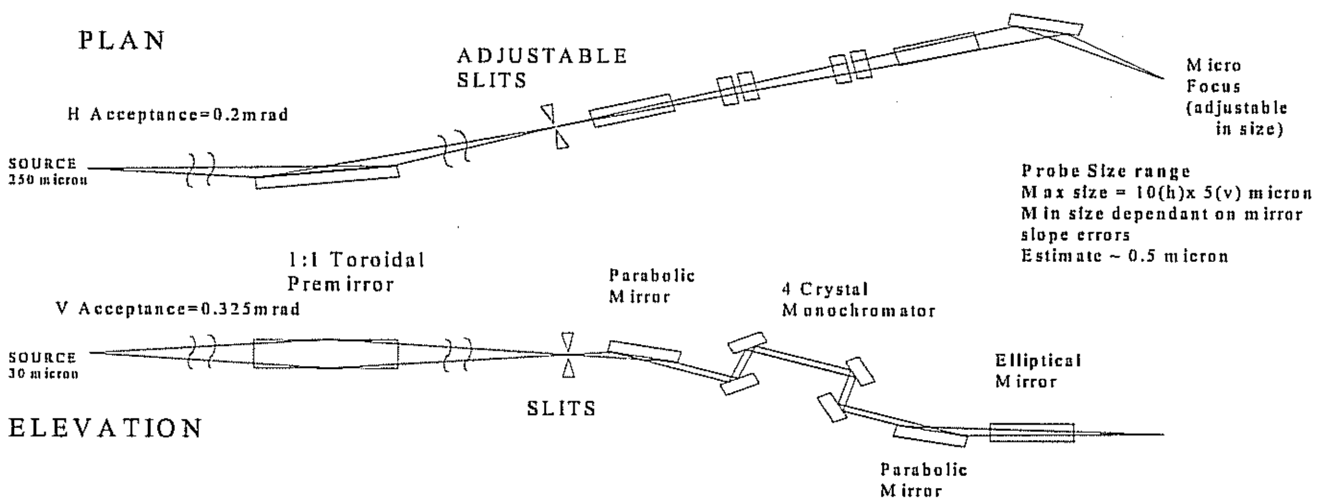

Figure 3: Schematic layout of ALS beamline 10.3.2.

Publications

A.A. MacDowell, H.A. Padmore, R Celestre, G.M. Lamble, A.C. Thompson, and D. Cambie, "Upgrading of the Micro-X Ray Absorption Spectroscopy Beamline 10.3.2 at the ALS," LSBL-539 (January 2000).

Laser-Assisted Photoabsorption of X-Rays by Atoms and Feasibility of a Femtosecond X-Ray Source

Principal Investigators: Ali Belkacem, Thornton Glover, and Wim Leemans

Project No.: 00005

Project Description

An important effect resulting from dressing an atom with a high-intensity laser is the change of its atomic structure. A combination of high-intensity laser and high-brightness of a synchrotron radiation source, such as the Advanced Light Source (ALS), offers a unique opportunity for probing inner-shell electrons and, in the process, opening the prospect of a new type of sub-picosecond x-ray atomic switch in the several keV energy-range. The study of the excitation of inner-shell electrons—the underlying process on which the "atomic" switch concept is based—requires a high degree of synchronization between the laser beam and a tunable x-ray beam that has a high energy resolution. This stringent requirement has limited the number of such studies reported in the literature, despite the critical role that inner-shell excitation processes play in many physical concepts including the x-ray laser. The state-of-the-art facilities at the ALS, in particular the new beamline 5.3.1, are uniquely suited for such studies.

An x-ray, with several keV energy, impinging on a high-Z atom will interact essentially with core electrons. The absorption crosssection of the x-ray by the atom can jump by an order-of-magnitude when the energy is tuned from below the K-absorption edge to above the K-absorption edge. Both initial and final state energy levels contain a sizable contribution from the strong electron-electron correlation of the multi-electron system. The application of a high-intensity laser field to a multi-electron atom adds another component. The structure of the laser-dressed atom will differ from that of the same atom in a field-free space as a result of two mechanisms:

- The electric field related to the short-pulse laser induces a linear and quadratic stark shift of the energy levels. This effect is larger for the outer atomic shells and continuum states.
- The outer electrons, strongly driven by the laser field, will rearrange and, in some cases, will move away from the ion core, decreasing the effect of their screening on the inner-shell. Consequently, the binding energy of the core-electrons will differ from that of the field-free atom. In the limit of ionization of the M-shell for argon, for example, the binding energy of the K-shell will sink in the Coulomb potential by 170 eV.

In the first stage of this project, we will use the laser facilities already existing at the ALS on beamline 7.3.1.2 to develop the diagnostic tools and endstation that are needed for the experiment. In the second stage, we will move the apparatus to beamline 5.3.1 to make use of the tunable femtosecond x-rays, a unique facility that is currently being built at the ALS.

Accomplishments

The challenge for performing these experiments is to develop the right diagnostic tools that can sign in a non-ambiguous way the creation of an inner-shell by the x-rays while the laser is acting on the atomic target. Once these diagnostic tools are identified and tested, the next step is to design, build, and install on the ALS beamline an endstation with all the peripherals, such as the detector systems and the electronic readout systems. Both of these tasks were achieved in FY2000.

The main problem that we had to address was the synchronization between the femtosecond laser and the ALS x-ray beam. In order to speed up our learning curve we collaborated closely in the first few months on an already existing project on beamline 7.3.2.1. The next problem we had to address was the identification, with a very high efficiency, of the creation of an inner-shell by the ALS x-ray. Once an inner-shell is removed from an atom, the resulting ion is left in an excited state and then relaxes through the emission of several Auger electrons. As opposed to the removal of an outer electron, the removal of an inner-shell electron results in an ion with a high charge state and the emission of several Auger electrons, including a KLL Auger electron. We tested this characteristic as a diagnostic tool by studying K-shell photo-ionization of neon.

On beamline 7.3.1.2, we built and installed a vacuum chamber with a time-of-flight system to identify the different charge states that are emitted when the x-ray energy of the ALS beam is varied through the K-shell threshold. The x-ray absorption is known to jump by an order-of-magnitude when the K-edge is crossed. We found that, when requiring the emission of a doubly-charged or triply-charged neon ion, the K-jump goes from one order-of-magnitude to two orders-of-magnitude. We also found that the probability of detecting a doubly-charged neon when the x-ray energy is tuned below the K-edge is extremely small.

This finding impacts two important aspects of the experiment. The high charge states identify in a very clear way the creation of a K-vacancy. The microchannel plate detectors used for the ions are very fast. Although the ions take a few hundred nanoseconds to reach the detector, the time resolution for a given charge state is on the order of a few nanoseconds. This resolution is narrower than the spacing of the ALS buckets around the camshaft pulse. This allows us to identify in a non-ambiguous way the ions that are created during the camshaft pulse. The next challenge was to find a technique that would allow the spatial and temporal overlap of the laser pulse and the camshaft ALS pulse. The spatial overlap is done with a charge-coupled device (CCD) camera and a YaG crystal inserted at the target location. We developed a new technique that insures the temporal overlap between the ALS pulse and the laser pulse using microchannel plate detectors. A metal wire is inserted at the location of the gas jet. The laser and the x-ray beam impinge on the wire and generate low-energy electrons that are extracted with a very high electric field (4000 V) toward a very fast microchannel plate. The initial energy of the electrons is low and the spread of this energy has a negligible effect on the time-of-flight to the detector. Time resolutions of at least 50—and in some cases 20—picoseconds were achieved. This resolution is better than the 70 to 100 picoseconds width of the ALS pulse. We use this novel technique to overlap the ALS pulse and the laser pulse in a very efficient manner.

These new detection techniques and diagnostics tools that we developed from our first measurements with the ALS x-rays and femtosecond laser were brought together and used to design a new endstation that is built and installed on beamline 5.3.1.

Selective Chemistry with Femtosecond Infrared Laser Pulses

Principal Investigators: C. Bradley Moore

Project No.: 99005

Project Description

The basic goal is to use the intense fields of 100-femtosecond (fs) infrared (IR) pulses to move a molecule from its equilibrium configuration to a desired transition state in a short time, compared to the time for vibrational energy randomization. In this way, it may be possible to carry out bond-selective and functional-group-selective reactions using IR photons.

Since the first experiments on infrared multiphoton dissociation (IRMPD) 25 years ago, chemists have wanted to be able to select specific reactions by using intense IR lasers to drive vibrational modes corresponding to the desired reaction coordinate. Attempts with nanosecond and microsecond lasers failed because intramolecular redistribution of vibrational energy (IVR) occurs on shorter timescales. Thus all modes are energized simultaneously. Inspired by the increasing availability of intense femtosecond IR pulses, a collaboration with Professor K.-L. Kompa and his group at the Max Planck Institute for Quantum Optics in Garching, Germany, has been initiated. Initially, a single tunable IR frequency will be used to excite a molecule, and products will be detected by standard methods. Ultimately, two tunable IR frequencies will be generated. Pulses of 100 fs duration are fast compared to many IVR processes. Theoretical and experimental studies on diatomic molecules suggest that substantial multiphoton vibrational excitation can take place at optical fields below that for which substantial non-resonant ionization takes place. In the event that selective reactions do not occur, time-resolved measurements of IVR rates may be carried out for individual modes, and relaxation pathways identified. These experiments are just on the edge of feasibility with current technology and, therefore, it is critical to design the excitation schemes correctly the first time. The measurements of spectroscopic-level widths and structures, of reaction rates, and of picosecond IRMPD in our lab and dynamical calculations in Kompa's lab, should allow the optimum conditions for these experiments to be defined in advance.

One approach heads directly toward the interests of synthetic chemists. Thus, the collaboration includes Chemical Science Division's Professor Robert Bergman. Many important synthetic reaction steps have activation energies that correspond to a few IR photons. This chemistry happens mostly in solution where energy is dissipated to the solvent, as well as to other vibrational degrees of freedom within the molecule. Our first target is to stimulate reaction of diazo groups. Jake Yeston (a Bergman/Moore student) has been studying ultraviolet (UV) photolysis of diazo compounds using an excimer laser for photolysis and a continuous-wave (cw) IR diode laser for measuring concentration-vs.-time for products. The asymmetric stretch of the diazo group near 2050 cm^{-1} is almost identical to the reaction coordinate:

$R_2C{=}N{=}N \rightarrow R_2C + NN$

where R is an alkyl or aryl group. If these reactions can be driven, we will look at molecules containing a second functional group with lower activation energy and see if the diazo can be driven to react without the normal thermal reaction occurring.

Accomplishments

The molecule initially chosen for IRMPD experiments was diphenyldiazomethane, $Ph_2C{=}N{=}N$ ($Ph{=}C_6H_5$). Preliminary studies of the thermal decomposition of this complex indicated that five IR photons at the CNN stretching frequency of 2050 cm^{-1} would furnish sufficient energy to cleave the C-N bond. The Ti:Sapphire-based laser system in the Kompa laboratories in Garching was employed to pump an optical parametric amplifier (OPA), producing IR pulses in the 2000 to 2100 cm^{-1} spectral region with 5 to 10 μJ of pulse energy and approximately 200 fs duration. To detect the dissociation product diphenylcarbene, Ph_2C, a laser-induced fluorescence scheme was employed, with excitation of the carbene to be achieved by a 400 nm probe pulse, also of approximately 200 fs duration. Experiments were carried out with the diazo compound dissolved in isooctane or cyclohexane solvent and recirculated in a liquid jet flowing at a sufficient rate for each laser pulse to impinge on fresh sample. To calibrate and optimize the detection scheme, a UV pump pulse at 266 nm was employed in place of the IR pulse for dissociation of Ph_2CN_2, and the dispersed fluorescence spectrum of the product carbene matched published literature spectra.

Digital photon counting techniques allowed a carbene detection sensitivity of 10^{12} molecules/cm^3 with the fluorescence scheme detailed above. No carbene formation was observed upon IR excitation of Ph_2CN_2 solutions in the 1 to 10 mM concentration range ($10^{17} - 10^{19}$ molecules/cm^3). The efficiency of IRMPD in this case must therefore be less than 0.001 %. Future studies may focus on increasing IR power and chirping the IR pulses to the red to compensate for anharmonicity in the higher vibrational energy levels of the CNN stretching mode.

Study of Radionuclide-Bacterial Interaction Mechanisms

Principal Investigators: Heino Nitsche and Petra Panak

Project No.: 99006

Project Description

This project is to determine the influence of microorganisms on radionuclide transport in the environment. A quantitative and mechanistic understanding will be developed of radionuclide interaction, in particular of the actinides uranium and plutonium, with aerobic soil bacteria. The information from this study is important for improving reactive transport models predicting the movement of actinides at contaminated sites and assessing the risk of potential nuclear waste disposal sites. Furthermore, the results will be transferable to possible biotechnology processes for stabilization and remediation of radionuclide-contaminated sites. The study has interdisciplinary character and combines actinide chemistry, microbiology and molecular environmental science.

The production and testing of nuclear weapons, nuclear reactor accidents, and accidents during the transport of nuclear weapons have caused significant environmental contamination with radionuclides. Due to their long half-lives and high chemical and radiotoxicity, the actinides pose a significant threat to human health. Their migration behavior is controlled by a variety of complex chemical and geochemical reactions such as solubility, sorption on the geo-medium, redox reactions, hydrolysis and complexation reactions with inorganic, organic, and biological complexing agents. In addition, microorganisms can strongly influence the actinides' transport behavior by both direct interaction (biosorption, bioaccumulation, oxidation and reduction reactions) and indirect interaction (change of pH and redox potential), thus immobilizing or mobilizing the radioactive contaminant. Very little information is available about these processes. Our research focuses on the interaction of aerobic bacteria that are present in the upper soil layers with plutonium and uranium.

Accomplishments

We studied the interaction of Pu(VI) with two representative strains of the main aerobic groups of soil bacteria present in the upper soil layers, *Bacillus sphaericus* ATCC 14577 and *Pseudomonas stutzeri* ATCC

17588. The accumulation studies have shown that under the same conditions these soil bacteria accumulated more U(VI) than Pu(VI). Using spores of *Bacillus sphaericus* instead of the vegetative cells, the binding capacity was significantly enhanced at low biomass concentrations (< 0.7 mg/L) for both, U(VI) and Pu(VI). At higher biomass concentrations (> 0.7 g/L), the biosorption efficiency decreased with increasing biomass concentrations due to increased agglomeration of the bacteria, and the vegetative cells of both strains and the spores of *B. sphaericus* showed comparable sorption efficiencies.

Spectroscopic studies (time-resolved laser fluorescence spectroscopy and x-ray absorption spectroscopy) of the U(VI)-*Bacilli* complexes proved that U(VI) phosphate complexes are formed. Uranium(VI) is the stable oxidation state in oxic environmental waters at near neutral pH, whereas plutonium can coexist in the oxidation states, 4+, 5+, and 6+ under these conditions. Spectroscopic methods and solvent extraction to separate different oxidation states of plutonium after contact with the biomass, and kinetic studies provided further information on the mechanistic details of the different processes resulting from the interaction with the bacteria. Based on our results, we developed a model to describe the interaction of Pu(VI) with aerobic soil bacteria. The overall mechanism includes three processes, which have different time scales. In a first step, Pu(VI) is bound to phosphate groups of the biomass. This process is characterized by very fast kinetics and depends strongly on the amount of biomass, which determines the amount of available binding sites of the cells. In a second step, a part of the cell-bound Pu(VI) is reduced to Pu(V) by interaction with the biomass. This is a much slower process compared to the binding of Pu(VI) to the biomass. After 24 hours, one third of the initial Pu(VI) was reduced. Due to the weak complexation ability of the PuO_2^+ ion, the formed Pu(V) was found in solution. This explains why, compared to uranium, less plutonium was found on the biomass under identical conditions. Uranium(VI) has a much lower redox potential than Pu(VI) and cannot be reduced under the experimental conditions. Long-term studies have shown that after a contact time of one month, 16.1 % Pu(IV) was formed (third process). Because of the very slow kinetics of the Pu(IV) formation, we conclude that under our experimental conditions the Pu(IV) was produced by disproportionation of Pu(V), and not by microbial reduction.

To characterize the bacterial complexes with Pu(VI) (formed in the first step) and U(VI), we used x-ray absorption spectroscopy [extended x-ray absorption fine structure (EXAFS) and x-ray absorption near-edge structure (XANES)] and time-resolved laser fluorescence spectroscopy (TRLFS) (see Figure), respectively. The analysis of the EXAFS spectra of the bacterial Pu(VI) complex provided information on the coordination and bond lengths (Pu-O_{axial}: 1.78 Å, Pu-$O_{equatorial}$: 2.42 Å and Pu-P: 3.70 Å). Using TRLFS, we were able to differentiate between phosphate complexes with organophosphate groups and inorganic phosphate complexes. Our investigations have shown that for the bacterial strains studied, the uranium was exclusively bound to organophosphate groups on the cell surface and not precipitated as uranyl phosphate.

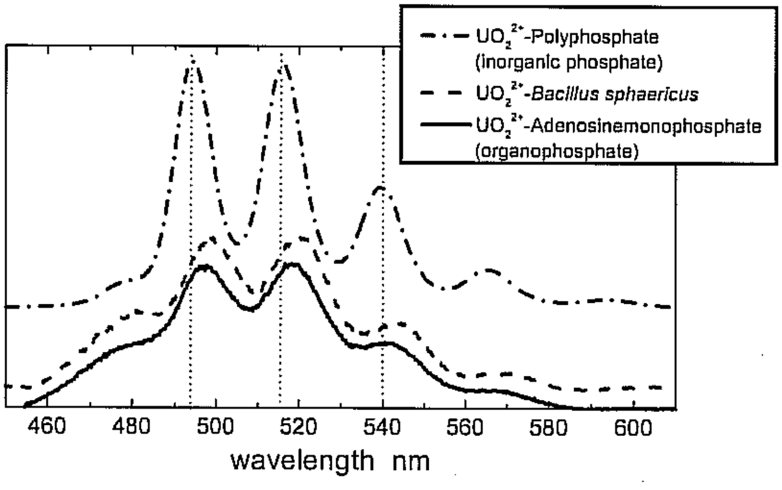

Figure 1: Time-resolved laser fluorescence spectra of the U(VI) complex with Bacillus sphaericus (dashed line) in comparison to the spectra of uranyl model compounds with organic phosphate (uranyl-adenosine monophosphate, solid line) and inorganic phosphate (uranyl polyphosphate, dashed-dotted line) The U(VI) in the Bacillus complex is bound to organophosphate groups on the cell surface (collaboration with R. Knopp, Berkeley Lab, The Glenn T. Seaborg Center).

Publications

P.J. Panak and H. Nitsche, "Interaction of Aerobic Soil Bacteria with Plutonium(VI)," LBNL-46688, (August 21, 2000) submitted to *Environmental Science and Technology*.

P.J. Panak, C.H. Booth, and H. Nitsche, "X-ray Absorption Spectroscopy of Plutonium Complexes with *Bacillus Sphaericus," Radiochim Acta*, (September 30, 2000) (draft).

P.J. Panak, and H. Nitsche, "Interaction of Aerobic Soil Bacteria with Hexa- and Pentavalent Plutonium," LBNL-45209 Abs, poster at Plutonium Futures-The Science, New Mexico, USA, (July 10-13, 2000).

P.J. Panak, and H. Nitsche, "Plutonium and Aerobic Soil Bacteria," LBNL-47060 Abs., talk given at 2000 International Chemical Congress of Pacific Basin Societies, Honolulu, Hawaii, U.S.A., (December 14-19, 2000).

High-Precision Arithmetic with Applications in Mathematics and Physics

Principal Investigators: David Bailey

Project No.: 99007

Project Description

For a growing number of investigators in mathematics, physics, and engineering, the standard computer hardware arithmetic typically found on today's computer systems (IEEE 64-bit format, accurate to approximately 16 digits) is no longer adequate. Some problems require only twice this amount ("double-double" precision), while others require substantially more, sometimes the equivalent of hundreds or thousands of decimal digits. High-precision arithmetic of this sort is typically performed by utilizing software packages, such as one that has been developed by the Principal Investigator.

One of the more interesting applications of very high-precision arithmetic is the discovery of new mathematical identities. Perhaps the most remarkable example of this is a new formula for the mathematical constant pi = 3.14159..., which was discovered recently. This new formula has the surprising property that it permits one to directly determine the n-th binary or base-16 digit of pi—without calculating any of the first n-1 digits—by means of a simple algorithm that can easily run on a personal computer. Numerous other formulas of this sort have subsequently been discovered. It now appears that these results have more than recreational value—they have important implications for some centuries-old mathematical questions.

Other applications of high-precision arithmetic to be explored in this activity include finding relationships between constants that arise in quantum field theory, the study of vortex roll-up phenomena in fluid dynamics, and the stabilization of climate modeling calculations.

This activity proposed to develop some new, faster high-precision arithmetic software, together with high-level language bindings, so that these routines can be accessed from a user's Fortran and/or C programs with only minor modifications. Some continuing studies in applications of this software were also proposed, including research in physics, applied mathematics, and pure mathematics.

Accomplishments

During this past year, two new high-precision arithmetic software packages were developed: one performs "double-double" arithmetic (approximately 32 decimal digits), while the other performs "quad-double" arithmetic (approximately 64 decimal digits). The latter software package was developed by Yozo Hida, a student at University of California (UC), Berkeley, as a summer activity sponsored by this grant. Both of these packages include Fortran-90 and C/C++ software bindings, so that scientists can utilize these facilities with only minor modifications to their computer programs.

Several vortex roll-up simulations were performed on the NERSC IBM SP parallel computer system using the quad-double package. These runs explored the question of whether or not these vortices always form perfect exponential spirals. The results appear to indicate that when the key "delta" parameter is pushed beyond a certain level, the vortex exhibits instabilities. This result appears to contradict the prevailing wisdom in the field. Further studies are continuing.

In another activity, a large library of extended and mixed precision linear algebra routines was developed. This work was done by Sherry Li of NERSC, in coordination with Professor James Demmel of the UC Berkeley computer science department, and several other colleagues.

Several studies have been done in the application of high-precision arithmetic calculations to mathematical theory. One breakthrough of sorts was a paper written by the Principal Investigator (PI) and his colleague Richard Crandall of Reed College. They showed that the new mathematical formulas that have recently been discovered using the PI's high-precision integer relation computer program have an important implication for the centuries-old question of whether the digits in mathematical constants are "random" in an appropriate statistical sense. In particular, they demonstrated that the existence of these formulas means that the question of digit randomness is reduced to a certain simple (and plausible) conjecture of mathematical chaos theory. More studies are continuing in this area.

During this past year, a special honor was given to the PI and his collaborator Helaman Ferguson of the Center for Computing Sciences in Maryland. The publication *Computing in Science and Engineering*, in its January 2000 issue, named the "PSLQ" integer relation algorithm, which they developed (and which is also a key focus of this research activity) as one of ten "algorithms of the century."

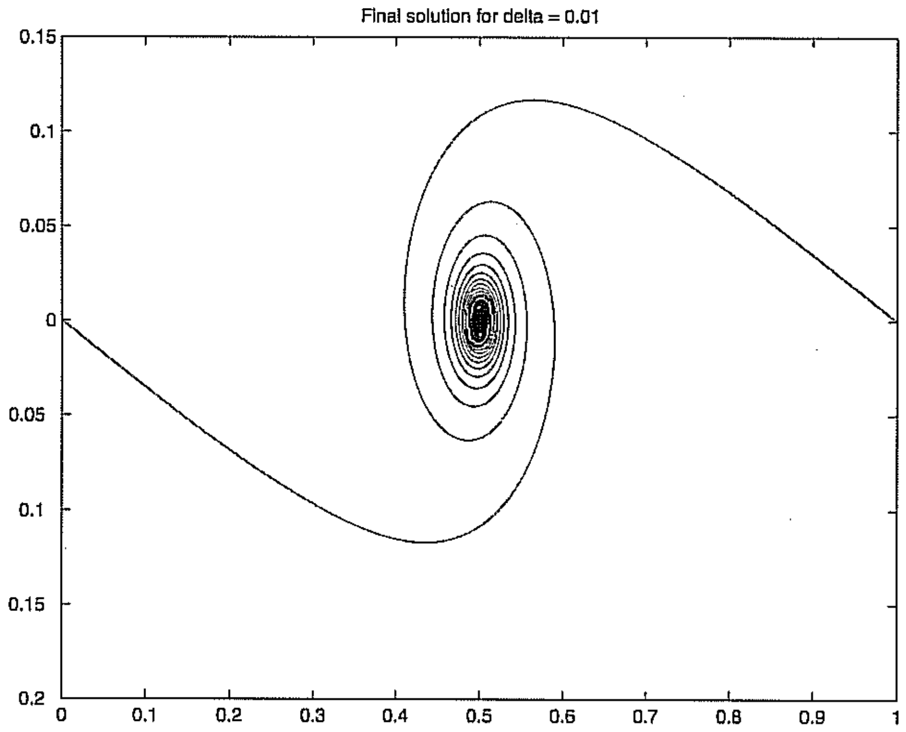

Figure 1: The result of a vortex sheet roll-up computation, performed on 256 processors of the IBM SP. This computation used our new "quad-double" arithmetic software to overcome numerical round-off error.

Publications

D.H. Bailey and D.J. Broadhurst, "Parallel Integer Relation Detection," accepted for publication in *Mathematics of Computation*" (October 1999).

D.H. Bailey, "Integer Relation Detection," *Computing in Science and Engineering*, (January-February 2000).

D.H. Bailey and J M. Borwein, "Experimental Mathematics: Recent Developments and Future Outlook," to appear in <u>Mathematics Unlimited—2001 and Beyond</u> (May 2000).

D.H. Bailey and R.E. Crandall, "On the Random Character of Fundamental Constant Expansions," to appear in *Experimental Mathematics* (October 2000).

Y. Hida, X. S. Li, and D. H. Bailey, "Algorithms for Quad-Double Precision Floating Point Arithmetic," submitted to ARITH-15 Conference (October 2000).

X. S. Li, J. W. Demmel, D. H. Bailey, and others, "Design, Implementation and Testing of Extended and Mixed Precision BLAS," submitted to *SIAM Journal on Mathematical Software* (October 2000).

All above publications available at:
<u>http://hpcf.nersc.gov/~dhbailey/dhbpapers/dhbpapers.html</u>

Numerical Methods for Time-Dependent Viscoelastic Flows

Principal Investigators: Grigory Barenblatt and Alexandre Chorin

Project No.: 98007

Project Description

The purpose of this project is the development and application of advanced computational techniques for simulating time-dependent Newtonian and non-Newtonian flows, with emphasis on flows studied experimentally by Berkeley Lab Material Sciences investigators as well as investigators in other laboratories (Illinois Institute of Technology, University of Illinois at Urbana-Champaign, NASA-Langley NTF, Royal Institute of Technology in Stockholm).

The approach was based on our recently developed computational technique for time-dependent high Reynolds number Newtonian flows. For the high Reynolds number flows, we used the modern asymptotic similarity methods based on the idea of incomplete similarity (asymptotic invariance with respect to a renormalization group).

Accomplishments

We have continued to construct accurate and robust schemes for incompressible viscoelastic flows. A key issue in this field is the use of accurate hyperbolic solvers. Recently, Kurganov and Tadmor developed a new semi-discrete scheme for hyperbolic systems. While this scheme has shown satisfactory performance in the context of hyperbolic systems, it has never been combined with incompressible flow solvers. We constructed a scheme for incompressible flows based on a pure stream function formulation of the Navier-Stokes equations. The pure stream function formulation obviates the difficulty associated with vorticity boundary conditions. The resulting biharmonic equation was discretized with a compact scheme and solved with an algebraic multigrid solver. The advection of vorticity was implemented with the Kurganov-Tadmor high-resolution solver, which proved to remain stable and accurate in the presence of large gradients. The accuracy and robustness of the method were demonstrated for high-Reynolds number Newtonian flows in a lid-driven cavity.

We processed all available experimental data (about 200 runs) concerning the Newtonian boundary layer flows with zero-pressure gradient, in particular the experimental data obtained in the above-mentioned laboratories. We found that in all cases, without exception, if the free stream turbulence is low, the basic intermediate layer between the viscous sublayer and the free stream consists of two self-similar parts, described by scaling laws. If the characteristic length scale that enters the Reynolds number is taken equal to approximately 1.5 thicknesses of the wall layer, the scaling law for the self-similar sublayer adjacent to the viscous sublayer (the wall layer) can be represented exactly in the form of a Reynolds-number-dependent scaling law, found by us earlier for the Newtonian pipe flows. The power in the scaling law adjacent to the free stream is shown to be strongly pressure-gradient-dependent; for zero-pressure-gradient flows it is around 0.2. The boundary between the wall-layer and the layer adjacent to the free stream is sharp. If the free stream turbulence is large, the self-similar layer adjacent to the free stream disappears.

For the case when the lower boundary is liquid, preliminary calculations were performed of the boundary layer flow acceleration by large drops. The calculations are related to a recently proposed model of tropical hurricanes by M. J. Lighthill.

The application of advanced similarity methods to the formulation of the boundary conditions in the numerical methods for viscous and viscoelastic flows was considered.

Publications

G. I. Barenblatt. "Scaling Laws for Turbulent Wall-bounded Shear Flows at Very Large Reynolds Numbers," *Journal of Engineering Mathematics*, **36**: 361-384 (1999).

G. I. Barenblatt, A. J. Chorin, and V. M. Prostokishin, "Analysis of Experimental Investigations of Self-similar Intermediate Structures in Zero-pressure-gradient Boundary Layers at Large Reynolds Numbers," Preprint No. 777, Ctr for Pure & Applied Mathematics, University of California, Berkeley (January 2000).

G. 1. Barenblatt, A. J. Chorin, and V. M. Prostokishin, "A Note on the Intermediate Region in Turbulent Boundary Layers," *Physics of Fluids* **12**, No. 9 (2000).

G.I. Barenblatt, A.J. Chorin, and V.M. Prostokishin, "Self-similar Intermediate Structures in Turbulent Boundary Layers at Large Reynolds Numbers," *Journal of Fluid Mechanics*, **410**, 263-283, (2000).

G.I. Barenblatt, A.J. Chorin, and V.M. Prostokishin, "Characteristic Length Scale of the Intermediate Structure in Zero-pressure-gradient Boundary Layer Flow," *Proceedings National Academy of Sciences USA* 97, No. 8, 3799-3802 (2000).

G.I. Barenblatt, A.J. Chorin, and V.M. Prostokishin, "A Note Concerning the Turbulent Boundary Layer Drag at Large Reynolds Numbers," Preprint No. 785, Ctr for Pure and Applied Mathematics, University of California, Berkeley (August 2000).

R. Kupferman, "A Central-difference Scheme for a Pure Stream Function Formulation of Incompressible Viscous Flow," *SIAM Jour. Sci. Comp.* (in press).

Science-Based Subgrid Scale Modeling in Fluid Turbulence

Principal Investigators: John Bell, Phillip Colella, Alexandre Chorin, Nancy Brown, and Michael Frenklach

Project No.: 00006

Project Description

We propose the development of an integrated approach to subgrid scale model development for reacting fluid flows. This project will build on the combined strengths of a number of groups at Berkeley Lab: in the understanding of fundamental analysis of fluid dynamics and chemical reactions; in large-scale simulations of fluid dynamics; and in parallel computing. We expect to develop and validate a number of new models for turbulence, in particular turbulent boundary layers and turbulent reacting fluid flows. In addition, we will develop the software capability required to support an integrated approach to model development, and will make this capability available to the Department of Energy (DOE) scientific community.

We will use new and more rigorous methodologies for developing subgrid scale models for two key problems in turbulence. For turbulent boundary layers, we will use the incomplete similarity and optimal prediction approaches developed in the Berkeley Lab Mathematics Department. For turbulent combustion modeling, we will use the Piece-Wise Reusable Implementation of Solution Mapping (PRISM) methodology for developing reduced descriptions of chemical reactions and transport. The development and validation of these models will be done using a state-of-the-art Computational Fluid Dynamics capability developed in the National Energy Research Scientific Computing Center (NERSC) Division, based on massively parallel implementations of adaptive mesh refinement methods.

Accomplishments

During the past year, we have made progress in two aspects of model development for time-dependent reacting flow. We have begun developing models for turbulent flow based on ideas of optimal prediction. Optimal prediction (OP) methods compensate for a lack of resolution in the numerical solution of complex problems through the use of an invariant measure as a prior measure in the Bayesian sense. In first-order OP, unresolved information is approximated by its conditional expectation with respect to the invariant measure. In higher-order OP, unresolved information is approximated by a stochastic estimator, leading to a system of random or stochastic differential equations. The stochastic variability in the system leads to a memory term that expresses the effects of the unresolved on the resolved scales. The memory term comes from the Mori-Zwanzig projection formalism, which yields an identity connecting the past and the future of reduced dynamical descriptions of complex systems and exhibits the memory term explicitly. We have applied this procedure to the solution of Averaged Euler equations in two space dimensions.

Another area of our research has concerned the development of reduced, high-fidelity representations of chemical kinetics. The GRI-Mech 3.0 reaction mechanism is dependable and accurate for CH_4 combustion. However, for performing highly resolved, three-dimensional (3-D) grid turbulent flow simulations, this reaction-set requires enormous computational resources. To alleviate this, Kazakov and Frenklach developed and applied a procedure to reduce GRI-Mech 1.2 (GRI-3.0 without nitrogen chemistry) obtaining a twenty-two species model, DRM22, and in the tests under laminar flame conditions, concentrations and enthalpy were reproduced to within 10% over a range of equivalence ratio ϕ from 0.8 to 1.5.

The reduction removed intermediate species if their rates were insignificant, relative to net production rates. The resulting effect of reducing induction time-scales by about 50ms, could cause a difference in a turbulent environment where velocity fields advect reactants/products around on time-scales a factor of 10 higher (0.5ms). We investigated this with a vortex-flame interaction (VFI) simulation: on a two-dimensional (2-D) grid, a laminar flame was set up in a premixed-air CH_4 flow, with the inlet stream set equal to the laminar velocity in order to keep the flame stationary. The velocity field of a self-propelled vortex pair was superimposed on the field and allowed to move into the flame. The velocities used in the vortex were on the order of 3 to 5 m/s and the turbulent intensity is at the high end of what is expected in commonly simulated situations. Identical simulations using both GRI-Mech 1.2 and DRM22 were conducted, and the results are in agreement with what is seen under laminar conditions. The time-scale associated with the turbulent intensity is shorter than that of chemistry.

Another effect of many interacting vortices in close proximity to each other is to create situations of reactant-product mixing (e.g., thin flames with reactant on both sides burning toward a common center, or pockets of hot product within non-burnt reactant) that never occur in laminar conditions. To simulate this effect, a well-developed turbulent field was impinged onto a steady 2-D laminar flame. The simulation was similar to the VFI above, except that instead of a vortex pair, a turbulent eddy field was superimposed. We investigated flows with mean turbulent intensities of 1 m/s, 10 m/s, and 100 m/s. The field moved toward the flame (self-propulsion and advection by inlet stream) and, depending on the intensity of turbulence, resulted in conditions ranging from slight deformation (turbulent intensity = 1 m/s) to a wrinkled flame (10 m/s) to a highly wrinkled, disconnected flame (100 m/s). Again, the simulations were conducted using both GRI-Mech 1.2 and DRM22. The result to date is not conclusive because, in two dimensions, vortices coalesce into larger structures, contrary to what is seen in three dimensions.

Publications

J. Bell, A. Chorin, and W. Crutchfield, 'Stochastic Optimal Prediction with Application to Averaged Euler Equations," *Proceedings of the 7th National Conference on Computational Fluid Mechanics* (August 2000).

J.B. Bell, N.J. Brown, M.S. Day, M. Frenklach, J.F. Grcar, and S.R. Tonse, "The Effect of Stoichiometry on Vortex Flame Interactions," *Proceedings of the 28th Combustion Institute* (July 2000).

J.B. Bell, N.J. Brown, M.S. Day, M. Frenklach, J.F. Grcar, R.M. Propp, and S.R. Tonse, "Scaling and Efficiency of PRISM in Adaptive Simulations of Turbulent Premixed Flames," *Proceedings of the 28th Combustion Institute* (July 2000).

Publications available at:

http://seesar.lbl.gov/ccse/Publications/pub_date.html

Computational Methods for Electronic Structure Codes in Materials Science: Ground-State and Excited-State Properties

Principal Investigators: Andrew Canning and Steven Louie

Collaborator: Lin-Wang Wang

Project No.: 00007

Project Description

A fundamental understanding of the properties of a material requires the knowledge of its electronic structure as determined by the valence electrons. In particular, as electronic components move towards the nanometer scale, quantum effects become increasingly important and can only be predicted and understood from accurate calculations of the electronic structure.

This project aims to develop state-of-the-art electronic structure methods and parallel codes and make them available to the materials science community and in particular the Department of Energy (DOE) community and National Energy Research Scientific Computing Center (NERSC) users. These codes will perform ground-state as well as excited-state electronic structure calculations. The ground-state calculations are based on density functional theory (DFT) using pseudopotentials to represent the atomic core regions and the local density approximation (LDA) or the generalized gradient approximation (GGA) for the electron-electron interaction. The wavefunctions for the electrons are expanded in plane-waves. Codes for electronically excited states will also be developed using a first-principles approach developed by Louie and collaborators based on the GW approach (The "G" in GW refers to the dressed Green's function of the electron and the "W" is the screened coulomb interaction.) In the case of optical properties where an electron-hole pair (exciton) is formed, the interaction between the excited electron and the hole is included through the two particle Green's function. The excited-state codes require the ground-state wavefunctions and energies as inputs, so the complete set of codes is required for an excited-state calculation. Development of these codes and methods will be applications-driven from physical problems relevant to the Materials Sciences (MSD) and Advanced Light Source (ALS) divisions at Berkeley Lab. These types of electronic structure calculations are very demanding of computer power and are a natural match for the large parallel computers at NERSC.

Accomplishments

Ground-State Methods and Code

The ground-state code PARATEC (PARAllel Total Energy Conjugate-gradient) has been further developed in this project. The code was originally developed to run efficiently on the Cray T3E at NERSC using the native SHMEM communication language but an efficient MPI (Message Passing Interface) version, which is portable across different machines, such as the new IBM SP at NERSC, has now been written. In the code, the electronic structure is determined by a self-consistent iteration loop on the charge density until a certain tolerance is reached. We have introduced a new charge-mixing scheme (Thomas-Fermi, based on an idea by Lin-Wang Wang at NERSC) that, for certain systems, gives faster convergence than previous methods. This new method helps avoid the so-called charge-sloshing problem associated with long unit cells. Another method is also being studied that minimizes the DFT function directly with a Grassmann conjugate gradient algorithm that updates the charge density and associated potential with every update of the wavefunctions.

Version 5.0 of PARATEC, which includes some of the above developments as well as bug fixes to the previous version, has been released to users. We are in the process of developing a web site for the code with a user's guide that will make it easier to distribute the code and keep users updated on new developments with the code.

Excited-State Methods and Codes

Preliminary parallel versions of the GW and exciton codes have now been developed and are being used by other groups who are part of the DOE computational materials science network (CMSN) project on excited states. The GW code has also been extended to deal with spin-polarized (i.e. magnetic) systems.

We have performed the first large-scale simulations using the GW code to calculate the quasiparticle electronic structure of ethylene adsorbed on the dimer reconstructed Si(001)-2x1 surface. Within the GW approximation, the self-energy corrections for the states derived from the molecular adsorbate are found to be much larger than those of the states derived from bulk silicon. The calculated quasiparticle band structure was found to be in close agreement with experimental photoemission spectra. The new spin-polarized code has been used to investigate the metal-insulator transition in BCC hydrogen, a classic Mott insulator. The calculated results are in excellent agreement with experiment in the limit of atomic hydrogen. The quasiparticle wavefunctions are found to be significantly more localized than the DFT LDA wavefunctions.

In the context of excited-state calculations, it is necessary to know the form of the interaction of the nonlocal part of the Hamiltonian with an electromagnetic field. In the past, there have been many attempts to find the correct description of nonlocal systems interacting with external fields, but these attempts have been heuristic or limited to weak and long wavelength fields. We now have a rigorous derivation of the exact, closed-form expression for the coupling of nonlocal electronic systems to arbitrary electromagnetic fields. Aside from justifying and illuminating the various forms used to date, the result is of essential value for systematic computation of linear and especially non-linear response functions, and our result provides the explicit mathematical starting points required for these calculations. These new exact expressions for the interaction of the nonlocal part of the Hamiltonian with an electromagnetic field are being added into the excited-state codes.

Publications

G.M. Rignanese, S.G. Louie, and X. Blase, "Quasiparticle Band Structure of C_2H_4 Adsorbed on the Si(001)-(2x1) Surface," submitted to *Phys. Rev. B*.

J.-L. Li, G.-M. Rignanese, E. Chang, X. Blase, and S.G. Louie, "GW Study of the Metal-Insulator Transition of bcc Hydrogen," (in preparation).

G.-M. Rignanese, X. Blase, A. Canning, and S.G. Louie, "Parallel Algorithms for the Calculation of Electronic Excitations," (in preparation).

D. Raczkowski, A. Canning, and L-W Wang, "Thomas-Fermi Charge Mixing for Obtaining Self-Consistency in Density Functional Calculations," submitted to American Physical Society March meeting (2001).

S. Ismail-Beigi, E. K. Chang, and S. G. Louie, "Coupling of Nonlocal Potentials to Electromagnetic Fields," submitted to *Phys. Rev. Lett.*

Electron Collision Processes above the Ionization Threshold

Principal Investigators: C. William McCurdy and Thomas Rescigno

Project No.: 99011

Project Description

The computational prediction of the electronic structure of atoms and molecules has become a practical task on modern computers, even for very large systems. By contrast, sophisticated calculations on electronic collisions have been limited in terms of the complexity of the targets that can be handled and the types of processes that can be studied. Collision processes are, nevertheless, central to the problems of interest to the Department of Energy (DOE), playing a key role in such diverse areas as fusion plasmas, plasma etching and deposition, and waste remediation. The intermediate energy region, extending from the ionization threshold to a few hundred eV, presents the greatest challenge for *ab initio* theory, since the infinity of energetically accessible final states precludes one from writing down a wave function that describes all possible scattering events, and is simply a reflection of the fact that ionization persists as one of the fundamentally unsolved problems of atomic collision theory.

A practical route to solving the intermediate energy electron collision problem cannot rely on close-coupling approaches, but rather must be based on formalisms that allow the wave function itself to be computed without recourse to the explicit asymptotic form, and on methods that extract cross section information from the wave function without knowing its detailed asymptotic form. The purpose of this project is to develop such an approach for both atoms and molecules. The approach will build on the algebraic variational formalism we have previously developed to study electron-molecule scattering. The approach will be extended to include the scattered-wave, flux operator formalism, which we have developed, complex optical potential interactions, and a variety of techniques based on analyticity. For atomic ionization problems, we will carry out direct solutions of the Schrödinger equation on a (complex) numerical grid and use the projected flux operator formalism to extract total and differential ionization cross sections.

Accomplishments

We extended our work on the three-body Coulomb problem, which was first reported in a 24 December, 1999 cover article in *Science*. A major paper on the electron-impact ionization of hydrogen will appear in *Physical Review A* detailing calculations of total, singly differential (energy-sharing) and triply differential (energy and angle) ionization cross sections at 17.6, 20, 25, and 30 eV, all in perfect agreement with experiment. We also completed a study of doubly differential ionization cross sections which, for the first time, accurately predict the behavior of the ionization cross sections at low impact energies for asymmetric energy sharing between the ejected electrons. Our calculations have revealed problems in the only measurements reported on this system and have prompted new experiments to be undertaken.

We have also made a number of improvements to the basic exterior complex scaling (ECS) methodology used to study ionization. We have developed a new discretization scheme, based on combining finite elements and the discrete variable representation, which is far more efficient than our original approach, which was based on finite difference. We have also developed new methods for using our computed wave functions in integral expressions for the ionization amplitude, which obviate the need for numerical extrapolation of the quantum mechanical flux and its associated errors and limitations. These new developments have allowed us to extend our studies to much lower energies, where we can begin to test threshold laws, and will hopefully allow us to extend our calculations to more complex three-electron systems. Finally, we have begun to explore the possibility of using ECS to study positron collisions, which will offer the possibility of studying rearrangement (positronium formation) scattering in the presence of ionization.

We have continued our work on low-energy electron CO_2 collisions, which play an important role in many gaseous electronics and atmospheric processes. We are particularly interested in probing the effects of nuclear motion on resonant electron impact processes such as vibrational excitation. Virtually all previous theoretical work in this area has been carried out with a simplified one-dimensional model for the nuclear motion, which is only correct for diatomic molecules. We have carried out a thorough study of the dependence of the electronic T-matrix in the vicinity of the 3.8 eV resonance on both symmetric stretch and bending motion. These amplitudes will be used in time-dependent wave packet studies of nuclear motion in several dimensions. Preliminary results suggest that the coupling of nuclear motion in several dimensions is very important in this system.

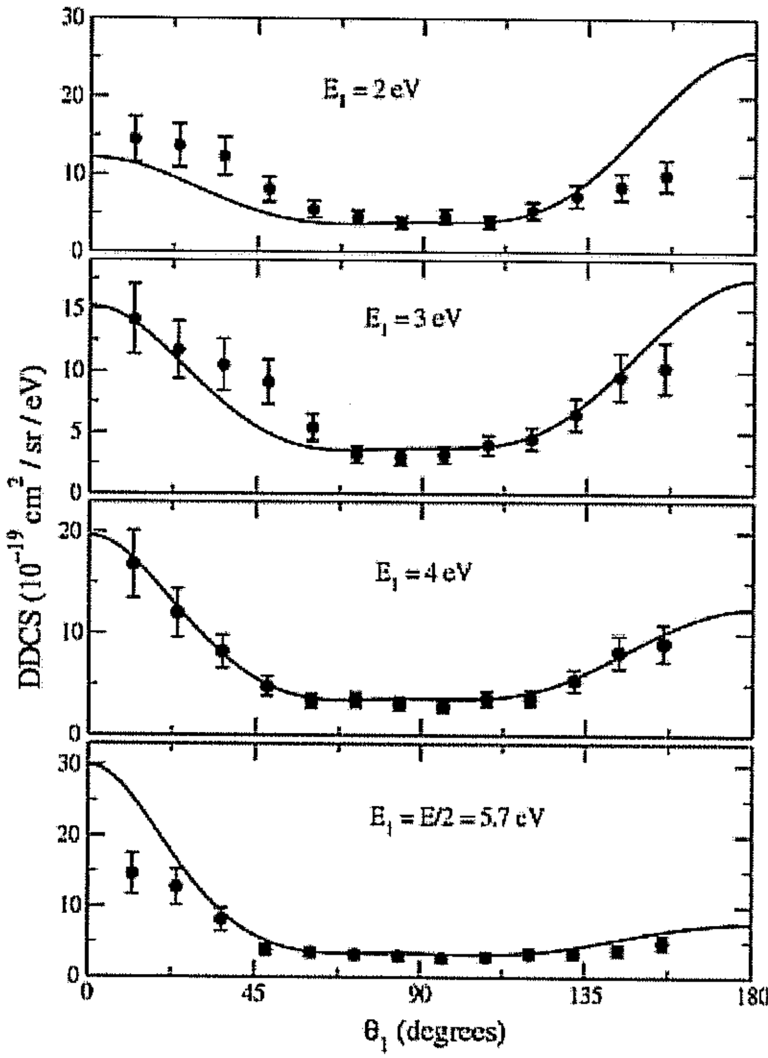

Figure 2: Comparison of calculated and measured doubly differential cross sections for electron-impact ionization of hydrogen at 25 eV. The four panels refer to different energies for the observed, secondary electron.

Publications

T.N. Rescigno and C.W. McCurdy, "Numerical Grid Methods for Quantum Mechanical Scattering Problems," *Phys. Rev. A* **62**, 032706 (2000).

C.W. McCurdy and T.N. Rescigno, "Practical Calculations of Quantum Breakup Cross Sections," *Phys. Rev. A* **62**, 032712 (2000).

C.W. McCurdy, D.A. Horner, and T.N. Rescigno, "Practical Calculations of Amplitudes for Electron Impact Ionization," *Phys. Rev. A* (2001) (in press).

M. Baertschy, T. N. Rescigno, W. A. Isaacs, X. Lee, and C. W. McCurdy, "Electron Impact Ionization of Atomic Hydrogen," *Phys. Rev. A* (2001) (in press).

W.A. Isaacs, M. Baertschy, C.W. McCurdy, and T.N. Rescigno, "Doubly Differential Cross Sections for the Electron Impact Ionization of Hydrogen," submitted for publication *Phys. Rev. Letts.*

M. Baertschy, T.N. Rescigno, C.W. McCurdy, J. Colgan, and M.S. Pindzola, "Ejected-Energy Differential Cross Sections for the Near Threshold Electron-Impact Ionization of Hydrogen," submitted for publication in *Phys. Rev. A.*

Feature-Based Representation and Reconstruction of Geophysical Data

Principal Investigators: Bahram Parvin and Qing Yang

Project No.: 99012

Project Description

This project aims at feature-based representation of large-scale geophysical data and the need for filling data in high-resolution observational platforms. Current environmental satellites generate a massive amount of sparse geophysical data, e.g., sea surface temperature (SST), ocean color, and precipitation data. These observations are collected through NASA MODIS (50-100 gigabytes/day of oceanic data) and NOAA AVHRR (4 gigabytes/day) spacecraft. Global AVHRR data are down-linked to several universities and managed by an automatic processing environment that navigates, calibrates, and computes the geophysical fields (e.g., SST) and combines the satellite swath data into daily, regional, and global fields. In the case of SST, the sparseness of data is due to cloud and aerosol contamination. These data need to be summarized and interpolated for effective visualization and subsequent analysis.

Accomplishments

We have focused on detection of fronts in low-resolution SST data and their corresponding climatic behavior as well as on feature-based reconstruction of high-resolution, spatio-temporal data.

Specifically, we have developed an approach for localization of fronts in low-resolution (18 km) sea surface temperature (SST) data. Aggregating fronts over a 12-year period clearly indicate preferred localization in 40° South and Gulf Stream.

We have developed and implemented a novel, feature-based approach for high-resolution (4 Km) reconstruction of SST data. The novelty of our approach is not just limited to the method, but also to the fact that the current reconstruction (interpolation) algorithms do not scale to 4 km data due to computational complexities. Our approach consists of three steps:

- Current operational reconstruction technique, based on objective analysis, has been leveraged to interpolate sparse images at low resolution. The low-resolution data has a grid point resolution of 18 km.
- Feature velocities of low-resolution, dense spatio-temporal SST data are computed and validated. Our computation model assumes incompressible fluid and uses the regularized flow equation for continuity and reduction in noise effect.
- Computed feature velocities are projected to 4 km sparse high-resolution data and the regularized flow equation is solved in reverse for intensity (as opposed to feature velocities). The results are validated through a number of analyses.

An example of the reconstruction algorithm is shown in Figure 3.

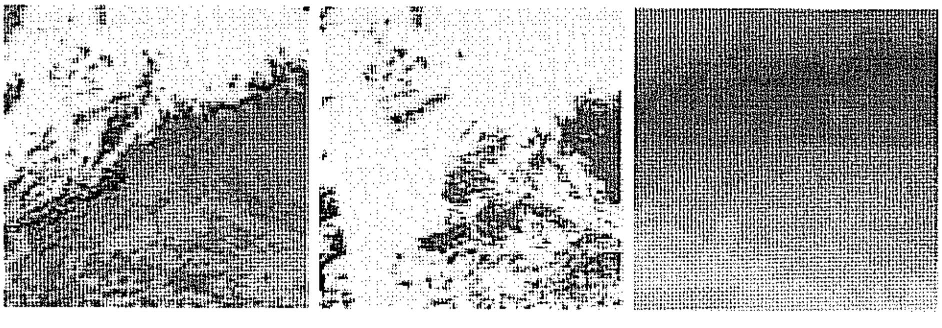

(a) (b) (c)

Figure 3: Reconstruction of high resolution SST data: (a) original SST data to be interpolated (Date: the 40th day of 1998, 130° to 150° W with 20° to 40° N); (b) quality field: white pixels indicate that the corresponding points in (a) are highly unreliable; (c) reconstruction results.

Publications

Q. Yang, B. Parvin, and A. Mariano, "Detection of Vortices and Saddle Points in SST Data," *Geophysical Research Letters* **V28** N2: 331-334 (January 15, 2001).

Q. Yang and B. Parvin, "Feature Based Visualization of Geophysical Data," IEEE Conference on Computer Vision and Pattern Recognition (June 2000).

Q. Yang and B. Parvin, "Singular Features in Sea Surface Temperature Data," International Conference on Pattern Recognition (September 2000).

Q. Yang and B. Parvin, "High Resolution Reconstruction of Sparse Data from Dense Low Resolution Spatio-Temporal Data," submitted to Internation Conference on Computer Vision.

Berkeley Lab Distribution (BLD): Software for Scalable Linux Clusters

Principal Investigators: Paul Hargrove, William Saphir, and Robert Lucas

Project No.: 99013

Project Description

An exciting development in scientific computing over the past few years has been the demonstration that clusters of personal computers (PCs) can achieve the performance of supercomputers for many problems of interest to the Department of Energy (DOE). Such clusters promise to greatly increase the impact of computation on science. Despite their promise, we believe that clusters are destined for only a minor role unless two critical barriers are overcome:

- Most existing and planned system software for clusters is not scalable, making infeasible large clusters that can be applied to DOE mission-critical applications.
- Cluster software is ad-hoc, poorly integrated, lacking in functionality, and difficult to use, making the setup and management of clusters very labor intensive, and limiting their flexibility.

We are designing, implementing, and integrating scalable system software and architectures for clusters. This software will form the basis of the "Berkeley Lab Distribution," or BLD, a complete package of plug-and-play software for configuring, managing, and using Linux clusters.

Accomplishments

In the first two years of this LDRD, we have focused on understanding cluster requirements, developing basic infrastructure for the cluster, and building collaborations with other labs that will eventually form the basis for coordinated multi-lab system software development.

The building block for the BLD architecture is a sub-cluster consisting of a filesystem server and one or more compute nodes that perform computations. The compute nodes require a root filesystem that may reside on a server, through a so-called diskless boot process, or may reside on a local hard disk through a diskfull boot process. There are trade-offs between these two exclusive approaches. Diskless boot is easy to administer, yet performance requirements prevent this method from being used on large clusters. Existing systems using diskfull boot have been shown to scale to the necessary system size, yet present formidable administrative challenges.

We have developed software called BCCM (Berkeley Cluster Configuration Manager), which makes it significantly easier for a system administrator to set up the compute node root filesystems using a minimum amount of storage on the server. It also handles other tasks required to add a compute node to a cluster. BCCM is designed to be scalable. We are adding functionality necessary for BCCM to support the diskfull boot process required by the largest clusters, while preserving the inherent administrative advantages of diskless clusters. A complete requirements definition for diskfull boot functionality was written earlier this year. We are currently redesigning BCCM to handle these new requirements.

We have evaluated dozens of tools to be used as software components in the BLD distribution. The results of these evaluations have been used to elicit requirements for future software development projects, and allowed us to act as participants in the open source community. We have integrated some of these tools into our existing cluster system. Tools evaluated include Chiba City, SCMS, Rexec, SGI ACE, Globus tools, FAI, SGI PCP, and PVFS.

We have also developed new tools for process startup and accounting on BLD clusters. Tmrsh is a tool for process startup that addresses some important deficiencies in current tools. Tmrsh starts jobs twice as fast as other tools, and provides for better fault tolerance while the cluster is operating. Acctpbs is a tool for analyzing cluster accounting data. Acctpbs allows the administrator to generate specialized reports to analyze all important aspects of cluster system utilization including total CPU time usage, total system utilization (average or interval), and other important metrics necessary in a production computing environment.

We have released a trial version of the BLD Distribution at a Linux cluster tutorial held at California State University at Sacramento (CSUS) earlier this year. This distribution allowed us to get early feedback from potential users of BLD systems, and allowed us to perform a detailed study of cluster software deployment. We were able to identify a need for further automation, better documentation, and better usability in our existing software tools, and we are currently designing solutions to these problems.

We have developed an extensive collection of benchmark results for processors used in Linux clusters. These results have become an important and highly visible resource for the community. These may be seen at http://www.nersc.gov/research/ftg/pcp/performance.html.

Sparse Linear Algebra Algorithms and Applications for Text Classification in Large Databases

Principal Investigators: Horst Simon, Chris Ding, and Parry Husbands

Project No.: 99014

Project Description

The goal of this research is to use high-performance computing to help understand and improve subspace-based techniques for information retrieval, such as latent semantic indexing (LSI). In the past, LSI has been used only on very small data sets. We are developing an environment and scalable linear algebra algorithms where LSI-based information retrieval can be applied to matrices representing millions of documents and hundreds of thousands of key words. The computational power of the T3E and SP are required to accomplish this.

There are two main components to this information retrieval: the retrieval accuracy and the efficiency of the algorithms used in retrieval algorithms. Specifically, we hope to:

- Further develop our subspace-based model and gain deeper understanding of the effectiveness of LSI. We will also explore the possibility of extending the subspace-based model for handling image and multimedia retrieval problems.
- Develop more robust and computationally efficient statistical tests for the determination of the optimal latent-concept subspace dimensions.
- Further explore the low-rank-plus-shift structures of the term-document matrices and develop fast and memory-efficient numerical algorithms for the computation of low-rank matrix approximations. We will also investigate linear-time partial Singular Value Decomposition (SVD) algorithms based on term and document sampling.
- Investigate a variety of spectral techniques for characterizing collections with hyperlinks (such as the world wide web) in order to improve retrieval performance.

This project is one of the first to compute decompositions of complete large-term-document matrices. Other efforts have had to resort to sampling to keep things computationally tractable. As such, we are in a unique position to study how scale affects subspace-based retrieval techniques.

We believe that the algorithms developed here will be of use not only in text retrieval, but also in more complicated settings, such as classification of image collections and extraction of images, with desired features, from large collections. Combining effective search and classification algorithms for image problems, with the compute and storage capabilities of future National Energy Research Scientific Computing Center (NERSC) systems, will also help the development of algorithmic techniques for the data and visualization corridors of the next decade.

Accomplishments

Our major accomplishment this year was a more complete understanding of LSI performance on large datasets. We examined the properties of SVD-based projections in order to determine whether they agree with our intuition about information retrieval concepts. The lower dimensionality of the space is intuitively desirable; terms that are related "should" be brought closer together (the cluster hypothesis). However, other properties of the SVD may not match our intuition. The focus of our work was the examination of the influence of term norm on retrieval performance. We discovered that rare terms (with low norm) contribute very little to the final LSI representation of documents, sometimes resulting in poor retrieval performance. We also investigated enhancements to standard LSI and verified an increase in performance on a large (500K document) dataset.

We have also started to explore the use of link data (as found in the world wide web) to augment text retrieval algorithms. To this end, we have secured a snapshot of the web from the Internet Archive and have begun preliminary analysis. We hope to determine (efficiently computable) features that would enable us to distinguish among different classes of sites and hopefully allow for more accurate searches.

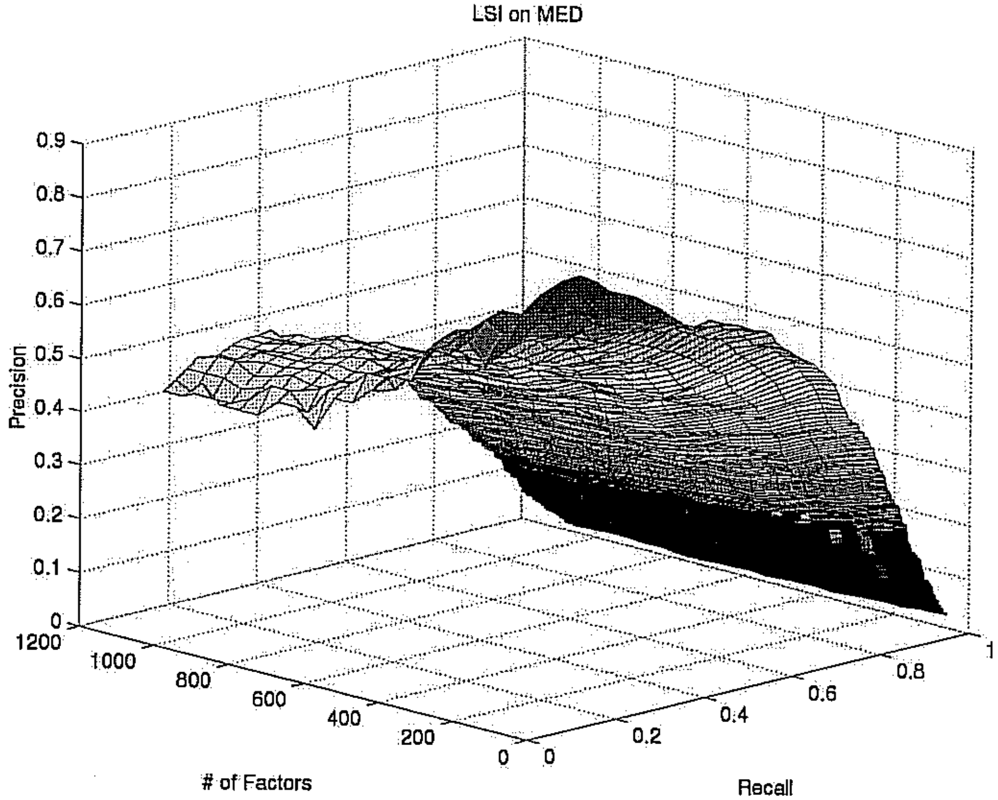

Figure 4: A graph showing the effects of changing the number of dimensions on the retrieval accuracy of LSI.

Publications

C. Isbell and P. Husbands, "The Parallel Problems Server: An Interactive Tool for Large Scale Machine Learning," *Advances in Neural Information Processing Systems 12 Proceedings of the 1999 Conference* (November29-December 4, 1999) LBNL Technical Report LBNL-45330, <u>*http://www.nersc.gov/~parry/text/hi.ps.gz*</u>

P. Husbands, H. D. Simon, and C. Ding, "On the Use of the Singular Value Decomposition for Large Scale Text Retrieval," *Proceedings of the First Workshop on Computational Information Retrieval*, (October 22, 2000) LBNL Technical Report LBNL-47170, <u>*http://www.nersc.gov/~parry/text/hsd.ps.gz*</u>

Geologic Sequestration of CO_2 Through Hydrodynamic Trapping Mechanisms

Principal Investigators: Sally Benson, Larry Myer, Curtis Oldenbury, Karsten Pruess, and G. Michael Hoversten

Project No.: 00008

Project Description

The climate of the earth is affected by changes in radiative forcing due to several sources including greenhouse gasses (CO_2, CH_4, N_2O). Energy production and the burning of fossil fuels are substantially increasing the atmospheric concentrations of CO_2. One of several proposed strategies to reduce atmospheric emissions is to capture CO_2 from fossil fuel final power plants and sequester it in the deep underground.

The Department of Energy is addressing sequestration through a broad program with the goal of developing "safe, predictable and affordable ways to prevent CO_2 from building up in the atmosphere" by 2025. The goals of this LDRD are to pursue research on key scientific issues concerning mechanisms for subsurface trapping of CO_2 and monitoring of CO_2 migration with the goal of establishing Berkley Lab's scientific leadership in this area.

Three projects were carried out: (1) An initial assessment of the statistical feasibility of using CO_2 to enhance gas recovery, (2) An initial evaluation of the sensitivity of geophysical technique for monitoring CO_2 movement, and (3) A preliminary estimate of the CO_2 sequestration capacity of California.

The technical approach involved numerical simulation, laboratory measurements, and/or data review, depending on the activity. The TOUGH2 reservoir simulator was used to perform process-based modeling of CO_2 in gas reservoirs. Forward geophysical modeling provided understanding of the seismic, electromagnetic and gravity response to CO_2 injection. Laboratory studies provide additional data on geophysical sensitivity to injection.

Accomplishments

Carbon Sequestration with Enhanced Gas Recovery (CSEGR)

One way to minimize the net cost of sequestration is to develop technologies that yield collateral economic benefit. The major technological challenge is to develop methods and processes to optimize both the amount of resource produced and the amount of CO_2 sequestered, an approach known as co-optimization. Little attention has been given to enhancing gas recovery while sequestering CO_2 even though the potential storage capacity of partially depleted natural gas reservoirs worldwide could be as much as 140 gigatonnes. In FY2000, this LDRD began the first fundamental process-based modeling of CSEGR. The focus of the work was use of numerical simulation to study CO_2 and CH_4 flow and transport, including gaseous interfingering, diffusive mixing, and mechanical dispersion of variable-density and variable-viscosity gases that may be approaching supercritical condition.

We have developed a module called EOS7C for simulating gas and water flow in natural gas reservoirs within the TOUGH2 framework. The module handles five components (water, brine, non-condensible gas, a gas tracer, and methane) along with heat. The non-condensible gas can be selected by the user to be CO_2, N_2, or air. The inclusion of optional N_2 and air allows testing against existing data and modeling results of traditional cushion gas processes. EOS7C includes the multiphase capabilities of TOUGH2 and allows a simulation of water drive and gas-liquid displacements. Molecular diffusion is simulated by a Fickian model that includes diffusion in both gas and aqueous phases.

Monitoring

Geophysical techniques provide the most cost-effective approach for obtaining the spatial coverage required for mapping the location and movement of CO_2 in the subsurface. However, the effectiveness of these techniques depends upon many factors. Contrasts in physical properties such as seismic wave velocity and electrical conductivity are of first-order importance, though only limited laboratory data are available to define these properties.

Two monitoring related activities were carried out in the FY2000 LDRD research. The first used numerical simulation to begin to assess the sensitivity of geophysical techniques for monitoring of CO_2 in oil reservoirs. The second activity was to perform laboratory measurements of physical properties.

Sensitivity studies began with three-dimensional reservoir simulation of a depleted petroleum reservoir in which a planer fracture connected a channel sand to an upper blanket sand. The reservoir parameters were used as a basis for simulation of time-lapse monitoring of surface and crosswell seismic, crosswell electromagnetic, and surface and borehole gravity.

Preliminary conclusions are that: (1) The presence of the leaking fault is indicated in the crosswell seismic tomographic models (although resolution is poor). (2) Surface seismic data provides a reasonable estimate of the position of the leaking fault, but no indication as to whether the fault is open or sealed. (3) When the fault location from surface seismic is used to constrain the crosswell electromagnetic imaging, the water content in the fault can be inferred indicating the presence of the leak.

The objective of the laboratory measurements is to obtain concurrent seismic and electrical properties of rock under reservoir conditions containing CO_2, brine, and oil. The first task was to assemble apparatus, which required modification of a test cell and fabrication of transducers. Samples 1.5 inches in diameter by 3 inches long are tested. Samples are placed in a rubber jacket containing electrodes used for electrical measurements. Seismic transducers were built which contain compressional and polarized shear wave elements with 1 MHz resonant frequencies. Pore fluids pass through the transducers into the core. An aluminum test vessel was employed so that x-ray computerized tomography (CT) imaging could be performed while the sample was under test conditions. The testing program is planned for FY2001.

Capacity Assessment

A preliminary sequestration assessment has been conducted for the State of California. Electricity generation in California results in emissions of about 60 megatonnes of CO_2 annually. Options for sequestration in California include oil, gas, and brine formations. Preliminary assessment indicates that on-shore gas fields and oil fields could each sequester from 40% to 60% of the CO_2 generated annually. Based on previously produced volumes of oil and gas, 30 and 60 years, respectively, of capacity are available. Brine formations suitable for sequestration are located in California's Central and Imperial Valleys. Several hundreds of years of sequestration capacity are available in the Central Valley alone.

Publications

S.M. Benson, "Comparison of Three Options for Geologic Sequestration of CO_2: A Case Study for California," *Proc. Fifth International Conference on Greenhouse Gas Control Technologies*, Cairns, Australia (August 13-16, 2000).

S.M. Benson and L. R. Myer, "The GEO-SEQ Project," *Proc. Fifth International Conference on Greenhouse Gas Control Technologies*, Cairns, Australia (August 13-16, 2000).

G.M. Hoversten and L.R. Myer, "Monitoring of CO_2 Sequestration Using Integrated Geophysical and Reservoir Data," *Proc. Fifth International Conference on Greenhouse Gas Control Technologies*, Cairns, Australia (August 13-16, 2000).

L.R. Myer, "A Strategy for Monitoring of Geologic Sequestration of CO_2," *ENERGEX'2000: Proceedings of the 8th International Energy Forum*, Las Vegas, pp. 1226-1231 (July 23-28, 2000).

C.M. Oldenburg, K. Pruess, and S.M. Benson, "Process Modeling of CO_2 Injection into Natural Gas Reservoirs for Carbon Sequestration and Enhanced Gas Recovery," *Proc. of the 220th National Meeting of the ACS, Washington D.C.*, **Vol.** 45, No. 4, pp 726-729.

Extended abstract, *Energy & Fuels* (August 20-24, 2000).

Ocean Particulate Carbon Dynamics

Principal Investigators: Jim Bishop

Project No.: 98035

Project Description

There is an urgent need to devise strategies to stabilize the levels of carbon dioxide in the atmosphere. The purpose of this project is to carry out fundamental research into the dynamics of particulate carbon off the coast of California and in the world's oceans. The sedimentation of particulate organic carbon is the ultimate burial of atmospheric carbon, but particulate carbon dynamics is not well understood because of the difficulty and exorbitance of direct high-precision measurements of trace constituents in the water column. This project seeks to explore the development of an economical autonomous device that profiles particulate organic carbon (POC) and particulate inorganic carbon (PIC) concentrations in the water column on time scales fast enough (~diurnal) to capture biological variability. Biological formation of PIC produces carbon dioxide as a byproduct and therefore counteracts the carbon dioxide drawdown due to formation of POC. The device and sensors will be inexpensive enough to permit the first large-scale quantification of the geographic and temporal distribution of POC and PIC. We will also study existing samples of particulate matter collected by large-volume, *in-situ* filtration from the North Pacific and other environments, and analyze them for compositional information that may yield insight into the processes of formation and removal of particulate organic and inorganic carbon.

Accomplishments

Our approach to understanding ocean particulate carbon dynamics will enable and refine strategies to meet targets for stabilizing carbon dioxide in the atmosphere. LDRD support in FY2000 initiated three activities in the area of ocean carbon cycle research at Berkeley Lab: selection/development of autonomous vehicles for carbon system monitoring; development of PIC and POC concentration sensors for the vehicles; data/sample analysis, synthesis, and publication. All activities strongly tie to the vision of the original LDRD proposal and Berkeley Lab now has several funded projects springing from LDRD support.

Specific accomplishments were:

- The Sounding Oceanographic Lagrangian Observer (SOLO) was selected as the autonomous vehicle for testing our carbon sensors. Developed at Scripps Institution of Oceanography (SIO), SOLO is capable of autonomously making 150 round trips between the surface and 1000 meters. Satellite telemetry of data after each surfacing permits real-time observational data to be obtained from remote locations. With twice-a-day profiling, SOLO can observe ocean carbon biomass variability for four months. The first POC concentration profile was obtained using SOLO in California coastal waters late last year (Figure 1).
- Our laboratory work has demonstrated that we can precisely and accurately measure particulate inorganic carbon (PIC) optically over the entire PIC concentration range in the oceans. A patent disclosure describing the PIC sensor concept was filed. The PIC sensor will be tested at sea in early 2001 in a follow-on effort.
- LDRD support has enabled the preliminary design of an autonomously operating POC and PIC flux monitoring device that can interface to SOLO floats.
- We participated in test deployments of the autonomously navigated miniature submarine glider "Spray" in the California coastal waters. Spray (also developed at SIO and Woods Hole Oceanographic Institution) is capable of 600 profiles to 1000 meters, for example providing twice-daily sampling for 10 months. Spray can navigate against currents and will be particularly useful for work in coastal waters. Furthermore, it shows great promise for monitoring the carbon cycle response to purposeful ocean carbon sequestration field experiments. We are developing carbon sensor strategies that are compatible with Spray's hydrodynamic shape.

LDRD continued to support the synthesis of data and samples on particulate matter dynamics obtained during four recent oceanographic cruises to the subarctic northeastern Pacific Ocean. Six publications and five conference proceedings abstracts related to this work appeared in 1999. We also contributed to an in-press paper on the supply and demand of iron to the global ocean.

In addition, LDRD supported research led to the establishment of the Department of Energy Center for Research on Ocean Carbon Sequestration (DOCS). This national center, co-located at Berkeley and Livermore Labs is investigating environmental acceptability and effectiveness of different ocean carbon sequestration strategies. Berkeley Lab's emphasis is on understanding carbon cycle dynamics and on carbon cycle perturbations resulting from ocean fertilization with iron.

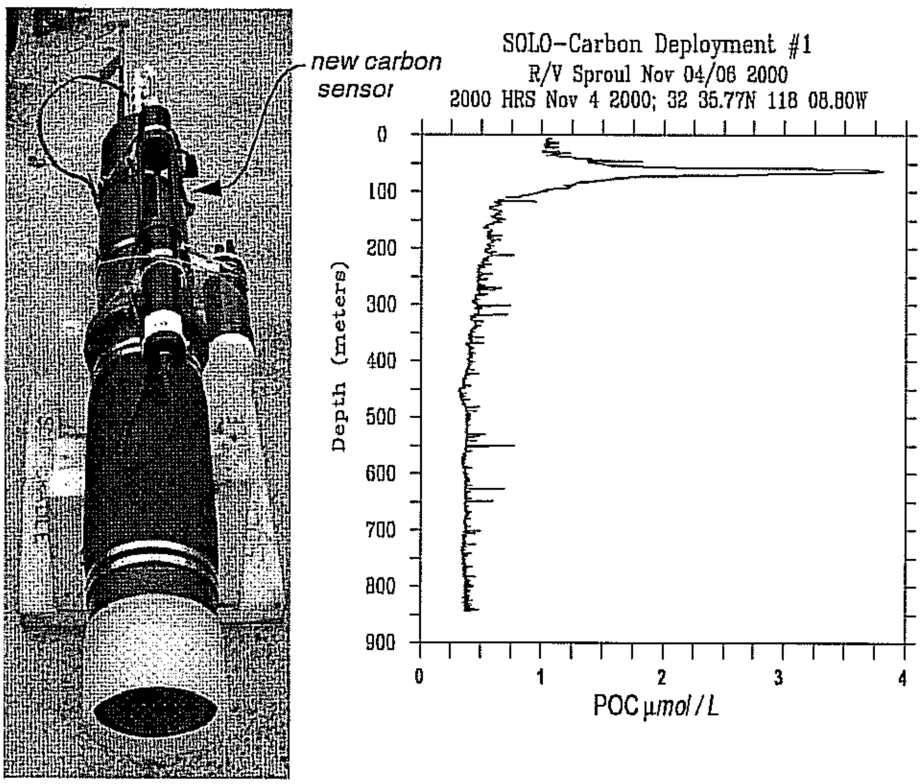

Figure 1: Left: Sounding Oceanographic Lagrangian Observer (SOLO) with attached POC sensor prior to deployment at sea Nov 4 2000. The SOLO, developed at SIO is shown configured to measure temperature and salinity. Right: Particulate Organic Carbon (POC) concentration profile recorded autonomously by SOLO.

Publications

I.Y. Fung, S.K. Meyn, I. Tegen, S.C. Doney, J.G. John, and J. K. B. Bishop, "Iron Supply and Demand in the Upper Ocean," *Global Biogeochemical Cycles* V14(N1):281-295 (2000).

J.K.B. Bishop and R.E. Davis, "Autonomous Observing Strategies for the Ocean Carbon Cycle," In ENERGY 2000, The Beginning of a New Millennium. Eds. P. Catania, B. Golchert, C. Zhou, Publ. Balaban International Science Services, L'Aquila, Italy. (2000) pp 1256-1261. ISBN 1-58716-016-1.

C.K. Guay and J.K.B. Bishop, "A Rapid Birefringence Method for Measuring Suspended $CaCO_3$ Concentrations in Water," *Deep-Sea Research* (in revision).

J.K.B. Bishop, "Prospects for a C Argo," *EOS, Trans. Am. Geophys. Union* 81 (48) (2000) OS62-D02, F660.

J.K.B. Bishop and K. Caldeira, "Purposeful Ocean Carbon Sequestration: Science and Issues," *EOS, Trans. Am. Geophys. Union.* 81 (48) (2000) B11-D02, F245.

C.K. Guay and J.K.B. Bishop, "A Rapid Birefringence Method for Measuring Suspended $CaCO_3$ Concentrations in Seawater," *EOS, Trans. Am. Geophys. Union* 81 (48) (2000) OS71-B01, F669.

C.K. Guay and J.K.B. Bishop, "A Rapid Birefringence Method for Measuring Suspended $CaCO_3$ Concentrations in Seawater," Ocean Optics XV, Monaco. (October 16-20, 2000).

Carbon-Climate Interactions

Principal Investigators: Inez Fung, Horst Simon, and Jim Bishop

Project No.: 00009

Project Description

Until now, climate model experiments have not accounted for feedbacks of the terrestrial and oceanic systems on the CO_2 growth rate, or feedbacks between plant uptake of CO_2 and transpiration of water or climate warming. The goal of this work is:

- To define the paradigm for investigating the co-evolution of $C0_2$, water, and climate,
- To advance the scientific understanding of how the climate system determines and responds to the rate of $C0_2$ increase in the atmosphere, and how the water cycle magnifies the $C0_2$ forcing, and
- To advance the scientific understanding of how climate change may alter the stability and efficacy of carbon sequestration.

To accomplish this, the project will do the following:

- A series of numerical experiments will be carried out at NERSC using the NCAR Community Climate System Model (CCSM). Active collaboration will be maintained with the NCAR CCSM group to take advantage of the cutting-edge model developed by the community effort. Senior consultants will be enlisted to participate in the experimental design and output analysis, and to link the Berkeley Lab effort to national and international programs and initiatives.
- Carbon isotopes will be implemented in the CCSM as additional diagnostics on the present-day simulations of the global carbon cycles.
- Water isotopes will be implemented in the CCSM as additional diagnostics on the water and carbon cycles.
- Analyses of the carbon and water isotope simulations will guide the development of an observational strategy.

Accomplishments

We have implemented the NCAR Community Climate Model (CCSM) at NERSC, and in the past year continued development of the CCSM to include an interactive carbon cycle. The CCSM is a physical climate model with the atmosphere, land, ocean, and ice components exchanging energy, momentum, and water. It has been widely applied to study climate change as a result of externally specified changes in atmospheric composition and/or surface boundary conditions.

Model development has focused on expanding the capability of the CCSM in biogeochemistry, so that atmospheric composition and boundary conditions are "internal" prognostic components of the model. This way, compositional changes would be interactive with the climate change. Firstly, we added a CO_2 tracer (in addition to the radiatively active CO_2) in the atmosphere of the coupled CCSM. This means that the three-dimensional distribution of CO_2 can be simulated as long as the source/sink functions are specified or calculated. This was validated by the simulation of CO_2/SF_6 distributions resulting from industrial emissions. Secondly, we have coupled the NCAR ocean carbon model into the CCSM, and have successfully initiated a CCSM experiment in which the air-sea exchange of CO_2—and hence the atmospheric and oceanic carbon distributions—are interactive with the climate of the coupled system. The experiment was initialized with an atmospheric CO_2 concentration of 280 ppmv—that of the pre-industrial Holocene—and is ongoing. We expect a spin-up of 500+ years.

Research into the processes of the carbon cycle has continued using atmospheric and/or oceanic circulation models separately and together. It is assumed that the biogeochemistry is influenced by the climate and not vice-versa. A first investigation is iron cycling in the upper ocean and its relationship to marine productivity and atmospheric CO_2 levels. We adapted our three-dimensional model of dust cycle—with uplift from arid lands, transport through the atmosphere, and wet and dry deposition—to simulate the aeolian source of iron to the oceans. The aeolian deposition was combined with an ocean model simulation of upwelling to yield the supply of iron to the upper ocean. The demand was estimated from satellite observations of marine productivity. The study revealed our general ignorance about the speciation, status, and fate of iron in soils and in the ocean, and posed a research agenda for improving our understanding. More importantly, our study shows that oceanic areas whose productivity is limited by iron availability are also areas in which the available nitrogen is not recycled efficiently to support the production. This finding links for the first time iron stress to nitrogen-use efficiency and introduces a new metric to quantify the potential for iron fertilization of marine productivity.

We have also investigated the atmospheric CO_2 distribution in the pre-industrial Holocene using the 3-D atmospheric and oceanic general circulation models. In the NCAR ocean carbon simulation of the pre-industrial era, the conveyor belt in the ocean transports carbon out of the North Atlantic and ultimately into the North Pacific, with near-zero net oceanic carbon transport across the equator. The resultant surface ocean carbon distribution leads, in our atmospheric simulation, to a near-neutral atmospheric CO_2 gradient in the north-south. In the east-west, however, our model yields an atmospheric CO_2 that is lower over the North Atlantic than over the North Pacific. This finding has tremendous significance for the inference of the North America-Eurasia partitioning of the contemporary carbon sink. Atmospheric CO_2 observations show a lowering over the North Atlantic 0.5 ppmv greater than that over the North Pacific. Our results show that the conveyor belt transport (plus the North Atlantic uptake of anthropogenic CO_2) predisposes the east-west gradient to that observed. This suggests that the east-west atmospheric CO_2 difference between the North Atlantic and North Pacific is not, by itself, a strong constraint on the continental distribution of the terrestrial carbon sink. Resolution of this carbon sink partitioning will require an augmentation of the atmospheric monitoring—especially over continental regions—and the use of carbon isotopes and other compounds as additional constraints in the problem.

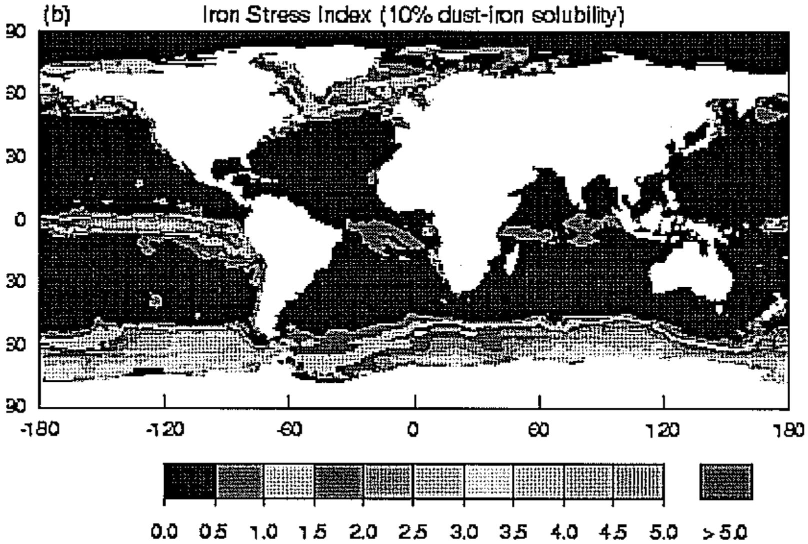

Figure 2: The iron stress index is the (Fe:N) in photoplankton relative to the (Fe:N) in upwelling and Aeolian deposition. High values of the iron stress index indicate recycling efficiency of Fe relative to N to support the production. The areas of high iron stress index are areas where addition of Fe may stimulate marine productivity. (Taken from Fung et al., Global Biogeochem. Cycles, 2000.)

Publications

I. Fung, "Variable Carbon Sinks," *Science* **290**: 1313. (2000).

G.J. Collatz, L. Bounoa, S. Los, D.A. Randall, I. Fung, and P.J. Sellers, "A Mechanism for the Influence of Vegetation on the Response of the Diurnal Temperature Range to Changing Climate," *Geophys. Res. Lett.* **27**: 3381-3384, (2000).

I. Fung, S. Meyn, I. Tegen, S.C. Doney, J. John, and J.K.B. Bishop, "Iron Supply and Demand in the Upper Ocean," *Global Biogeochem. Cycles:* **14**: 281-296 (2000).

Publications available at :
http://www.atmos.berkeley.edu/~inez/#pubs

Aerobic Bioremediation of Landfills

Principal Investigators: Terry Hazen, Curtis Oldenburg, Sharon Borglin, and Peter Zawislanski

Project No.: 00010

Project Description

The purpose of this research is to demonstrate and model aerobic bioremediation of municipal solid landfills as a more cost effective and environmentally sound way of managing municipal solid waste. This work is applicable not only to municipal solid waste, but also to remediation of solid waste landfills created by industry and the industrial processes of Department of Energy (DOE) and Department of Defense (DOD). The goals are to determine the critical biological and chemical parameters that control the ability of air injection and leachate recirculation in landfills to: (1) increase the biodegradation rate of the refuse mass, (2) decrease production of greenhouse gases (CH_4), (3) regulate biogenic temperature, (4) reduce metals leaching, (5) increase short-term subsidence, and (6) increase the long-term stability of the refuse mass. An increased subsidence of only 15% could translate to over $1 billion in additional revenues for the 3500 landfills currently in operation in the United States.

Using data collected over the last year from a demonstration conducted at the Columbia County, Georgia, Landfill, and a literature evaluation, critical biological, physical, and chemical parameters have been identified during the first year of the project. These potentially controlling parameters will be tested in the laboratory at Berkeley Lab using landfill simulation columns. The columns will be tested using various types of compaction, air injection strategies and rates, and leachate recirculation strategies and rates. During the first year, the landfill columns were designed and constructed and testing should begin shortly. The tests will be evaluated in relationship to the six goals stated above. These tests will be used to develop a numerical simulation model of aerobic bioremediation of landfills, building on the TOUGH2 code of Berkeley Lab. This approach will then be field demonstrated in the more arid environments at California municipal landfills and western DOE sites. Both the Yolo County and University of California at Davis landfills have been contacted.

Accomplishments

During the first six months, we conducted an extensive literature review on aerobic landfill bioremediation. The literature review was used to definitively establish the state of the science and what critical parameters would need to be monitored in the landfill column simulations, the model, and the field studies. We have a proposed model and have begun developing it. This TOUGH2 model will be oxygen limited and contains the following chemical components: water, acetic acid, carbon dioxide, methane, air (proxy for oxygen and nitrogen), and heat. The critical reactions have been determined to be: hydrolysis [creation of acetic acid from reaction of raw waste (e.g. cellulose)] using GENER; and biodegradation (aerobic or anaerobic), including a number of kinetic equations. (Note: biomass will be monitored but will not be part of the TOUGH2 mass balance.) The model will also take into consideration coupling of all kinetics with substrate and heat transfer by adding biogenic heat formation terms to TOUGH2. We have designed and constructed a Plexiglas chamber to simulate the landfill. We have three of these set up in Building 70A. All three have been operational since July and are generating data that we can use to start testing our draft model. We have also made contact with the landfill operators at Yolo County Landfill. This landfill has been testing innovative designs and is interested in using the aerobic landfill concept. They have agreed that we can collect samples at their sites and may be willing to set up a field demonstration in collaboration with us.

In more detail, this study consists of laboratory experiments on the biodegradation of municipal landfill materials. Three 55-gallon clear acrylic tanks have been fitted with pressure transducers, thermistors, neutron-probe access tubes, and leachate and air injection and collection ports. Air can be injected into the bottom of the tanks, and gas vented out the top. Gas compositions are monitored at the top of the tanks. Leachate can be collected at the bottom of the tanks, recirculated, and sprinkled over the top of the refuse. The neutron probe is used to estimate average moisture content of the refuse. The tanks contain 10 cm of pea gravel at the bottom, overlain by a mixture of fresh waste materials consisting of (by weight): 24% dry paper, 11% fresh food waste, 7% metal (5% steel, 2% aluminum), 8% glass, 7% plastic, 8% garden waste, 24% soil, and 11% miscellaneous building materials and wood. The materials were crushed, chipped, and broken into pieces approximately 5 to 10 cm in size to simulate actual landfill materials. Three different treatments are being applied to the tanks: (a) air injection with leachate recirculation and venting from the top, referred to as Tank A; (b) a sealed system with gas venting from the top, referred to as Tank B; and (c) an air-sealed system with leachate recirculation with venting from the top, referred to as Tank C. Tank A is an aerobic system while Tank B and C are anaerobic. Tank A and Tank C absorbed 5 to 10 kg of water sprinkled on the top before producing leachate. This water is assumed to have been absorbed mostly by the paper, which appears wet when viewed through the clear walls of the tank. We have observed rises in temperature and changes in gas composition in Tank A consistent with rapid aerobic biodegradation. The temperature in Tank A increased to 30°C upon initial air injection at a rate of 3 L/min. In the following ten days, the temperature decreased to approximately 20°C as additional water and air were injected. The tanks are partially insulated but temperature trends have largely paralleled the diurnal temperature variations in the laboratory. A shut-in experiment was conducted in Tank A by stopping the air injection and leachate recirculation while allowing leachate to continue to drip from the bottom of the tank. The gas venting from the top became depleted in O_2 in one day, and CO_2 concentrations increased from 1% to 21%. Temperatures in the tank increased as the cooling effects of the air and water injection stopped. Ongoing work will focus on identifying optimal moisture contents and air injection rates for enhancing the aerobic biodegradation of landfill materials.

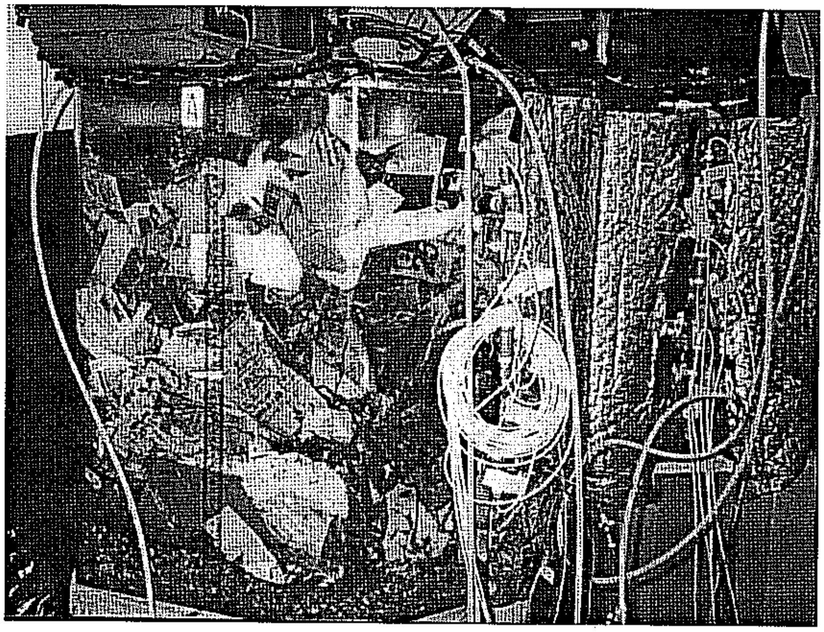

Figure 3: Fully instrumented aerobic refuse bioreactor in 55-gallon Plexiglas vessels can measure moisture, oxygen, carbon dioxide, methane, temperature, and moisture continuously.

Publications

T. C. Hazen, "Aerated Landfills," presented at Annual Meeting of the Society of Industrial Microbiology (July 2000), abstract published.

T. C. Hazen, "Aerobic Landfill Bioreactors," presented at Prague 2000, Fifth International Symposium and Exhibition on Environmental Contamination in Central and Eastern Europe, Environmental Issues in Central and Eastern Europe (September 2000), abstract published.

T. C. Hazen, "*In Situ* Bioremediation of Solvent Contaminated Sites Using Gaseous Nutrient Injection," presented at Department of Biology, Chico State University (October 2000), abstract distributed at University.

T. C. Hazen, "Aerobic Landfills: Changing the Subtitle D 'Dry Tomb' Paradigm," presented at New Mexico Environmental Health Conference (October 2000), abstract published.

T. C. Hazen, "Aerobic Bioremediation of Landfills: Changing the 'Dry Tomb' Paradigm," presented at Environmental and Water Resources Engineering Series, University of California at Davis (October 2000), abstract distributed at University.

Effects of $2xCO_2$ Climate Forcing on the Western U.S. Hydroclimate using the High-Performance Regional Climate System Model

Principal Investigators: Jinwon Kim, Norman L. Miller, and Chris Ding

Project No.: 99015

Project Description

Understanding the impacts of increased atmospheric CO_2 concentration on the regional climate, water resources, and socioeconomics is a growing concern (*Kyoto Protocol* 1997). The goal of this project is to study the climate and water resources in the western U.S. under a doubled carbon dioxide ($2xCO_2$) condition using recent General Circulation Model (GCM) projections as input to a high-performance Regional Climate System Model (RCSM.hp). Detailed objectives include: (1) investigate the effects of $2xCO_2$ on the climate and water resources in the western U.S., (2) examine the Sensitivity Imposition Method (SIM) for downscaling GCM ensemble predictions, (3) contribute to the Intergovernmental Panel on Climate Change (IPCC) 2000 Regional Assessment Report and the U.S. National Assessment, and (4) develop the RCSM.hp.

We will investigate the effects of $2xCO_2$ on the western U.S. climate using the RCSM.hp to downscale global climate data for the present-day and GCM-projected $2xCO_2$ scenarios. The RCSM has been used in climate studies for the western U.S., eastern Asia, and northeast Australia with good results. We will calculate the regional climate sensitivity from the National Center for Environmental Prediction (NCEP) reanalysis (control simulation) and a $2xCO_2$ climate projection from the Hadley Centre (sensitivity simulation). The sensitivity run will be made by modifying the present-day temperature and water vapor fields by the amount projected by the GCM. We will focus on precipitation, snow, soil moisture, and basin-scale hydrology for water-resource assessments. Development of the high-performance RCSM is a crucial part of this project, as climate simulations require a large amount of computational resources. A message-passing method will be used for efficiency and portability across a variety of high-performance computing platforms. New techniques will be used to match cache-based processor architectures. Efficient schemes to improve data input and output will be developed.

Accomplishments

A prototype high performance version of the Mesoscale Atmospheric Simulation (MAS) has been developed and tested. Due to the limited size of the model domain (160x120), scalability tests were performed up to 96 SP3 processors. Initial tests of the prototype model show good scalability. Even with relatively small domain size, performance of the model continued to increase with increasing number of processors. With a successful development of the prototype version, the next step is to improve the load balance of the model and to incorporate advanced model formulations developed in parallel with the development of the high performance version.

We have completed four multi-year regional climate simulations for the western U.S. during the project period. The climate simulations completed in this project include a multi-year regional climate hindcast for 1988-1995 and a five-year simulation of $2xCO_2$ climate using the SIM method. We also performed two ten-year simulations in which scenarios representing today's climate and a projected $2xCO_2$ climate for the years 2040 to 2049, are produced by directly downscaling the global data from the Hadley Center GCM2 (HadCM2). Based on the downscaled regional climate data, we have completed initial projection of precipitation, temperature, and streamflow for $2xCO_2$ climate.

In an eight-year regional climate hindcast, in which the large-scale forcing was obtained from the NCEP-NCAR reanalysis, the MAS model showed good skill in simulating the hydrologic cycle of the western U.S. The simulated precipitation is in good agreement with observations throughout the eight-year period. Other variables (e.g., low-level air temperature, upper-level geopotential fields, winds) are also close to observations and analysis. The simulated short- and longwave budgets showed a systematic bias when compared to a large-scale analysis of satellite observed values. The bias, however, is small and systematic. This suggests that the MAS can generate climate sensitivity consistent with the changes in the global scenarios. In the $2xCO_2$ climate experiments, the MAS has predicted that there is a strong possibility for extreme events to increase in California, especially during winter seasons. The prediction suggests a significant increase of wintertime precipitation in Washington, Oregon, and California, decrease (increase) of wintertime snowfall (rainfall), and early snowmelt in the spring. Effects on summertime climate are relatively small, but summertime precipitation may decrease in a part of the southwestern U.S.

Our hydrologic investigation has been focused on simulating stream flow of major river basins in California. In collaboration with the National Oceanic and Atmospheric Administration /National Weather Service

California-Nevada River Forecast Center (CNRFC), and the Scripps Institution of Oceanography (SIO) at University of California at San Diego, we have prepared the Sacramento Model (CNRFC), the Precipitation-Runoff Modeling System (PRMS) (U.S. Geological Survey and SIO), and the TOPMODEL (Berkeley Lab) for stream flow simulations in eleven river basins in California. Using the forcing generated in the regional climate hindcast and forecasts, we have investigated the stream flow climatology, and the effects of $2xCO_2$ on stream flow in major river basins. The early results suggest a significant increase of wintertime precipitation and streamflow in California, and reduced streamflow in spring and early summer, especially in the high elevation basins. Predictions from both the MAS and stream flow models suggest increased chance of wintertime flooding and reduced water resources in the summertime in Sierra-Nevada basins.

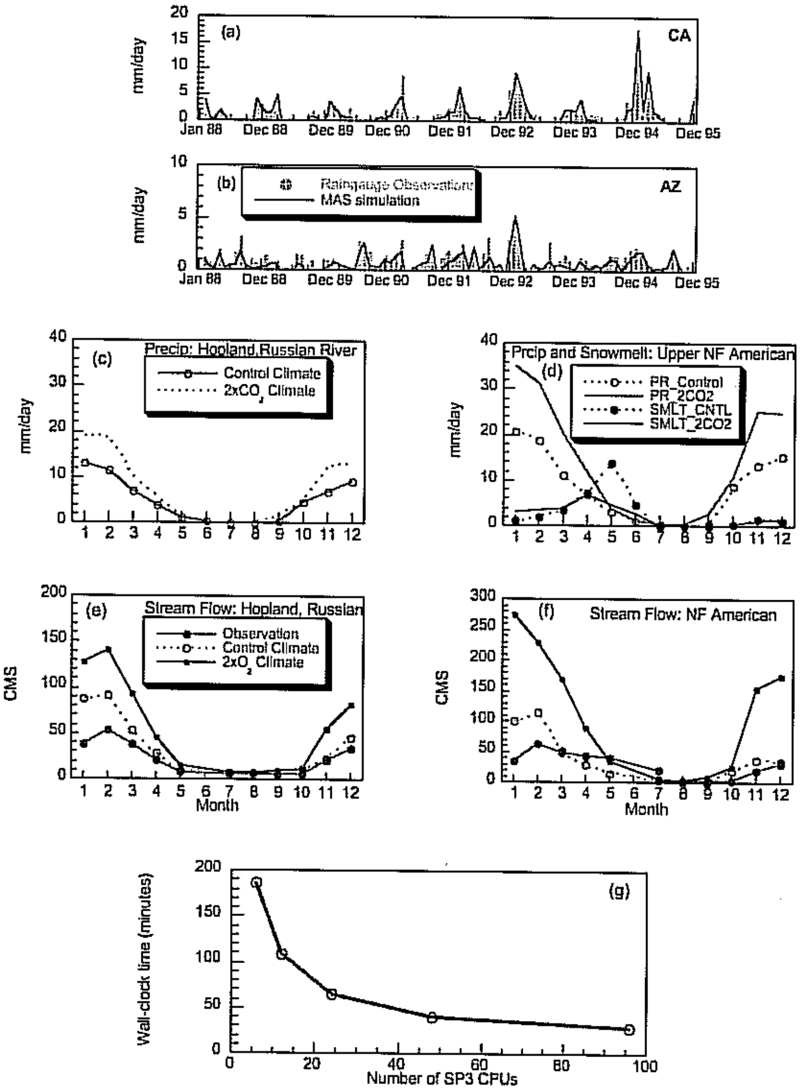

Figure 4: Regional Climate Simulations:(a) Simulated and observed monthly precipitation in California for 1988-1995. (b) Same as (a), but in Arizona. (c) Simulated precipitation in the Hopland basin under today's and $2xCO_2$ climate regimes. The large-scale forcing is from the Hadley Centre GCM 2 (HadCM2). (d) Same as (c), but in the Upper North Fork American River. (e) Effects of $2xCO_2$ on the stream flow in the Hopland basin. (f) Same as (e), but in the North Fork American River. (g) Speed-up of the high performance version MAS model in the IBM SP3.

Publications

J. Kim, N.L. Miller, J.D. Farrara, and S.-Y. Hong, "A Seasonal Precipitation and Stream Flow Hindcast and Prediction Study in the Western United States during the 1997/98 Winter Season using a Dynamic Downscaling System.," *Journal of Hydrometeorology* (August 2000).

J. Kim, J.-E. Lee, and N.L. Miller, "A Multi-year Regional Climate Simulation for the Western United States using the Mesoscale Atmospheric Simulation Model," *Journal of Geophysical Research-Atmosphere* (July, 2000) (accepted with minor revisions).

J. Kim, N.L. Miller, T.-K. Kim, R. Arritt, W. Gutowski, Z. Pan, and E.S. Takle, "Downscaled Climate Change Scenario for the Western U.S. using MAS-SPS Model," to appear in *Proceedings of the 12th Symposium on Global Change and Climate Variation, Amer. Meteorol. Soc. Annual Meeting, January 14-19, 2001 Albuquerque, New Mexico* (January 2001).

N.L. Miller, J. Kim, R.K. Hartman, and J.D. Farrara, "Downscaled Climate and Streamflow Study of the Southwestern United States," *Journal of American Water Resources Association* (1999).

N.L. Miller and J. Kim, "Climate Change Sensitivity for Two California Watersheds: Addendum to Downscaled Climate and Streamflow Study of the Southwestern United States," *Journal of American Water Resources Association* (2000).

N.L. Miller, W.J. Gutowski Jr., E. Strem, R. Hartman, Z. Pan, J. Kim, R.W. Arritt, and E.S. Takle, "Assessing California Stream Flow under Present Day and a Climate Change Scenario," to appear in *Proceedings of Climate Variability, the Oceans, and Societal Impacts, Amer. Meteorol. Soc. Annual Meeting,* January 14-19, 2001, Albuquerque, New Mexico.

Isotopic Analysis of Carbon Sequestration in Terrestrial Ecosystems and Global Change Impacts

Principal Investigators: Margaret Torn

Project No.: 00011

Project Description

This is a project to develop advanced isotopic techniques to quantify carbon fluxes and storage in terrestrial ecosystems, and apply them to a California global change experiment. Field experiments combined with measurements of ^{13}C and ^{14}C will be used to study soil respiration, decomposition, and long-term carbon stabilization. The primary research questions are: (1) How do changes in climate and nutrients influence carbon loss through respiration by plants and microbes? and (2) How does soil mineralogy influence the response of soils to global change and their capacity to stabilize organic carbon for long-term storage? The research will be expanded to address the question: (3) How do changes in climate and nutrients influence microbial communities and the pools of carbon available for decomposition by different microbial communities?

The approach employs specialized field sampling and rapid, automated isotope analysis being developed under the LDRD project. The Jasper Ridge Global Change field experiment, in an annual grassland, is the first to address the integrated suite of environmental changes predicted to occur over the coming decades: elevated $C0_2$, warming, increased rainfall, and nitrogen fertilization. The elevated $C0_2$ creates isotopically labelled plant material that is used to quantify carbon fluxes and sources. The isotopic content of soil respiration, soil gas, and dissolved inorganic carbon are used to estimate the relative contribution to effluxes from recent plant photosynthate vs. decomposition of older soil organic matter. The influence of soil mineralogy on sandstone and serpentine soils is being tested by analyzing physically (density) fractionated soil for carbon and carbon isotopic content. This approach amplifies the signal of changes in carbon stocks and of mineral associations.

Accomplishments

In the first year, we developed the field collection and automated analysis system for isotopic analysis of replicated ecological samples. System performance is described in a manuscript in preparation. Application of this system at Jasper Ridge was successful; preliminary results were presented at several meetings and are described briefly below.

The isotopic content of soil respiration is being used to distinguish sources of CO_2 flux, from root respiration, exudates, and soil organic matter. At the end of the first experimental growing season (May 1999), approximately 70% of respiration derived from root respiration and 30% from microbial decomposition. At the beginning of the second growing season (October 1999), before roots had begun to grow, we partitioned sources of microbial respiration as 55% to 70% from the first year's photosynthesis and the remainder from older soil organic matter. Treatments receiving nitrogen had higher root inputs, higher rates of respiration, and a greater proportion of new carbon in respiration. Thus, we were able to document that although nitrogen treatments increased plant carbon inputs, nitrogen treatments also had higher carbon losses—indicating that there might be limited carbon gains from fertilization in this grassland. Preliminary analysis of soil leachate indicates that the warming treatment increased the contribution of roots to dissolved inorganic carbon losses from soil. This is the first *in situ* experimental test of the influence of these environmental factors on root carbon cycling in either respiration or leachate.

In the soil organic matter study, the light (labile) fraction showed a detectable increase in soil carbon ($p<0.031$, $n=10$) in the elevated CO_2 treatment. The ^{13}C isotopic analysis confirmed that the light fraction was new carbon, and that the heavy fraction contains more of the older (i.e., more stable) mineral-associated carbon. The ^{14}C content of heavy fraction carbon from sandstone and serpentine soils was used to estimate the turnover times of mineral-stabilized carbon on these soil types, and thus their capacity to stabilize organic carbon for long-term storage (Torn, *et al.* 1999). The turnover time of mineral stabilized organic carbon in the top 15cm of soil is 270 years in sandstone and 450 years in serpentine.

Publications

S. Davis, M.S. Torn, M.R. Shaw, and M.E. Conrad, "Automated Analysis of $^{13}C/^{12}C$ in Soil CO_2 and Dissolved Inorganic Carbon," *Soil Biology and Biochemistry* (draft in preparation).

E.S. Zavaleta, M.S. Torn, and C.B. Field, "Storage of Soil Carbon Due to Elevated CO_2 Detected by Stable Isotope Analysis," *Biogeochemistry*.

M.S. Torn and J. Southon, "A New ^{13}C Correction for Radiocarbon Samples from Elevated-CO_2 Experiments," *Radiocarbon*, (accepted, in press).

M.S. Torn, E.S. Zavaleta, and C.B. Field, "Combining ^{14}C and ^{13}C Measurements to Quantify Changes in Soil Carbon Cycling in Elevated CO_2 experiments," paper presented at 17th Annual Radiocarbon Conference (2000).

M.S Torn, E.S. Zavaleta, and C.B. Field, "Quantifying Soil Carbon Dynamics with Carbon Isotope Tracers: Carbon Turnover in a California Grassland," Fall meeting and *EOS Bulletin of American Geophysical Union* (1999). (Paper presented and abstract published).

E.S. Zavaleta, M.S. Torn, and C.B. Field "Soil Carbon Responses to Elevated CO_2 in Two Annual Grassland Ecosystems: a Stable Isotope Approach," Fall meeting and *EOS Bulletin of American Geophysical Union* (1999) (paper presented and abstract published).

M.R. Shaw, M.S. Torn, and C.B. Field, "The Effects of Global Change on Belowground Carbon Storage: Under Elevated CO_2, increased N-deposition does not Lead to Increased C Storage in a California Grassland," presented at Fall meeting of the Ecological Society of America and abstract published in *Bulletin of the Ecological Society of America* (2000).

C.A. Masiello, M.S. Torn, J. Southon, and O.A. Chadwick, "Effects of Mineralogy on the Storage Rates of Organic Carbon Classes across a Soil Chronosequence," paper presented at 17th Annual Radiocarbon Conference (2000).

Development of the High-Performance TOUGH2 codes

Principal Investigators: Yu-Shu Wu, Karsten Pruess, and Chris Ding

Project No.: 99017

Project Description

TOUGH2, a general-purpose numerical simulation program for simulating flow and transport in porous and fractured geological media developed and maintained at Berkeley Lab, is now being used in over 150 organizations in more than 20 countries. The largest user community is within the U.S., where TOUGH2 is being applied to problems in geothermal reservoir engineering, environmental remediation, and nuclear waste isolation. TOUGH2 is one of the official codes selected by the Department of Energy (DOE) for its civilian nuclear waste management program to help evaluate the suitability of the Yucca Mountain site as a repository for nuclear wastes.

The largest and most demanding applications of TOUGH2 currently arise in the context of nuclear waste isolation work. Berkeley Lab is in charge of developing a three-dimensional (3-D), site-scale flow and transport model at the Yucca Mountain site for DOE. The model involves using unstructured computational grids of 100,000 blocks and more, and hundreds of thousands of coupled equations of water and gas flow, heat transfer, and radionuclide migration in subsurface. These large-scale simulations of highly-nonlinear multiphase flow and multicomponent transport problems are being run on workstations and PCs, and are reaching the limits of what can be accomplished on those platforms.

The purpose of this project is to explore whether TOUGH2 can be upgraded to take full advantage of modern supercomputing capabilities. This will be accomplished by the following steps:

(1) Analyze and restructure the TOUGH2 codes for implementing a parallel scheme.

(2) Develop a parallel scheme for partitioning grid blocks for processor sub-domains of simulated systems. This includes examining for load balance involving both the Jacobian matrix element calculations and the later linear equation solution. We also need to investigate the suitability of the Metis partitioner software and integrate it into the codes.

(3) Restructure the linear solver part to incorporate the AZTEC parallel solver into the codes, and investigate the solver suitability for large-scale problems.

(4) Enhance computational performance of TOUGH2 on the T3E, or on other multi-processor computers, by one-to-two orders-of-magnitude improvement, both in size of problems to be solved (up to 105 to 106 grid blocks) and in CPU time required.

(5) Create a TOUGH2 computing environment on the T3E, and make it available to the TOUGH2 user community worldwide.

Accomplishments

We have made continual progress in the parallel computing version of the TOUGH2 code, for significant improvement of both computing time and memory required for large-scale reservoir simulations. For a typical, large-scale, three-dimensional simulation, a minimum memory of several gigabytes is required, which is generally too large for a single processor to handle. Therefore, it is necessary to distribute the memory requirement to all processors. We have optimized the data input procedure and the efficient usage of the computer memory in the parallel code.

In addition, certain parts of the parallel code require full-connection information of grid blocks, which can cause a bottleneck of memory requirement when solving a large problem. We have implemented a new method to avoid the bottleneck and to make it possible to model a large-scale simulation problem using the parallel TOUGH2 code.

Other improvements include: optimization of local connection index searching; introduction of a 4-byte integer for index arrays to reduce the memory requirement; consideration of memory requirement balance between all processors; and enhancement of input and output (I/O) efficiency. In addition, several programs for input data preparation, data transformation, and domain partitioning have also been developed.

The parallel code has been successfully used to develop a 3-D model of two-phase fluid flow and heat flow in variably-saturated fractured rocks. The 3-D model uses 1,075,522 gridblocks and 4,047,209 connections to represent the unsaturated zone of the highly heterogeneous, fractured tuffs of Yucca Mountain, Nevada. This problem involves solving 3,226,566 linear equations at each Newton iteration step. Simulation results indicate that the developed code is a powerful reservoir simulator for large-scale problems with multi-million gridblocks. The major benefits of the code are that it: (1) allows accurate representation of reservoirs with sufficient resolution in space and time, (2) allows adequate description of reservoir heterogeneities, and (3) enhances the speed of simulation.

A user manual for using the developed parallel TOUGH2 code has been prepared. The code is ready for the worldwide TOUGH2 user community for large-scale (in the range of 106 gridblocks) reservoir simulations on the Cray T3E-900.

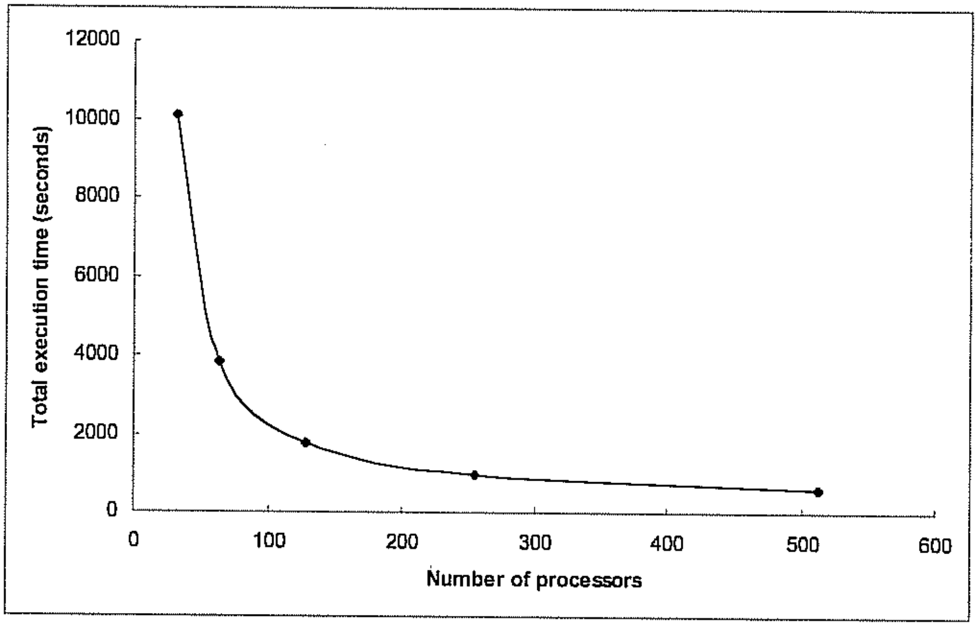

Figure 5: Reduction of execution time with the increase of processor number for a one million gridblock problem on Cray T3E-900.

Publications

K. Zhang, Y.S. Wu, C. Ding, K. Pruess, and E. Elmroth, "Parallel Computing Technique for Large-scale Reservoir Simulation of Multi-component and Multiphase Fluid Flow," accepted for Society of Petroleum Engineers 16th Reservoir Simulation Symposium (February11-14, 2001).

K. Zhang and Y.S. Wu, "Parallel Version TOUGH2 User's Guide," LBNL report (in preparation).

K. Zhang, Y.S. Wu, C. Ding, and K. Pruess, "Application of Parallel Computing Techniques to Large-scale Reservoir Simulation," accepted for Twenty-Sixth Workshop on Geothermal Reservoir Engineering (January 29-31, 2001).

Instrumentation for Sorting Individual DNA Molecules

Principal Investigators: Henry Benner

Project No.: 99018

Project Description

An ion detector recently developed at Berkeley Lab and implemented in a new type of mass spectrometer, provides a way to measure the mass of individual ions nondestructively on-the-fly. This proposal defines the design and fabrication of a new technique, based on this detector, to sort individual molecular ions according to their mass. The goal of the project is to evaluate how reliably individual ions can be sorted on demand.

To accomplish this, a charge detection mass spectrometer, developed and recently patented by Berkeley Lab, will be modified to release individual molecular ions into collection wells. Initial evaluation of the procedure will be conducted by attempting to sort large DNA molecular ions and fluorescently-labeled polystyrene latex (PSL) particles. Sorted molecular ions or charged PSL particles will be guided through an aperture and detected with a microchannel plate ion detector. Attempts will be made to collect sorted molecular ions or charged PSL particles on appropriate substrates and analyze them via secondary techniques, such as epi-fluorescence microscopy and electrospray ion mobility. The polymerase chain reaction replicates single target molecules and it may be possible to develop a single-molecule detection capability for confirming the sorting of single DNA molecules into a well in a microtiter plate.

The term sorting, as used in this proposal, is the process of isolating one molecule out of many by first performing a measurement on a single molecule and then either choosing or eliminating it according to a predetermined selection criterion. The technological basis supporting our attempt to develop an instrument to sort individual molecular ions derives from the recent invention of charge detection mass spectrometry (CDMS) at Berkeley Lab. The proposed technology relies on the nondestructive determination of the mass of individual ions as they fly through a small metal tube detector. The detector tube captures the image charge of passing ions. The approximately square-shaped image-charge output pulse has width proportional to ion velocity and amplitude proportional to ion charge. Ion mass is determined on-the-fly by software from these measurements and knowledge of ion energy. We propose to modify a charge detector and construct a capability to deflect ions, after measuring their mass, into collection wells. One application of this technology is to sort individual DNA molecules for the purpose of supplying a single copy template for amplification by polymerase chain reaction (PCR). The concept of sorting single molecules has been addressed previously in terms of sorting ions in solution, such as fluorescently labeled DNA ions, but has not been extended to gas-borne ions like those manipulated in the vacuum environment of a mass spectrometer. The approach we investigated is closely related in concept to fluorescent activated cell sorting but extends the concept to single ions.

Accomplishments

Our goal for the current year's work was to evaluate several ion optics designs for deflecting ions having a predetermined mass onto a prescribed collection substrate. We evaluated the system with DNA molecular ions or electrosprayed PSL particles because they carry a large number of charges and are readily detected and weighed by our charge detection scheme. In our system, DNA ions will be generated by electrospray, then weighed and gated into a collection well if they fall within a predetermined mass range.

We have two ways to measure the mass of ions with CDMS. We obtain the most precise measurements with a technique that relies on a matched pair of electrostatic ion mirrors to reflect ions back-and-forth through our image-charge detector tube. The reflections allow us to make multiple measurements of ion charge and velocity. This provides the highest precision for mass measurements. A less precise measurement is obtained by our one-pass method, which does not rely on the ion mirrors and thus produces one measurement of the ion. This latter measurement approach was used to evaluate the possibility for sorting because it can be operated to deliver many more ions to the sorting (deflection) electrodes.

We constructed a switched power supply to produce the necessary signals for deflecting individual ions or particles onto collection substrates. The system, shown in the attached figure, deflects single ions away from a beam of ions that pass through a detector tube. The current design of the charge detection electronics requires that ions with 250 eV/charge are produced by the electrospray source. This requirement is defined by the need to generate image charge signals with rise times on the order of a few microseconds. The highly charged megadalton DNA ions, which we generated, carry more than a thousand charges, and thus break apart when they hit a collection surface because their total energy is more than 250 keV. This impact-induced breakup complicated the use of single-molecule PCR analysis of deflected DNA molecules. It was nevertheless possible to detect DNA ions that were deflected onto collection surfaces using image-enhanced epi-fluorescent microscopy. Deflected DNA ions remained intact enough to be visualized after fluorescent staining as small dots when megadalton and larger DNA ions were collected on transparent substrates. The use of fluorescent staining to detect deflected DNA ions demonstrated proof-of-concept for sorting individual ions. The use of fluorescent staining to verify the collection of deflected DNA ions was extremely time consuming and did not provide a way to tune up the sorting system in real time. Therefore, most of the measurements that were made after the proof-of-concept were performed by either deflecting ions through an aperture—used to simulate a well in a microtiter plate, placed in front of a microchannel plate (MCP) ion detector—or by deflecting PSL particles onto a collection surface. With the apertured MCP detector, it was possible to characterize the sorting efficiency of the system and to evaluate several approaches for producing 'soft-landing' conditions for the ions so that they would not fragment upon impact. Deceleration ion optics, designed for this purpose using SIMION software, provide a way to focus and slow down deflected ions to velocities small enough to preclude fragmentation. The test results confirm that it is possible to sort single ions, providing they carry enough charge (> 250 charges) to be weighed by the CDMS technique.

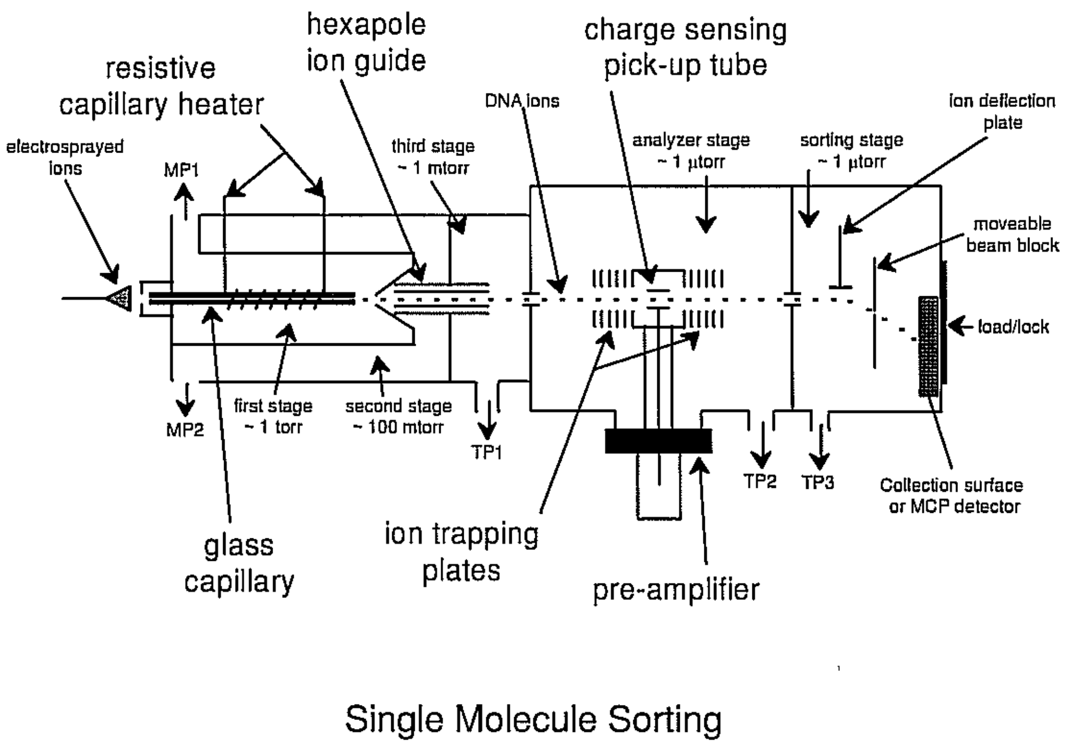

Figure 1: System used to demonstrate ion sorting.

Publications

W. H. Benner, G. Rose, E. Cornell and E. Jackson, "Mixtures of High Mass Electrospray Ions Analyzed with a Gated Electrostatic Ion Trap," *Proceedings of the 47th Am. Soc. Mass Spectrom. Conference On Mass Spectrometry and Allied Topics* (June 13-17, 1999).

W. H. Benner, Gated-Charged Particle Trap, U. S. Patent #5,880,466, (1999).

Transformation Pathways of Biogenic Organic Emissions in the Formation of Secondary Organic Aerosol

Principal Investigators: Melissa Lunden, Laurent Vuilleumier, Nancy Brown, and Mark Levine

Project No.: 00029

Project Description

The objective of this research project is to determine the chemical pathways by which biogenically-emitted organic vapors form secondary organic aerosol particles, as well as aerosol mass yields from these biogenic precursors. This will be achieved by conducting particle characterization measurements in concert with the measurement of gas phase biogenic emissions as a function of time at a site in the Sierra foothills.

Formation of secondary organic aerosols (SOA) is important because it has been estimated that SOA can contribute up to 50% of particle mass in urban areas. The contribution of SOA to particle mass in rural areas is not well characterized, but has been shown to be significant, for example, in the region surrounding Atlanta. Our knowledge of the chemistry of SOA formation is not well understood particularly in rural environments where the role of biogenic SOA formation is of greater importance. Secondary organic aerosols form when organic vapors emitted into the atmosphere are oxidized to produce less volatile products. These products then partition between the gas and particle phase. Much of the research on biogenic emissions has been performed in the Eastern and Southern United States. Research on SOA formation from biogenics is very sparse in general with very little occurring in the West and under actual field conditions. SOA production from a given volatile organic compound (VOC) depends on: (1) the abundance and reactivity of the given VOC compound; (2) the abundance of radicals in the atmosphere; (3) the nature of its reaction pathways; (4) the volatility and gas-to-particle partitioning properties of its products; (5) the ambient aerosol mass concentration; and (6) temperature.

The sets of experiments conducted are aerosol characterization studies in the ambient environment in the foothills of the Sierra. Fieldwork at the remote site includes measurements of total particle mass, total particle number, and particle size distribution as a function of time for a four-to-six-week period. Allen Goldstein and group, under sponsorship of the California Air Resources Board (CARB), are conducting measurements of the gas phase species that are emitted from biogenic sources, along with meteorological measurements. The research on aerosol characterization consists of five tasks: Task I: Plan particle characterization experiments in concert with those conducted for gas phase species. Task II: Assemble instrumentation for field study and render it field worthy. Task III: Develop sampling protocols for the entire measurement set. Task IV: Conduct particle characterization measurements in the field as a function of time. Task V: Analyze results. Two approaches that are being considered are the conduct of principal component and/or factor analysis to investigate correlations of particle loading characteristics and gas phase measurements. Our research will have as its product a completely unique set of measurements that describe SOA formation from the birth of precursor compounds resulting from emissions from biogenic sources, through various stages of chemical transformation and particle growth. These measurements, which are conducted using the atmosphere as a laboratory, offer the advantage of having all reactants present in realistic concentrations and reducing the role of artificial surfaces that often plague traditional smog chamber experiments. Our research provides data for determining aerosol yields, contributes to the understanding of the chemical steps involved in SOA formation, and provides critical understanding required for the modeling of SOA.

An additional component to this LDRD project involved research that adds the dimension of policy analysis to our air quality work, by addressing the issue of low-cost means of reducing air emissions in developing countries. This issue is one that is certain to be of increasing importance over the coming decades. It ties in extremely well with the international energy work of the Laboratory as well as being of interest to environmental policy staff of the Environmental Protection Agency (EPA) and the World Bank. The first step in the research was to review studies relevant to the overall problem of reducing environmental impacts of energy production, transport, and use in developing countries, and, in particular, methods of cost-benefit analysis of mitigation measures for prioritization of air pollution policy initiatives. The next step was to develop/modify a model that could be used to evaluate economic impact of air pollution from various energy sources used in different sectors, including both ambient and indoor pollution sources. We plan to perform one or more case studies, and assemble data to analyze the costs, benefits, and uncertainty of estimates, of different environmental damages. We will publish work to describe the nature of the problem in developing countries, including the need to more aggressively pursue relatively low-cost solutions. Finally, we will develop a design to extend the study to: one country in greater depth; to many countries to demonstrate the breadth of the issues; or to work with others, including researchers in developing countries, to refine and apply the methods demonstrated in the project.

Accomplishments

Aerosol Characterization

Progress was achieved on all five tasks of the proposal. A set of field experiments were planned in conjunction with research conducted on gas phase organic compounds (Task I). Aerosol measurements were performed at the University of California Blodgett Forest Research Station (Georgetown, California, 38°53'42.9"N, 120°37'57.9"W, 1315 meter elevation), which lies approximately 75 km northeast of Sacramento. The field site is located in a Ponderosa pine plantation that consists of evenly aged trees (6 to 8 years old) that were 3 to 5 meters tall. Local infrastructure consists of a 10-meter measurement tower, where sample inlets for all the relevant atmospheric measurements were located, and two enclosed buildings for storage of the gas phase analysis instrumentation, supplies, and data acquisition computers. Power is provided to the site by a 30 kW diesel generator located 130 meters northwest of the tower, as far outside of the major airflow paths as possible. Its presence has been shown to affect measurements at the tower location less that 5% of the time.

A suite of aerosol characterization instruments were assembled for the field study and rendered field worthy (Tasks I and II). The remote location of the experimental site posed a number of challenges. It was imperative that the aerosol sampling instruments be located on the tower because aerosol particles are lost during transport through sampling tubing. This is particularly true for the ultrafine particles that are of interest for biogenically influenced SOA production. These small particles are lost by diffusion to tubing walls, and any significant length of inlet line can significantly degrade the sample. Field worthy enclosures for each instrument were identified and mounted on the tower, shielding instrumental exposure to the elements thereby allowing for aerosol sampling with limited bias. A sampling manifold was developed to sample and transport the aerosol to the measurement instrumentation. The entrance to the manifold consisted of a PM-10 inlet, which samples aerosols of size 10 μm or smaller through an inlet designed to be insensitive to wind speed and wind direction. This aerosol was then passed through a PM-2.5 size cut, which removes the larger particles (10 – 2.5 μm) that are not of interest for this study. Sample flows for each individual instrument were drawn isokinetically from the main flow.

Installation of the equipment was performed during the month of September. The aerosol instruments at the site included a condensation particle counter (CPC), an optical particle counter (OPC), an aethalometer, and a nephelometer. Each instrument measured a different aspect of the aerosol population. The CPC measures total particle count. Any significant rise in this count signals either a recent nucleation event or a significant source of small particles being transported to the site. The aethalometer measures light absorption by the aerosol, indicating the concentration of light absorbing black carbon aerosol particles. In addition, the aethalometer gives a qualitative indication of the amount of ultraviolet-absorbing aerosol, which may serve as a marker for the presence of SOA. The OPC measures the size distribution of aerosol particles in the 0.1 to 2.5 μm size range, which is an indication of the presence of aged atmospheric aerosol that has been formed elsewhere and transported to the site. The nephelometer measures total particle scattering, which is an alternate measure of total particle number. Scattering is also sensitive to relative humidity. Data from the suite of instruments were obtained using a computer-controlled data-acquisition system with a time resolution of three minutes.

Data was collected in late summer (Task IV). This time period provided a number of meteorological conditions starting with the tail end of the hotter summer season through several storms and generally falling temperatures. A preliminary analysis of the data has been performed (Task V). Data from both the aethalometer and the CPC clearly reveal when the urban plume from the Sacramento region arrives at the Blodgett forest. The data set shows a number of particle concentration bursts that appear to be due to particle exhaust from the diesel generator arriving at the measurement tower. However, there are increases in particle concentration that do not appear to be affected by the generator and seem to indicate local particle nucleation and growth. Further analysis of the data, in conjunction with the data from Allen Goldstein's group, is underway.

Pollution Prevention in Developing Countries

High levels of particulate matter are present in many urban regions in low- and middle-income countries, causing higher levels of respiratory illness and sometimes cases of premature death. Indoor exposure to particulate matter in these countries is of particular concern because particulate emissions from stoves and heating sources are often high, and the population spends a great amount of time indoors. To determine which sources lead to high health costs from elevated exposure levels, as well as other environmental costs, the World Bank has developed a rapid assessment model to value air pollution damages. The model includes emissions from power plants, large industry, small industry, transportation, and residential areas. In the original model, costs associated with local health, local non-health, and global effects are calculated.

We developed and integrated a separate module to determine the indoor particle concentrations, for all of the fuel types. The local non-health effects of particles generated outdoors are accounted for because we allow the particles that do not deposit indoors to be released to the outdoor source. There were no changes made to the model for pollutant releases other than particles.

Case studies have been completed with Shanghai and Bombay. When the indoor air model was not included, the largest environmental costs were due to health effects associated with exposure to particles resulting from small industrial sources and transportation. The addition of the indoor air model shifts the major environmental costs to include health effects from exposure to particles from indoor sources. We also performed a sensitivity analysis to understand which model assumptions and inputs have a large effect on the results.

Improvements in fuel use indoors will have a greater impact on health costs than decreases in energy use by power plants and industry. Results from the Shanghai case study are displayed in Figure 2, which shows a breakdown of estimated damages by type of damage and source of damage. When only damages from ambient air pollution resulting from fossil fuel use are considered, total damages in 1995 are estimated to be US$1.3 billion, with 56% from health damages alone. When indoor air pollution is considered, the total damage estimate rises to US$2 billion, with 70% from health damages. Including indoor air also raises the contribution of residences from 5% to 37% of total damages. These results emphasize that indoor air quality is a crucial area to consider in assembling air-pollution mitigation measures; focusing only on mitigating ambient air pollution narrows opportunities for reducing health and environmental damages.

Similar shifts in priorities could result from modeling indoor exposure for small industry. The sensitivity analysis showed that expected health effects and the cost of health effects are both very dependent on a variety of economic and energy-use characteristics—ranging from fuel use and residence characteristics to valuation of specific types of damages—that will need to be better specified in applying this model in a policy-making setting.

Both the USEPA and the World Bank have expressed interest in this study and the improved methodology embodied in the modified model. Potential opportunities for extending this work include: applying the model to a case study of Beijing; focusing on power plant improvements (USEPA); applying the model to a different case study of Beijing; focusing on the impact of switching from coal to natural gas in residential heating boilers (World Bank); and providing training to researchers in developing countries in the use of the model (World Bank).

Results of the study were presented at the Society for Risk Analysis conference in Washington D.C. in December 2000, and were well received.

Figure 1: The 10-meter measurement tower located at the University of California Blodgett Forest Research Station. The aerosol instrumentation and sampling inlet were located on the upper two platforms of the tower. The Ponderosa pine plantation can be seen around the tower. The white object to the right of the tower is one of the two instrumentation buildings.

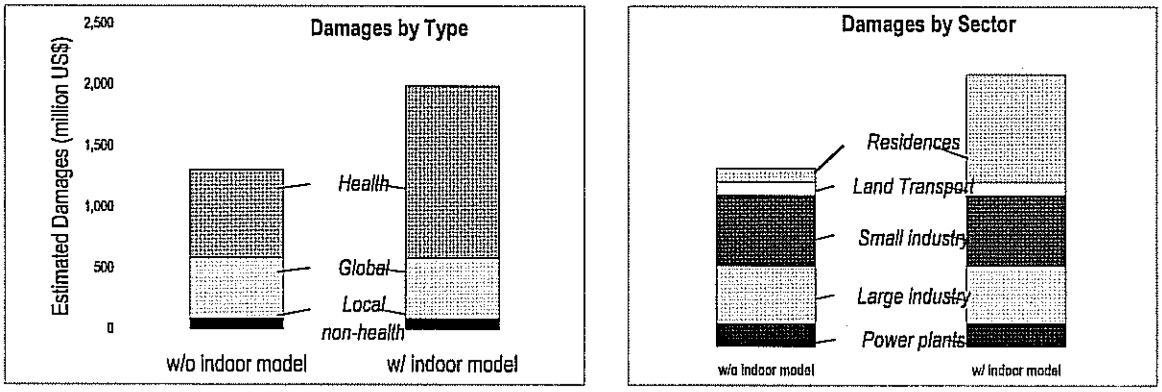

Figure 2: Shanghai Case Study, economic damages with and without Indoor Air Module, 1995.

Publications

D.H. Bennett and J.E. Sinton, "Environmental Costs for Urban Regions in Low- and Middle-income Countries", Society for Risk Analysis Conference, Washington D.C. (December 4, 2000).

D.H. Bennett and J.E. Sinton, "Environmental Exposure Modeling for Urban Regions in Low- and Middle-income Countries," (in preparation, selection of journal for submission in progress).

Atmospheric Chemistry: Changes at the Interface Between Urban and Regional Scales

Principal Investigators: Ronald Cohen, Nancy Brown, Allen Goldstein, Robert Harley, and Haider Taha

Project No.: 00012

Project Description

A critical challenge for the atmospheric sciences is to understand the anthropogenic impacts on atmospheric chemistry over spatial scales ranging from the urban to the regional, and, ultimately, to the global. Using LDRD funding as a seed, we plan to conduct research focused on exploring, characterizing, and understanding these impacts. This problem is energy relevant because the majority of emissions that affect atmospheric change are combustion generated. The problem is challenging due to the inherent non-linearity of the photochemistry at all spatial scales; the difficulties in simultaneously representing atmospheric fluid dynamics at different scales within a numerical model; the large demands placed on computational resources by solving the chemical rate equations; and the limitations of observations that are too sparse, infrequent, and inaccurate. To address these issues, we propose to continue developing a combined experimental and modeling program whose objective is to understand: 1) the dependence of O_3 sensitivity to precursors; 2) how the sensitivity changes as one moves from urban to regional scales; and 3) the relationship of O_3 sensitivity changes to particle loading. The program we envision will include a network of comprehensive, chemical observing stations along a West-East transect extending from the Marin Headlands to Lake Tahoe, along the prevailing synoptic wind direction. The observing program is intimately integrated with a state-of-the-art coupled photochemical-meteorological model. Even the initial fraction of this capability that can be supported by LDRD would advance understanding of the chemical, meteorological, engineering, and public policy issues that are intertwined in the subject of urban, regional, and global pollution. To date, we have initiated construction of a second mobile laboratory and the instruments it would contain and have begun a comprehensive assessment of meteorological modeling appropriate for Central California.

Accomplishments

Modeling: We have performed an assessment of meteorological modeling appropriate for Central California. This effort guides our ongoing development of meteorological modeling capabilities for the region, and provides requisite information to help us select the most appropriate model(s) for use in future work. Modeling Central California air quality is made difficult by complex terrain and a number of significant emission sources within the region. Our current effort involves intercomparison of two competing prognostic meteorological models (numerical solutions to the coupled system of mass, momentum and energy conservation equations) with an interpolation-based diagnostic model using common data sets. We have installed the latest generation and version of the PSU/NCAR MM5 mesoscale meteorological modeling system (MM5V3.3) on local Berkeley Lab and NERSC computers. We have initiated an uncertainty analysis of MM5 using the data from the 1990 San Joaquin Valley Air Quality Study (SJVAQS) to determine the effects of uncertainties in the meteorological model on the air quality model predictions for the August 1990 episode. Uncertainty is quantified by withholding selected radar wind profiler data, and comparing model predictions to withheld data. This will be used to enhance meteorological modeling capabilities for Central California, and to select the model(s) to use in future work.

In a study using a simpler one-dimensional model for the Sacramento plume, we show that the plume has unusually high efficiency for ozone production by nitrogen oxides. Approximately 10 O_3 are produced for each NO_x oxidized. In a more typical plume, measured values for efficiency are 6 or 7. This analysis provides coarse scale insight into what might be expected from the high-resolution models. We show that the background atmosphere at Blodgett Forest in California's Gold Country is comparable to clean continental sites and that a daily cycle mixes the urban plume from the Sacramento Valley into this clean background in the afternoon. Typical early evening conditions at Blodgett Forest, at the peak of the Sacramento plume, are a mixture of 78 % background and 22 % Sacramento plume. Analysis of observations of short-lived hydrocarbons provides a strict constraint on the product of the reaction time and the OH concentration during transport of the plume. The analysis also quantifies the total deposition rate of all nitrogen oxide species 0.015 $\mu gN/sec/m^2$ and the gross ozone production rate—7 parts per billion by volume (ppbv)/hour in the evolving plume. Two papers describing the details of this research are in draft form and will be submitted in the near future.

Results from analysis of hydrocarbon measurements confirm the overwhelming importance of biogenic hydrocarbons to the photochemistry of the Sacramento plume in general and to ozone production rates specifically. One paper describing these results is in press.

The experimental effort has been to define the layout of a mobile laboratory and contract for its construction. We are focusing on a cargo container that could be used at a single site or installed aboard the freight trains that travel the state.

The lab will be capable of supporting about a half dozen different instruments simultaneously. Components for assembly of instruments to measure NO and NO_y from this trailer have been ordered. Components to measure CO and to augment our capabilities to measure a suite of speciated organic nitrates have been assembled. We have identified components for an instrument that will make continuous hydrocarbon observations. The CO and speciated organic nitrate instruments will initially be deployed at Blodgett Forest while we determine the optimal location for the second observing site.

Publications

M.B. Dillon, A.H. Goldstein, and R.C. Cohen, *et al.*, "Chemical Evolution of the Sacramento Urban Plume: Transport and Oxidation," draft in preparation for *J. Geophys. Res.* (November 2000).

M.B. Dillon, A.H. Goldstein, and R.C. Cohen, *et al.*, "On the Role of Nitrogen Oxides in the Sacramento Urban Plume," draft in preparation for *J. Geophys. Res.* (November 2000).

D. Day, and R.C. Cohen, *et al.*, "Observations of HNO3, Alkylnitrates and Peroxynitrates in the Sacramento Urban Plume," AGU Fall Meeting (2000).

G.W. Schade and A.H. Goldstein, "Fluxes of Oxygenated Volatile Organic Compounds from a Ponderosa Pine Plantation," *J. Geophys. Res.* (in press, November 2000).

G.B. Dreyfus, G.W. Schade and A.H. Goldstein, "Investigating the contribution of Isoprene Oxidation to Ozone Production," AGU Fall Meeting (2000).

Diesel Particle Detection and Control

Principal Investigators: Donald Lucas and Arlon Hunt

Project No.: 00013

Project Description

Combustion is the primary source of fine particles (<2.5μm) in the atmosphere. These particles are linked to significant human health effects, but they are extremely difficult to measure and control. Conventional particle characterization techniques are inadequate, and cannot provide information at time scales necessary for active feedback control in engines or other combustion devices. We are designing and building transportable, low-cost particle sources that are well characterized and allow variations in the post-flame environment. The evolution and control of these particles are being studied using methods developed at Berkeley Lab, including the Diesel particle scatterometer (DPS) and excimer laser fragmentation fluorescence spectroscopy (ELFFS).

We are using two different laboratory-scale engines to study the region between the engine cylinder and the atmosphere. This work extends ongoing research in the combustion region to the post-flame region, where the temperature, residence time, and concentrations of particles and other species are high enough to allow considerable chemical and physical reactions, and expands on the diagnostics used to measure particles. Different sampling and dilution methods are being tested with the DPS, ELFFS, and conventional methods to determine the effects of varying temperature, humidity, dilution, and residence time. Our initial results show that the particle size and composition are strongly influenced by the nature of the dilution and the time-temperature history of the exhaust. We propose to continue our efforts to develop a reliable, well-characterized source of combustion particles, new diagnostic methods to measure them, and control methods.

Accomplishments

We have conducted experiments with two engines: a one-cylinder Diesel/generator and a two-stroke spark-ignited engine. We also built a small flame/dilution system to test the effect of different dilution properties on soot particles. The system uses an ethylene/air flame impinging on a stainless steel screen to produce particles in the 10^6 to 10^7 cm^{-3} range. The particles from these systems are being measured using the DPS and ELFFS diagnostics, as well as other particle sampling methods.

The characteristics of exhaust from the Diesel test generator were studied using the DPS. It provides the size distribution and the complex index of refraction (n, k) for various operating conditions. Cycle-by-cycle variations in particle loading were also studied on a microsecond time scale. In addition, loading and unloading conditions were measured to study transient behavior. In all cases, rapid and complex variations in particle loading were observed down to the sub-millisecond time scale.

The DPS was also used to study the operation of a Diesel particle afterburner connected to the Diesel generator. The afterburner consisted of two counterflow heat exchangers used to thermally isolate an electrically heated box capable of reaching temperatures of about 800°C. The DPS measurements showed that as the temperature in the heater box increased, the particles decreased in size to less than 20 nanometers as the hot box reached about 700°C. However, the nanoparticles did not burn out entirely. The size distribution became broader, and both the refractive and absorptive components (n, k) of the index of refraction of the particles decreased. The remaining particulate component had a low index of refraction and no absorption. This was interpreted as demonstrating the "burn out" of the carbon component of the particulate leaving a non-volatile nanoparticle component (probably sulfate). In addition to characterizing the effectiveness of the afterburner, the measurements provided a demonstration of the range and sensitivity of the DPS.

The ELFFS experiments revealed that the atomic carbon signal at 248 nanometers could be used as a marker for soot particles. The signal is linear with particle density, but we have not yet determined how the particle size affects the signal. We noted that CH and C_2 emission from the soot could be measured, and conducted experiments to determine the origin of these signals. The signals appear to arise from hydrocarbons coated on the soot particles, as engine exhaust sent though a denuder (which effectively removes lighter hydrocarbons and water) has only the atomic C signal, similar to pure carbon particles made from India ink solutions.

Publications

C.J. Damm, D. Lucas, C.P. Koshland, and R.F. Sawyer, "Measurement of Combustion Generated Particles with Excimer Laser Fragmentation Fluorescence Spectroscopy," presented at Spring Meeting of the Western States Section of the Combustion Institute (March 2000) (available as Conference Proceedings CD).

C. J. Damm, D. Lucas, C.P. Koshland, and R.F. Sawyer, "Real Time Measurement Of Combustion Generated Particles With Photofragmentation Fluorescence," in preparation for *Applied Spectroscopy* (December 2000).

Ion-Beam Thin-Film Texturing: Enabling Future Energy Technologies

Principal Investigators: Ron Reade and Paul Berdahl

Project No.: 99042

Project Description

Ion-beam assisted deposition (IBAD) processes have shown great potential for fabricating template buffer layers for epitaxial crystalline thin film growth without the need for expensive single-crystal substrates. However, current IBAD processes are very slow and thus too expensive for industrial application in cost-sensitive energy technologies such as high-temperature superconductor tapes. We are testing and developing a new concept for much more rapid processing—ion-beam thin film texturing (ITEX). To further develop ITEX processing, a better understanding of the fundamental mechanisms of ion-beam crystalline texturing processes is needed. The purpose of this project is to experimentally probe these mechanisms, and utilize this information to improve the fabrication processes for energy technologies. A new reflection high-energy electron diffraction (RHEED) system, installed in our pulsed-laser deposition system, has provided *in situ* information on film surface crystallinity and texture.

Accomplishments

In the past year, we further modified our ion-assisted pulsed-laser deposition (PLD) system for use with RHEED. The magnets in the ion source inside the PLD system initially caused a distortion of the electron beam from the RHEED system. To reduce this distortion, it was necessary to cut a new port in the chamber for reinstallation of the ion source further from the electron beam path. In addition, the chamber pressure during the ITEX process was found to cause degradation of the RHEED images. Improvements to the differential pumping system (evacuating the electron gun), including the purchase of a new pumping station, have improved imaging during the processing, allowing for further analysis of ITEX surface texture.

The ITEX method was applied to a yttria-stabilized zirconia (YSZ) film. YSZ is a key material used as a textured-template layer for $YBa_2Cu_3O_7$ (YBCO) superconductor deposition on stainless metal substrates. The RHEED images that we have obtained have shown that the surface is crystalline and in-plane oriented. In particular, when the sample is rotated about its surface normal, the RHEED pattern exhibits the desired four-fold symmetry. This is the first direct observation of biaxial surface texture of an ITEX film. A YBCO layer deposited on a similar ITEX YSZ layer on Haynes Alloy #230 (a nickel-based stainless alloy) was found to have a critical current density (J_c) of $0.25 MA/cm^2$. This J_c demonstrates that the ITEX process may lead to suitable template layers for future application to high-temperature superconductor tapes. Further analysis by θ-2θ and ϕ-scan x-ray diffraction showed that the ITEX YSZ layer seeded a well-crystallized YBCO film.

We are near submission of a patent application for the ITEX method.

This LDRD project has sharpened our expertise in the area of ion texturing, has resulted in improved equipment for film synthesis and characterization, and forms the basis for the new partnership with the Department of Energy Superconductivity for Electric Systems Program and private industry.

Publications

P. Berdahl and R. Reade, "Ion-Beam Texturing Mechanisms by Oblique Ion Beams Impinging on Metal Oxides," abstract and presentation at MRS Spring Meeting (April, 2000).

R.P. Reade, P. Berdahl, and R.E. Russo, "Ion-Beam Nanotexturing of Buffer Layers for Near-Single-Crystal Thin Film Deposition: Application to YBCO Superconductor Films," prepared for expected submission to *Applied Physics Letters* (submission delayed due to patent issues).

R.P. Reade, P. Berdahl, and R.E. Russo, "Particle Beam Biaxial Orientation of a Substrate for Epitaxial Crystal Growth," Patent Application, (December 2000, in final preparation).

Transgenic Mouse Models for DNA Damage Sensing, Repair and Aging

Principal Investigators: David Chen

Project No.: 00015

Project Description

The purpose of this proposal is to understand the role of DNA repair proteins in cellular senescence and telomere maintenance in mammals. We hypothesize that DNA double-strand break repair proteins are involved in telomere metabolism at the end of chromosomes. Cellular deficiency in expression of DSB repair proteins would lose the ability to protect the chromosome ends. We propose to construct knockout transgenic mice deficient in DNA double-strand break repair and DNA base damage repair. Cellular senescence in primary fibroblasts and telomere length maintenance in embryonic stem (ES) cells will be determined. The specific aims are:

- To generate knockout transgenic mice involved in DSB repair.
- To determine the telomere maintenance and cellular senescence in mouse embryonic fibroblasts (MEFs) isolated from transgenic mice deficient in Ku70, Ku80, DNA-dependent protein kinases (DNA-PKcs) and the double knockout Ku80/DNA-PKcs.

We will test whether deficiency in DNA double-strand repair proteins in mammalian cells would accelerate telomere shortening, thereby resulting in premature cellular senescence. We will analyze primary fibroblasts from our existing knockout mice, Ku70, Ku80, DNA-PKcs, and the double knockout Ku80/DNA-PKcs to determine their possible role in cellular senescence.

Accomplishments

Construction of Nijmegen Breakage Syndrome (NBS) +/- Heterozygote Knockout Mice

The targeting vector for NBS was constructed by substituting the NBS promoter region (about 200 base pairs upstream of ATG start codon), entire exon 1, and 2kb of intron 1 with the PGK-neo gene. This substitution removes the transcription and translation initiation sites, resulting in null expression of the NBS gene. Transfection of the linearized targeting vector to CJ7 ES cells was performed by electroporation. About 400 of the G418-resistant ES clones were screened at first by polymerase chain reaction (PCR), and then confirmed by Southern hybridization. A total of six ES clones showed homologous integration at the targeting site resulting in disruption of one of the NBS alleles.

Three targeted ES clones were then injected into C57BL/6 blastocysts to generate chimeric mice. Only one of the three ES clones showed good contribution towards chimera formation as assayed by analysis of coat color. These chimeras were crossed with C57BL/6 females to generate F1 progenitors. Among the17 F1 mice that were obtained, 7 males and 5 females showed successful transmission of the targeted allele as assayed by PCR and Southern blotting analysis. These NBS+/-mice are now being used to generate homozygous NBS-/- blastocysts for further analysis (NBS-/- mice are embryonic lethals).

Characterization of the Embryonic Lethality of NBS Knockout Mice

1. The NBS knockout mice are embryonic lethal.

NBS +/- mice were generated as described above. Upon crossing F1 NBS heterozygote mice (+/- x +/-), we were unable to obtain any NBS-/- mice from the 78 F2 progeny obtained. Genotyping analysis of these 78 F2 mice revealed that 24 mice were wild type (+/+) and 54 mice were heterozygous (+/-), a ratio of 1: 2.25. This strongly suggests that our NBS homozygous knockouts (possibly null knockouts rather than hypomorphs) are embryonic lethal.

We then analyzed embryos from e8.5 to e13.5 after crossing heterozygous mice (+/- x +/-). Of the 20 embryos obtained at e8.5-9.5, 13 embryos showed normal development and 7 embryos showed undeveloped and atrophic appearance. During e10.5 to 13.5, we observed 14 normal embryos and 11 small undeveloped, adsorbed embryos. We speculate that the growth of NBS -/- embryos is arrested before e7.5, and NBS-/- cells die after e10.5. Thus, our null NBS knockout mice show early embryonic lethality even though human NBS patients are viable and show relatively normal development until their birth. Therefore, it is possible that human patients may have low levels of hypomorphic truncated NBS protein and that NBS-/- knockout mice may be a better model system to understand all the functions of NBS protein.

2. Characterization of NBS-/- blastocysts for apoptosis and DSB repair.

We have isolated blastocysts at e3.5 and cultured *in vitro* to further analyze the growth abnormality of early NBS-/- embryonic cells. After five days of culture, cells derived from the inner cell mass (ICM) of NBS-/- blastocysts fail to grow and show massive apoptotic cell death by the TUNEL assay. On the other hand, NBS+/+ or -/- blastocysts show only a trace amount of cell death. Our results suggest that NBS knockout cells start dying by apoptosis at an early embryonic stage probably because of inability to repair endogenous DNA damage.

3. Construction of conditional NBS knockout mice.

In order to avoid the lethality associated with NBS gene knockout, we are in the process of establishing conditional knockouts for NBS using the tetracycline (tet) inducible system (Tet-On system, available from Clonetech). Also, viable mice which escape from embryonic lethality and whose NBS gene expression can be turned off after birth would be a good model for human NBS patients and would be useful for analyzing basic functions of NBS protein *in vivo.*

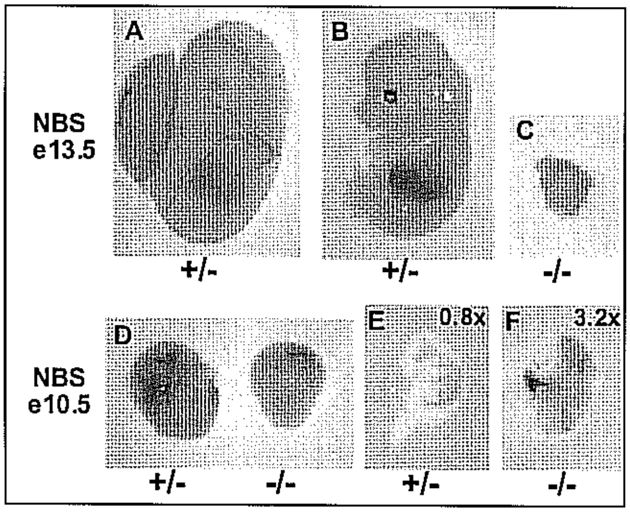

Figure 1: Early embryonic lethality of NBS knockout mice.

Publications

A. Kurimasa, *et al.*, "Targeted Disruption of the NBS Gene Leads to Early Embryonic Lethality in Mice," (in preparation).

S. Burma, *et al.*, "DNA-dependent Protein Kinase-independent Activation of p53 in Response to DNA Damage," *J Biol Chem.* (June 11, 1999).

R. Araki, *et al.*, "Enhanced Phosphorylation of p53 Serine 18 Following DNA Damage in DNA-dependent Protein Kinase Catalytic Subunit-deficient Cells," *Cancer Res.* (August 1, 1999).

S. Burma, *et al.*, "Roles of ATM, DNA-PK, and Nbs1 in the Phosphorylation and Activation of p53 in Response to Ionizing Radiation," 47th Annual Meeting of the Radiation Research Society (April 29, 2000).

Structural Cell Biology of Multi-Component Protein Complexes Essential for Genomic Stability

Principal Investigators: Priscilla Cooper and John Tainer

Project No.: 99019

Project Description

A major challenge in structural cell biology concerns the structural chemistry of large multicomponent protein complexes. We propose the development and application of structural and computational technologies for characterization of such complexes via a closely coordinated range of approaches involving molecular and cell biology, biochemistry, electron microscopy, crystallization, and x-ray diffraction. The research will initially focus on complexes that are essential for maintaining genomic integrity through two critical processes: transcription-coupled DNA repair of oxidative damage, and DNA double-strand break repair. The techniques developed for characterizing these will be applicable to defining the structural biology of other critical multicomponent complexes. Thus, an overall goal is to provide the technical basis for structural characterization of large complexes in contrast to the biophysical chemistry of single proteins.

This research will provide over-expression and purification of component proteins involved in transcription-coupled base excision repair and double-strand break repair complexes. It will also address their biochemical characterization, atomic resolution x-ray diffraction structures of individual components, and cryo-electron microscopy characterization of the complexes, including diversity and conformational states. It will advance current barriers for x-ray crystallography and begin filling the gap between high-resolution structures for individual proteins and medium resolution electron microscopy (EM) of multiprotein complexes. Initially, we will make and characterize the complexes and develop the technical tools for linking EM and x-ray structures, including beamline design for low- and high-resolution data collection on crystals of multi-component complexes. The follow-on goal is for combined EM and diffraction studies of the components and complexes, with results linked to coupled cell biology studies in an experimental cycle in which each builds on information from the other.

Accomplishments

The fundamental goal of this research program is development of techniques and capabilities to bridge the size and resolution gap between electron microscopy of biological assemblies and x-ray diffraction structures of separate proteins in order to advance the interpretative framework for molecular and cellular biology. The program focus is on two complexes that are essential for maintaining genomic integrity. Scientific progress has centered upon identifying and characterizing transcription-coupled repair (TCR) complexes and upon the structural biochemistry of the double-strand break repair complexes (DSBR) involving Rad50 and Mre11. These TCR and DSBR complexes were chosen as prototypes for the development of integrated structural biology programs in Life Sciences centered on macromolecular DNA repair machines essential for maintaining genomic integrity.

TCR research results underlying these efforts include discovery of a network of interactions of XPG—a key human protein essential for TCR—with a number of other crucial DNA repair proteins. These interactions have been characterized *in vitro*, and in some cases identified *in vivo*, and their functional significance has been established by the observed consequent stimulation of substrate binding or enzymatic activity. Such specific interactions of XPG include those with the base excision repair proteins hNTH1 and APE1. For the XPG partner APE1, enzyme:DNA co-crystal structures and mutational analysis identified a structural basis for DNA product binding and subsequent handoff during DNA repair pathway progression. We have found that XPG also interacts directly with a number of DSBR proteins including Mre11 and Rad50 as well as with the mismatch repair binding protein hMutSβ, which is required for TCR in an as-yet poorly understood role. Our observation that XPG strongly stimulates binding of hMutSβ to loop-, lesion-, or bubble-containing DNA substrates suggests that participation of mismatch repair proteins in TC-BER is direct. Furthermore, we have identified and characterized high affinity binding of XPG to DNA containing bubble structures, and have mapped this DNA binding to the R-domain region we first identified. Significantly, XPG greatly prefers to bind bubbles of 10 to 20 nucleotides, which resemble the region of helix opening in transcription. We postulate that this bubble-binding activity of XPG is central to its role in TCR. An examination of DNA repair protein structures and conformational changes has provided a unified understanding of DNA damage recognition and repair pathway regulation. Taken together, our results are providing a basis for the development of a new conceptual framework for studying and understanding DNA repair interactions and pathways.

DSBR results include multiple structures of Rad50 and Mre11 coupled to mutational and biochemical analyses. Rad50 catalytic domain crystal structures with and without ATP reveal ATP-driven conformational changes that control DNA binding. These structures furthermore suggest general principles for ATP-driven conformational switching in DNA repair processes including mismatch repair, nucleotide excision repair, and DSBR. Structures of the Mre11 nuclease/phosphatase reveal its resemblance to the calcineurin family, identify its DNA binding site, and establish a catalytic site containing two manganese ions. Finally, our co-expression experiments have identified the interaction sites between Mre11 and Rad50 and defined a "minimal core" for crystallization of an Mre11-Rad50 complex. Incorporating ~50 residues of the coiled-coil adjacent to the ATPase domain resulted in a tight complex of the ATPase domain with Mre11, suggesting that Mre11 binds to Rad50 in the coiled-coil region adjacent to the ATPase domain. Combined EM and x-ray diffraction results promise to provide the basis to bridge the gap between EM reconstructions of large complexes and high-resolution x-ray crystal structures (see figure).

Beyond these tangible research accomplishments, the ideas and approaches developed through this LDRD project have provided the basis for a multi-investigator DOE program proposal on the "Structural Biology of DNA Repair Complexes: Double-strand Break Rejoining and Transcription-Coupled Repair," which was funded at $770,000 for FY01. Furthermore, based upon concepts developed under this LDRD funding, we proposed an initial design for a new synchrotron beamline at Berkley Lab, which was approved by the Scientific Advisory Committee of the Advanced Light Source (ALS). This approval allowed us to apply for major funding for this beamline, which we have named SIBYLS for "Structurally Integrated BiologY for Life Sciences." In recognition of the importance of this new facility to conquer the current limitations of crystallography for characterizing multi-protein macromolecular machines, DOE has awarded $4.5 M to support the design, development, and construction costs for this tunable wavelength beamline at the ALS. The optimization of the SIBYLS beamline for DNA repair complexes will furthermore provide a unique resource to synergistically support and unify our proposed project "Structural Cell Biology of DNA Repair Machines," (SBDR) that has been submitted to the National Cancer Institute (NCI).

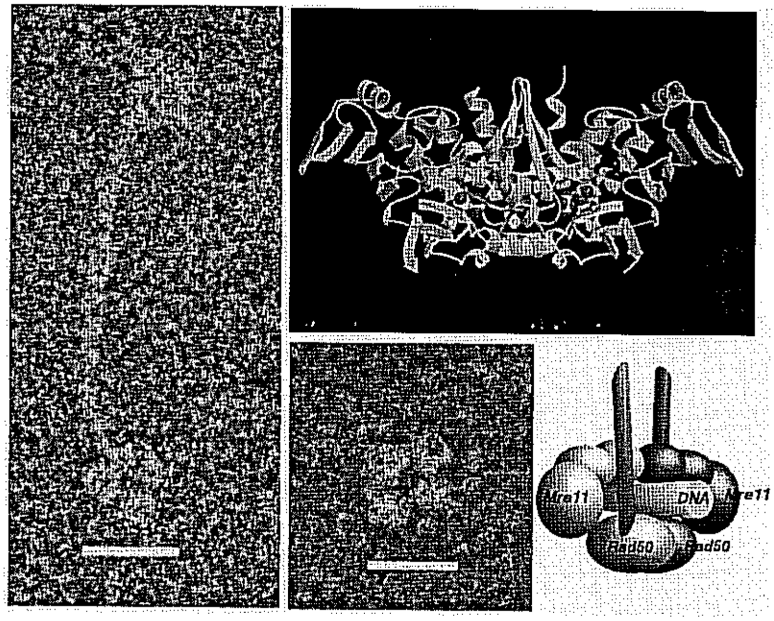

Figure 2: The Mre11/Rad50 DNA double-strand break repair complex structure. EM images (left) reveal the four domains of Mre11:Rad50 at the ends of the long helical coiled-coil and provide a basis for reconstructing the EM structure (bottom center) with the high-resolution x-ray diffraction structure of the Rad50 dimer (top, right) as shown schematically (bottom right).

Publications

C.D. Mol, T. Izumi, S. Mitra, and J.A. Tainer, "DNA-bound Structures and Mutants Reveal Abasic DNA Binding by APE1 and DNA Repair Coordination," *Nature* **Vol. 403**, pp. 451-456 (2000).

K-P. Hopfner, A. Karcher, D.S. Shin, C. Fairley, J.A. Tainer, and J. P. Carney, "Mre11 and Rad50 from *Pyrococcus furiosus*: Cloning and Biochemical Characterization Reveal an Evolutionarily Conserved Multiprotein Machine," *Journal of Bacteriology* **Vol. 182**, pp. 6036-6041 (2000).

J.A. Tainer and E.C. Friedberg, "Dancing with the Elephants: Envisioning the Structural Biology of DNA Repair Pathways," *Mutation Research* **Vol. 460**, pp. 139-141 (2000).

K-P. Hopfner, A. Karcher, D.S. Shin, L. Craig, L.M. Arthur, J.P. Carney, and J.A. Tainer, "Structural Biochemistry of Rad50 ATPase:ATP-driven Cooperativity and Allosteric Control in DNA Double-strand Break Repair and the ABS ATPase Superfamily," *Cell* **Vol. 101**, pp. 789-800 (2000).

K-P. Hopfner and J.A. Tainer, "DNA Mismatch Repair: the Hands of a Genome Guardian," *Structure, Folding and Design* (2000) (in press).

K-P. Hopfner, S.S. Parikh, and J.A. Tainer, "Envisioning the Fourth Dimension of the Genetic Code: the Structural Biology of Macromolecular Recognition and Conformational Switching in DNA Repair," *Symposium 65 in Quant. Biol.: Biological Responses to DNA Damage,* Cold Spring Harbor Press (2000) (in press).

A.H. Sarker, S. Tsutakawa, D. Shin, C. Ng, E. Campeau, J.A. Tainer, and P.K. Cooper, "A Novel DNA Binding Domain of XPG and its Implication in Transcription-coupled Repair" (2000) (in preparation).

Analytical Tools for Gene Expression and Genome Sequence

Principal Investigators: Michael Eisen

Project No.: 00016

Project Description

Our focus is on two fundamental problems relating to the use of genome-wide expression measurements in biology.

The first project involves the yeast *Saccharomyces cerevisiae*. Using DNA microarrays based on the complete yeast genome sequence, the variation in abundance of every yeast transcript has been measured across a wide variety of conditions and during diverse biological processes. We seek to understand the relationships between this gene expression data and the molecular function and cellular role of yeast's 6,200 genes, especially the 3,000 or so whose functions remain unknown. We also seek to understand the relationships between gene expression and the yeast genome sequence so that we can begin to unravel the cis-regulatory code.

The second project involves the use of gene expression patterns to characterize and classify human tumors. Clinical heterogeneity remains a major obstacle to the successful management of cancer. Even tumors that are identified as the "same" in the currently recognized cancer taxonomy differ considerably in their response to therapy and in outcome. Our premise in this work is that this clinical heterogeneity represents unrecognized molecular heterogeneity, and that genome-wide expression measurements can, by providing a window onto this molecular heterogeneity, form the basis for a new and more clinically relevant molecular taxonomy of tumors.

Our approach to the yeast project involves both computational and statistical analysis of existing data, as well as the development and application of new experimental methods that are designed to provide additional experimental data to address ambiguities in our current analyses. Our approach to building tumor taxonomies is to use DNA microarrays to survey the variation in gene expression in archived clinical specimens whose clinical histories are known and available. This enables us to immediately investigate the relationships between variation in gene expression and variation in clinical parameters, and, we hope, to develop models that will allow us to predict the prognosis and optimal treatment of newly diagnosed tumors.

To utilize all of the data in both projects, we will also build integrated databases and analytical tools that will facilitate the discovery of meaningful patterns within gene expression data and between gene expression and other important biological properties. These analytical tools include a variety of statistical and more complex analyses specifically developed for the problems we address.

Accomplishments

Yeast

We have completed the analysis of a complex set of gene expression experiments examining the response of yeast to diverse environmental transitions. DNA microarrays were used to measure changes in transcript levels over time for almost every yeast gene, as cells responded to temperature shocks, hydrogen peroxide, the superoxide-generating drug menadione, the sulfhydryl-oxidizing agent diamide, the disulfide-reducing agent dithiothreitol, hyper- and hypo-osmotic shock, amino acid starvation, nitrogen source depletion, and progression into stationary phase. A large set of genes (900) showed a similar drastic response to almost all of these environmental changes. Additional features of the genomic responses were specialized for specific conditions. Promoter analysis and subsequent characterization of the responses of mutant strains implicated the transcription factors Yap1p, as well as Msn2p and Msn4p, in mediating specific features of the transcriptional response, while the identification of novel sequence elements provided clues to novel regulators. We have also developed a method for directly associating sequence elements in cis-regulatory regions with gene expression patterns. This method is conceptually distinct from previously published methods in that it does not depend upon clustering. Tests of this method demonstrate that it successfully identifies most known sequence motifs and identifies a series of new motifs. We are working on a manuscript describing the method and these results.

Tumors

We have completed two initial studies examining the relationship between gene expression data and phenotypes of human tumors. In the first study, a collaboration between myself, Stanford University Medical School, and the Norwegian Radium Hospital, we used cDNA microarrays to measure gene expression in a set of 65 surgical breast specimens from 42 individuals. Two tumor samples were taken from 20 of the patients, one prior to, and one following, a standard course of doxirubicin-based chemotherapy. Remarkably, the gene expression patterns of 17 of these 20 before-after tumor pairs were more similar to each other than they were to any other tumor sample. This important observation demonstrates that gene expression patterns represent a truly intrinsic property of human tumors that is relatively insensitive to variation in patient condition or other clinical parameters, or to artifacts introduced by sample acquisition and handling. Applying a new statistical method I developed, we identified a set of genes "intrinsic" to these paired tumor samples. Using expression levels of these genes as the basis for a hierarchical classification of the tumors revealed, generated a clear taxonomy that included a previously unrecognized class of breast tumors. Strikingly, there was considerable variation in survival between patients in these different groups, a finding that has now been confirmed in a secondary analysis of over 600 patients.

The second initial study involved diffuse large B-cell lymphoma (DLBCL), the most prevalent form of non-Hodgkin's lymphoma in the U.S., and a disease that rapidly claims the lives of approximately half the people it strikes. Using cDNA specifically designed to study DLBCL and other tumors of lymphoid origin, we surveyed gene expression in 96 normal and malignant lymphocyte samples including 42 DLBCL patients. Within the DLBCL samples, we observed significant variation in the expression of genes characteristic of germinal center B-cells. Since DLBCL is thought to arise in the germinal center or from B-cells that have passed through the germinal center, we classified the tumors based on expression of these germinal center genes and a set of genes whose expression complemented these germinal center genes. (This last set of genes, induced during *in vitro* activation of resting B-cells, was not expressed in the tumor samples that showed the highest level of expression of the germinal center genes.) This analysis identified two subgroups of DLBCL (germinal center B-cell-like DLBCL and activated blood B-cell-like DLBCL) that showed marked and statistically significant differences in outcome. Again, subsequent analysis of additional tumor samples supports the clinical significance of this classification. Using the data, we have also developed a series of new methods for analyzing tumor data and for detecting association between gene expression and clinical parameters.

Both of these projects are now in their second stages during which we will collect data from thousands of tumor samples to further confirm and extend our initial finding to further confirm and extend our initial finding.

I have greatly expanded and improved the software programs Cluster and Tree View, which form the core of all of the analyses of these yeast and tumor experiments. This software is now quite popular, with over 4,000 registered users worldwide, and been cited in over 300 refereed scientific publications.

Publications

Perou, *et al.* "Molecular Portraits of Human Breast Tumors," *Nature* (August 2000)
http://rana.lbl.gov/papers/Perou_Nature_2000.pdf

Alizadeh, *et al.*, "Identification of Molecularly and Clinically Distinct Types of Diffuse Large B-cell Lymphoma by Gene Expression Profiling," *Nature* (February 2000)
http://rana.lbl.gov/papers/Alizadeh_Nature_2000.pdf

Hastie, *et al.*, "'Gene Shaving' as a Method for Identifying Distinct Sets of Genes with Similar Expression Patterns," *Genome Biology* (August 2000)
http://www.genomebiology.com/2000/1/2/research/0003/

Gasch, *et al.*, "Genomic Expression Programs in the Response of Yeast Cells to Environmental Changes," *Molecular Biology of the Cell* (December 2000)
http://rana.lbl.gov/papers/Gasch_MBC_2000.pdf

Chiang and Eisen, "Direct Association of Genome Sequence Words and Gene Expression Patterns," (in preparation).

Teraflop Challenges in Single-Particle Electron Crystallography

Principal Investigators: Robert Glaeser, Esmond Ng, and Ravi Malladi

Project No.: 00017

Project Description

The goal of this project is to define efficient mathematical approaches (and algorithms) that produce a three-dimensional reconstruction from high resolution, cryo-electron microscopy (EM) images of single protein molecules. These tools must make it possible to automatically identify between 10^5 and 10^6 single particles and automatically merge these images to produce the three-dimensional reconstruction. In order for this to be practical, identification and merging should be accomplished with less than ~10^{17} floating point operations (~10^5 teraflop). The long-term goal is to be able to carry out structural studies of large, multi-subunit protein complexes at high resolution, using electron microscope images of fields that contain ~100 particles each. Merging data from single particles is equivalent to crystallization *in silico*. By eliminating the need for biochemical crystallization, and by reducing data collection and three-dimensional reconstruction to about one day each, single-particle electron crystallography will achieve a level of high throughput that is similar to the speed of x-ray crystallography. There will be no delay in screening for crystallization conditions, however. Furthermore, structural studies will be made possible for complex molecular assemblies that represent increasingly problematic challenges for x-ray crystallography, but which are increasingly more favorable for cryo-EM.

To accomplish this, existing methods of automatic particle identification will be refined by the addition of conceptually new mathematical tools. The goal is to improve particle identification to a level such that false negatives fall below 25% and false positives fall below 10%. In parallel with this effort, we will port existing software suites (SPIDER, EMAN, and others) to the SP computer at the National Energy Research Scientific Computing Center (NERSC), and we will use existing data sets (one with almost 10^5

particles) to demonstrate that routine, high throughput merging of very large data sets is feasible on this machine.

Accomplishments

By the end of the first year, we had successfully recruited for a postdoctoral position in the Mathematics department, an entry-level career scientist was recruited into the Scientific Computing group, and an entry-level career scientist was hired within the Life Sciences Division (now transferred to the Physical Biosciences Division). Together with collaborators in Albany, New York, and in Houston, Texas, we were able to port some of the most time-consuming pieces of the SPIDER and EMAN software packages to the IBM SP machine at NERSC. We thus were able to run preliminary tests to evaluate the performance of these packages. We found that the size of jobs that could be completed did indeed scale as the number of processors. Substantial diagnostics have also been started to look for places where legacy code could be replaced by faster and more robust algorithms.

New work was started to look for improvements in the way in which single particles are identified and "boxed" within electron microscope images. This work began with a thorough review of the literature of automated particle boxing. Attention has focused on sophisticated techniques of image smoothing that have been developed by the Berkeley Lab Mathematics department. This work has led to good success in contouring images of single particles, a step that may next allow us to apply strong criteria for rejecting the false-positive particles that result from existing methods of automated particle identification.

Publications

W.V. Nicholson and R.M. Glaeser, "Automatic Particle Detection in Electron Microscopy," in preparation for *Journal of Structural Biology.*

DNA Microarray Analysis of Metabolic Regulatory Genes in the Mouse

Principal Investigators: Ronald Krauss

Project No.: 99020

Project Description

The overall aim of this project was to develop a system for identifying and characterizing key genes involved in metabolic regulation on a genome-wide scale using cDNA microarray methodology. Our primary approach was to examine alterations in tissue gene expression in mice with specific genetically-induced abnormalities in lipid metabolism. For these initial studies, we chose to analyze changes in adipose tissue gene expression profiles in mice with knockout of the gene for hepatic lipase, an enzyme with critical functions related both to regulation of plasma lipoprotein metabolism and adiposity.

Accomplishments

Pilot studies indicated changes in expression of several genes involved in lipid metabolism in three hepatic lipase knockout mice compared to three wild-type littermates. In order to confirm and expand these results, we bred a larger mouse population and compared adipose tissue gene expression in eight hepatic lipase knockout mice and eight wild type controls. For these studies, we used a microarray panel of approximately 10,000 genes including 300 involved in lipid metabolism. To determine significant changes in gene expression, we applied a new statistical analysis procedure developed in collaboration with Dr. Matt Callow and Professor Terry Speed of the University of California (UC), Berkeley Department of Statistics. The expression ratios for each knockout vs. wild type comparison were displayed in a two-dimensional matrix with rows corresponding to array elements and columns corresponding to different arrays. In order to test the null hypothesis of equal mean expression for array element j in the control and test group, a two-sample t-statistic was used. To account for multiple hypothesis testing, adjusted p-values were determined. A suitable permutation distribution of the test statistics was used to deal with these problems. In this algorithm, the permutation distribution of the t-statistics was obtained by permuting the columns of the data matrix. This strategy has the advantage of allowing the detection of small but potentially significant changes in expression using microarrays, and represents a statistically straightforward approach to data analysis comparing two different conditions. Unfortunately, this more extensive analysis, both in terms of number of animals and statistical methodology, did not confirm our previous findings: none of the lipid metabolism genes previously identified showed significant changes, and no new candidates were revealed. These results were confirmed by real-time quantitative polymerase chain reaction (PCR).

Follow-up studies were directed at using cDNA microarray analysis to specifically address the genetic basis for the association between hepatic lipase activity and adiposity. This has involved collaboration with Craig Warden (University of California, Davis) whose group has created a spontaneously obese mouse model (BSB) by crossing *M. musculus* C57/B16 with *M. spretus*, and backcrossing the F1 generation to C57/B16. They also created BSB mice heterozygous for the hepatic lipase deletion, where the functional hepatic lipase allele was derived from either C57/Bl6 or *M. spretus*. Interestingly, mice carrying the C57/Bl6 hepatic lipase allele had significantly lower gonadal fat mass than mice with the spretus allele (0.30 g vs. 3.02 g, P <10-9) and had correspondingly lower plasma hepatic lipase activity. This observation is consistent with a relation between hepatic lipase activity and adiposity, and suggests the presence of a modifier gene on chromosome 9, on which the hepatic lipase gene is located. In order to identify this and other genes that may modulate the adipose tissue response to hepatic lipase deficiency, cDNA microarray analysis was used to compare adipose tissue gene expression in the two BSB strains ("fat", n=8 and "lean", n=16) carrying single copies of the spretus and C57/Bl6 hepatic lipase alleles, respectively. Interestingly, expression of the leptin gene (on chromosome 6) was 13-fold lower in the lean vs. fat mice. Leptin is a hormone that regulates body weight through decreasing food intake and increasing energy expenditure. This result suggests an interaction of hepatic lipase deficiency with one or more genes in C57Bl/6 or spretus mice that modulate leptin gene expression. Based on the microarray analysis, we found 23 other genes that showed significant differences in adipose tissue expression between the fat and lean strains. None of these genes were on chromosome 9, none have obvious connections to lipid or energy metabolism, and most are non-annotated expressed sequence tags (ESTs). We now intend to confirm these results in additional mice, and to further characterize the nature and function of the genes showing the largest changes in expression in the fat vs. lean mice.

In summary, these initial studies indicate the feasibility of using cDNA microarray methodology to identify genes (both known and as yet uncharacterized) whose functional importance can be revealed by altered regulation in response to specific metabolic perturbations. We have recently received support from the National Dairy Council to extend this approach to the study of metabolic regulation in humans by analysis of altered adipose tissue gene expression in response to change in dietary composition and body weight. Future plans are to develop, with UC Berkeley and other institutions, a Center for Nutritional Genomics aimed at identifying interactions between genes and nutrients that could lead to specific, individualized dietary recommendations for optimizing health.

Cryo X-Ray Microscopy And Protein Localization

Principal Investigators: Carolyn Larabell

Project No.: 99021

Project Description

The purpose of this project is to examine the distribution of specific proteins using soft x-ray microscopy at the Advanced Light Source (ALS). Whereas the amount of certain proteins often remains the same in normal and tumor cells, the distribution is frequently altered. For example, it has recently been shown that the protein beta-catenin is located at the cell surface of normal cells but in the nucleus of tumor cells. In fact, an increasing number of proteins have recently been found in the nucleus of tumor cells, where it is believed they activate or repress gene transcription. The distribution of proteins is typically determined using immunolocalization analyses, but spatial resolution within the nucleus is difficult to determine using light microscopy. We will examine the distribution of proteins in normal human mammary epithelial cells and tumor cells, using soft x-ray microscopy to obtain higher resolution information. This requires a three-dimensional analysis that can only be accomplished with a cryo-tilt stage that can image specimens at multiple angles.

Human mammary epithelial cells will be grown on silicon nitride windows and fixed at various time intervals. They will then be incubated in the specific primary antibodies, followed by the gold conjugated secondary antibodies. The gold particles will then be enhanced with silver until approximately 45 to 50 nm in size. The hydrated, labeled cells will then be examined using the soft x-ray microscope at the ALS. The precise three-dimensional localization of these proteins, however, depends on the ability to obtain three-dimensional information from either stereo or tomographic images.

Accomplishments

One of our goals was to develop improved protocols that would preserve cellular organelles in chemically fixed cells for immunolocalization studies. We tested a number of permeabilization reagents that would facilitate passage of antibodies without destroying structural information. We have decided that one of these, saponin, fulfills these criteria. The addition of saponin to the fixative provides a simultaneous permeabilization/fixation with excellent preservation of the plasma membrane and subcellular organelles. This approach is now being used to localize specific proteins to subcellular structures, which are now much better preserved and easily recognized.

We also tested the use of other techniques that would enable visualization of the antibodies while reducing the background non-specific labeling. Although silver-enhanced gold labeling provided proof-of-principle results that we can visualize labeled proteins in the x-ray microscope, this approach often generated excessive non-specific labeling. Instead of silver, we are now using a gold-enhancement of the gold-tagged antibody. This approach allows us to reduce both the incubation time required as well as the artifactual non-specific labeling.

Finally, using x-ray immunocytochemistry, we have labeled cytoplasmic and nuclear proteins in normal and tumor human mammary epithelial cells.

Publications

C.A. Larabell, D. Yager, W. Meyer-Ilse, and B.A. Rowning, "From Dynamics to Details: Live-Cell Light Microscopy and High-Resolution Soft X-ray Microscopy," *Microscopy and Microanalysis* Pp 84-85 (August 2000).

W. Meyer-Ilse, D. Hamamoto, A. Nair, S.A. LeLievre, G. Denbeaux, L. Johnson, A. Lucero, D. Yager, M.A. LeGros, and C.A. Larabell, "High Resolution Protein Localization Using Soft X-ray Microscopy," *Journal of Microscopy* (2001, in press).

Cryo-Electron Microscopy Studies of the Eukaryotic Transcriptional Basal Factor TFIID

Principal Investigators: Eva Nogales

Project No.: 99022

Project Description

Regulation of gene transcription is essential in the process of cell differentiation and development of the organism, as well as for the survival of each cell in changing environmental conditions. The importance of gene transcription and its regulation is underlined by the myriad of human disorders that result from the malfunction of the molecular components involved in this cellular process. Initiation of gene transcription in eukaryotes starts with the binding of TFIID, containing the TATA binding protein (TBP), to the DNA core promoter, and the consequent assembly of the general transcriptional machinery. Six general transcription factors and RNA Pol II constitute the minimal protein assembly for transcription, adding up to several million Daltons. TFIID is also involved in the interaction with gene-specific activators. Our ultimate goal is to understand how the eukaryotic transcription initiation machinery assembles and functions, and the structural mechanisms for gene transcription regulation. To this end, we will characterize the structure of TFIID and its interaction with other general factors and with activators, using cryo-electron microscopy and single-particle image reconstruction. We have recently obtained an initial structure of TFIID and its complex with full length TFIIA and TFIIB at 35 Å resolution by negative stain, and localized, by antibody mapping, the position of TBP within the complex. One of our immediate priorities is to obtain a 3-D reconstruction of frozen-hydrated human TFIID complexes at a resolution better than 25 Å. We are interested in following the structural assembly and conformational changes of this complex machinery by generating medium resolution structures of increasingly larger complexes, with TFIID as the central core. Our final goal is to characterize the structural basis of transcription regulation by the interaction of the general transcriptional machinery with activators.

Accomplishments

Cryo-Electron Microscopy (EM) of Frozen-Hydrated TFIID

We have started our study of TFIID in a frozen-hydrated state. We found that although the number of particles per micrograph was high in negative stain studies, the low concentration of TFIID (~0.05 mg/ml) was limiting in cryo-EM experiments. Our initial attempts to visualize TFIID in vitreous ice through the holes of perforated carbon grids—a generally used support for cryo-EM experiments—were generally unsuccessful. Only a few TFIID particles were found, mostly bound to the edges of the holes. We are now using a technique that should help us increase the concentration of particles in the EM grid by providing a thin and continuous carbon surface for interaction with the protein complex. The regular holey carbon grids are covered with a very thin film of carbon, so that background in the images is minimized while providing a surface of interaction for the protein and a means for the correction of the CTF (contrast transfer function). Pretreatment of the EM grids to modify the hydrophilicity and/or charge of the carbon is also being optimized to maximize particle attachment. Given the relatively small size of the particles, and the added difficulty of blotting the grid previous to cryo-freezing when the second layer of carbon is present, our initial trials were negative but inconclusive—it was difficult to differentiate between whether particles were not visible because of the thickness of the ice or because they did not remain on the carbon.

To discriminate between these two possibilities we have used cryo-negative staining. In this case, the samples are still prepared in an aqueous layer, but a low percentage of stain is added to the solution before blotting. This method, together with the inclusion of tobacco mosaic virus (TMV) in the solution as a reference, has allowed us to clearly differentiate between lack of contrast (due to the thickness of the ice or insufficient defocus), and general lack of TFIID particles. With this setup, we are in the process of searching for conditions for which the number of particles per micrograph is maximized. Figure 3 shows a region of a micrograph taken using this methodology. The image clearly shows both TMV and TFIID particles. The density of TFIID complexes is already high enough to allow efficient collection of particle images, and we are now moving onto traditional cryo-EM experiments. These initial efforts will be invaluable for our studies not only of TFIID but also of larger complexes, where the concentration of particles will remain low.

Atomic Force Microscopy (AFM) studies of TFIID-A-B complexes bound to DNA

Recently we have obtained some preliminary results on the binding of TFIID and TFIID-A-B complexes to DNA using AFM of these complexes in air. The DNA template is from the G3ADMLBCAT plasmid, containing about four kilobases and has the adnl (adeno-virus major late) promoter that will also be used for cryo-EM studies (see Research Design and Methods). Images—obtained in tapping mode by scanning 2µm x 2 µm surfaces at a rate of 2-3.5 Hz—show the location of the TATA box within the DNA segment. Selected areas correspond to TFIID-A-B complexes bound to the DNA fragment. Most of the images were similar, in that they show TFIID-A-B bound preferentially at DNA ends. The proximity of the TATA box to one of the ends, and the limited resolution of the AFM, which will not allow the visualization of small DNA segments, makes it difficult to assess if these complexes were bound at the core promoter. Generally, there is a wide range of binding locations along the DNA, indicating that specificity is not very high. While much work still needs to be done on the optimization of the deposition conditions, these initial studies prove the feasibility of visualizing TFIID bound to DNA.

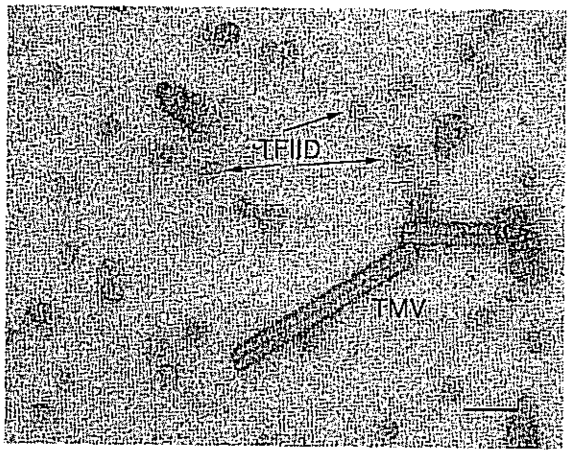

Figure 3: Cryo-negative stain images of TFIID complexes obtained using low-dose methods on a 200 keV, FEG scope. The bar corresponds to 500 Å.

Publications

A. Andel III, G. Ladurner, C. Inouye, R. Tjian, and E. Nogales, "Three-Dimensional Structure of the Human TFIID-IIA-IIB Complex," *Science* (December 10, 1999) http://www.sciencemag.org/cgi/content/full/286/5447/2153

E. Nogales, "Recent Structural Insights into Transcription Preinitiation Complexes," *J. Cell Sci.* **113**, 4391-4397 (2000).

Nanoscale Transport in Ultra-Thin Films

Principal Investigators: Michael Crommie

Project No.: 00018

Project Description

The purpose of this project is to experimentally probe electron and mass transport at the angstrom level in ultra-thin metal films. We wish to understand the influence that well characterized nanostructures have on the electrical conductivity of metal overlayers. Electromigration (mass transport) occurs hand-in-hand with electrical conductivity, but is not well understood at the atomic scale. An important goal here is to elucidate the local mechanisms of electromigration and to observe how nanostructures evolve under the influence of flowing current. We want to know if electromigration can be converted from a "problem" to a new and useful tool for fabricating novel nanostructures.

Thin metal overlayers will be grown under ultra-high vacuum conditions and probed with a variable temperature scanning tunneling microscope (STM). Local electronic structure and conductivity in the films will be investigated using the combined techniques of STM spectroscopy, four-point resistivity probe, and scanning tunneling potentiometry. The effects of electromigration on nanostructures will be investigated by directly probing local structures before, during, and after current injection. Novel nanostructure growth modes will be explored by varying overlayer composition, as well as electromigration parameters.

Accomplishments

The bulk of our efforts in this project have gone into developing a new ultra-high vacuum (UHV) scanning tunneling microscope (STM) capable of operating at temperatures between 15°K and 300°K. This instrument will allow us to grow ultra-thin films *in situ* using molecular beam epitaxy techniques, and to perform simultaneous STM and transport experiments. In addition, the instrument is designed to allow optical access during STM operation, so that the effects of optical stimulation on nanostructures can be measured at microscopic length scales.

Our instrument uses a Pan-type coarse approach mechanism suspended by springs inside an enclosed copper heat shield. The heat shield is cooled via gas-flow techniques (See Figure 1.). *In-situ* sputtering, surface analysis, and cleaving will all be possible in the surrounding UHV chamber. The STM has been designed for ultra-stable operation and should be capable of atomic manipulation and high-resolution local spectroscopy.

The STM mechanism and sample-handling equipment were designed and fabricated over the last year. We are currently assembling these pieces and they all appear to perform as desired. Figure 1 shows an image of the instrument. Piezo actuators and coarse approach electronics are currently being fabricated and integrated into the STM body. The UHV chambers have been designed and purchased, and should be delivered within a month. The optical table, pumps, and manipulators have already been delivered and are currently being assembled. We expect to pump the chamber down in January, and to begin final STM installation in February. We are currently wiring up the STM.

We will be taking data this coming year, and we expect to study molecular-mechanical actuation in collaboration with other Berkeley Lab researchers.

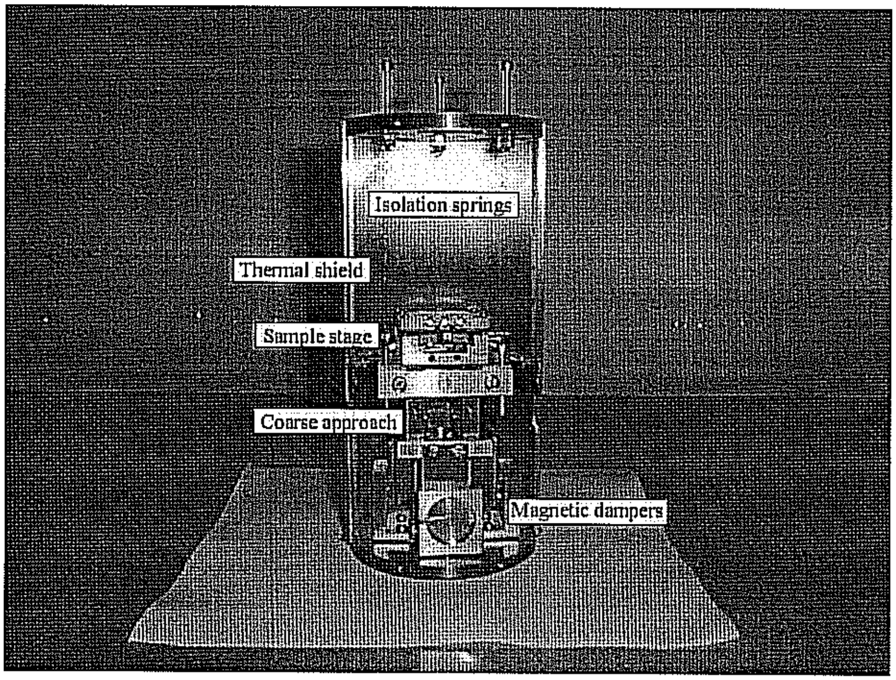

Figure 1: Variable temperature UHV STM with in-situ transport capability and optical access.

Atomically Resolved Spin-Polarized Imaging with Superconducting STM Tips

Principal Investigators: J.C. Séamus Davis

Project No.: 99024

Project Description

The goal of this proposal is to create techniques of scanning tunneling microscopy (STM) with superconducting tips that will allow imaging of the spin polarization, and thus the magnetic moment, of individual atoms on a surface.

A combination of the superconducting tip, very low temperatures, and high magnetic fields will allow us to create a 100% spin-polarized source of electrons in the tip by using the Zeeman splitting of the quasiparticle density of states at the gap edge of the superconductor. The polarization is possible when $\mu_B B \gg k_B T$. With the available magnetic field of up to 7.25 Tesla in our STM cryostat, we should easily be able to achieve this condition and thus split the spin polarization states completely. The peaks in the DOS then occur at voltages given by $V_+ = (\Delta + \mu_B B)/e$ and $V_- = (\Delta - \mu_B B)/e$ where Δ is the energy gap of the superconducting tip, and e is the charge on the electron. Tunneling at bias V_+ uses only electrons of one polarization, and tunneling at V_- only those of the other. Using this Zeeman polarized superconducting tip, in combination with an atomic resolution STM, will give us a unique opportunity to create the first spin-sensitive imaging technique at the atomic scale. Should this be achieved, it will revolutionize the way that magnetic materials are studied on the atomic scale.

Accomplishments

To realize atomic resolution controllable spin-polarization contrast STM three elements are required: (1) atomic resolution STM, (2) magnetic field and temperature such that $\mu_B B \gg k_B T$, (3) superconducting STM tips, and (4) appropriate conducting samples which have spin-polarized surface states. We have recently succeeded in the first use of Nb superconducting tips with atomic resolution. We have also successfully integrated a high field magnet with our atomic resolution STM and 250 mK refrigerator. We are currently studying highly correlated electronic materials in magnetic fields with conventional tips to help choose appropriate spin-polarized surface state systems. Following is a more detailed description of the steps taken.

Imaging and Spectroscopy of Magnetic Vortices in of $Bi_2Sr_2CaCu_2O_{8+\delta}$ (BSCCO)- Discovered Core States

We have spent much effort in understanding and characterizing $Bi_2Sr_2CaCu_2O_{8+\delta}$, with our low-temperature STM, since it is the type of cuprate-oxide perovskite that is a potential target for spin-polarized STM. As reported previously, while studying the magnetic properties of BSCCO in high magnetic fields, we demonstrated for the first time the existence of localized core states in BSCCO whose properties are consistent with a locally nodeless order parameter. We also showed that atomic scale scattering centers can influence vortex structure by pinning vortices.

Discovered Spin-Split Scattering Resonances in $Bi_2Sr_2CaCu_{2-x}Ni_xO_{8+\delta}$

We studied magnetic Ni atoms that were deliberately introduced in BSCCO. Ni doping is known to suppress the superconducting transition temperature. Spectroscopy on the Ni atoms and surrounding sites revealed the presence of two particle-hole symmetric resonances at 9mV and 18mV[2]. Surprisingly, the coherence peaks of the superconductor survive the perturbation created by the Ni atom. Comparison of our data with theory leads us to the conclusion each resonance has a definite spin associated with it. These spin-split resonances are a good candidate for testing the ultimate atomic resolution spin-polarized STM.

Discovered Spatial Inhomogeneities in the Gap Magnitude in Underdoped $Bi_2Sr_2CaCu_2O_{8+\delta}$

While measuring the local spectroscopic properties of BSCCO, we made a surprising discovery about spatial variations in the magnitude of the superconducting gap. Our high-resolution STM data have revealed that the HTSC state, rather than being homogeneous, is a collection of nanoscale regions in which the superconducting energy gap varies from one place to another. Figure 2a shows a nanoscale image of the superconducting gap magnitude as a function of position. In Figure 2b, the boundary regions between two distinct electronic characteristics are identified for exactly the same surface. This data gives indisputable evidence for nanoscale inhomogeneity and, in combination with experimental evidence from other groups, points towards nano-segregation of superconducting droplets by another non-superconducting phase. Since the electronic properties of the bulk superconductor are strongly influenced by oxygen doping, a study of the segregation as a function of oxygen doping will clarify issues about the identity of the two phases.

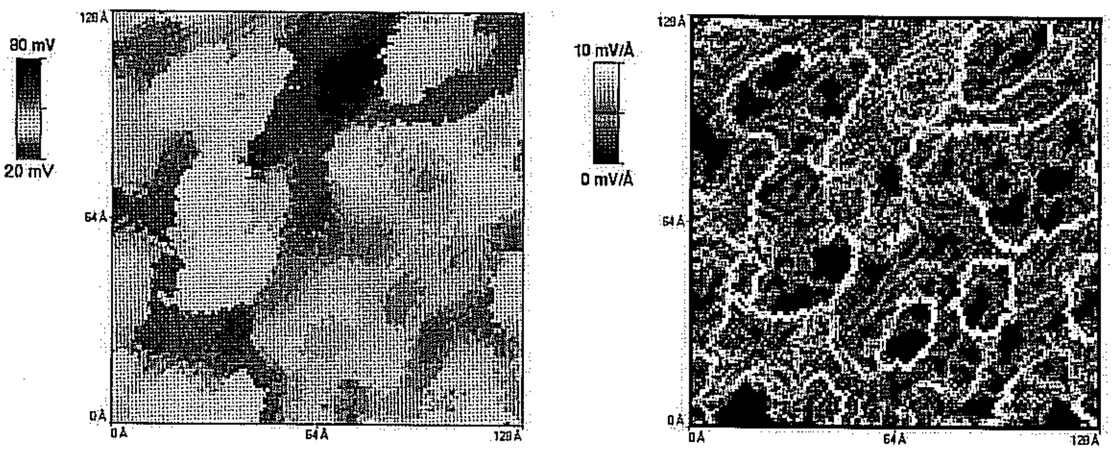

Figure 2: A map of the magnitude of the superconducting gap (left) on a 128 Å area of BSCCO. The 'low gap' regions (lighter tones) are surrounded by 'high gap' regions (darker tones). On the right is a derivative map showing the boundaries between the two regions clearly.

Publications

S. H. Pan, E.W. Hudson, A. K. Gupta, K-W Ng, H. Eisaki, S. Uchida, and J.C. Davis, "STM Studies of the Electronic Structure of Vortex Cores in $Bi_2Sr_2CaCu_2O_{8+\delta}$," *Phys. Rev. Lett.* **85**, 1536 (2000).

E.W. Hudson, K. M. Lang, V. Madhavan, S. H. Pan, H. Eisaki, S. Uchida, and J.C. Davis, "STM Studies of Magnetic Impurity Atoms in $Bi_2Sr_2CaCu_2O_{8+\delta}$: Implications for Magnetic Mechanism for High-TC Superconductivity," in preparation for *Nature*.

Holographic Imaging with X-Rays: Fluorescence and Fourier Transform Holography

Principal Investigators: Charles Fadley and Malcolm Howells

Project No.: 00030

Project Description

The purpose of this project is to develop two promising new techniques for imaging matter in three dimensions using x-rays. The first technique is hard x-ray fluorescence holography, which has already demonstrated the ability to image atomic positions in three dimensions with accuracies of ~0.2 Å over a range of about 10 Å around a given emitter. This will be extended to 0.1 Å resolution over larger spatial regions and to yield enhanced elemental and magnetic sensitivity. The second technique is soft x-ray Fourier transform holography, which currently is able to image wet life-science samples at 50 nm resolution in two dimensions. This will be further developed to yield ultimate resolutions of ~10 nm in three dimensions.

To accomplish this, an existing x-ray fluorescence holography experimental station will be upgraded in several ways for use at the Advanced Light Source (ALS), first, on a bend-magnet beamline (9.3.1), and, ultimately, on a superbend or wiggler beamline in the future. The x-ray energy discrimination and detection will be via high-speed solid-state detectors (making use of special Berkeley Lab expertise). Experiments will be performed in both the direct (single-energy) and inverse (multi-energy) modes, as well as with resonant absorption, to enhance contrast, elemental sensitivity, and magnetic sensitivity. An existing soft x-ray holography experimental station will also be modified to permit the use of ALS beamline 9.0.1 for Fourier transform holography with a complex reference object (e.g., a random array of ultrasmall pinholes). New theoretical methods for inverting both hard x-ray and soft x-ray Fourier transform holograms will also be explored, and there will be a high degree of synergism between the two aspects of this work.

Accomplishments

X-Ray Fluorescence Holography (XFH)

In order to obtain the highest quality holograms, we have upgraded the previous experimental setup in several ways so as to remove different sources of noise or unwanted signals, as well as to maximize count rate. A schematic of it is shown in Figure 3a.

Statistical noise minimization and energy discrimination: A high count-rate germanium solid-state detector developed at Berkeley Lab and provided by the Bucher/Shuh group has been installed in the experimental chamber.

Count rate maximization and elimination of the direct hologram: The sample rotation axes are positioned off-center in the experimental chamber in order to increase the detector solid angle. This was done not only to increase the count-rate but also to average out intensity oscillations due to the motion of the sample with respect to the detector (the direct hologram).

Minimization of beam instabilities: To average out intensity fluctuations in the ALS or the beamline, we have built a stand-alone motion control and data acquisition setup able to perform a full holographic measurement in one minute. The acquisition is performed by synchronizing the high-speed rotation of the sample (600 rpm) with rapid acquisition capability (1 MHz maximum count rate, 10 kHz sampling rate), and with the use of direct memory access for the high-speed data storage. By repeating the measurement several times, various instabilities will be averaged out. Acquisition and diagnostics of the system are controlled by dedicated software developed by us. In addition, we have developed the theoretical basis of a new technique, resonant-XFH (RXFH), based on the anomalous scattering effect, which is already successfully applied in x-ray diffraction to solve the phase problem. In holography, the phase information is directly available; but by working in resonance and by properly subtracting images off and on resonance, we can suppress non-resonant atoms and image only selected atomic species. In addition, new algorithms based on iterative deconvolution methods are being studied. Although preliminary results show only a small improvement of the reconstructed images, several other possibilities for improvement will also be tested.

Soft X-Ray Holography (SXH)

The development of new types of reference objects and the use of the Fourier transform geometry will enable high resolution to be obtained with a relatively low-resolution detector via diffraction tomography. Such a reference object must have good x-ray transmission and possess structure on the interesting 0.1 to 0.001 $Å^{-1}$ scale, such that it fills the detector with diffracted x-rays out to the desired angle. We have made experimental tests of pinhole arrays and silica aerogels as candidate reference objects. The pinholes were about 10 nm in diameter and were produced by etching damage tracks made in 5-μm-thick mica plates by a 4 MeV α–particle beam. The aerogels were of pure silica, 3 to 4% dense and with peak pore size of 10 to 20 nm. Such materials have been shown to have about the right spatial-frequency coverage, 0.1-0.001 $Å^{-1}$, for high-resolution x-ray imaging. The aerogels used were provided by Dr A. Hunt of the Division of Environmental Energy Technology. The candidate reference objects were illuminated by non-monochromatised undulator radiation ("pink beam") on beam line 9.0.1 at the Advanced Light. The beam consisted of essentially 100% of 560 eV x-rays (for maximum absorption by mica) in the third undulator harmonic and with a coherence length of 120 waves and nominally perfect spatial coherence. We were not able to observe the expected diffraction pattern and wave. The problem has been traced to the energy and type of ion used in forming the damage tracks. New tracking experiments are planned using the 88-Inch Cyclotron at Berkeley Lab as the source for damage tracks. On the other hand, the aerogels gave good soft-x-ray scattering patterns with a spatial frequency cutoff corresponding to about 20 Å resolution, with results shown in (Figure 3b).

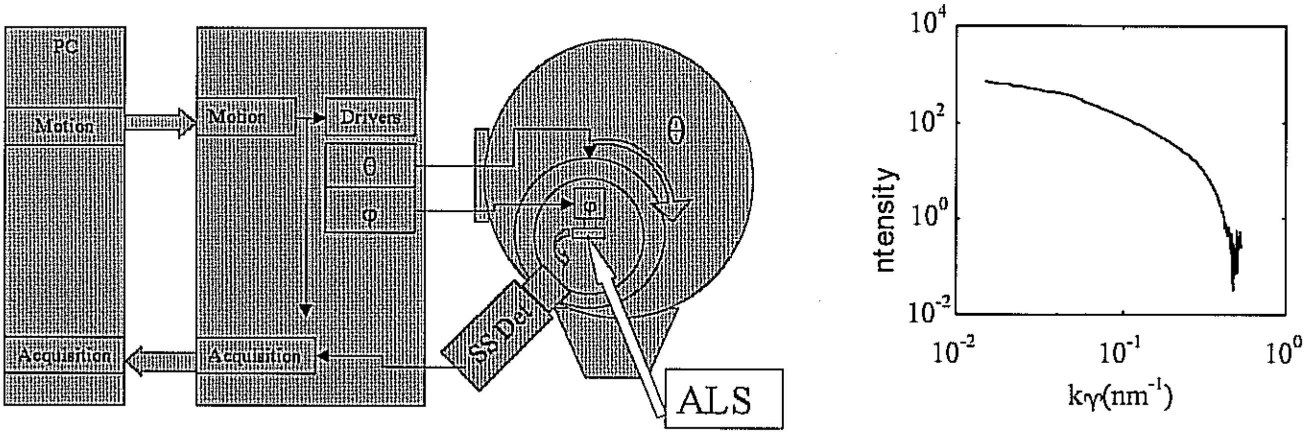

(a) (b)

Figure 3a: XFH—New experimental setup: pc and motion/acquisition, experimental chamber with off-centered goniometer mounting. 3b: SXH—Scattering intensity of an aerogel sample.

Publications

M.R. Howells, C.J. Jacobsen, S. Marchesini, S. Miller, J.C.H. Spence, and U. Weirstall, "Toward a Practical X-Ray Fourier Holography at High Resolution," accepted for publication by *Nuclear Instruments and Methods (2000).*

Novel Routes to the Fabrication of Microdesigned Grain Boundaries via Solid-State Methods

Principal Investigators: Andreas Glaeser and Ronald Gronsky

Project No.: 00019

Project Description

A dominant goal of materials science is to establish the microstructure-property-processing relationships essential to the intelligent fabrication and application of advanced materials. The spatial arrangement of solid-vapor interfaces (surfaces), solid-solid interfaces (grain boundaries), and/or solid 1-solid 2 interfaces (heterophase boundaries) establishes the microstructure of a material. The structure and chemistry of interfaces, their energetic and kinetic attributes, influence the spatial arrangement of interfaces and establish the properties of a material. Consequently, the importance of interfaces and microstructure in affecting or controlling material properties transcends all restrictions associated with material type and material application. A better understanding of the properties of surfaces and interfaces has a beneficial impact on a broad range of material applications, bridging many scientific disciplines. This applies especially to nanostructured materials, due to their high intrinsic spatial density of surfaces and interfaces.

Grain boundaries play a particularly important role in influencing the microstructure and properties of advanced ceramics. Bicrystals provide a vehicle for model studies of such interfaces. In principle, the geometry of the interface and the compositions of the contacting phases can be controlled, and the properties of the grain boundary can then be examined under a wide range of conditions. However, systematic fundamental studies of grain-boundary structure-property relationships have been limited because producing high-quality bicrystals is particularly difficult. As a result, the supply of ceramic bicrystals is limited.

This LDRD has focused on this limitation by exploring and developing new methods of producing controlled misorientation grain boundaries in aluminum oxide, a model ceramic material. The effort has been successful, and has prompted international interest and offers of future collaboration. Future studies can develop the idea that nanostructured two-phase materials interface properties (chemistry) can become size dependent; and bicrystals define the reference behavior.

Accomplishments

Novel solid-state methods of producing three distinct types of bicrystals by tandem epitaxial growth of single crystal seeds into theoretically dense, doped or undoped polycrystals have been developed. In principle, the methods should be applicable to any material (metal, semiconductor, and ceramic) for which single crystals are available. Such samples simplify and indeed enable systematic study of the effects of grain boundary geometry, chemistry, and environment on grain boundary structure and properties. The methods provide samples that will allow systematic studies of grain boundary structure and chemistry, and of grain boundary phenomena, e.g., grain boundary grooving, grain boundary diffusion, solute segregation to grain boundaries, grain boundary corrosion, penetration by intergranular phases, and phase formation at grain boundaries.

In the present program, the method has been applied to Ti-doped aluminum oxide, a material of central interest in the ceramics community for more than forty years. Although Ti is known to fundamentally alter the thermodynamic and kinetic properties of surfaces and interfaces, and thereby the rate and nature of microstructural development, the true basis for this change has eluded definition. The effect of Ti additions on the properties of grain boundaries has been particularly controversial.

It has been demonstrated that bicrystals can be produced by using two individual single crystals misoriented in a controlled manner as a template. These misoriented seed crystals are bonded by solid-state methods to a sacrificial polycrystalline layer of controlled chemistry. The grain boundary is produced by the "collision" of the two growth fronts. Two different types of controlled-misorientation, controlled boundary-plane orientation bicrystals have been produced. Both low-angle and high-angle controlled misorientation twist boundaries were fabricated by growing two rotated (0001) undoped sapphire seeds into a thin intervening layer of polycrystalline Ti-doped alumina. Controlled-misorientation tilt boundaries were produced by 1) removing a wedge from a single crystal substrate, 2) bringing the two remaining pieces of substrate into contact, 3) bonding the two seeds to a single layer of polycrystalline material, and 4) allowing growth of the seeds into the polycrystal. Methods of sample fabrication and appropriate growth conditions required for the fabrication of such bicrystals were established. Grain boundary grooving studies were initiated to study interface energetics. Polycrystalline material containing controlled and systematically incremented levels of Ti were prepared to allow studies of the effect of bulk composition on grain boundary chemistry and structure. Efforts were also made to produce tilt grain boundaries in which the grain boundary misorientation is fixed, and the full range of grain boundary plane orientation is sampled. Ideally, a large circular grain embedded in a larger single crystal is produced. This effort was a partial success; complete impingement of the growth fronts occurred only along one-third of the perimeter, but the directions for achieving 360° impingement have been defined.

Of the numerous bicrystals that were produced, a subset was evaluated using high-resolution transmission electron microscopy. The results show that high-quality grain boundaries—free of unwanted contaminant phases and with the imposed misorientation—can be produced. Atomic resolution imaging is possible. For tilt grain boundaries, analysis of the dislocation structure can be performed, as illustrated in Figure 4 for a 9.8° tilt grain boundary. Interfacial chemistry was also assessed by spatially-resolved energy-dispersive spectroscopy (EDS) using the x-ray signal generated by the electron beam in an analytical electron microscope. An enhanced Ti level at the interface was indicated for all grain boundaries examined. Results suggest Ti is in the 4+ state. Interestingly, cosegregation of Ca^{2+} was also observed, with indications of a fixed Ti^{4+}:Ca^{2+} ratio in the near grain boundary region. Such cosegregation may result in charge mismatch compensation, and account for the unusual migration properties of grain boundaries in this material. These results clearly illustrate the potential of the epitaxially-seeded growth method inaugurated here for solid-state growth of controlled-misorientation bicrystals. The samples produced are of exceptionally high quality and are amenable to characterization by phase contrast imaging and nanoscale spectroscopy for simultaneous assessment of structure and composition at the atomic level.

This research has developed a powerful tool. A process was developed that has the potential to produce controlled interfaces at a minimal cost. Programs extending this approach to interfaces between dissimilar materials should soon provide the basic scientific understanding required to provide the foundation underlying intelligent design of materials with "conventional" microstructural scales as well as nanostructured materials. This approach allows a major reduction in the capital investment required for studies of controlled interfaces, and thereby should enable broader participation in this vital research area.

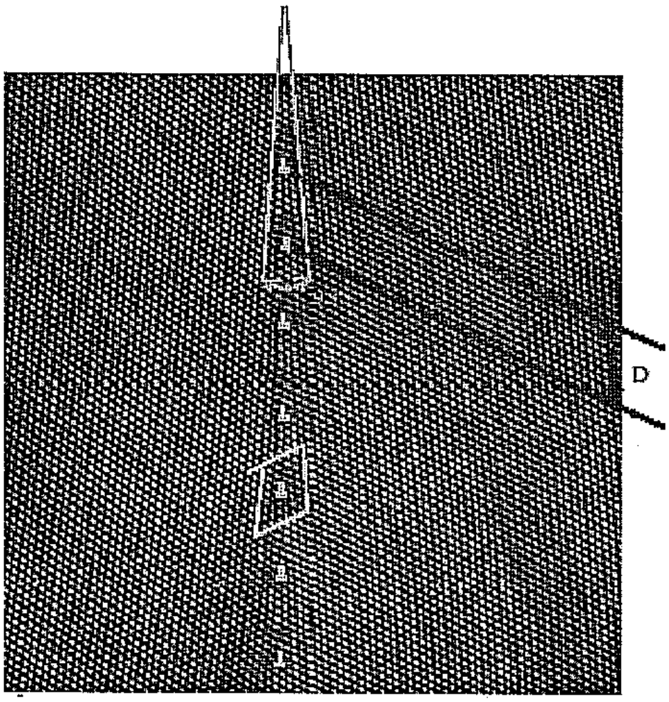

Figure 4: An atomic resolution image of a tilt grain boundary intended to have a $\theta=10°$ misorientation. Such grain boundaries can be described in terms of periodic arrays of edge dislocations, the positions of which are indicated on the figure by the symbol $\perp$. The Burgers vector, b, of the edge dislocations is shown to be along <2110>, and to have magnitude 4.7588Å. The dislocation spacing D is shown to be 27.55Å. Application of Frank's rule ($\sin\theta = |b| / D$) indicates a misorientation of 9.8°, illustrating the high level of control possible over the grain boundary misorientation.

Publications

M. Kitayama, T. Narushima, R.A. Marks, S. Taylor, R. Gronsky, and A.M. Glaeser, "Model Studies of the High-Temperature Properties of Surfaces and Interfaces via Microdesigned Interfaces," invited talk at 10th Iketani Conference, Karuizawa, Japan (June 28th, 2000).

M. Kitayama, T." Narushima, R.A. Marks, S. Taylor, R. Gronsky, and A.M. Glaeser, "Model Studies of the High-Temperature Properties of Surfaces and Interfaces via Microdesigned Interfaces" invited talk at JSPS Workshop of Future Directions in Materials Science (July 1, 2000).

R.A. Marks, S. Taylor, R. Gronsky, E. Mammana, and A.M. Glaeser, "Bicrystals via Epitaxially Seeded Transformations" in preparation for submission to *Nature.*

Graphite: The Rosetta Stone of Current Two-Dimensional Condensed Matter Physics

Principal Investigators: Paul McEuen and Dung-hai Lee

Project No.: 00020

Project Description

The "Fermi-manifold" of a metal is the set of points in momentum space where gapless fermionic excitations exist. In ordinary metals, the Fermi-manifold is a surface, and in artificial two-dimensional systems, such as two-dimensional electron gas, it is a closed curve. However, interesting exceptions occur in nature. For example, the Fermi-manifold of a single sheet of graphite consists of isolated points. The electronic dispersion near these points is of the relativistic Dirac form. Another important example of the point-like Fermi-manifold occurs in the superconducting state of the high-transition-temperature superconductors. There, due to the d-wave symmetry of Cooper pairing, the quasiparticle spectrum is gapless and consists of four Dirac points just like graphite.

Our goal is ambitious and long term in nature. We want to understand the impact of the Fermi-manifold topology on the low-temperature properties of these materials. At this initial stage spanned by the LDRD project, we approach this goal separately from experimental and theoretical points of view. Experimentally, we try to fabricate single graphite sheets, in hoping to perform in-depth study of its physical properties. Theoretically we take one prototype system—the cuprate superconductor—and try to understand the effects of the Dirac-like quasiparticle excitations on the superconducting properties.

Accomplishments

Theoretically we focused on two issues. The first is the effect of strong electron-electron interactions on the Dirac quasiparticles in the cuprate superconductors. Per our first publication, we performed the first exact treatment of the continuum gauge theory of high temperature superconductors. There we show that strong electron-electron interaction can significantly renormalize the quasiparticle charge. The second issue we addressed is the effect of external perturbations on the quasiparticle spectrum. In our second publication, we study the effect of local destruction of superfluid on the quasiparticles in the core of a superconducting vortex. We have shown that the density of low-energy excited states is very robust against such strong perturbation.

Experimentally, we have made significant progress towards measurements of a single graphene sheet. Figure 5 shows an atomic force microscopy (AFM) micrograph of a graphene platelet, consisting of approximately 10 graphene sheets, that is contacted by gold electrodes. The graphite rests on top of an insulating silicon dioxide layer grown on a silicon wafer. Initial transport measurements demonstrate that the silicon substrate can be used as a gate to adjust the electron density in the graphene sample. Other measurements show evidence for the quantum Hall effect in this system in an applied magnetic field. These are important steps forward toward isolating and measuring a single graphene sheet.

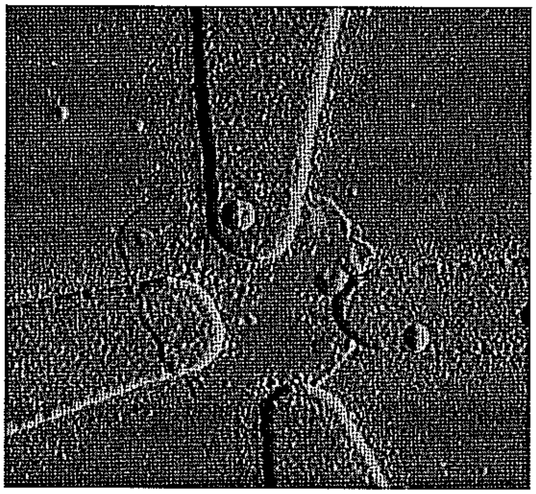

Figure 5: Submicron graphite platelet with attached electrodes.

Publications

D.H. Lee, "Superconductivity in a Doped Mott Insulator," *Phys. Rev. Lett.* **84**, 2694 (2000).

J.H. Han and D.H. Lee, "Structure of a Vortex in the t-J Model," *Phys. Rev. Lett.* **85**, 1100 (2000).

Infrared Spectroscopy of Complex Materials

Principal Investigators: Joseph Orenstein

Project No.: 99026

Project Description

Infrared (IR) spectroscopy is a powerful probe of new materials, enabling, for example, the discovery of gap-opening phase transitions and "pseudogaps" above the transition temperature. The goal of this project is to establish a capability for IR reflection and transmission measurements at the Advanced Light Source (ALS) and initiate the first experiments. IR spectroscopy will function synergistically with the angle resolved photoemission spectroscopy (ARPES) program at the ALS. ARPES is a powerful, but time intensive, technique. Characterization by IR spectroscopy can dramatically shorten the time for discovery of materials that have the most exciting and useful properties.

Synchrotron-based IR beamlines are considerably brighter than conventional (thermal) IR sources. At present, Beamlines 1.4.2 and 1.4.3 make use of the high brightness of the ALS to perform room temperature IR micro-spectroscopy using a Bruker IFS 66v/S spectrometer. We have added a cryostat, reflection optics, and a visible-light interferometer to enable variable-temperature reflection and transmission spectroscopy as well. The cryostat allows vertical positioning of up to three samples (typically one reference and two samples), as well as rotational alignment of the sample with respect to the IR beam.

Accomplishments

Initially, we successfully recruited student Chris Weber, who has extensive experience in far-IR spectroscopy, to work together with Michael Martin on the project. The first year of the project, FY1999, led to the following accomplishments:

- All the component parts have arrived and have been tested: cryostat, cryostat-spectrometer interface, helium-cooled bolometer, and sample mounts.
- Detailed characterization of the substrates, on which the thin film samples will be grown, has been performed. The substrates were found to be sufficiently transparent to permit transmission measurements from 20cm^{-1} to 200 cm^{-1}, which is the region of interest.

In the end year of this project, FY2000, we have performed the first successful measurements using the system described above. Steve Dodge, Chris Weber, and Michael Martin obtained far-infrared transmission spectra of two classes of oxide materials: the bismuth-based high-T_c superconductor and $SrRuO_3$, which is a ferromagnetic ruthenate. In the latter system, the far-infrared measurements were combined with other spectroscopic techniques to obtain the optical constants over unprecedented range, from approximately 3 to 3000 cm^{-1}. Using a variety of analytical techniques, the optical conductivity was determined over this entire range. The temperature dependence of the optical conductivity showed that the $SrRuO_3$ can not be described by Fermi liquid theory, which is the cornerstone of our understanding of more conventional metals. Instead, the conductivity obeys an extremely simple scaling law proposed in the context of high-T_c superconductors by Ioffe and Millis. The implications of the remarkable similarity between the optical conductivity of $SrRuO_3$ and that of high-T_c superconductors are currently under investigation.

Measurements were also performed on films of BSCCO, which is a high-T_c superconductor, at several values of the carrier concentration. The far-infrared spectra join together accurately in the region of overlap with transmission spectra obtained previously at lower frequencies using coherent time-domain terahertz spectroscopy. Together, the measurements add considerably to our understanding of charge transport in the controversial pseudogap region of the high-T_c phase diagram.

Publications

J. S. Dodge, C.P. Weber, J. Corson, J. Orenstein, Z. Schlesinger, J.W. Reiner, and M.R. Beasley, "Low-Frequency Crossover of the Fractional Power-Law Conductivity in $SrRuO_3$," *Phys. Rev. Lett.*, **85**, 4932 (2000).

J. Corson, C.P. Weber, J. Orenstein, S. Oh, J. O'Donnell, and J.N. Eckstein, "Carrier Concentration Dependence of the Optical Conductivity of $Bi_2Sr_2CaCu_2O_{8+\delta}$," (in preparation).

Investigation of the Quantum Well States in Magnetic Nanostructures

Principal Investigators: Zi Q. Qiu

Project No.: 98041

Project Description

Quantum Well (QW) states in layered nanostructures are generated by electron confinement in the surface normal directions. In magnetic nanostructures, a spin-dependent energy band produces spin-dependent QW states. This general character leads to our motivation to carry out an investigation on the QW properties and their relation to the recently discovered fascinating phenomena in magnetic nanostructures. In particular, we would like to understand the intrinsic relation between the QW states and the oscillatory interlayer magnetic coupling.

Photoemission is currently the most direct experimental technique for QW study as QW states can be easily identified as peaks in the photoemission spectrum. To have a systematic photoemission study of metallic QW states at the atomic scale, we proposed to perform photoemission on wedged sample, which can control film thickness continuously. Wedged sample, however, requires local probe, which is not common in photoemission. The beamline 7.0.1.2 at the Advanced Light Source (ALS) has the capability of fine photon beam size (~50-100μm) with high brightness (>10^{12} photons/sec at resolution power of 10,000). This unique capability makes it possible to perform photoemission experiments on wedged sample.

Accomplishments

Magnetic measurements suggest that the long- and short-period couplings are correlated with a relative phase and amplitude. Recent experiments revealed that the relative amplitudes depend sensitively on the interfacial roughness. However, the origin of the relative phase between the long- and short-period couplings remains unclear. To better understand the origin of the interlayer couplings with different oscillation periodicities, it has become very important to identify the relation of different QW states in k-space to explore the relative phase of the long- and short-period interlayer couplings. In this work, we obtained results on the momentum-resolved QW states using angle resolved photoemission spectroscopy (ARPES) as well as on the interlayer coupling using the magnetic x-ray linear dichroism (MXLD) on the Cu/Co(100) system. We first investigated the QW states in k-space by doing ARPES on a Cu wedge grown on Co(100) (Figure 6b and 6c). We then studied the interlayer coupling using the MXLD technique (Figure 6d). With a direct comparison to the QW results obtained from the ARPES (Figure 6e), we show that the QW phases at the Cu/Co interface in the k-space determine the relation of the long- and short-period oscillations in the interlayer coupling.

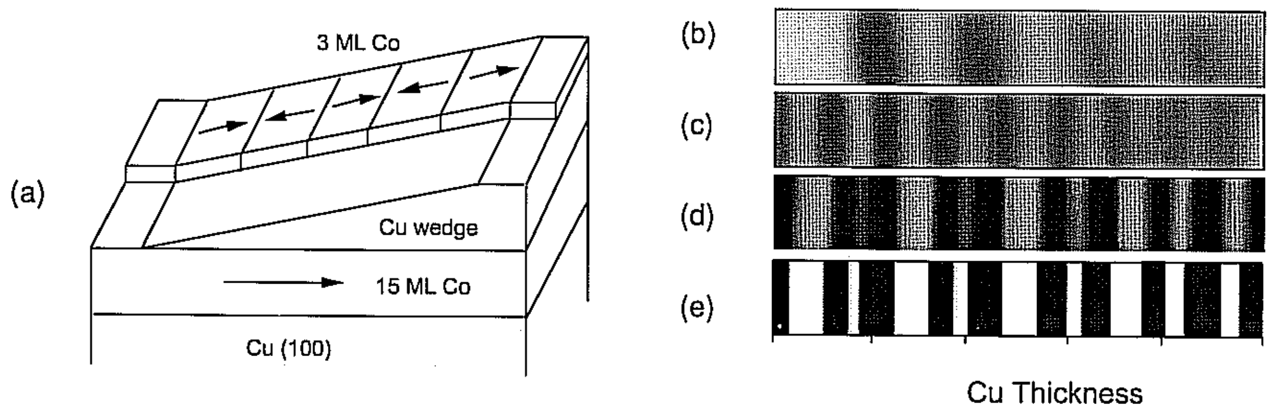

Figure 6: (a) Schematic drawing of the sample from which both QW states and the interlayer coupling were obtained. (b) Density of state (DOS) at the belly of the Fermi surface oscillates with 5.6 monolayer (ML) periodicity of the Cu thickness. (c) DOS at the neck of the Fermi surface oscillates with 2.7 ML periodicity of the Cu thickness. (d) Interlayer coupling from the MXLD measurements. The white and dark regions correspond to the antiferromagnetic and ferromagnetic interlayer couplings. (e) Interlayer coupling calculated from QW results of (a) and (b). The white and dark regions correspond to the antiferromagnetic and ferromagnetic interlayer couplings.

Publications

R. K. Kawakami, *et al., Phys. Rev. Lett.* **82,** 4098 (1999).

Z. D. Zhang, *et al., Phys. Rev. B,* **61,** 76 (2000).

Hyuk J. Choi, *et al. Phys. Rev. B,* **62,** 6561 (2000).

Results of these works were reported as invited talks in the 2000 APS March Meeting and 16th International Colloquium on Magnetic Films and Surfaces (ICMFS) (August, 2000).

Spatially-Resolved Residual Stress Characterization at Microstructural Dimensions

---

Principal Investigators: Robert Ritchie and Howard Padmore

Project No.: 99027

Project Description

A broad range of issues exists in materials science which have eluded full understanding due to an inability to experimentally quantify local micro-strains at spatial dimensions comparable to, and below, microstructural size-scales. The resultant stresses arising from such micro-strains are critical as they are additive to any applied stresses, and thus significantly affect any local defect mobility, deformation, and fracture behavior. As no techniques to date have been capable of quantifying the magnitude and gradient of such stresses/strains over micron-sized dimensions and under *in situ* loading conditions, this work was focused on the development of experimental methods and analysis for this purpose through the use of ultrahigh-brightness, x-ray micro-diffraction techniques at the Advanced Light Source (ALS), and the application of such techniques to several critical problems in materials engineering. The ALS provides the unique ingredient here due to its ability to produce high photon fluxes over spot sizes of micron dimensions, thus permitting three-dimensional stress and strain measurements within a single microstructural feature.

The approach involved three stages: (1.) the development and calibration of techniques, to measure the micro-strain gradients under *in situ* loading conditions and to determine three-dimensional strain states over microstructural dimensions, (2.) the refinement of these techniques to the problem of impact damage in titanium alloys, and (3.) the relaxation and redistribution of such residual stresses during subsequent *in situ* loading.

It is believed that the uniqueness of this work, i.e., the ability to measure local strain gradients to 1 part in 10,000 over micron-scale dimensions, the possibility of determining the complete three-dimensional stress and strain tensors within a single grain, and the capability of measuring such residual micro-strains during *in situ* loading experiments in the x-ray beam, provides new mechanistic insight into the problem of impact damage in metallic materials and the propensity of such damage to promote subsequent cracking under applied cyclic loading.

Accomplishments

While the application of the x-ray diffraction technique to the determination of residual stress fields has been well documented for several decades, the problem of a projectile impact provides several unique complications preventing the use of traditional techniques. These complications are: (a) the need for a small spot size (~300 μm or less) to correctly sample the strain gradient over millimeter dimensions and (b) the need for a highly parallel x-ray source to prevent divergence errors while sampling a non-planar surface (i.e. the indent ridge and concave floor). For these reasons, two synchrotron-based techniques have been applied to characterize the residual stresses produced from a projectile impact. A mesoscale technique (spot size ~300 μm) has been used to characterize stresses using traditional polycrystalline methods (i.e. the $\sin^2\psi$ technique). A microscale technique (spot size ~1μm) has been used to measure residual stresses in individual grains by observing distortion of each grain using Laue micro-diffraction recently developed at the ALS.

The primary conclusions from this work are as follows:

First, the surface-normal residual strain field has been determined experimentally by symmetric powder diffraction and numerically verified using finite element methods (FEM). Good agreement was found between these two results when the impact was formed at moderate velocities (200 m/s), Figure 7. However, when the impact was formed at high velocities (300 m/s), there is a notable discrepancy between the FEM and experimental x-ray results, the latter showing a less-intense residual strain field. These discrepancies are attributed to the quasi-static nature of the first-cut FEM simulation, and subsequent reanalysis, taking into account time-dependent effects, has shown that the discrepancy between the FEM and x-ray methods diminishes.

Second, each impact velocity produces very different levels of residual stress at the surface of the base of the crater. The equibiaxial stresses measured at the base of the crater are approximately -1000 MPa, -500 MPa, and +50 MPa at 0 m/s, 200 m/s, and 300 m/s respectively. Interestingly, in the 300 m/s case, which has the highest tensile stresses of the three cases, fatigue cracks do not tend to form at the crater floor, but instead, form at the crater rim due to the formation of incipient microcracks at the rim during the impacting process.

Third, the relaxation of residual stresses after impact due to subsequent fatigue cycling (maximum applied stress of 500 MPa, stress ratio of 0.1) has been experimentally observed. This relaxation, however, is only observed when (a) the magnitude of the residual stresses is sufficiently high, and (b) the residual stresses are sufficiently close to the crater to promote stress-amplitude magnification via the stress-concentration factor of the indent. Moreover, there is an indication that more relaxation occurs at the crater floor than at the rim of the crater. Such information has been incorporated into a fracture mechanics based model for the threshold conditions for high cycle fatigue failures from impact damage.

Finally, there is a high degree of point-to-point variability in the observed residual strain field. A fully annealed sample with no macroscopic residual stresses, can exhibit ~500 $\mu\varepsilon$ (~50 MPa equivalent uniaxial stress) of variability depending on the location of the spot when interrogated with a 300 mm x 300 mm spot size. This observed variability is well above the resolution of the technique (~100 $\mu\varepsilon$ or 10 MPa equivalent uniaxial stress). This variability is associated with local residual stresses (so-called "microstresses") locked in during the formation and cool-down of the anisotropic microstructure. The ALS microdiffraction technique verified that the grain-to-grain stress variations are on the order of 50 MPa (500 $\mu\varepsilon$)—providing for the first time a direct observation of the origins of these microstresses. Ongoing investigation should prove that the formation of fatigue cracks is at the location of most intense microstresses (in the absence of microcracks or other defects).

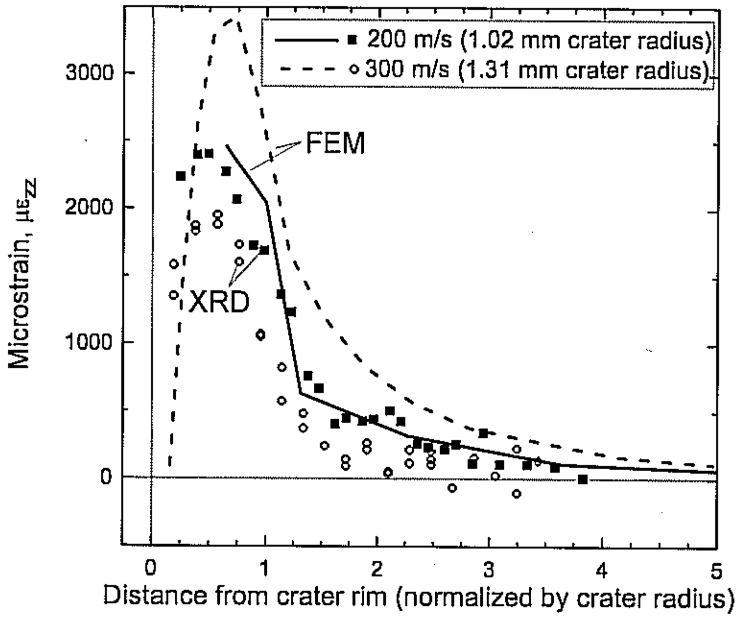

Figure 7: Survey of residual strain gradient emanating away from the crater rim at the surface of the specimen. The FEM results (lines) compare well to x-ray diffraction experiments (points) at 200 m/s, although there is significant discrepancy at higher impact velocities, i.e., 300 m/s, due to rate effects.

Publications

J.O. Peters, B.L. Boyce, A.W. Thompson, and R.O. Ritchie, "Role of Foreign-Object Damage on High-Cycle Fatigue Thresholds in Ti-6Al-4V." *Proceedings of the Fifth National Turbine Engine High Cycle Fatigue (HCF) Conference,* M. J. Kinsella, ed., Universal Technology Corp., Dayton, Ohio, 2000, CD-Rom, session 1, pp. 28-37 (2000).

B.L. Boyce, X. Chen, J.W. Hutchinson, and R.O. Ritchie "Residual Stresses Associated with Spherical Hard-Body Impacts in Foreign-Object Damage: Quasi-Static Numerical Analysis and Experimental Verification." to be submitted to *International Journal of Solids and Structures* (2000, draft).

Electron Spectroscopy of Surfaces under High-Pressure Conditions

Principal Investigators: Miquel Salmeron, Zahid Hussain, and Charles Fadley

Project No.: 99028

Project Description

The goal of this project is to build a special environmental chamber to perform studies at the liquid-gas and solid-gas interface at high pressures (up to 20 torr), using the high beam intensity of the synchrotron radiation at the Advanced Light Source (ALS). In its first phase, it will be applied to the study of the surface structure of ice near the melting point. The existence of a liquid-like layer on the ice surface at temperatures well below its triple point plays an important role in a wide variety of phenomena, such as ozone depletion in the upper stratosphere, acid rain, and the reduced friction of ice near its melting point. In another important application, the chamber and spectrometer should be invaluable in studies of catalysis, biological, and environmental sciences where surfaces are exposed to high pressure of gases or liquids. Until now, surface electron spectroscopy could only be performed in high vacuum conditions.

The purpose of the second-year was twofold. One was to complete the instrument development initiated in FY99 to develop capabilities for photoelectron spectroscopy studies of surfaces in high-pressure gas environments at the ALS. The successful development of such an instrument will revolutionize surface science, catalysis, environmental, and biochemistry studies. This development is possible thanks to the high intense photon flux and brilliance available at the ALS. The second objective was to apply the new instrument to spectroscopic studies of nanoscale wetting phenomena, i.e., the formation of liquid films a few monolayers thick in equilibrium with vapor in the torr pressure range.

The present FY00 LDRD was to complete the instrument development initiated in FY99, and to demonstrate its usefulness. One specific application will be the study of water and ice films. Ice below 0°C has a special surface structure consisting of several liquid-like layers. This is not well understood but is crucial in environmental and biological processes.

Accomplishments

A high-pressure electron transfer system (HPETS) was designed and parts were fabricated during the first year of this LDRD project in FY99. The HPETS system was assembled at the start of FY00 and the initial successful tests were made in December of 1999.

Operating parameters were determined for the differential pumping system and the electrostatic electron optics and HPETS control software was implemented and integrated into existing control software for the hemispherical electron energy analyzer.

A prototype experimental cell was constructed that could vary the distance between the sample surface and the HPETS entrance lens while controlling sample temperature in the –50° to +50°C range and delivering a controlled mass flow of water vapor or other gases.

Photoemitted electron spectra have been successfully obtained for several insulating and conducting samples at gas pressures up to 5 torr.

A series of HPETS experiments have been carried out to investigate the pre-melting of the ice surface. This problem has significant implications for environmental chemistry. A "liquid-like layer" is believed to exist at the ice surface below the bulk melting point, however there is no general agreement on the temperature dependent thickness of this liquid-like layer. Surface melting must be investigated with the ice sample in thermodynamic equilibrium with the vapor. The vapor pressure of ice varies from less than 0.01 torr at –85°C to 4.6 torr at the melting point.

We have used near edge x-ray absorption fine structure (NEXAFS) to investigate the structure of the ice-vapor interface. In this experiment at the LBNL ALS beamline 9.3.2, the oxygen 1s core level excitation cross section is measured as a function of incident photon energy in the range of 520-600 eV. In particular, this measurement probes the density of unoccupied molecular states, and spectra of solid ice, liquid water, and water vapor can be clearly distinguished. We monitored core-level excitation by using the HPETS to transfer photo-emitted electrons from the ice surface to a hemispherical electron energy analyzer, which measured the oxygen KLL Auger electron signal as a function of photon energy. In this way we obtained surface-sensitive NEXAFS spectra, since the Auger electrons come from the top ~2 nm of the sample surface—Auger electrons created deeper in the sample were attenuated by inelastic electron scattering and never reached the analyzer.

We have obtained important new results (see figure), which are being prepared for publication. Some key points include:

- We obtained Photoelectron spectra and Auger-yield NEXAFS spectra from the surface of liquid water above 0°C and, also, of super-cooled water.
- No changes were observed in the surface NEXAFS spectra for ice between –85°C and –10°C.
- A liquid-like layer in the top 2 nm of the ice surface was evident above –5°C.
- Even at –1°C the surface NEXAFS spectrum of the ice liquid-like layer could be clearly distinguished from that of liquid water.
- Monolayer contamination of the ice surface by organic molecules had a significant influence on the liquid-like layer of ice above –5°C.

Photoelectron spectra of –10°C ice, water vapor, and -85°C ice, showing core-level Auger emission and valence-level photoemission

Auger-yield NEXAFS spectra of liquid water, warm (-5°C) ice, and cold (-25°C) ice, showing premelting

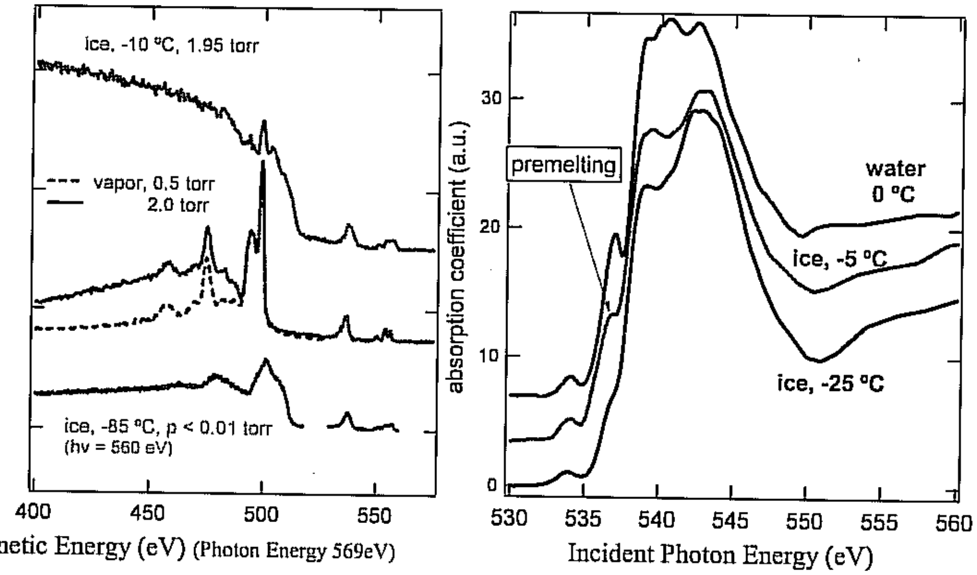

Figure 8: Auger-yield Surface NEXAFS spectra showing ice premelting.

Publications

H. Bluhm, D.F. Ogletree, C.H.A. Huan, C. Fadley, Z. Hussain, and M. Salmeron, "Photoelectron Spectroscopy of Water near the Triple Point," delivered at Western Regional Conference of the American Chemical Society, San Francisco, California, (October 2000).

H. Bluhm, D.F. Ogletree, C.H.A. Huan, C. Fadley, Z. Hussain, and M. Salmeron, "X-ray Absorption and Photoelectron Spectroscopy on Ice," delivered at ICESS (International Conference on the Electronic Structure of Surfaces) Berkeley, California, (August 2000).

D. F. Ogletree, H. Bluhm, C. Fadley, Z. Hussain, and M. Salmeron, "Photoemission at 5 Torr," delivered at ICESS 8 (International Conference on the Electronic Structure of Surfaces), Berkeley, California, (August 2000).

H. Bluhm, D.F. Ogletree, C.H.A. Huan, C. Fadley, Z. Hussain, and M. Salmeron, "The Liquid-like Layer on Ice: A NEXAFS Study" delivered at EMSL 2000 (Environmental Molecular Sciences Symposia), Pacific Northwestern Laboratory, Richland, Washington (June 2000).

H. Bluhm, D.F. Ogletree, C.H.A. Huan, C. Fadley, Z. Hussain, and M. Salmeron, "Thickness of the Liquid-like Layer on Ice Determined by Fluorescence Yield NEXAFS," (in preparation).

H. Bluhm, D.F. Ogletree, C. Fadley, G. Lebedev, Z. Hussain, and M. Salmeron, "Development of a High Pressure Electron Transfer Lens for Photoelectron Spectroscopy Up to 10 Torr," (in preparation).

Single-Molecule Protein Dynamics

Principal Investigators: Shimon Weiss

Project No.: 99030

Project Description

This project seeks to develop methods to study conformational changes and folding/unfolding pathways of single macromolecules by novel single molecule fluorescence spectroscopy techniques. Fluorescence resonance energy transfer (FRET), which measures the proximity between two fluorophores, is used to measure distance changes, and therefore conformational dynamics, between two points on a macromolecule. This distance serves as a reaction coordinate for folding/unfolding, denaturation and charge screening reactions. Performing such measurements on the single molecule level has important advantages over conventional ensemble measurements, since it (1) resolves and quantitatively compare distinct sub-populations of conformational states, otherwise invisible at the ensemble level; and (2) resolves dynamic conformational changes, otherwise hidden at the ensemble level because of lack of synchronization.

Two kinds of molecules have been investigated: single stranded DNA (ss-DNA) and the protein Chymotrypsin Inhibitor 2 (CI2). In the first experiment, ss-DNA is used to study the statistical and dynamical properties of a short polymer, with only very few Kuhn segments. While the conformational statistics of long single- and double-stranded DNA have been studied extensively using traditional methods such as sedimentation velocity, light scattering, and optical tweezers, these methods are inadequate for the studies of polymers on the 100Å scale, far from the infinite chain limit. Properties such as the persistent length and the characteristic ratio of DNA oligonucleotides in this distance range (15 to 60 bases in length) change significantly with increasing chain length. While models have been proposed to calculate the end-to-end distance distributions and scaling properties in such oligonucleotides, they have not been systematically tested experimentally. Such scaling issues and the effects of solvent environment on the polymer conformational properties are being studied.

The molecule CI2 is used for single-molecule protein-folding experiments. The problem of protein folding is of great significance from both fundamental and practical points of view. How a relatively unstructured protein in its unfolded state finds its way through a huge conformational space to a small ensemble of structures that is the native state is a question that has fascinated physicists, chemists, and biologists for many decades. Furthermore, the current effort in genome research is producing massive quantities of protein sequence information that needs to be converted into structural and functional information. A detailed understanding of protein-folding mechanisms is therefore a very important piece of this puzzle. Although much has been learned about the issue, especially in the last decade, the complexity of protein structure precludes detailed studies from being carried out using ensemble methods. These methods lose a lot of the dynamic and stochastic information that is both fascinating and crucial to the understanding of the physics of protein-folding mechanisms.

Accomplishments

ss-DNA

Using single-stranded DNA (ss-DNA) as a model polymer system, single-pair FRET (spFRET) was used to study polyelectrolyte chain distributions, dynamics, and scaling properties in the short chain regime. There are several outstanding fundamental questions regarding polyelectrolytes in solution, especially due to the complexity resulting from Coulomb interactions. Single-molecule studies on relatively isolated polyelectrolytes could help answer these questions. In order to study scaling issues in this length regime, a series of short poly-dT oligonucleotides ($(dT)_{15}$, $(dT)_{20}$, $(dT)_{30}$, $(dT)_{40}$, and $(dT)_{50}$), end labeled with donor and acceptor dyes were synthesized. Poly-dT sequences were chosen to minimize specific interactions between residues in the chain for this first set of experiments, and lengths were chosen by considering isomeric state simulations. We calculated the characteristic ratio for ss-DNA as a function of length in bases. The characteristic ratio provides a measure of the polymer stiffness. The points are averages from simulations based on the rotational isomeric model, while the line is a fit of this simulation data to the worm-like chain model. This model assumes a continuum form for the polymer chain, with a certain amount of rigidity. The fit gives a persistence length of 15Å for these idealized conditions, which is within the range of recent experimental estimates. An important point to note is that although C_n eventually levels out for ss-DNA with N>100, it has a strong, non-linear dependence for shorter lengths. Additional histograms for $(dT)_{20}$ as a function of salt concentration were produced, showing the collapse of the DNA molecule at higher concentrations where electrostatic screening between the DNA backbone negative charges becomes more effective. Fits to the histograms allow the calculation of modified characteristic ratios ($\langle R^2 \rangle / N$), as a function of length, for several salt concentrations. A downward slope in 100mM and 1M salt means that the size of the ss-DNAs increases more slowly than one would expect for a Gaussian chain. This could indicate poor solvent conditions and a collapsed structure for high salt. Several corrections must be included to improve the accuracy of the above results—these issues are under current investigation. Thus, the spFRET method allows measurement of polymer end-to-end distances at low concentrations, which minimizes any intermolecular interaction between strands. Furthermore, it provides a simple test for heterogeneity in the sample due to such aggregation effects.

CI2

The spFRET distance measure provides an effective reaction coordinate that affords a global view of the conformational distributions and dynamics during the folding reaction. CI2 was chosen for two major reasons, the wealth of existing ensemble folding data for this protein, and the relative ease of synthesis of site-specifically donor-acceptor labeled protein. The presence of many common elements of secondary structure and the simple two-state folding behavior exhibited by CI2 make the protein an ideal model system for these first single-molecule folding investigations. We prepared spFRET histograms at three different concentrations along the denaturation curve. At or below 3M GdmCl, a peak at around 0.95 energy transfer efficiency (E) is observed, corresponding to the folded state. At high denaturant concentration (6M), only a peak at around 0.65 E is detected, corresponding to the unfolded state. As intermediate denaturant concentrations are scanned, varying ratios of the two peaks are observed; the sample histogram at 4M GdmCl shows approximately equal 0.65 and 0.95E peaks. The assignments of the peaks were confirmed by comparison to data from a destabilized mutant of CI2 (K17G), which shows the same peaks in the histogram, and whose relative ratio is a different function of denaturant concentration, consistent with its lowered stability. Hence, using these spFRET histograms, the folded and unfolded states of CI2 can be directly observed and quantified, and this work provides a direct confirmation of the two-state folding model previously inferred from ensemble data. Since the areas of the peaks are a measure of the occupation probabilities for the two states, a fractional occupation for the folded state can be extracted. A plot of this fraction versus denaturant concentration results in a single-molecule denaturation curve. Such curves derived from ensemble data are routinely used to quantify protein stability. GdmCl denaturation curves for pseudo wild-type CI2 and the destabilizing mutant were also done.

It is noteworthy that the single-molecule curves are indistinguishable within error of the ensemble curves, showing that the equilibrium properties of the system are faithfully reproduced by the single-molecule diffusion experiment, providing a validation of the methodology for such studies. An interesting distinction may be drawn between the ensemble and single-molecule curves. In equilibrium ensemble experiments, direct information concerning the fraction of the protein in a particular state is not available since only average properties are measured. In contrast, the single-molecule approach analyzes the occupation probabilities of the individual states directly. Potentials calculated using the E histograms show the presence of a double-well shape in the transition region. The figure depicts upper bounds on widths of these wells, and lower bounds on the barriers between them, due to the width contributions described earlier. Such potentials can be used for comparisons to theory. While the reported potentials are crude approximations, better analysis methods and future experiments on immobilized molecules will allow the calculation of more accurate potentials. Intriguingly, the mean E measured for the denatured peak shows a poorly resolved shift close to the transition region, which might correspond to changes in the overall dimensions of the protein as a function of denaturant (the 'fast collapse').

Publications

A. Deniz, T. Laurence, G.S. Beligere, M. Dahan, A.B. Martin, D.S. Chemla, *et al.*, "Single Molecule Protein Folding: Diffusion Förster Energy Transfer Studies of the Denaturation of Chymotrypsin Inhibitor 2," *Proc. Natl. Acad. Sci.* USA, 97, 5179-5184 (2000).

S. Weiss, "Measuring Conformational Dynamics of Biomolecules by Single Molecule Fluorescence Spectroscopy," *Nature Structural Biology*, 7, 724-729 (2000).

A. Deniz, T. Laurence, M. Dahan, *et al.*, "Ratiometric Single-molecule Studies of Freely Diffusing Biomolecules," *Annual Reviews in Physical Chemistry* (2000, in press).

Improved Temporal Resolution Femtosecond X-Ray Spectroscopy

Principal Investigators: Robert Schoenlein, Alexander Zholents, Max Zolotorev, Phillip Heimann, and T. Glover

Project No.: 98023

Project Description

We propose a novel technique for generating femtosecond x-ray pulses from the Advanced Light Source (ALS). This will improve the temporal resolution available at an existing bend-magnet beamline from 30 ps to ~250 fs. The availability of ultrashort x-ray pulses from a synchrotron source will open new areas of research in physics, chemistry, and biology, by allowing the motion of atoms in materials to be directly probed on the time scale of a vibrational period, which is the fundamental time scale for structural dynamics, chemical reactions, phase transitions, etc. High brightness femtosecond x-rays will allow researchers to combine powerful x-ray structural probes such as diffraction and extended x-ray absorption fine structure (EXAFS) with ultrafast pump-probe techniques. In addition to being a significant enhancement of the ALS, this proposal is an important first step toward the development of a fourth generation synchrotron light source, providing two to three orders-of-magnitude improvement in time resolution over existing synchrotron sources. The main components (femtosecond laser system and modifications to the ALS storage ring) are already in place, and considerable progress has been made towards the development of the source. This proposal seeks funding to complete the development and characterization of the femtosecond x-ray source. We expect that a successful demonstration of this source will serve as the basis for proposing the construction of a beamline specifically for femtosecond x-ray science at the ALS.

The temporal duration of synchrotron light pulses is determined by the duration of the stored electron bunches, typically >30 ps. We propose to reduce the duration of the x-ray pulses by more than two orders-of-magnitude by selecting radiation which originates from a short (~100 fs) temporal slice of the electron bunch. Such a slice can be created through the interaction of a femtosecond laser pulse co-propagating with an electron bunch in an appropriate wiggler. The high electric field of the laser pulse modulates the energy of a slice of the electron bunch. The accelerated and decelerated electrons are spatially separated from the main electron bunch by a bend magnet. Femtosecond x-rays will be generated at an existing beamline by imaging the synchrotron radiation from the displaced femtosecond electron slice. Initial measurements of the pulse duration will be made by cross-correlating visible light from the beamline with laser pulses in a nonlinear crystal.

Accomplishments

We have demonstrated, for the first time, the generation of femtosecond synchrotron pulses from a storage ring. We have developed sensitive diagnostics for monitoring the interaction between the laser and the electron beam. We have made detailed measurements of the femtosecond time structure, created in the stored electron bunch by a femtosecond laser pulse, and manifest in the synchrotron radiation from an ALS bend-magnet beamline. This was accomplished by cross-correlating visible light from the beamline with ~50 fs pulses from the laser in a nonlinear crystal. The measured pulse duration (~300 fs) is determined by the time-of-flight stretching of the electron bunch as it propagates from the wiggler to the bend-magnet beamline ($1/8^{th}$ of a storage ring orbit). The agreement between model calculations and experimental measurements of the time structure gives us confidence that for an optimally-placed beamline (immediately following the wiggler), synchrotron radiation pulses of 100 fs duration may be generated using this technique.

Based on these results, we have designed and constructed a bend-magnet beamline specifically for time-resolved experiments using the laser/electron-beam modulation technique. The beamline collects radiation from the middle bend magnet immediately following the wiggler (in which the laser/electron-beam interaction occurs). In this location, the expected x-ray pulse duration is 100 fs. The beamline consists of a toroidal mirror, which images the source onto a pair of slits for selection of the femtosecond synchrotron radiation. A double-crystal monochromator (interchangeable with a plane-grating spectrometer) is used for wavelength selection. Differential pumping allows operation from ~0.1 to 10 keV.

The laser system used for the demonstration experiments has been upgraded for operation with the new bend-magnet beamline. Using a larger pump laser and cryogenic cooling of the Ti:sapphire crystal in the amplifier enables operation of the laser at 5 kHz. In addition, the beam transport and alignment optics, which control the laser interaction with the electron beam, have been upgraded and automated with computer controls.

Finally, we have designed and proposed a femtosecond undulator beamline for the ALS. This beamline is based on a small-gap undulator and a 40 kHz laser system, and will provide ~10^3x more flux and ~10^4 higher brightness than the bend-magnet beamline over the range from 0.3-8 keV. The following figure illustrates the expected flux and brightness from the bend-magnet beamline, which is presently being commissioned, and the proposed undulator beamline. Such a beamline adds a capability for ultrafast x-ray science and will open new areas of research in physics, chemistry, and biology by allowing the direct study of structural dynamics on the time scale of a vibrational period, ~100 fs.

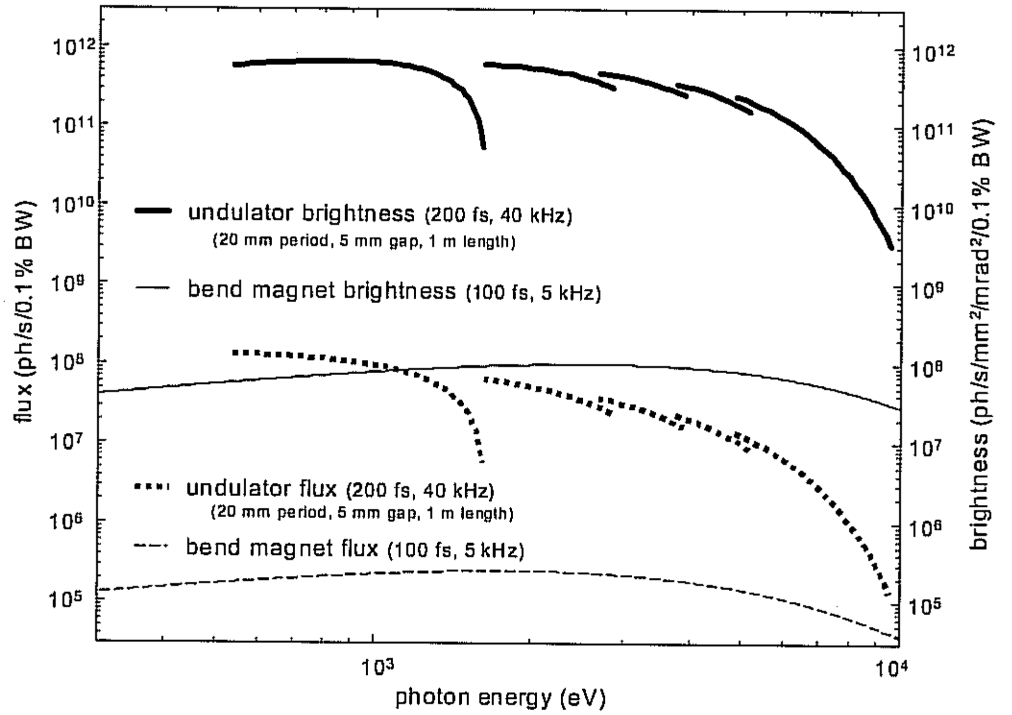

Figure 9: Average femtosecond flux and brightness from the proposed undulator beamline compared with that of the existing bend-magnet beamline.

Publications

Schoenlein, Chattopadhyay, Chong, Glover, Heimann, Shank, Zholents, and Zolotorev, "Generation of Femtosecond Pulses of Synchrotron Radiation," *Science*, (2000).

Schoenlein, Chattopadhyay, Chong, Glover, Heimann, Leemans, Shank, Zholents, and Zolotorev, "Generation of Femtosecond X-rays via Laser-Electron Beam Interaction," *Applied Physics B* (2000).

Schoenlein, Chong, Glover, Heimann, Shank, Zholents, and Zolotorev, "Femtosecond X-ray Pulses from a Synchrotron," *Ultrafast Phenomena XII, Springer-Verlag Series in Chemical Physics* (in press, December 2000).

Nuclear Science Division

New Exotic Nuclear Beams by Implementation of the "Recyclotron Concept"

Principal Investigators: Joseph Cerny

Project No.: 98024

Project Description

For the past two years, LDRD funding has supported the BEARS (Berkeley Experiments with Accelerated Radioactive Species—see the FY99 LDRD annual report for more detailed background). The BEARS project has now successfully accelerated its first radioactive beam, Carbon-11, at the 88-Inch Cyclotron. In the final year the goal of this joint Nuclear Sciences Division/Life Sciences Division project was to extend the complement of short-lived beams that can be provided by BEARS, in particular Oxygen-14. In addition, development of a radioactive-beam technique termed a "recyclotron" was to be performed. In this method, the 88-Inch Cyclotron is used first to produce the radioactive isotope of interest, and then later, to accelerate it as a beam. Fifteen-hour half-life Krypton-76 was selected for this demonstration.

Accomplishments

Production of Oxygen-14 in a suitable chemical form, carbon dioxide, has proved much more difficult than first expected, due to a combination of high levels of radiation-induced chemistry in the production target and the need for much higher specific activities than has been achieved in past work with oxygen isotopes (Oxygen-15 used in medicine for PET scans). Much effort has gone into exploring different, new techniques. The most promising has been the production of Oxygen-14 in the form of water vapor, that is then catalytically converted by a two-step process to carbon dioxide. Extension of the BEARS automated system to include this procedure was incorporated in this project.

One advantage of the new work is its applicability to the development of an Oxygen-15 beam, with only a little extra effort. The difficulties with oxygen chemistry have also increased our understanding of techniques that will be useful in the future development of radioactive-fluorine beams.

On the "recyclotron" method, test runs have been performed, looking at the production and release of krypton isotopes by two different nuclear reactions. Engineering and design of a remotely-operated target and activity-handling system was also addressed.

Gamma Ray Studies using the 8π Spectrometer Array

Principal Investigators: I-Yang Lee, Lee Schroeder, and David Ward

Project No.: 98025

Project Description

The 8π Spectrometer, on loan from McMaster University, has been operating in Cave 4C at the 88-Inch Cyclotron since April 1998. The instrument is made up of a high-quality Bismuth-Germanate (BGO) spherical shell of 72 detectors and an array of twenty HPGe detectors with BGO Compton-Suppressor shields. A number of auxiliary detectors and special equipment developed for the spectrometer have also been employed, including the computer-controlled recoil-distance apparatus. The combination of these apparatus makes the 8π a unique gamma-ray spectroscopy instrument and this capability was applied to the observations specified below and in the publications.

Accomplishments

The following are a few highlights of the experimental program:

Jacobi Shapes

This experiment received very little beam-on-target because of the problems with the Cyclotron. However, it provided very important checks on the complementary experiments with Gammasphere done previously at Argonne National Laboratory. A central issue in studies of the Jacobi shapes is isolating spectra corresponding to a selected Gamma-ray multiplicity, which, in turn, is related to the spin at the top of the Gamma-ray cascade. This multiplicity selection is done by gating on the number of Gamma-ray hits on the array. Since the 8π Spectrometer differs considerably from Gammasphere in how this quantity is measured, experiments may be viewed as independent determinations of the multiplicity spectra associated with a particular reaction and, as such, must give the same result. A major paper on the Jacobi effect in atomic nuclei is in preparation.

Precision Studies of Transitional Nuclei

For isotopes of Sm, Gd, and Dy there is a transition from well-deformed shapes at N=92, to near-spherical shapes at N=86. Surprisingly, there is still much experimental spectroscopy to be performed following beta decay in such well-studied systems as 152Eu→152Sm.

Modern arrays, such as the 8π Spectrometer, have revealed much more detail concerning the spectroscopy of vibrational bands than was previously possible. Many earlier studies are being found to be incorrect in some crucial details. These details usually involve the strengths of very weak gamma-branches, which determine whether a level belongs to a particular collective structure or not. The theoretical understanding of these bands is incomplete and very controversial at the present time.

The spectrometer operation was terminated in FY2000. Up to that time, there were seven experiments carried out, using a total of 384 hours of beam time. In addition to Lawrence Berkeley National Laboratory staff, other users included groups from three U.S. universities, and eight foreign institutions. The spectrometer was decommissioned and shipped to the TRIUMF facility in Vancouver, Canada.

Publications

C.M. Petrache, D. Bazzacco, T. Kroell, S. Lunardi, R. Menegazzo, C. Rossi Alvarez, G. LoBianco, G. Falconi, P. Spolaore, A.O. Macchiavelli, D. Ward, R.M. Clark, M. Cromaz, P. Fallon, G.J. Lane, A. Galindo Uribarri, R.M. Lieder, W. Gast, I. Ragnarsson, and A.V. Afanasjev, "Stable Triaxiality at the Highest Spins in ^{138}Nd and ^{139}Nd," *Physical Review C* **61**, 011305-1 (1999).

B. Djerroud, B. Schaly, S. Flibotte, G.C. Ball, S. Courtin, M. Cromaz, D.S. Haslip, T. Lampman, A.O. Macchiavelli, J.M. Nieminen, C.E. Svensson, J.C. Waddington, D. Ward, and J.N. Wilson, "Fission Barriers, Coupled-Channel and Shell Effects at the Coulomb Barrier in the A~190 Mass Region," *Physical Review C* **61**, 024607-1 (2000).

D.E. Appelbe, G. Martinez-Pinedo, R.A. Austin, G.C. Ball, J.A. Cameron, B. Djerroud, T.E. Drake, S. Flibotte, A. Melarangi, C.D. O'Leary, C.E. Svensson, J.C. Waddington, and D. Ward, "High-Spin Structure of $^{58}{}_{26}$Fe$_{32}$," accepted for publication in *PRC.*

J. Domscheit, A. Görgen, J. Ernst, P. Fallon, B. Herskind, H. Hübel, W. Korten, I.Y. Lee, A.O Macchiavelli, N. Nenoff, S. Siem, D. Ward, and J.N. Wilson, "Angular Momentum Limit of Hf-Isotopes Produced in Three Fusion-Evaporation Reactions," accepted for publication in *Nuclear Physics A.*

D.E. Appelbe, R.A. Austin, G.C. Ball, J.A. Cameron, B. Djerroud, T.E. Drake, S. Filbotte, C.D. O'Leary, A. Melarangi, C.E. Svensson, J.C. Waddington, and D. Ward, "Gamma-Ray Spectroscopy of $^{57}{}_{25}$Mn$_{32}$ and $^{58}{}_{25}$Mn$_{33}$," *European Physical Journal A* **8**, 153-155 (2000).

A. Görgen, H. Hübel, D. Ward, S. Chmel, R.M. Clark, M. Cromaz, R.M. Diamond, P. Fallon, K. Hauschild, G.J. Lane, I.Y. Lee, A.O. Macchiavelli, and K. Vetter, "Spectroscopy of ^{200}Hg After Incomplete Fusion Reaction," *European Physical Journal A* **6**, 141-147, (1999).

A. Görgen, H. Hübel, D. Ward, S. Chmel, R.M. Clark, M. Cromaz, R.M. Diamond, P. Fallon, K. Hauschild, G.J. Lane, I.Y. Lee, A.O. Macchiavelli, and K. Vetter, "Search for Magnetic Rotation in ^{202}Pb and ^{203}Pb," (to be published).

G.J. Lane, A.P. Byrne, R.M. Clark, M. Cromaz, M.A Deleplanque, R.M. Diamond, G.D. Dracoulis, P. Fallon, A. Görgen, H. Hübel, I.Y. Lee, A.O. Macchiavelli, S. Schmel, F.S. Stephens, C.E. Svensson, K. Vetter, and D. Ward, "Resolution of the Anomalous Shape Coexistence in ^{185}Hg and Observation of a Signature-Dependent Prolate-Oblate Interaction Strength," (to be published).

D.E. Appelbe, G. Martinez-Pinedo, R.A. Austin, J.A. Cameron, J. Chenkin, T.E. Drake, B. Djerroud, S. Flibotte, D.N. Parker, C.E. Svensson, J. C. Waddington, and D. Ward, "√-Ray Spectroscopy of $^{56}{}_{26}$Fe$_{30}$," *Physical Review C* **Volume 62**, 064314.

Vacuum, Radio Frequency (RF), and Injection Systems for High-Intensity Stable Beams

Principal Investigators: Claude Lyneis and I-Yang Lee

Project No.: 99032

Project Description

The goal of this LDRD was to identify and make an engineering evaluation of potential improvements to the 88-Inch Cyclotron to create a premier stable beam facility. A Department of Energy (DOE) decision to move forward with an advanced isotope separator on line (ISOL) capability —the Rare Isotope Facility (RIA)—follows the completion of the ISOL white papers, which identified several key areas in nuclear physics. These include nuclear astrophysics, nuclear structure, exotic nuclei, and heavy elements and will require both stable and radioactive beams. For that reason, we envision there will be a need for a premier stable beam capability to complement the planned ISOL facility. The main focus of this proposal is to study the re-engineering of the cyclotron to modernize it and provide new capabilities and scientific opportunities.

The first task is reconstruction of the vacuum system, including the vacuum enclosure, to produce very high vacuum for the transmission of very heavy ions made by the Advanced Electron-Cyclotron Resonance ion source (AECR-U), now, and, in the future, by the Versatile Electron-Cyclotron Resonance ion source for Nuclear Science (VENUS), which is under construction. Measurements of the transmission of high charge-state ions, coupled with an analysis of the cyclotron vacuum and losses due to charge pickup and charge stripping, indicate that significantly higher transmission could be achieved by improving the cyclotron vacuum to 1×10^{-7} Torr.

The second task is redesign of the center region geometry and improvement of the RF system to provide single-turn extraction and improved beam timing. Analysis and particle tracking need to be done to explore the possibility of achieving precise single-turn extraction. In addition, upgrade of the axial injection system is necessary to increase the transmission of high-intensity heavy-ion beams. Beam optics calculations, including space charge, can now be done to evaluate methods for compensating for the space-charge effects observed with high-intensity beams.

Accomplishments

The beam optics for the injection line between the AECR-U and the cyclotron were calculated in detail for the first time. The calculations included full space-charge effects and realistic source emittances. The AECR-U emittances were measured for a wide range of beam species, charge states, and intensities, to provide starting conditions for the optics calculations. These experiments showed that the emittance is relatively independent of beam intensity, but that it depends strongly on ion mass and charge state. In addition, plasma instabilities cause significant emittance growth. Figure 1 shows the excellent emittance measured for a high-intensity (50 eμA) $^{86}Kr^{19+}$ beam with the very stable plasma conditions. The beam transport calculations demonstrated that high-intensity beams become too large in the lower half of the axial injection line due to the space charge of the beam. The most straightforward solution to this is to increase the injection voltage. To test this idea, a new mirror inflector that can operate at higher voltages was developed and a radial probe was installed on the cyclotron so that beam centering at higher injection voltages could be experimentally studied. These measurements indicated that it is possible to increase the injection voltage from 10 to 15 kV and still center the beam. This increases the transmission of high-intensity beams through the axial line by 30%. Operation at injection voltage significantly above 15 kV will require the design and construction of a spiral inflector and changes in the center region geometry. This design process will benefit from the complete set of beam transport codes and tools developed as part of this LDRD.

An engineering analysis determined that the best approach to improve the cyclotron vacuum would be to construct a central cryopanel. A low-profile cryopanel could be built and installed on the cyclotron trim coil platter just opposite to the Dee. This would provide up to 30,000 l/s of additional pumping close to the center of the machine, where beam loss due to charge pickup is most severe. Excess refrigeration capacity from the pair of 1400 helium refrigerators could be used to keep the inner panel at 20°K for optimum pumping.

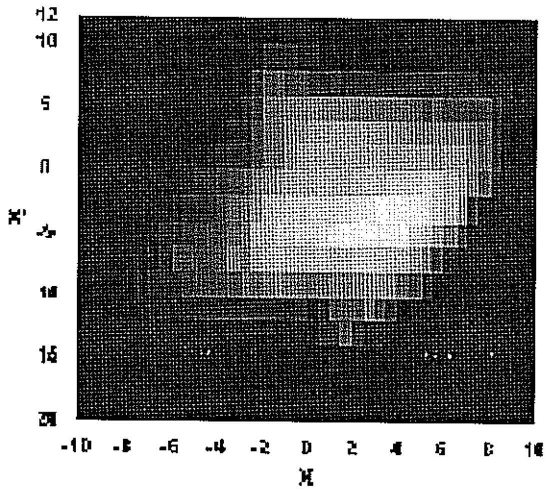

Figure 1: An emittance plot for a 50 eμA beam of $^{86}Kr^{19+}$ from the AECR-U with a normalized root mean square value of 03. π mm-mrad.

Publications

D. Wutte, M.A. Leitner, and C.M. Lyneis, "The Berkeley 88-Inch Cyclotron Injector System," submitted for publication in *Proceedings of the European Particle Accelerator Conference (EPAC-2000)* (June 6, 2000). *http://ecrgroup.lbl.gov/NEWS/EPACPapers/index.htm*

D. Wutte, M.A. Leitner, and C.M. Lyneis, "Emittance Measurements for High Charge State Ion Beams Extracted from the AECR-U," submitted for publication in *Proceedings of International Conference on the Physics of Highly Charged Ions,* (July 30, 2000) *.http://ecrgroup.lbl.gov/papers_pdf/MP058WUTTE.pdf*

D. Wutte, "The 88-Inch Cyclotron External Injector System," Lawrence Berkeley National Laboratory Internal Report LBID-2349 (September 2000).

First Chemical Study of Element 108, Hassium

Principal Investigators: Heino Nitsche and Uwe Kirbach

Project No.: 99033

Project Description

The purpose of this project is to develop the pre-requisites for and carry out a first-time study of the chemical properties of hassium (Hs), element 108. The major goals of the program are:

- Development, construction, and testing of the Recoil Product transfer Chamber (RTC) interfaced to the Berkeley Gas-filled Separator (BGS) and a chemical reaction unit where the hassium undergoes chemical conversion.
- Design and testing of a Cryo-Thermochromatographic Separator (CTS). The CTS thermochromato-graphically separates the hassium reaction products from other actinide reaction products and identifies them by α decay.

- Study for the first time the chemical properties of hassium and determine if it behaves in a similar manner as its chemical homologues ruthenium (Ru) and osmium (Os).

The chemical identification will be achieved by combining a novel chemical separation system with the advantages of the BGS. The BGS provides good and fast separation of transfer products stemming from impurities of the nuclear target and from long-lived spontaneous fission products. The novel chemical separator is based on the expected high volatility of the tetroxides of hassium and consists of a chemical reaction chamber and the CTS.

The development of the RTC is an important part of this project and is needed to directly couple the BGS with the chemical separation system, which will facilitate further separation from the actinides and detection by nuclear counting. In the chemical reaction chamber, the nuclear reaction products coming from the RTC via a gas jet are subjected to an oxygen/helium gas mixture at a reaction temperature of 1200°K to form volatile hassium tetroxides. The volatile oxides are then transported via the gas stream through a capillary to the CTS, leaving behind non- and less-volatile compounds. The CTS consists of an assembly of two rows of 32 silicon PIN-diodes arranged opposite each other, forming a narrow rectangular channel through which the transport gas flows. A negative temperature gradient ranging from room temperature to about 150°K is applied to the PIN-diode assembly. This results in the deposition of the hassium tetroxide on one of the detectors, where it can be identified by α-counting. We expect a separation factor of 10^7 to 10^9 for actinides from the combined BGS-CTS system.

For the production of hassium, which has an estimated half-life of about 9.3 seconds, we will use the reaction ^{26}Mg (^{248}Cm, 5n) ^{269}Hs. As model experiments, the chemical volatility and the chromatographic properties of the oxides of the lighter hassium-homologue osmium will be studied in on-line experiments using short-lived α-decaying isotopes.

Accomplishments

In FY99, we designed and constructed the Recoil product Transfer Chamber (RTC), the transfer device between the BGS and a chemical separation system. It was mounted on the back-end of the BGS focal plane detector chamber to allow a fast transfer of pre-separated recoil nuclei from the BGS to the chemistry system. A wire-grid-supported thin mylar foil with a thickness down to 200 $\mu g/cm^2$ was used to separate the BGS detector chamber, at 1.3 mbar pressure, from the chemistry system at different pressures ranging from 480 mbar to 2000 mbar. Thin windows are necessary to accommodate penetration of the recoil nuclei with relatively low kinetic energy. We tested the RTC in different experiments to determine the transfer efficiency. The reactions ^{164}Dy(^{40}Ar, xn)$^{204-n}$Po and ^{197}Au(^{22}Ne, xn)$^{219-n}$Ac were used to measure the efficiencies of the evaporation residues (EVR) at different kinetic energies of 43 MeV and 11 MeV, respectively. The overall efficiencies of the transport ranged between 30% and 15%, compared to the activity measured in the focal plane detector of the BGS. These experiments encouraged us that the RTC can be used to connect the BGS with a chemical separation system like the CTS or the automated liquid-liquid extraction system SISAK 3.

In FY00, the CTS was designed as a separation and α-decay detection system for the highly volatile tetroxides of osmium and hassium, element 108. The CTS consists of two rows of 32-α detectors arranged along a negative temperature gradient. The tetroxides adsorb on the surface of one of the silicone photodiodes at a certain deposition temperature, and the nuclide is then identified by the α-decay. To test the CTS with the expected hassium homologue osmium, different α-active osmium isotopes were produced using the nuclear reactions ^{118}Sn(^{56}Fe, 4,5n) ^{170,169}Os and ^{120}Sn(^{56}Fe, 4,5n) ^{172,171}Os. After pre-separation in the BGS, a mixture of 90% helium and 10% oxygen was used to transport the osmium to a quartz tube heated to 1225°K, where OsO_4 was formed. The negative temperature gradient in the CTS ranged from 248°K to 173°K. Using a flow rate of 500 mL/min most of the osmium activity was adsorbed at a temperature of about 203°K. From the measured α-activity distribution, an adsorption enthalpy of 40±1 kJ/mol for OsO_4 on the detector surface was calculated using Monte Carlo simulations. The results show that the CTS is working properly and can be used in an experiment to study the chemical properties of hassium.

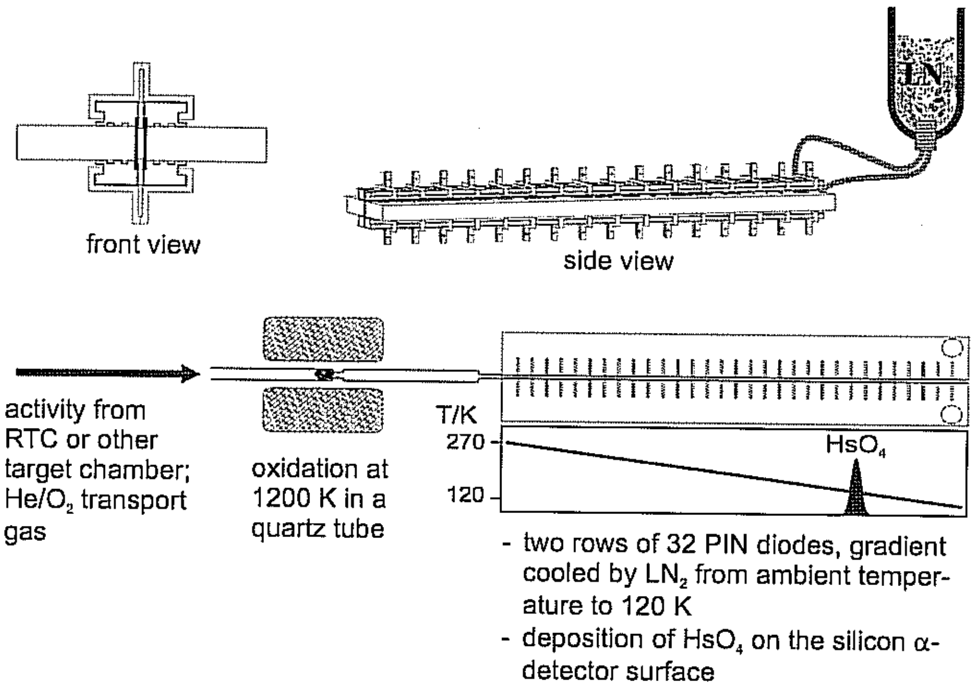

Figure 2: Schematic and working principle of the Cryo-Thermochromatographic Separator (CTS) and detector that was used to identify volatile osmium tetroxide, a homologue of hassium (Hs, element 108). This experimental set-up will be used for the first chemical identification of hassium.

Publications

U.W. Kirbach, *et al.*, "CTS, A Cryo-thermochromatographic Separation and α-Detection System for Volatile Heavy Ion Reaction Products," in preparation for *Nucl. Instr. Meth. A*.

U.W. Kirbach, *et al.*, "RTC, A Recoil Product Transfer Chamber for Heavy Element Chemistry at the Berkeley Gas-filled Separator," in preparation for *Nucl. Instr. Meth. A*.

U.W. Kirbach, *et al.*, "A New Interface for Heavy Element Studies at the Berkeley Gas-filled Separator," invited presentation at the 220th ACS National Meeting, Washington, D.C. (August 20-24, 2000).

U.W. Kirbach, H. Nitsche, K.E. Gregorich, D.C. Hoffman, and V. Ninov, "Superheavy Element Chemistry Studies at the Berkeley Gas-filled Separator," invited presentation and poster at the Heavy Element Chemistry Contractors' Meeting, Argonne National Laboratory, Chicago, IL (November 19-21, 2000).

Integrated Physiome Analysis

Principal Investigators: Adam Arkin, Inna Dubchak, Teresa Head-Gordon, Stephen Holbrook, and Saira Mian

Project No.: 00022

Project Description

This project is an integrated computational and experimental program to elucidate the molecular basis for type-1 pili phase variation in uropathic *E. coli* and the sporulation initiation program of *Bacillus subtilis*. Both these pathways represent genetic switches that respond to environmental signals in order to change the behavior of a population of bacteria. In addition, both these switches are "imperfect" in that the population splinters into heterogeneous subpopulations that have different behaviors. Both pathways are also involved in the pathogenic potential of the organism or a closely related microbe. Type-1 pili mediate adherence of uropathic *E. coli* to the urinary track epithelium, and the sporulation pathway in *Bacillus subtilis* is nearly identical to that in *B. cereus B.* and *anthracis* both of which are human and animal pathogens. The biochemical and genetic networks underlying these switches are of sufficient complexity that it is nearly impossible to reason qualitatively about their function. Thus, we propose to further develop an integrated database and data-mining tool called Bio/Spice specialized for the kinetic simulation and analysis of biochemical and genetic reaction networks. We have found such a tool necessary for systematizing, consistency checking, and hypothesis testing experimentally derived information about any biological process of even moderate complexity (without the tool, an experimentally validated model of the λ-phage lysis lysogeny decision, sufficient for prediction, took over two years). The combined research program will deliver Bio/Spice to the biomedical community as a useful new bioinformatics tool, and will yield insight into two industrially and medically important pathways. Once these pathway models are validated against experimental data (from our own laboratory and our collaborators), we will explore the means of pharmaceutical control of these processes (e.g. to force 100% sporulation of a *B. subtilis* population) and test how well such interventions fare when parameters change due to mutation. A central goal is to further develop the Bio/Spice platform.

Accomplishments

The findings and outcomes of this project are of two types. Bio/Spice technology development has proceeded on all fronts: the central database has been completed; a number of ontologies for data, models, analyses, biological experiment, and data types have been developed to aid in classification and mining of data; the simulator has been updated with new theory on stochastic simulations and heuristic algorithms for mixed stochastic/deterministic/algebraic equation simulation; and the graphical user interface has been further developed. On the biological side, description and analysis of the type-1 pili control system has been completed and an extension to host/pathogen interactions has been embarked upon. In addition, the results gathered herein have led to further funding from Defense Advanced Research Projects Agency (DARPA) and Office of Naval Research (ONR).

Bio/Spice

The Bio/Spice tool is meant to be an integrated suite of database and data-analytical and pathway-analytical tools for understanding cellular dynamics on the genomic scale. The tool is constructed from a database that holds edited biological information on cellular pathways, genetic sequence, strain information, etc., as well as primary data from technologies such as gene chips and two-dimensional protein gels. Also in the database are sets of bio-object models for processes as diverse as gene expression and cell locomotion and integrated models of biological processes composed from these bio-objects and parameterized with data from the edited database. We have finalized design of version 0.2 of the database integrating National Center for Biotechnology Information (NCBI) standards as part of the design. We have also built additions for storage of primary biological data. A working example of the haploinsufficiency profiling databases is now on the web. The database supports different chip designs, tag assignments, normalization methods, and experimental types. The full database has hundreds of tables and relations and updates will be made periodically. The user interface has undergone a number of revisions in design to incorporate thoughts on cytomechanics and transport phenomena, as well as more phenomenological modeling methods (scheduled events and algebraic and logical statements).

Type-1 Pili Phase Variation:

In order to make sure that Bio/Spice covers data and biological processes of sufficient breadth and flexibility to simulate any process in a cell, we have chosen a number of focusing problems on which to hone the technology. One of these is a model of environmental control of type-1 pili phase variation in uropathic *E. coli*. This system is controlled by the stochastic flipping of a 314-basepair piece of chromosomal DNA that includes the promoter for the pili structural genes. The inversion is mediated by two proteins: one that mediates inversion from the "ON" to the "OFF" orientation, the other that mediates inversion in both directions. A number of biochemical sensing systems [(H-NS and leucine-responsive regulatory protein (Lrp)] impinge on the ability of these proteins to mediate the flipping. We discovered that the network structure is such that the percent of the population that is piliated in the environment and the time it takes to move from one percentage of piliation to another are independently controlled. In addition, we uncovered the source of the temperature sensor in the circuit that is controlled by the H-NS protein: a particular configuration of binding sites in the promoter regions of FimE and FimB (the invertases). These two former system outputs are regulated by the ratio of FimE and FimB activity, and the method by which the ratio affects these variables is further switched by the activity of Lrp.

Publications

C. Rao and A. Arkin, "Control Principles in Biological Networks," *Annual Review of Biomedical Engineering* (in press).

D. Wolf and A. Arkin, "Control of the Type-1 Pili Phase Variation Switch," (draft).

C. Rao and A. Arkin, "A Singular Perturbation Theory for the Master Equation: Application to Simulation of Enzymatic Reactions," (draft).

Structural/Functional Genomics and Pathways: D. radiodurans and B. subtilis

Principal Investigators: Adam Arkin, Teresa Head-Gordon, Stephen Holbrook, and Daniel Rokhsar

Project No.: 00023

Project Description

The sequencing of the complete genomes of a variety of microbes, the metazoan *C. elegans, Drosophila* and the soon to be completed human genome, are a driving force for understanding biological systems at a new level of complexity. The goal of the computational structural and functional genomics initiative of the future is to link these sequencing efforts to a high-throughput program of annotation and modeling of both molecular structures and functional networks. We propose to build a coherent computational biology program at Berkeley Lab by linking research in DNA modeling; protein fold recognition, comparative modeling, and *ab initio* prediction of individual gene products; molecular recognition of protein-protein and protein-nucleic acid complexes; and modeling biochemical and regulatory pathways, using *Deinococcus radiodurans* and *Bacillus subtilis* as our test beds.

To explore the basis for survival of *D. radiodurans* under extreme conditions of DNA damage, and the sporulation/competence switch in *B. subtilis* under nutrient stress, we will construct molecular models of the key components of the DNA repair system including damaged DNA, multigenomic repair intermediates such as Holliday junctions, proteins known or yet to be discovered that are involved in DNA repair, as well as higher order protein-protein or protein-nucleic acid complexes implicated in repair, replication, and transport. A model for sporulation of *B. subtilis* will be developed using Bio/Spice and other modeling tools to identify the control mechanism of the sporulation/competence switches in cell nutrition. An essential element of the proposed program is to develop connections between the analyses of single molecules, complexes, and networks, to establish a coherent program for integrating structural and functional annotation into systems-level understanding for any organism.

Accomplishments

Prediction of Protein Function

Our functional assignment of hypothetical and unknown proteins identified in genomic sequences assumes that proteins having a common function will also have common sequence characteristics that allow them to perform that function. If these sequence characteristics can be extracted, they can be used to predict whether hypothetical or unknown proteins have that function. We have tested this assumption on the general class of nucleic acid binding proteins. A compilation of these sequences can be used to compute parameters for training neural networks and to identify novel nucleic acid binding proteins. An initial database of ~100 nucleotide binding proteins and ~100 non-nucleotide binding proteins were selected from the annotated genome of *M. genitalium*. Global sequence descriptors, previously utilized in protein fold recognition, were used as input parameters to train computational neural networks on this protein database. Neural networks were trained for these descriptors and voting between these predictions was conducted. Using jackknife cross-validation, remarkably accurate predictions were possible considering the crude approximations of clustering all nucleic acid proteins together and lack of parameter and network optimization. After training, these neural networks can be used to identify novel nucleic acid binding proteins among the hypothetical and unknown proteins of the *M. genitalium* genome. Several predicted nucleic acid binding protein genes are clustered along the genome. For example, MG055, MG057, and MG059 are all predicted to code for nucleic acid binding proteins. Interestingly, tentative annotations of MG057 (as a primase-like DNA binding protein) and MG059 (as a homologue of the RNA binding protein smpB) have been made (www.tigr.org) in agreement with our predictions.

Prediction of Protein Structure

Our most recent research has involved the determination of the structure of helical proteins with about 70 amino acids, utilizing networks of workstations at Colorado and the Cray T3E at the National Energy Research Scientific Computing Center (NERSC). The results of our global optimization approach appear to be at the leading edge of protein structure determination for α-helical proteins via optimization. Starting with predictions of secondary structure from neural networks that are incorporated as hints within the global optimization algorithm, and utilizing global optimization techniques, these algorithms have determined the structure of two helical proteins with 70 and 71 amino-acids, the A-chain of uteroglobin, 2utg A, and a four-helix bundle DNA binding protein, 1pou. 1pou is a transcription factor that binds specifically to the octamer motif (ATTTGCAT) of immunoglobulin promoters, and activates these genes in eukaryotes, and binds DNA in a similar way to the prokaryotic transcription factors Cro and repressor. Our resulting predictions for the entire structures are within 6.3Å r.m.s. deviation of the nuclear magnetic resonance (NMR) structure for 1pou. Substituting correct secondary structure prediction for the hints within the global optimization for 1pou resulted in structures with r.m.s. deviations of under 5.0Å. According to a recent article, the probability of obtaining a 6Å r.m.s. deviation by chance is so remote that a prediction algorithm obtaining such structures should be considered quite successful. We believe that this common structural motif for DNA-binding proteins found in *D. radiodurans* and *B. subtilis* is something that we can predict with quite good accuracy *ab initio*.

Considering the computational complexity of predicting protein structure and function for whole genomes like Deinococcus, or for protein members of DNA-repair pathways, we have also directed this year's effort to improving the parallelization of the global optimization algorithm. Protein structure prediction presents a tree search problem (to be precise, exploring nodes of a forest of dynamically generated trees of configurations) that is extremely difficult to solve. Our hierarchical approach is scalable to large-scale parallel computers, and we have demonstrated that it runs effectively on 400 processors on the Cray T3E at NERSC and on a network of DEC/alpha workstations at the University of Colorado. In fact, as the number of processors increases new categories can be added to the hierarchy to avoid communication bottlenecks. This is an important feature for even larger problems.

Prediction of Protein Structural Domains

Many of the proteins involved in DNA repair are known to be multi-domain both in structure and in function. Our plan is to develop approaches for assignment of domain structure directly from sequence (global and local) and apply these methods to the prediction of proteins involved in DNA repair, specifically in *D. radiodurans*. To test the hypothesis that multi-domain proteins can be distinguished from single-domain proteins and their own sub-domains based on their amino acid sequence, we compiled local databases from the RCSB (Research Collaboratory for Structural Bioinformatics) Protein Data Bank and the SCOP (Structural Classification of Proteins) database. After extensive manual editing to remove fragments—homo and hetero-multimers and proteins that are not clearly a single structural domain—we compiled a database of single domain proteins consisting of 170 examples. We have also compiled databases of homodimers, homotrimers, homotetramers, and heterodimers. A database of sub-domains of the multi-domain database was also constructed, as was a database of linker sequences of various sizes connecting the constituent domains of multi-domain proteins.

A variety of sequence-related parameters can be calculated from these various databases that may be useful in distinguishing domain structure. One of these is amino acid composition, which we calculated for each of the multi-domain proteins, their sub-domains, and the single domain proteins.

In contrast to the global sequence methods described above, local sequence information can also be used. An approach to finding the domain boundaries of multi-domain proteins is to identify the linker sequences between the domains. From these same databases, we analyzed preferences in the sequences of linkers, which join protein domains.

Protein Function Analysis

We have also studied several models for deriving low-frequency protein dynamics from low-resolution structures. Such low-frequency motions have been consistently implicated in protein function, either as large-scale conformational changes or smaller-scale active-site adaptations. Since homology modeling typically yields low-resolution structures, the models we are considering are well suited to genome-scale analyses. In addition, the formation of protein complexes often involves the deformation of the participating partners, and a characterization of the energies and entropies of deformation is essential for understanding complex formation and function. Models introduced earlier by Jernigan and his collaborators model the dynamics of proteins by a one-dimensional network of springs connecting nearby alpha-carbons; we have extended this model to a full three-dimensional network. We showed that the crystallographic "B-factor," which is well predicted by these models, can in fact be related (by an analytical perturbation theory calculation) directly to the effective coordination number of each residue. The normal mode calculations and a general-purpose graphical viewer for examining protein motions have been implemented and are currently being applied to several proteins of local interest at Berkeley Lab and University of California, (UC) Berkeley.

Regulation of Sporulation/Competence in B. subtilis

In this last year, we have been filling out our knowledge of the *B. subtilis* sporulation cascade. To aid in this work, we started collaboration with an experimental group on UC Berkeley campus to understand the timing and regulation of asymmetric development and develop assays for population heterogeneity that are important to deducing the structure and function of the sporulation network. While cultures of *B. subtilis* can be induced to sporulate en mass by resuspension in a specialized medium, the resulting sporulating cells are by no means synchronized. The sporulating population represents a rather broad distribution of progress through the various developmental stages of sporulation. This dispersion complicates the interpretation of experimental results obtained from the population as a whole, as in the measurements of enzyme activity taken from whole culture homogenates. A quantitative understanding of the dispersion is also important in drawing inferences as to which microscopic processes occur deterministically in time and which are stochastic, a distinction that can significantly accelerate the development of a quantitative microscopic model.

Publications

S. Crivelli, T. Head-Gordon, R.H. Byrd, E. Eskow, and R. Schnabel, "A Hierarchical Approach for Parallelization of a Global Optimization Method for Protein Structure Prediction," *Lecture Notes in Computer Science, Euro-Par '99*, P. Amestoy, P. Berger, M. Dayde, I. Duff, V. Fraysse, L. Giraud, and D. Ruiz (eds.), pg. 578-585 (1999).

S. Crivelli, T.M. Philip, R. Byrd, E. Eskow, R. Schnabel, R.C. Yu, and T. Head-Gordon, "A Global Optimization Strategy for Predicting Protein Tertiary Structure: α-Helical Proteins," *Computers & Chemistry* **24**, 489-497 (2000).

A. Azmi, R.H. Byrd, E. Eskow, R. Schnabel, S. Crivelli, T. M. Philip, and T. Head-Gordon, "Predicting Protein Tertiary Structure Using a Global Optimization Algorithm with Smoothing," Optimization in Computational Chemistry and Molecular Biology: Local and Global Approaches, C. A. Floudas and P. M. Pardalos, editors (Kluwer Academic Publishers, Netherlands) 1-18 (2000).

T. Head-Gordon and J. Wooley, "Computational Challenges in Structural and Functional Genomics," *IBM Systems Journal on Deep Computing in the Life Sciences*, B. Robson, J. Coffin, W. Swope, editors (2000, in press).

S. Crivelli and T. Head-Gordon, "A Hierarchical Approach for Parallelization of Large Tree Searches," submitted *to J. Parallel and Distributed Computing* (2000).

Development and Application of the General Theory of Hydrophobicity to Interpret Stability and Dynamics of Biological Assemblies

Principal Investigators: David Chandler

Project No.: 00024

Project Description

While hydrophobic interactions are of fundamental importance in structural biology, a general theory for these forces has not existed. The primary source of the difficulty is the well known yet puzzling multifaceted nature of hydrophobic interactions. We have shown that the resolution of the difficulty is found in the different roles of hydrophobicity at small and large length scales. We have derived equations that describe these different roles and the competition between them. This development opens the way for a quantitative understanding of microscopic and mesoscopic assembly and adhesion. The purpose of this research is to carry out such extensions and applications of the theory, specifically to systems of biological interest.

Specifically, we will develop generally applicable algorithms to apply the Lum-Chandler-Weeks theory equations. These algorithms will be applied in conjunction with molecular dynamics. This approach, coupled with a course-grained dielectric description of electrostatics, provides an implicit solvent model for biomolecule solvation.

Accomplishments

During the first year of this project, we began by studying the temperature dependence of hydrophobic effects, especially the concept of entropy convergence often used to interpret the thermodynamic properties associated with protein folding. Contrasting experimental observations of the temperature variation for hydration-free energies for small alkane chains and for extended oil-water interfaces shows that temperature dependence at small length scales is markedly different that at large length scales. Our recent work has shown that the Lum-Chandler-Weeks (LCW) theory can successfully interpret the contrasting temperature variations. Our analysis shows why entropy convergence temperatures for protein folding are universally lower than those for small hydrophobic molecules, and the amount by which it is lower can be understood in terms of the number of hydrophobic residues and the size of the folded protein.

A longer-term development has focused on creating a computationally efficient method for using LCW theory to estimate solvent-mediated forces in proteins and protein assemblies of arbitrary shape and composition. Here, we have succeeded at constructing what the theory implies for the free energy surface governing a slowly varying density field, $n(r)$. This field lives on a cubic lattice, with lattice spacing given by the course graining length of LCW theory (roughly 0.4 nm, the correlation length of bulk water at ambient conditions). The field's free energy Hamiltonian is of the Ising form, where $n(r)$ takes on the values of 0 and 1 corresponding to vapor and liquid, respectively. "Bare" nearest neighbor couplings coincide with the liquid-vapor surface tension of water. In the presence of hydrophobic species, density fluctuations on length scales smaller than the course graining length renormalize these nearest neighbor couplings and also the chemical potential. In the simplest case, these hydrophobic species are cavities. The cavities move through the lattice in continuous space. The renormalizations are functions of the composition and configuration of the hydrophobic species.

For a given configuration of hydrophobic solutes, the mean field equations that follow from the Hamiltonian for $n(r)$ are LCW's principal equations of the average field $\langle n(r) \rangle$. For arbitrary compositions and configurations, it is difficult to solve these equations. Since the task is carried out numerically, one may dispense with mean field approximation altogether. Instead, since it is a field of binary numbers, numerical simulations of its behavior by stochastic methods, such as Monte Carlo, may be easily performed.

A dynamical model for hydrophobic solutes moving in water employs this model to determine solvent-averaged forces affecting the hydrophobic species. The solvent averaging is done by averaging over a specified number of Monte Carlo passes over the field, $n(r)$. The particular number of passes sets the time scale for course-grained solvent motions relative to the molecular dynamics time steps for the solutes. The solutes move according to Newton's laws with the solvent averaged forces. This scheme provides a remarkably simple computational means for capturing collective solvent effects. With modest modification, it can be generalized to include the role of polarity. In a preliminary application, we have used it to study the nucleation of a hydrophobic cluster in water. A few pictures illustrating results from this work are shown in Figure 1.

Drying Induced Nucleation of Oil Droplets in Water

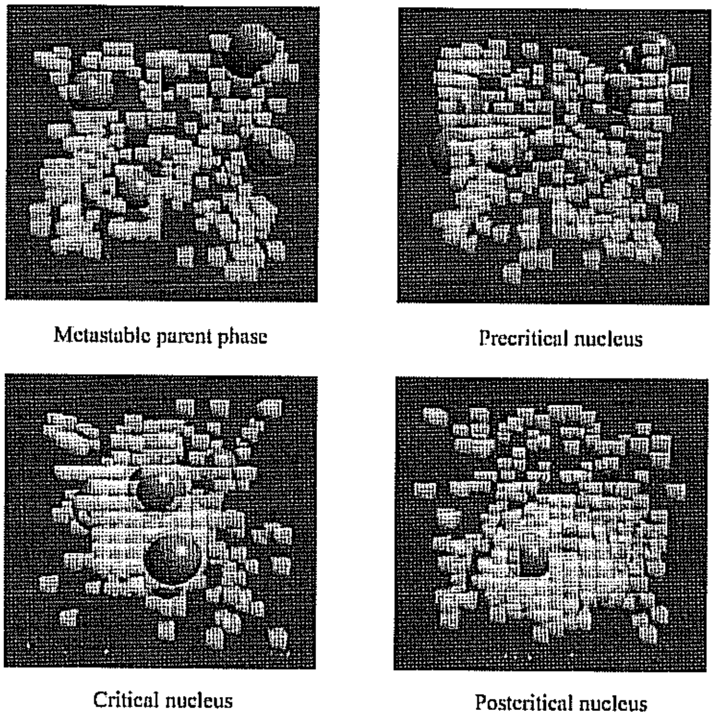

Figure 1: Nucleation of an oil droplet in water. The aggregation of the hydrophobic objects is driven by a drying transition (transparent cubes indicate cells that are "vapor") of the hydrophilic solvent.

Publications

D.M. Huang and D. Chandler, "Temperature and Length Scale Dependence of Hydrophobic Effects and Their Possible Implications for Protein Folding," *Proceedings of the National Academy of Science* (April 18, 2000).

P.R. TenWolde, S. Sun, and D. Chandler, "Manifestations of Phase Equilibria in the Solvation of Microscopic Solutes," (in preparation).

Structural Biology of Large Biomolecular Complexes

Principal Investigators: Thomas Earnest

Project No.: 99035

Project Description

This project seeks to understand how biomolecular assemblies are formed, and how complexes of proteins and nucleic acids activate and modulate biological function. This includes the transient recognition and assembly of these molecules to define their role in signal transduction, and the investigation of large permanent assemblies. This research depends on tools and methods from a number of disciplines—molecular biology, biochemistry, and cell biology—along with access to a bright, tunable synchrotron crystallography beamline. There are two main components that serve as the basis of this project.

Wnt Receptor Pathway Proteins and Protein Complexes

The *Wnt* gene products are a family of secreted glycoproteins, which bind to transmembrane receptors and transduce developmental signals. In the past few years, there has been extensive research into the role of the *Wnt* gene products in cellular proliferation and the establishment of cell fate in both invertebrates and vertebrates. There has been a concurrent identification of the role of several members of the *Wnt* signal transduction pathway in cellular development, and in certain cancers. The misregulation of members of cellular development pathways is commonly seen in several types of cancer.

Since a number of these proteins are involved in more than a single pathway, it is critical to study the interactions of the molecules, which lead to differential activation. The atomic-resolution structure of the biologically-relevant complexes will illuminate how the interactions of these proteins mediate the function of these pathways. Since these are typically weak, transient interactions among large molecules, structural studies of these proteins typically will require high-brightness synchrotron-radiation sources. The requirement of multiwavelength anomalous diffraction (MAD) for phase information requires the tunability that only bright synchrotron sources offer.

Members of the *Wnt* family bind to the membrane-bound receptor, *frizzled*, which appears to consist of seven transmembrane helices. The proposed extracellular region of *frizzled* contains a conserved cysteine-rich domain. An extracellular protein, *frzB*, contains a homologous cysteine-rich domain and acts as an endogenous antagonist of *Wnt* signalling. It is believed that *frzB* binds to *Wnt*, preventing binding of *Wnt* to *frizzled*. The binding of *Wnt* to *frizzled* activates *dishevelled*, which then negatively regulates glycogen synthase kinase (GSK-3). GSK-3, *dishevelled*, axin, beta-catenin, and adenomatous polyposis coli (APC) protein form an intracellular complex of more than 600,000 daltons, which regulates beta-catenin levels. This regulation of beta-catenin, which later forms an intranuclear complex with LEF/TCF proteins and other transcriptional co-activators to regulate transcriptional activity, is a key step in the development of the organism. The misregulation of beta-catenin has been definitively linked to various forms of cancer.

The 70S Ribosome and Functional Complexes

The ribosome is the machinery that translates information from the genome into the production of proteins. The 70S ribosome is a massively large complex of 3 RNA and 52 protein molecules with a total molecular weight of over 2.5 million daltons, and consists of two subunits, 30S and 50S. The 50S subunit contains the peptidyl transferase activity responsible for amino acid ligation, while the interaction between the messenger RNA template and the aminoacylated transfer RNAs is mediated by the 30S subunit. The determination of the atomic structure of the 70S ribosome will serve as a basis for understanding ribosomal function, as well as a broader understanding about how these complexes are assembled and stabilized. Thus the significance of elucidating the structure of the 70S ribosome, as well as the technical difficulties of this task, makes it an ideal target for a full-scale effort for structure determination by the Macromolecular Crystallography Facility at the Advanced Light Source (MCF/ALS).

In an effort led by Dr. Harry Noller at University of California at Santa Cruz—who has extensive experience in RNA and ribosomal molecular biology, biochemistry, and crystallization—we undertake the determination of the structure of the 70S ribosome at atomic resolution, along with the structure of its functional complexes. Dr. Noller's group has obtained crystals that yield native data to 6-angstrom resolution at the MCF/ALS. Electron density maps to 7.8-angstrom resolution have been calculated that reveal the structural arrangement of a number of components of the ribosome. One particularly useful approach, which is unique to the MCF/ALS, is the ability to perform MAD experiments around the absorption edges of several atoms, including the uranium Mv edge at 3.55 keV. This is useful since the anomalous signal at this energy is large enough to phase a complex as massive as the 70S ribosome. We will continue to develop methods and instrumentation to improve the quality of the data from the MCF/ALS for this project, which will be generalizable to other large complexes. Furthermore, we will develop computational methods for determining structures of this size and difficulty. This will include multi-solution phasing approaches to determining the structure of large macromolecules.

Accomplishments

Over the past year, we have continued to pursue two primary projects that seek to understand the biomolecular structure and function of large complexes: the 70S ribosome in collaboration with Dr. Harry Noller and complexes of the *Wnt* signal transduction pathway in collaboration with Dr. Randall Moon, Howard Hughes Medical Institute (HHMI)/ Washington. We are also seeking to develop methods to express, purify, and crystallize proteins and protein complexes of large size and with intrinsically weak, but biologically-relevant, interactions.

70S Ribosome

The resolution of the 70S ribosome has been extended to 5.0 angstroms leading to a large enrichment of the details of this large multi-component complex of RNA and protein. These studies have contributed significantly to our understanding of ribosomal function, as well as ribosomal structure, for large RNA molecules. In addition, methods and protocols for collecting and processing data were explored and optimized. These structures were solved by MAD experiments using the iridium anomalous signal.

Wnt pathway complexes

Three structures of the PDZ domain from *Xenopus disheveled* have been solved by independent MAD experiments using the selenomethionine-derivatized protein. These structures are: monomeric, homodimeric, and in complex with the C-terminal peptide of a protein, *Dapper*—discovered by two-hybrid analysis with *disheveled* PDZ as bait. This eight amino-acid peptide was tightly bound and has been observed to lose binding upon deletion of the C-terminal, which has the consensus PDZ binding domain sequence, -MTTV. These structures indicate different conformational substates, which are being correlated with developmental states with cellular assays based on these structures. A number of other proteins and protein complexes have been expressed and purified and are in crystallization trials.

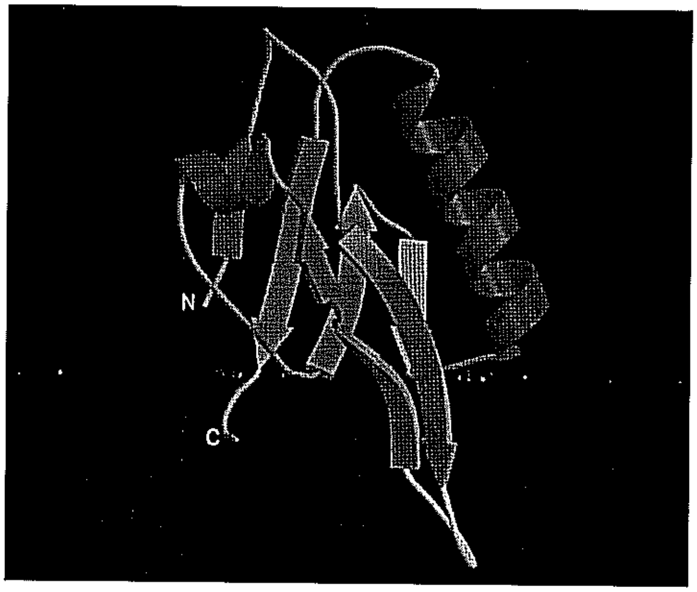

Figure 2: Structure of the PDZ domain of Xenopus disheveled.

Publications

N. Khlebtsova, L. Hung, K. Henderson, R. Moon, and T. Earnest, "Crystallization and Preliminary X-ray Studies of the PDZ Domain of *Dishevelled* Protein," *Acta Cryst. D.* **56**, 212-214 (2000).

J.H. Cate, M.M. Yusopov, G.Z. Yusopova, T.N. Earnest, and H.F. Noller, "X-ray Crystal Structures of 70S Ribosome Functional Complexes," *Science* **285**, 2095-2104 (1999).

N. Khlebtsova, L. Hung, B. Cheyette, J. Miller, R. Moon, and T. Earnest, "Structure of the Xenopus PDZ Domain in Monomeric, Homodimeric, and Peptide-complexed Forms," (in preparation).

B. Cheyette, N. Khlebtsova, J. Miller, T. Earnest, and R. Moon, "Novel *Dishevelled* PDZ Domain Interacting Protein, *Dapper*," (in preparation).

Novel Approaches to the Study of Molecular Organization in Living Cells

Principal Investigators: Jay Groves

Project No.: 99044

Project Description

The purpose of this project is to develop new strategies for imaging and studying the dynamic spatial organization of molecular components in living cells. In recent work, we have introduced the concept of using microfabricated substrates to impose patterns and structure on fluid lipid bilayer membranes. This fairly general technique combines standard microfabrication processes with membrane self-assembly to produce lipid membranes with precisely defined patterns. The aim of the current research is to develop micropatterned membranes, along with more general structures, as novel means of examining the role of dynamic organization in cell membranes on the micrometer and nanometer scale.

This project involves a cross section of several rather different technologies. Conventionally microfabricated substrates will be used to guide the assembly of membranes and proteins into desired geometries. These hybrid bio-solid-state structures will then be employed in various experiments with proteins and living cells. Information will be gathered largely by fluorescence microscopy.

Accomplishments

In this work, phospholipid bilayers were employed as biomimetic coating materials to modulate the adhesion and growth of cells on solid substrates. We have explored the use of lipid composition in supported membranes as a means of controlling the adhesion and growth of cells on solid substrates. Two naturally adherent cell lines, HeLa (human cervical carcinoma) and NIH3T3 (mouse fibroblast), were cultured on a panel of supported membranes covering a range of lipid compositions and charge densities. All of the membrane compositions examined block cell adhesion except those containing phosphatidylserine (PS). PS is known to promote the pathological adhesion of erythrocytes (abnormally expressing PS in the outer leaflet of their membrane) to endothelium in conditions such as sickle cell disease, falciparum malaria, and diabetes. In our studies, PS-containing membranes strongly promoted adhesion and growth in both cell lines studied. This finding allowed us to use lipid bilayer patterning technology to selectively direct cell adhesion to specified elements in a membrane microarray.

Membrane microarrays displaying alternating corrals of PS-containing and PS-free membrane were deposited on prefabricated substrates with either 200 μm or 500 μm grid sizes. The membrane within each corral in the microarray is fluid while grids of chrome barriers on the silica substrate prevent mixing between separate corrals. Different fluorescently labeled lipids were incorporated in the various membrane types, allowing them to be distinguished in the microarray. Cells cultured on microarray surfaces selectively adhered to and grew on the PS-containing membrane corrals. Figure 3 illustrates fluorescence (3A) and phase contrast (3B) images of a 4-corral section of a microarray. The fluorescence from the membrane in the upper two corrals identifies them as PS-containing, while membrane in the lower two corrals is PS-free. The corresponding phase contrast image illustrates the distinct segregation of the cells onto the PS-containing membrane corrals. The nearly complete lack of cell deposition on the identically-charged PG-containing membrane (lower two corrals in Figure 3) underscores the chemical specificity of the PS effect. In multiple experiments with various membrane combinations, cells were observed to proliferate to near confluence on the PS-containing membrane, while PS-free membrane corrals remain essentially devoid of cells.

This work represents the first application of membrane microarrays to assay cell discrimination characteristics. The microarray format allows cells to sample many different membrane targets before a commitment is made. Follow-on projects, seeded by these initial results, will explore the capabilities of reconstituted membrane recognition systems and compare them to those of living cells using the microarray discrimination assay introduced here.

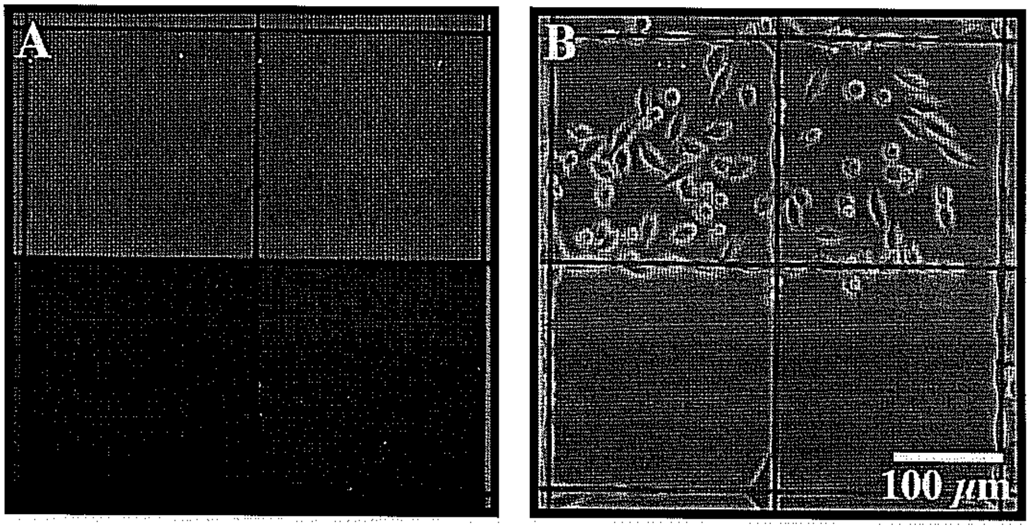

Figure 3: Patterned cell growth on membrane microarrays.

Publications

J.T. Groves, L.K. Mahal, and C.R. Bertozzi, "Control of Cell Adhesion and Growth with Micropatterned Supported Lipid Membranes," to be submitted (November 2000).

Identification of Novel Functional RNA Genes in Genomic DNA Sequences

Principal Investigators: Stephen Holbrook and Inna Dubchak

Project No.: 99037

Project Description

The long-term objective of this proposal is to develop an automatic computational method for the identification of RNA genes and functional RNA elements encoded in the genomic DNA sequences of procaryotes, archaea, and eucaryotes including human. Such a system will enable the discovery of new RNAs potentially having novel biological functions. Currently, no procedure exists for the location of unknown functional RNA molecules. Based on the rate of discovery of new RNA genes and control sequences, we expect that many functional RNAs remain to be identified in genomic sequences. Once the RNA products are identified, traditional biochemical methods such as northern blotting, microarray hybridization, and gene disruption or deletion can be used to verify their presence, level, and function.

We intend to verify and apply the hypothesis that RNA genes can be characterized and identified by local and global sequence patterns that are intrinsic to their structure and function. Our approach is to use machine-learning methods to learn and generalize sequence differences between known RNAs and non-annotated regions for the purpose of prediction of new functional RNAs. This requires compilation of RNA and non-RNA sequence databases, parameterization of this sequence data, training with these parameters, cross-validation testing to assess accuracy of prediction, and finally prediction of putative RNA genes. The optimal set of input parameters for representation of the sequence is determined by maximizing accuracy in cross-validation testing. Assuming that functional RNA sequences will be conserved among related organisms, computational verification (or pre-screening) of potential functional RNAs will be done through application of low stringency nucleic acid sequence or sequence/structure alignment using standard software.

RNA gene identification methods are developed initially using *E. coli* and other bacterial genome sequences. Next, these methods will be tested and modified where necessary for archaeal and eucaryotic genomes, including the human genome. Predictions in *E. coli* and other bacteria will be tested and verified biochemically and genetically with feedback to the gene prediction algorithms. Improved annotation of RNA genes will be provided to public databases and the prediction software made available for distribution and access through the internet.

Accomplishments

As the most well studied bacteria in terms of both genome structure and function, we chose to formulate and test our predictive methods on the *E. coli* genome. The M52 version of the *E. coli* K-12 genome sequence was used to compile a database of functional RNA and non-annotated sequences. The functional RNA sequences include 86 tRNAs, 22 rRNAs, and 11 other small RNAs. The non-annotated, or "non-coding" sequences were obtained by removing all protein and functional RNA coding regions from the genome along with a buffer on both the 5' and 3' sides of 50 residues so as to remove promoter, terminator, and other untranslated control elements. Sequences in both strands were removed when there was a coding region on either strand. The complete genome consists of 4,697,212 nucleotides on each strand (9,394,424 total). After removal of all protein coding and RNA coding genes (except the recently discovered *oxyS, micF, csrB*, and *rprA*) 340,375 nucleotides remained on each strand for a total of 680,750 nucleotides. The RNA database consisted of 40,966 nucleotides. Each RNA and non-annotated intergenic sequence was divided into sequence windows of 80 residues with a 40 nucleotide overlap between windows (i.e., each window slides 40 residues along the sequence). A window of less than 40 residues at the end of the sequence was omitted from the calculations. A total of 6108 windows from each strand were used for calculation of input parameters of the non-annotated sequences, while 305 windows were available from the known RNA sequences for input parameter calculation. Each sequence window was converted to a set of input parameters for training a computational neural network to learn characteristics that distinguish RNA genes from non-coding sequences. An equal number of windows of each type were used in training the networks that were then tested for prediction accuracy by a jackknife procedure.

Based on the observation that all known, stable, functional RNAs share common structural elements and that sequences corresponding to these elements would occur preferentially in RNA genes, we explored the hypothesis that novel RNAs could be predicted based on the occurrence of these features in local sequences. We therefore chose to use the prevalence of several common, well-known, structural elements including double helices, UNCG and GNRA tetraloops, uridine turns, and tetraloop receptors as potential discriminators of RNA genes. By analysis of the known RNA genes and non-annotated sequences in *E. coli* and the archaea *Pyrococcus horikoshii*, we determined that these elements do occur with higher frequency in RNA genes and thus are useful in their identification.

Since neural networks based on the occurrence of RNA structural elements cannot be expected to identify non-RNA sequences in a positive manner, we used additional global sequence descriptors to discriminate RNA genes from non-RNA genes. These descriptors include 4 composition (C), 20 distribution (D), and 16 transition (T) parameters, for a total of 40 parameters (C+T+D). Testing indicated that the distribution parameters did not improve prediction and so only the composition and transition parameters were used (20).

A database of 730 sequence windows of length 80 residues (in some cases between 50 and 80 residues) from 115 *E. coli* RNAs and 730 sequence windows from non-annotated intergenic regions were used to calculate the input parameters for the neural networks. Networks were tested by a full jackknife procedure (removing one example at a time, retraining, testing on the single example, and averaging over all examples). In order to optimize the number of RNA sequence windows, redundant sequences were not removed from the database (i.e. multiple ribosomal and tRNA genes), therefore some bias was present in the testing results. The results of training/testing experiments are shown in Table 1.

Table 1. Testing of neural networks for prediction of RNA genes in *E. coli*

	Structure (6 params)		**Sequence (20 params)**		**Voting (Struc., Seq.)**	
Threshold	**%Correct**	**%Predicted**	**%Correct**	**%Predicted**	**%Correct**	**%Predicted**
	RNA/Non	**RNA/Non**	**RNA/Non**	**RNA/Non**	**RNA/Non**	**RNA/Non**
20%	80.2/88.6	96/77	93.2/95.9	101/94	93.3/94.6	100/97
30%	82.5/90.1	85/72	93.4/96.4	100/91	93.7/95.4	99/96
40%	84.3/91.7	75/66	94.0/97.2	98/89	94.3/95.9	98/96
50%	86.8/93.8	64/62	94.6/97.5	96/87	94.5/96.3	97/92
60%	88.3/95.0	53/55	95.0/97.6	93/86	94.7/97.1	95/90
70%	92.4/95.8	35/49	95.2/98.0	91/84	95.1/97.1	95/90
80%	96.9/97.7	13/41	95.9/98.1	71/81	95.4/97.6	93/89
90%	100./98.5	1/27	NA/98.1	0/74	97.3/98.8	57/68

Networks used 2 hidden nodes. Threshold=(pred1-pred2)*100./(pred1+pred2) where pred1 and pred2 are output activities.

Table 1 illustrates that neural networks are able to learn to distinguish between RNA genes and non-coding regions with high accuracy using either structural or global sequence parameters as input. A second-level network incorporating output from both structural and global sequence networks is the most accurate and predicts the greatest percent of the data at all threshold levels. We thus feel justified to use a voting network trained with the architecture and parameters described above to search the intergenic regions of *E. coli* for novel RNAs.

We have applied and tested the prediction scheme to several other organisms including *Mycoplasma genitalium* (Mg), *Mycoplasma pnuemoniae* (Mp) and *Methanococcus jannaschii* (Mj). The Mg and Mp have small and highly related genomes, with the Mg genome almost a subset of Mp. Testing and training of neural networks for RNA prediction in Mg was 94% correct, and Mp 95% correct. When the network trained on Mg was used to predict Mp RNAs, it was 98% accurate, and the Mp networks were 94% accurate in predicting Mg RNAs. This cross prediction between organisms suggests we may be able to predict RNA genes in many organisms from related species rather than having to make individual networks for each organism. It also is possible that we can use RNAs from many genomes to compile a larger database and make more accurate predictions. This approach remains to be tested.

The prediction of RNAs in Mj, a hyperthermophilic archaeal organism, was extremely accurate on cross-validation testing with 98% of predictions correct. This accuracy may arise from differences in the G+C content of RNAs in this hyperthermophile relative to the rest of the genome. The success discussed above in predicting RNA genes suggested the possibility that the same or similar algorithms could be used to predict other functional RNAs such as the untranslated control regions (UTRs) of some mRNAs that are also generally highly structured. We tested this idea on an evolutionarily conserved RNA stem-loop in the 5' UTR of RNaseE mRNA. This regulatory element was strongly predicted by our method with the boundaries well defined by the prediction. Much more extensive testing remains to be done to determine whether the same or related prediction methods can be used in identifying all functional RNAs, be they individual genes or control regions of mRNA.

These programs are implemented and accessible on the world-wide-web through the "RNAGENiE" interface (http://rnagene.lbl.gov). Here users type or paste a sequence of interest into a text-window. The program then splices the data into windows of the appropriate size, converts them to the proper input parameters, and performs a prediction using the stored neural network weights. The results from RNAGENiE are then e-mailed to the users giving scores corresponding to the likelihood of any window being part of an RNA gene.

Although initial attempts to use machine learning methods to distinguish RNA genes in genomic DNA sequences was successful as judged by cross-validation and prediction of newly identified RNAs not included in the training database, several potential improvements came to light during the development process. A second generation RNA gene predictor is under development to incorporate these improvements.

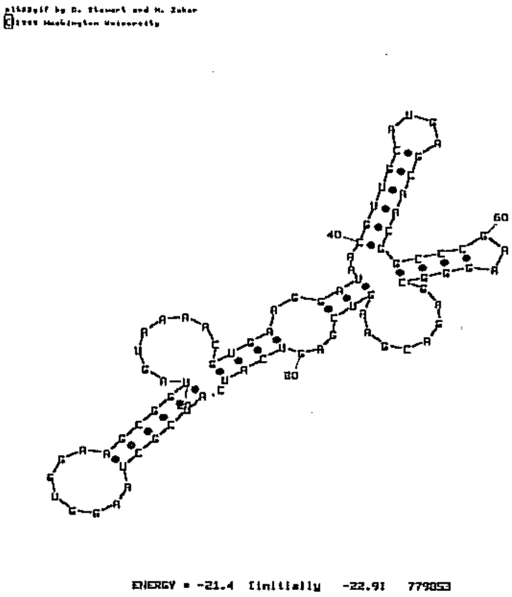

Figure 4. Predicted secondary structure of intergenic sequence found in lysT operon.

Publications

I.L. Dubchak, S.R. Holbrook, and I. Muchnik, "Global Description of Amino Acid & Nucleotide Sequences: Application to Predicting Protein Folds, Intron-Exon Discrimination & RNA Gene Identification," *Proc. of the Second Intl. Conf. on Modeling and Simulations of Microsystems*, San Juan, Puerto Rico, p38-41 (1999).

I.L. Dubchak, C. Mayor, and S.R. Holbrook, "Identification of Novel Functional RNA Genes in Genomic DNA Sequences," presented at RNA 2000, 5th Annual Meeting of the RNA Society, Madison, Wisconsin (2000).

R.J. Carter, I.L. Dubchak, C. Mayor, and S.R. Holbrook, "RNAGENiE: The Identification of Novel Functional RNAs in Genomic DNA Sequences," (2000, in preparation).

Transgenic Optical Sensors for Live Imaging of Neural Activity

Principal Investigators: Ehud Isacoff

Project No.: 00025

Project Description

We have designed a new class of optical sensors of cellular signaling, which converts signaling proteins into sensors. This approach allows us to harness the high sensitivity and specificity of the biological molecules that transduce, transmit, and receive cellular signals. Our approach has been to modify signaling proteins in such a way that changes in their biological activity are converted into changes in fluorescence emission that can be detected non-invasively with standard imaging techniques. Our aims for the LDRD have been two-fold: (1) to optimize our optical sensors of membrane potential for use in the model organisms, and (2) to deploy our sensors and a protein-based optical sensor of cellular Ca++ made in Roger Tsien's lab in these organisms.

Accomplishments

Rational Tuning of a Protein-based Optical Sensor of Membrane Potential

In FY2000, we succeeded in modifying the kinetics, dynamic range, and color of our optical voltage sensor FlaSh, made from a fusion of a Green Fluorescent Protein (GFP) "reporter domain" and a voltage-gated Shaker K+ channel "detector domain." In our original work, we engineered FlaSh in such a way that changes in membrane potential changed the conformation of the Shaker channel and this, in turn, induced a rearrangement of GFP that changes its brightness.

We have now altered, in a directed manner, the response properties of FlaSh in order to optimize it for sensing particular classes of signals in particular cell types. By modifying both the GFP reporter and detector domains, we produced sensors with improved folding at 37° C, enabling use for the first time in mammalian preparations. We also made variants with distinct spectra, improving the signal to background readout in cells. In addition, we have modified the kinetics and voltage dependence of the sensor, thus expanding the types of electrical signals that can be detected. The optical readout of FlaSh has also been expanded from single-wavelength fluorescence intensity changes to dual-wavelength measurements based on both voltage dependent spectral shifts and changes in fluorescence-resonance-energy transfer (FRET), thus providing ratiometric readouts. Different versions of FlaSh can now be chosen to optimize the detection of either action potentials or synaptic potentials, to follow high versus low rates of activity, and to best reflect voltage waves in cell types with distinct voltages of operation.

Deploying Sensors in Model Preparations

One advantage of using proteins, rather than organic compounds, as detectors is they can not only be rationally tuned, but they can be targeted to specific protein complexes located in specific subcellular compartments. In recently completed work, we have proven that this principle can work by localizing a membrane-bound GFP to post-synaptic membrane *in vivo* using a PDZ-interaction domain that we showed earlier to be responsible for synaptic targeting. This PDZ-targeted GFP expresses so well and is localized so efficiently that it makes it possible to visualize synapses in unanesthetized *Drosophila* larvae through their opaque cuticle, over the high autofluorescence of the entire animal, permitting a time-lapse visualization of synaptic growth and remodeling. We have now carried out the first steps of equipment construction and molecular and cell biology necessary to express the protein-based optical sensors in a model organism, *Drosophila*, and in model cells, and to detect them rapidly and efficiently. This work is a prelude to the use of these sensors in the mammalian central nervous system (CNS). So far, we have demonstrated the following:

- We can reconstitute in cells the synaptic clustering between synaptic proteins and our reporters and use this to target sensors to the synapse and visualize the synapse easily in a manner compatible with vital recording of synaptic transmission.
- We can use the sensors to report activity as well as morphological development of the synapse, to thus identify mature and immature connections and compare their function.
- We have made various constructs of Tsien's Cameleon with varying affinities for calcium and various cellular targets.
- We have devised a method for high-speed ratiometric imaging of the FRET signal with a system that is not rate-limited by rotating filters, but acquires synchronous images in both emission colors and thus permits ratiometric images to be obtained at the rate of the camera (meaning now, in principle, up to 1000 frames per second).
- We have detected calcium signals in model heterologous cells with targeted Cameleons.

Together, these achievements now place us in the position to use viral, transgenic, and particle gun delivery of sensors into the mammalian CNS.

In summary, our work so far takes a significant step toward developing tools for the *in-vivo* measurement of neural activity from whole neural circuits, with the kinetic resolution and analog precision of intracellular electrophysiology and the spatial resolution of single identified cells. This unprecedented resolution emerges from our ability to target fluorescent protein sensors to specific cell types and subcellular locations. Beyond increasing the resolution of neural imaging, our approach provides a huge potential for the expansion of the kind of biological signals that can be measured from neurons. These detectors are compatible with concurrent electrophysiological recording. We expect them to provide new insights into the mechanism of synaptic function and plasticity. An analogous approach can be taken toward the design of detection methods for practically any signaling event in a cell for which signaling proteins have been cloned. This means that biochemical events that have so far only been studied *in vitro* can now be measured in their cellular context during biological activity. Optical monitoring of biochemical activity with high spatial and kinetic resolution promises to provide the next generation of tools for systems neuroscience.

Publications

G. Guerrero, M.S. Siegel, B. Roska, E. Loots, and E.Y. Isacoff, "Tuning FlaSh: Redesign of the Dynamics, Voltage Range and Color of the Genetically-Encoded Optical Sensor of Membrane Potential," submitted to *PNAS* (2001).

Computational Modeling of Protein Folding and Unfolding using Lattice Models and All-Atom Molecular Dynamics

Principal Investigators: Daniel Rokhsar

Project No.: 98044

Project Description

The goal of this project is the construction of quantitative theoretical models of biological materials and systems. Our primary focus is two-fold: (1) the thermodynamic and kinetic properties of proteins and (2) the development and organization of neuronal networks in the mammalian visual system.

Studies of protein folding require extensive Monte Carlo simulation for thermodynamic properties and molecular dynamics and Langevin analysis for kinetics. Because all-atom calculations are limited to nanoseconds of real time (while real proteins fold in milliseconds), progress demands the construction of faithful yet tractable models to make the best use of available computational resources. We use lattice models, simplified representations of proteins, and all-atom molecular dynamics with solvent to study the nature of folding and unfolding pathways.

Simulation and analysis of retinal and cortical patterns and their projections requires both image processing and dynamical simulations. Parallel simulations of a range of control parameters for these realistic networks is the best way to accumulate sufficient data to understand these complex dynamical systems. The goal of this effort is (1) a quantitative model of the developing mammalian retina and (2) the ability to make specific predictions for the behavior of this network under various conditions.

This computational effort relies heavily on the computational resources of National Energy Research Scientific Computing Center (NERSC), specifically the Cray T3E.

Accomplishments

Unfolding a Beta Hairpin by Mechanical Forces

Single-molecule mechanical unfolding experiments have the potential to provide insights into the details of protein-folding pathways. To investigate the relationship between force-extension unfolding curves and microscopic events, we performed molecular dynamics simulations of the mechanical unfolding of the C-terminal hairpin of protein G. We studied the dependence of the unfolding pathway on pulling speed, cantilever stiffness, and attachment points. Under conditions that generate low forces, the unfolding trajectory mimics the untethered, thermally accessible pathway previously proposed based on high temperature studies. In this stepwise pathway, complete breakdown of the backbone hydrogen bonds precedes dissociation of the hydrophobic cluster. Under more extreme conditions, the cluster and hydrogen bonds break simultaneously. Transitions between folding intermediates can be identified in our simulations as features of the calculated force-extension curves. Our results are relevant for the comparison between thermal and mechanical unfolding events.

Protein Dynamics

We have also studied several models for deriving low-frequency protein dynamics from low-resolution structures. Such low-frequency motions have been consistently implicated in protein function, either as large-scale conformational changes or smaller-scale active-site adaptations. Since homology modeling typically yields low-resolution structures, the models we are considering are well-suited to genome-scale analyses. Furthermore, the formation of protein complexes often involves the deformation of the participating partners, and a characterization of the energies and entropies of deformation is essential for understanding complex formation and function. Models introduced earlier by Jernigan and his collaborators infer the dynamics of proteins by a one-dimensional network of springs connecting nearby alpha-carbons. We have extended this model to a full three-dimensional network. We find that the crystallographic "B-factor," which is well predicted by these models, can in fact be related (by an analytical perturbation theory calculation) directly to the effective coordination number of each residue. The normal mode calculations and a general-purpose graphical viewer for examining protein motions have been implemented and are currently being applied to several proteins of local interest at Berkeley Lab and University of California (UC), Berkeley, including tubulin (with E. Nogales and K. Downing) and ubiquitin (T. Handel). The dynamics of ubiquitin have been studied extensively by Nuclear Magnetic Resonance (NMR) in Handel's lab, and we are correlating the model predictions and experimental measurements as a test of the model. The various polymers of tubulin can be used to characterize the importance of protein deformation in packing and docking.

Retinal Waves and Collective Network Properties

Propagating neural activity in the developing mammalian retina is required for the normal patterning of retinothalamic connections, specifically the refinement of retinotopy in the lateral geniculate nucleus and superior colliculus. This activity exhibits a complex spatiotemporal pattern of initiation, propagation, and termination. We have explored the information content of this retinal activity, with the goal of determining constraints on the developmental mechanisms that use it. Through information theoretic analysis of multi-electrode and calcium imaging experiments, we have shown that the spontaneous retinal activity present in early development provides information about the relative positions of the retinal ganglion cells that produce it, and can, in principle, be used to refine retinotopy. Remarkably, we find that most of this information exists on relatively coarse time scales (0.1 to 2 seconds) which implies a correspondingly long integration time in the synapses that use it. These findings are consistent with the idea that bursts of action potentials, rather than single spikes, are the unit of information used during development. Our approach to describing the developing retina provides new insight into how the organization of a neural circuit can lead to the generation of patterns of complex correlated activity.

DNA Microarray Analysis

We are developing GUACAMOLE, a comprehensive software package for the analysis of DNA microarray data. This integrated package combines image analysis and quantification, graphically-oriented, user-guided sorting, classification and visualization of single microarray datasets, and higher-level analyses across multiple experiments, including complex queries, sorting, clustering, pattern recognition, etc. The package provides a single, user-friendly platform for navigation and exploration across single and multiple experiments. Results are stored in a relational database, BEANDIP, with a database schema that has been designed to be compatible with a wide range of other analysis tools, including especially the SCANALYZE series, and Laboratory Information Management Systems (LIMS) systems including Stanford University, UC Berkeley, and Berkeley Lab versions. The implementation of a relational database permits high-level statistical analyses to be performed across multiple experiments. A simple web interface allows multiple users (with suitable identification/passwords) to access and search large collections of microarray data.

GUACAMOLE is currently in a beta-testing stage, with several groups at UC Berkeley and Berkeley Lab currently testing it using microbial, fly, mouse, and human arrays.

Publications

Z. Bryant, V.S. Pande, and D.S. Rokhsar, "Pulling Apart a Beta Hairpin," *Biophysical Journal* **78** (2): 584-9 (2000).

D.A. Butts and D.S. Rokhsar "The Information Content of Spontaneous Retinal Waves," to appear in *Journal of Neuroscience* (February 2001).

Physics Division

Silicon-on-Insulator Technology for Ultra-Radiation Hard Sensors

Principal Investigators: Kevin Einsweiler, Naimisaranya Busek, Roberto Marchesini, Gerrit Meddeler, Oren Milgrome, Helmuth Spieler, and George Zizka

Project No.: 98038

Project Description

A paradigm shift is underway in the design of radiation-resistant integrated circuits. Previous designs have emphasized specially designed fabrication technologies, using non-standard processes to optimize gate oxides and inter-device isolation structures. In contrast, standard commercial "deep submicron" (<0.3 μm feature size) processes are now becoming viable for circuits operating up to tens of Mrad or more. The critical ingredient is not the small feature size *per se*, but the thin gate oxides needed for good operation of submicron channel length MOSFETs (Metal-Oxide Semiconductor Field Effect Transistors). At oxide thicknesses <10 nm, electron tunneling fills the hole traps in the oxides and practically eliminates the effects of oxide charge buildup. Thin gate oxides do not solve the problem of inter-device isolation. Field oxides in deep-submicron process are still thick enough for substantial radiation-induced charge buildup, which forms surface channels by local band bending at the oxide-silicon interface. This problem is mitigated by using closed geometry transistors. This comes at the expense of circuit density, but since the feature sizes are substantially smaller than in certified radiation-hard processes, the overall circuit area is comparable or even smaller, depending on the specific implementation. Work at CERN has demonstrated radiation hardness to >30 Mrad using a 0.25 μm IBM process. Since deep sub-micron processes are now readily available for small-scale prototype runs through MOSIS, the emphasis of our work has shifted from the Honeywell and Temic radiation-hard SOI processes to the investigation of 0.25 μm technologies.

Accomplishments

Given the complexity of chips needed in the most demanding radiation regions of next-generation collider detectors, assessing the suitability of a process for this environment must go beyond merely determining whether devices "die" or not. Instead, a detailed evaluation of many electrical parameters is necessary to determine how the individual device parameters can be balanced against one another to mitigate the effects of radiation damage. The available deep-submicron processes are all designed for digital applications, so we conducted a detailed set of measurement to assess the analog properties of these devices.

Since the IBM process has been studied at CERN, we elected to investigate the TSMC (Taiwan Semiconductor) 0.25 μm CMOS (complementary metal oxide semiconductor) process, available through MOSIS.

Initial data showed the expected behavior of transconductance vs. drain current, which is quite different from conventional devices. In devices with channel lengths >0.5 μm channel length the transconductance increases with drain current until it is limited by the parasitic source resistance. In short channel devices, velocity saturation sets in at much lower currents, so the transconductance saturates, as shown in last year's report. This carries a penalty for the low-power operation essential in high-density analog circuits. In conventional processes, the current density for the onset of weak inversion increases as the channel length is reduced. As a result, a given transconductance (i.e. speed and noise level) can be achieved at lower current when the channel length is reduced. The dependence of the normalized transconductance g_m/I_D vs. normalized drain current I_D/W is shown in Figure 1 for a Honeywell 0.8 μm and a TSMC 0.3 μm device. Apart from the smaller transconductance in weak inversion (the low current asymptote), the curves are quite similar. Moderate inversion is in the same regime for both devices ($I_D/W \approx 1$). Although the current at which the weak inversion reaches 50% is slightly higher in the 0.3 μm device, the improvement is much smaller than would be expected from previous data.

The second concern in sub-micron devices is output resistance. Data from experimental 0.25 μm IBM devices measured about ten years ago, show triode-like output characteristics with much smaller output resistance than long channel devices. Presumably, this was due to the relatively deep source and drain implants, which led to a greater spread of the channel into the bulk (two-dimensional channel effects). In contrast, the current devices show very good output characteristics, with an intrinsic voltage gain $g_m R_D$ comparable to the 0.8 μm devices measured previously. Typical output curves for a 0.8 μm channel length device have been measured, as shown in Figure 2. The maximum output resistances are in the range 150 kΩ for $V_{GS} = 1$ V to 8 kΩ for $V_{GS} = 3$ V.

The early onset of velocity saturation implies high fields in the channel, which raises the concern of impact ionization. Impact ionization can increase the noise of the device and also reduce reliability, because of oxide damage from "hot" electrons. The presence of impact ionization can be detected by measuring the substrate current, as this is the only current path for the holes formed in the ionization process. Current vs. gate voltage for fixed drain voltages ranging from 1 to 3 V have been plotted. Significant impact ionization occurs at drain voltages greater than 1.5 V. The shape of the ionization current curves follows theoretical expectations. However, a surprising result is pronounced impact ionization at $V_{DS} = 1.1$ V, since impact ionization requires at least 1.5 eV energy. The impact ionization current is roughly 10^{-9} of the drain current, so this may be due to tails in the thermal distribution in combination with fields due to oxide charge. The tunneling current through the gate oxide was also measured and found to be normal. In any case, impact ionization of this magnitude is not typical of other processes we have investigated and it warrants further investigation.

In summary, the 0.25 μm channel length devices investigated here have characteristics that are quite suitable for analog circuitry. They show pronounced velocity saturation effects, which reduce the maximum transconductance. Velocity saturation also obviates the reduction in power that one would extrapolate from data on longer channel devices. An area of concern is the rather high level of impact ionization, even at low drain voltages.

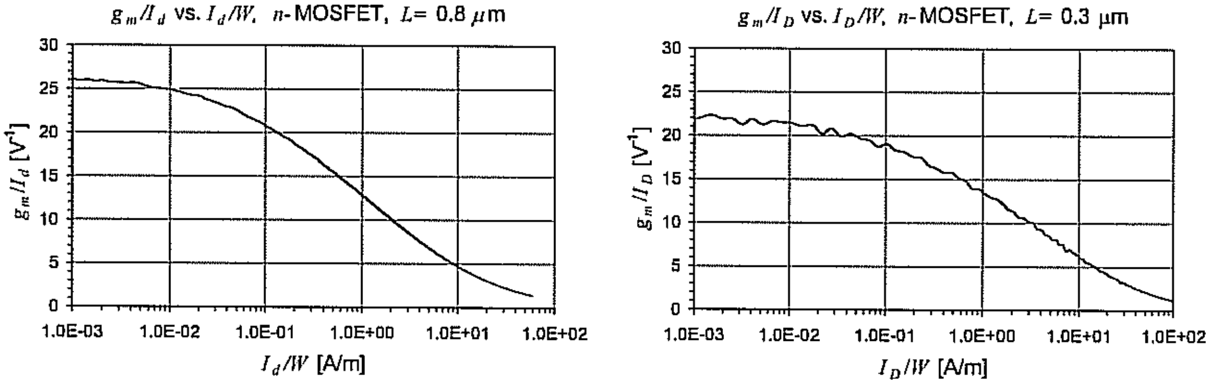

Figure 1: Normalized transconductance g_m/I_D vs. normalized drain current I_D/W is shown for a Honeywell 0.8 μm and a TSMC 0.3 μm device.

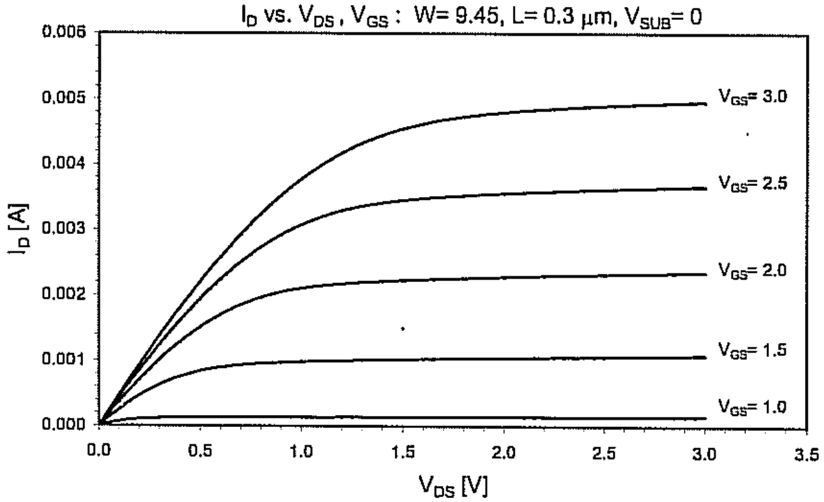

Figure 2: Measured output curves of an n-MOSFET with 0.3 μm channel length.

Foundations for a SuperNova Acceleration Probe (SNAP)

Principal Investigators: Michael Levi and Saul Perlmutter

Project No.: 00026, 00027

In FY2000, Berkeley Lab funded two separate projects. Project 00026 is to tackle technical challenges in developing a large charge-coupled device (CCD)-mosaic camera having near-infrared (IR) sensitivity. Project 00027 is to develop techniques to significantly increase discovery of nearby supernovae—which is particularly constrained by data handling bottlenecks—for reducing the systematic uncertainties in our current understanding of supernova observations. Consequently, the two self-contained reports follow.

For FY2001, because both scientific problems are crucial to the possible development of the proposed Department of Energy/National Aeronautics and Space Administration SNAP satellite, they are considered effectively a single project this coming year. Nonetheless, both scientific problems are crucial for further general advances in astrophysics and astronomy and therefore are of ongoing significance independent of the ultimate success of the SNAP satellite proposal.

Sub-Project 00026: Development of an Advanced Imaging Array

Project Description

A major milestone has been achieved with the recent success in fabricating near-IR sensitive, large-format 2kx2k pixel CCDs. We must now find ways to exploit this technology to the fullest. In particular, these devices can be placed in advanced cameras for observational astronomy and lead the new development of major scientific instruments for astrophysics research. We intend to develop a small-scale instrument, optimize it, and then use the demonstrated performance as a centerpiece for several new directions, which could include a major instrument for ground-based astronomy.

For this project, we propose developing the capability to produce large CCD-mosaic cameras, from the design stage, to a complete scientific camera that can be used at a major telescope facility. The design would be applicable to many of the next-generation ground- and space-based observatories. The currently available CCD camera designs are not as sophisticated—in their mechanical, electronics, readout, or computing designs—as the state-of-the art high energy physics detector systems. Thus, at Berkeley Lab, we are well suited to developing very-large-area CCD arrays that can be used for very-deep high-resolution surveys of the early universe. The development would be in the context of creating a large instrument for a world-class wide-field telescope. This would allow us to aggressively pursue the uniqueness of our technology while exploiting the strengths of Berkeley Lab in creating large multi-faceted instruments.

Accomplishments

We proposed to proceed in three main steps:

- First, to develop the lab-bench test capabilities necessary to illuminate and read out a mosaic of CCDs and to tune their performance characteristics.
- Second, electronics and mechanical camera design of a 3 by 3 mosaic of large-format CCDs, the dewar, and the testing of component parts and design elements.
- Third, camera assembly, and testing of the full 3 by 3 mosaic of large-format CCDs.

The following things were done in the process of completing the first step:

- We have built a 200 square foot, Class 10000 cleanroom where we will attach CCDs to their mounts and perform wire bonding to the signal pads. The room incorporates a laminar flow bench, a manual wire-bonder, a low-temperature refrigerator for storing adhesives, and a vacuum oven for curing the adhesives.
- Two commercial liquid nitrogen dewars have been purchased and a third one has been built in-house. The latter was designed to overcome the slow cycle time of the commercial dewars. We anticipate being able to do a complete load, pump down, cool, and warm up cycle with this dewar in two hours or less. This is to be compared to the 24^{+} hour cycle time for the other two. The two commercial dewars are in use and the other one is now being wired.
- We have purchased two commercial CCD controllers and interfaced each to a SUN workstation. We have built support electronics to process analog signals at the dewar and to generate additional voltage levels for biasing and clocking the CCDs. A scheme to

control fall and rise time of clock signals is designed and being implemented.

- The commercial CCD controllers come with some data acquisition software. We have made enhancements to this to control sealed sources, erase the CCDs, and enter parameters in units of volts instead of digital units. For online analysis of data, we have established an Interface Definition Language (IDL) framework to which we are continually adding functionality. To date we have automated dark current, read noise, charge transfer efficiency measurements, x-ray peak reconstruction, and some image processing.

- All CCD testing so far has been with CCDs mounted directly to conventional printed circuit boards (PCBs) or with indirect PCB mounting with an aluminum nitrate substrate for better cooling and thermal match. In both cases, the CCD signal pads are wire-bonded to the PCB and the signals routed to convention connectors. We have also been building models of final production mounts that support backside illumination where a CCD is glued directly to a compatible metal. The metal serves as the CCD support, acts as an attachment mechanism to the cooling system, and holds a PCB with connectors to which the CCD signals are wire-bonded. This scheme supports four-sided, close packing of the CCDs so that large-area arrays can be assembled.

Sub-Project 00027: Nearby Supernova Search with Ten-Fold Increase in Efficiency

Project Description

The study of cosmology has entered a new era in which empirical data can play a decisive role in determining the correct theory of the history and fate of the Universe. While previously this theory was heavily dependent on esthetic considerations, we now are beginning to have a range of experimental /observational tools that can directly measure the relevant cosmological parameters. Among these tools, supernovae stand out as potentially the most direct, least model-dependent, for studying the energy-densities of the universe and the relative contributions of mass energy and vacuum (or "dark") energy. Over the past 15 years, Berkeley Lab has developed this supernova tool to the point that its current main result—the evidence for the existence of significant vacuum energy—is now considered to be a crucial element of the current State of the Universe report by much of the astrophysics community.

The next key step is to take the range of techniques that we have developed and perform the definitive measurements that will make the supernova results one of the solid foundations on which future cosmological investigations will build. By studying an order-of-magnitude more supernovae in a much larger, systematic program, we can address each of the main remaining sources of uncertainty (primarily systematics). The "supernova values" for the mass density, vacuum energy density, and curvature of the universe will then become the benchmarks for the other, more model-dependent cosmological measurement techniques. In particular, the cosmic microwave background measurements will be able to use these values as both a starting point and a benchmark as they fit the eleven or so parameters to which their power spectrum is sensitive.

This project will provide Berkeley Lab with the capability to dramatically scale up discovery of nearby-supernovae. Instead of finding dozens of supernovae during a semester, we would gear up the search to discover several hundred and therefore are calling this a Supernova Factory (SNfactory). We are learning how to do this in an efficient manner, and learning which telescopes are most suitable for the task. In particular, the NEAT [Near Earth Asteroid Tracking program operated by the Jet Propulsion Laboratory (JPL)] search runs are going to increase. Over a three-month span, we would expect NEAT to find over 200 supernovae in the Hubble Flow. In addition to NEAT, the LINEAR (Lincoln Near Earth Asteroid Research) team will be surveying the entire visible sky twice a month. Discussions concerning a collaboration are underway and we will look to characterize their telescope in the near future for use in a supernovae search.

We must greatly improve the computational tools for managing the dataflow, data analysis, scheduling, and multi-telescope coordination. We have identified the following items as critical tasks. They are all feasible, but will require innovative large-data-set handling, and novel software for coordination of an international collaboration of humans, computers, and telescopes.

- *More complete automation of the search.* Just controlling and monitoring the dataflow, required most of the time of two experienced scientist/ programmers during the period of the pilot study search. This will have to be automated for year-round searching.

- *Automation of target sky-field selection, and distribution to the appropriate telescopes (e.g., NEAT).* We will need automation of the evaluation process of search observations and appropriate rescheduling.

- *Improve automated candidate pre-screening by at least a factor of 30.* We will not be able to repeat our current feat of 30,000 candidates searched by eye, and we need to be able to handle at least 10 times more data.

- *Develop more reliable network connections and use dedicated machines.* We will need automation of follow-up observation scheduling for the multiple telescopes that will observe the supernovae after discovery. Automation is also needed of analysis of follow-up data feedback of these results for the planning and scheduling of further follow-up observations.

- *Queue scheduled spectroscopy and photometry (VLT, Gemini North and South SOAR).* The final siting and operation of our own Berkeley Lab 30" telescope at Chews' Ridge, California, will provide a northern hemisphere automated queue-scheduled photometry telescope.

Accomplishments

The project depends of the use of the Near Earth Asteroid Telescope (NEAT) to find large numbers of Supernova candidates. Part of our effort has focused on developing improved supernova-searching capabilities with NEAT. The NEAT Team at JPL has moved to a larger telescope (1.2-meter diameter, formerly 1.0-meter diameter) on Haleakala, Hawaii, and has increased the number of search nights from 6 to 18 per month. The telescope is now equipped with a re-imaging camera built by Boeing for the United States Air Force at a cost of $USD 500,000. NEAT has also added water cooling (previously thermal-electric cooling) to its CCD detector, enhancing its sensitivity to faint targets by lowering the dark current. This facility is to be the primary source of supernova discoveries for the SNfactory, so these improvements lead directly to improvements in the baseline performance of the SNfactory. Besides the greater depth attainable with the improved NEAT, it will be possible to search patches of sky for supernovae more frequently, allowing supernovae to be discovered much earlier after explosion.

Since NEAT has resumed search operations with these new capabilities, we have provided them with scripts needed to automatically transfer imaging data from Haleakala to Berkeley Lab for processing, and these scripts have been tested on a run of real data. In March 2001, NEAT will further expand its searching capabilities by installing a 3-CCD camera at the Palomar 1.2-meter telescope (the telescope responsible for the famous Palomar Observatory Sky Surveys). This will more than double NEAT's search abilities, compared to the new improved capabilities at Haleakala.

Another priority is the acquisition of a telescope for follow-up of nearby supernovae. We have been in negotiation with the University of Hawaii (UH) regarding the use of their 2.2-meter telescope on Mauna Kea in Hawaii to obtain follow-up observations (spectra and lightcurves) for supernovae discovered by the SNfactory using NEAT data. Mauna Kea is the world's premier site for astronomical observations, providing the best image quality available from the ground. One setback has been the postponement of a decision by the European Southern Observatory (ESO) regarding the fate of its 2.2-meter telescope in the Chilean Andes (another excellent site renowned for the large fraction of clear nights), originally viewed as a very likely prospect as a second SNfactory telescope.

The major instrumentation effort has gone into creating baseline design for a supernovae follow-up spectrograph. The SNfactory concept for an integral field unit (IFU) spectrograph for use in obtaining supernovae spectra and lightcurves has been much more fully developed. With the help of the OASIS/Sauron group at the Observatory of Lyon (France), a prototype optical and mechanical design has been developed for an IFU spectrograph for the UH 2.2-meter telescope. This spectrograph will have both a blue and a red optical channel, allowing optical elements and detectors to be optimized for each channel. The estimated 'average' efficiency for this spectrograph of 20% (including telescope and atmosphere) is better than the typical "peak" efficiency of spectrographs currently available. Because the integral field unit obtains a spectrum of the 122 0.5 x 0.5 sections of sky from the 6 x 6 arcsecond region of sky around and including each supernova, all the supernova light is captured. This allows not only spectroscopy, but also synthetic photometry, to be obtained. Synthetic photometry is obtained over the entire optical spectral region, making this approach much more efficient than typical photometry, which involves serial observations in up to 6 separate filters. Because, for synthetic photometry, filter bandpasses can be defined in software, the photometry can be more precise and can be checked for a wider range of potential systematic errors. Moreover, the large region covered by the IFU means that precise pointing of the telescope is not required. Therefore, we expect to be able to automate the acquisition and subsequent observation of each supernova. This minimizes our reliance on a night assistant at the telescope; the night assistant will need to do nothing more than point the telescope using standard procedures (accurate to typically a few arcseconds) and then press a mouse button to commence observations. This instrument will be truly revolutionary. Funds and manpower in France has been earmarked for construction of the first follow-up spectrograph, pending completion of a Memorandum of Understanding between Lyon and Berkeley Lab.

A key feature of the project is new supernova search software. Graduate student Michael Wood-Vasey has now implemented an adaptive kernel image subtraction package into the code used to discover supernovae in the NEAT images. This is a critically important addition since the wide field covered by the NEAT images can result in changes in the point-spread function (PSF) over the field. Images taken weeks apart can have different PSF gradients, leading to subtraction errors and the detection of spurious supernova candidates. Since, on average, there will be only one supernova per 25 NEAT images, it is critical that the number of spurious candidates be kept to much less than one per NEAT image. Spurious candidates can usually be eliminated by human inspection, but the flow of data from NEAT will be so large that the commitment of manpower would be ridiculous without this important control. This improved software is now ready for testing on real NEAT data, and that work will take place over the coming summer.

Solutions to Data Handling Constraints for Large High Energy and Nuclear Physics Experiments

Principal Investigators: David Quarrie

Project No.: 99045

Project Description

The current generation of large-scale High Energy and Nuclear Physics experiments are characterized by significant data management problems. This is because of the sheer quantity of the information (0.3-1.0 petabytes per year), as well as the large size and geographical dispersion of the collaborations. Current experiments such as BaBar at Stanford Linear Accelerator Center (SLAC) and the Solenoidal Tracker at the Relativistic Heavy Ion Collider (STAR at RHIC) have 500 to 1000 physicists, spread across 80 to 100 institutions in eight to ten countries. The next generation of experiments at the Large Hadron Collider (LHC), in particular the ATLAS and CMS experiments, will require further scaling of five to ten. Thus the problems of data storage and more importantly data access, are scaling faster than those of processing needs, particularly when contrasted with the performance growth of commercial hardware. Processing speeds are increasing faster than network speeds, which in turn are increasing faster then the performance of rotating disks and lastly, tape storage media.

Since the days of the Superconducting Super Collider (SSC), Berkeley Lab scientists have been at the forefront of applying innovative techniques to these data management problems. These techniques include the use of object-oriented programming languages and database management systems, distributed object brokers, and data indexing. These efforts have most recently focused on the BaBar and STAR experiments. This LDRD is designed to build upon the experience gained from these projects, to generalize the solutions so they are applicable across a broader range of experiments, and to address scalability and distributed-access issues that remain to be solved before the advent of the LHC experiments.

The BaBar data management system is based upon a commercial object-oriented database, but has added significant domain-specific software. This not only deals with the complex data model of the experiment data, but also adds several security and data-protection tools. This also provides monitoring tools to allow re-optimization of the data placement across a hierarchy of data servers. The management system includes the ability to iterate across so-called collections of events in order to select candidate events of interest for a particular physics analysis. However, indexing techniques offer the potential for significant performance enhancements relative to conventional iteration, and these are being developed, but are not yet in production. In addition, a mixed language environment based on both Java and C++ is now feasible, and the implications of this are beginning to be understood.

The LDRD proposes, therefore, to continue the development of the BaBar data management system, and to review the techniques and lessons with a view for their adoption by other experiments.

Accomplishments

The major accomplishments are the following.

Performance Scaling

A major focus of the LDRD has been to understand and overcome performance limitations in several areas. These include:

- *Parallel write performance from a number of data generators and activation startup and closedown overheads.* While good results had been attained last year for the steady-state throughput from the online event processing farm of 150 nodes, the average throughput lagged behind the nominal because of edge-effects—the relatively long ramp-up time when starting a data processing run, and a similar closedown time. Extensive efforts at minimizing these effects include the development of a CORBA-based caching server for conditions database access. This set of databases holds time-varying information, such as calibration and alignments, for the equipment. This server reduces the startup time by almost 50% by caching the requests for identical information from the 150 nodes. A similar server is being tested that reduces the overheads associated with database creation and extension, and which will reduce the lock server traffic significantly. This traffic results from the locking and transaction management that provides protection against incompatible simultaneous modification attempts within the database management system. A bug was discovered in the closedown handling (which is where the partial calibration information from the 150 nodes are summed together to provide high statistics summaries), and the average number of events processed in each run was increased. The net effect of these changes has been to increase the average throughput to the design specifications, and to provide a path towards increasing the throughput to at least twice the design limit to accommodate the higher event rate expected during 2001.

- *Parallel read performance for physics analysis.* This is characterized by being almost entirely random read, with the number of client applications being determined by administrative limits placed on batch queues. Investigations of the limitations to scaling determined that the RAID (short for Redundant Array of Inexpensive Disks) disk controllers were inefficient for this. In the short term, this resulted in the addition of more such controllers, and a longer term solution has been achieved following intensive disk performance studies, resulting in a factor of four improvement in the random read performance of the RAID controllers.

Space Optimization Studies

Another area of concern that has been addressed is that of the disk space used per event. This was three-to-four times the design number, and significant progress has been made in understanding the sources of this overhead. The detailed contents of each database have been reverse engineered so that there is a complete understanding of wasted space, whether within the event data model itself, or packing of the objects into the database. This has triggered a re-engineering of the event data model in certain areas to provide better packing of information and some reworking of the application code to pre-size arrays rather than extend them. A compression scheme has also been implemented for the database files themselves. These optimizations are still underway, but early indications are that they will achieve the desired compression such that the design size per event will be achieved.

Transient/Persistent Separation

The success of this approach on BaBar has resulted in its adoption by other High Energy Physics experiments, most notably the ATLAS experiment at the LHC. The advantages of the approach are the independence of most of the application software from the underlying persistency mechanism, support for multiple persistency mechanisms, good support for schema evolution, and the ability to monitor and police access.

Multi-Petabyte Scaling

Earlier preliminary studies of the scaling to multi-petabytes, based on an extended 128-bit object identifier, proved not to be viable. However, an alternative approach has been adopted that will achieve the desired scaling. This is based upon support for multiple federations, each of which is limited in the number of databases that it supports. The model that is under development is based on the use of a single federation per week of experiment running, and an extension of the data model to accommodate hierarchical federation-spanning collections that can be used to aggregate events from across extended running periods. In a follow-on effort, the design and implementation of this is well advanced, with initial deployment scheduled for February 2001.

Publications

D. Quarrie, *et al.*, "Operational Experience with the BaBar Database," *Computing in High Energy Physics* (February 2000).

J. Becla, *et al.*, "Improving Performance of Object Oriented Databases," *BaBar Case Studies, Computing in High Energy Physics* (February 2000).

S. Patton, *et al.*, "Schema Migration for BaBar Objectivity Federations," *Computing in High Energy Physics* (Feb, 2000).

E. Leonardi, *et al.*, "Distributing Data Around the BaBar Collaboration's Objectivity Federations," *Computing in High Energy Physics* (February 2000).

S. Patton, *et al.*, "Practical Constraints and Solutions for a Large Object Database in High Energy Physics," *High Performance Databases 2000* (July 2000).

Research on High-Luminosity Tracking Sensors

Principal Investigators: James Siegrist

Project No.: 99039

Project Description

Charged particle tracking in high-luminosity experiments such as those planned for the Large Hadron Collider (LHC) depends heavily on measurements using pixel and silicon strip detector devices. The LHC groups, including the Berkeley Lab ATLAS group, have been developing such detectors for use at high-rate hadron colliders, but many of the components still need research and development to provide a tracker designed to run for many years at a luminosity of $10^{34}cm^{-2}sec^{-1}$. Silicon trackers, even at the LHC, cannot survive at full machine design luminosity at the innermost radii.

This project is to concentrate on some outstanding technical questions relating to silicon tracker development, both in the pixel system and the silicon strip systems. Not yet resolved, under the constraints noted above, is the comparison of measured signal development to simulated signal development in undamaged and radiation-damaged devices. Work on this project is to measure actual devices and compare the results with simulations. Various test devices excited by lasers, sources, and/or cosmic rays will be used in the measurements. Devices will be characterized, analyzed, and modeled after irradiation at the Berkeley Lab 88-Inch Cyclotron and with cobalt sources.

Accomplishments

Previous work in the context of this LDRD project resulted in a computer program that numerically determines the instantaneous signal current produced by a detector for an arbitrary field profile and arbitrary arrays of electrodes. This is especially interesting in radiation-damaged strip and pixel detectors, where the field distribution and time dependence of the induced charge have yet to be measured accurately.

The code SIGSIM was originally written for use on UNIX workstations and could only run on a cluster of SGI processors in the Physics Division. In the past year, the code was modified and ported to a PC.

The detector signal is given by the following equations:

- If a charge q moves along any path s from position 1 to position 2, the net induced charge on electrode k is

$$\Delta Q_k = q(V_{q1}(2) - V_{q1}(1)) \equiv q\left(\Phi_k(2) - \Phi_k(1)\right)$$

- The instantaneous current can be expressed in terms of a weighting field

$$i_k = -q\,\vec{v}\cdot\overrightarrow{F_k}$$

The weighting potential Φ_K and the corresponding weighting field $\vec{F}_k$ are determined by applying unit potential to the electrode of interest and setting the potentials of all other electrodes to zero.

In a pad detector the weighting field is simple, as it is the field of a parallel plate capacitor, which is uniform throughout the volume, and the potential is a linear function of position. In a strip detector the situation is much more complicated. The weighting potential in a strip detector was used with a 50 μm electrode pitch of and 300 μm thickness. Two special cases are useful in testing the code. When a track is centered on a strip, ultimately all of the induced signal is registered on that strip. When a track is centered between two strips, both strips receive equal charge. Cuts through the weighting potential and weighting field for these two track positions were calculated.

For all of the induced charge to transfer to the desired strip, it is essential that all charges reach their destinations. Consider an electron-hole pair q_n, q_p originating on a point x_0 on the centerline of two opposite strips of a double-sided strip detector. The motion of the electron towards the n-electrode x_n is equivalent to the motion of a hole in the opposite direction to the p-electrode x_p. The total induced charge on electrode k, after the charges have traversed the detector, is

$$Q_k = q_e[\Phi_{Qk}(x_p) - \Phi_{Qk}(x_0)] - q_e[\Phi_{Qk}(x_n) - \Phi_{Qk}(x_0)]\,,$$

since the hole charge $q_p = q_e$ and $q_n = -q_e$. If the signal is measured on the p-electrode, collecting the holes,

$$Q_k = q_e[\Phi_{Qk}(x_p) - \Phi_{Qk}(x_n)]\,,$$

$$\Phi_{Qk}(x_p) = 1\,,$$

$$\Phi_{Qk}(x_n) = 0$$

and $Q_k = q_e$. Assume, for example, that the electrons are stationary, so they do not induce a signal. Then the second term of the first equation above vanishes, which leaves a residual charge

$$Q_k = q_e[\Phi_{Qk}(x_p) - \Phi_{Qk}(x_0)] \, ,$$

since for any coordinate not on an electrode $Q_k(x_0) \neq 0$.

If, however, the charge is collected on the neighboring strip $k+1$, then $Q_{k+1}(x_p) = 0$, $Q_{k+1}(x_n) = 0$ and $Q_{k+1} = 0$. In general, if moving charge does not terminate on the measurement electrode, signal current will be induced, but the current changes sign and integrates to zero.

This framework is used to calculate the current pulses and the total induced charge vs. time, shown in Figure 3. Signals are shown for both *p*- and *n*-strips, representing opposite sides of a double-sided detector. Note that the pulse shapes on the two sides are very different, unlike pad detector signals, which have the same shape on both sides, albeit of opposite polarity. For comparison, the signals calculated for a pad detector operating at the same field were examined. Again, the pulse shapes differ dramatically from the strip detector, due to the different weighting field, although the transit times are the same.

In summary, the two-dimensional detector simulation code SIGSIM has been ported to PCs. The simulations provide valuable insights into the signal formation of strip detectors and can be applied to more complicated electrode geometries.

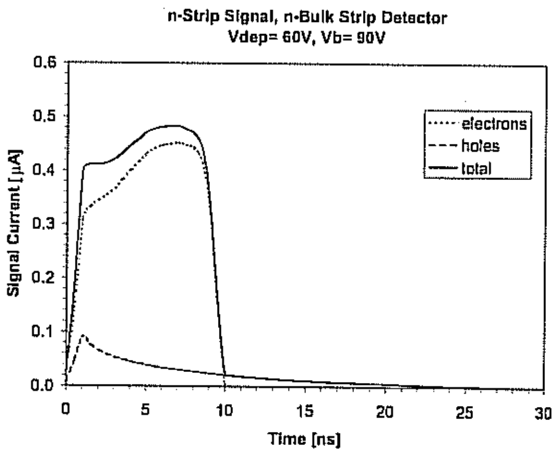

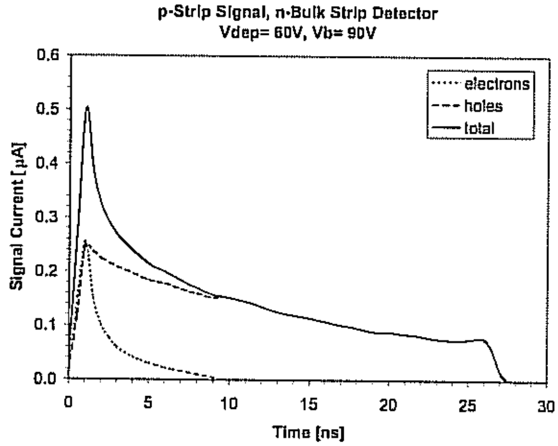

Figure 3: Calculated current pulses in a strip detector with a 50 μm pitch and 300 μm thickness. The figure on the left shows signals induced on the n-strips (ohmic side), the figure on the right shows signals on the p-strips (junction side). The detector is operated beyond depletion, i.e. with a voltage of 90 V (1.5 times depletion voltage).

Extraction of Fundamental Parameters from the Cosmic Microwave Background Data

Principal Investigators: George Smoot

Project No.: 97038

Project Description

The Cosmic Microwave Background (CMB) is the universe's wallpaper. It is what is leftover when all the radiation from astronomical objects is subtracted from what we observe. Theoretically we understand it as the faint echo of the Big Bang itself.

As the universe expands, its temperature falls. Some 300,000 years after the Big Bang the Universe had cooled to the ionization temperature of hydrogen, and the free protons and electrons coupled to form atoms. In the absence of free electrons to scatter off, the photons simply continued in the direction they were last moving. These photons constitute what we call the Cosmic (because it fills the universe so completely uniformly) Microwave (because of the frequency at which its spectrum peaks today) Background (because it originated further away from us than all other electromagnetic radiation we detect).

Despite its stunning uniformity—isotropic to a few parts in a million—it is the tiny perturbations in the CMB that contain its unprecedented view of the early universe. Already present before gravitationally-bound objects had formed, these temperature variations are an imprint of the primordial density fluctuations that seeded the formation of galaxy clusters and superclusters. These variations also retain the imprint of any other energetic effects from primordial times. With such retained evidence, their study promises to be an exceptionally powerful discriminant between competing cosmological models.

How to extract information about the tiny CMB fluctuations from a thermally noisy measurement of the sky temperature is a serious problem. However, at least formally, we can iteratively make maximum likelihood estimates of first the noise temporal power spectrum, then from this a pixelized sky temperature map and its pixel-pixel noise correlations, and finally from these the desired CMB temperature angular power spectrum.

The development and implementation of algorithms to realize this formalism for the current generation of balloon-borne CMB measurements is a significant computational challenge, and as such is the primary goal of this LDRD. It has been met in the development of the Microwave Anisotropy Dataset Computational Analysis Package (MADCAP).

Accomplishments

We have been very fortunate that throughout this project our work has been informed by the need to analyze real datasets from the MAXIMA (Millimeter Anisotropy eXperiment Imaging Array) and BOOMERANG (Balloon Observations of Millimetric Extragalactic Radiation and Geophysics) CMB observations. In the final year of this LDRD, we have seen this synergy come to fruition with the publication of results from the three most significant CMB datasets since the COBE experiment. In each case, the results were obtained using the MADCAP software running on National Energy Research Scientific Computing Center (NERSC)'s Cray T3E.

In November 1999, the results of the BOOMERANG North American test flight were published. These demonstrated that the Universe was undoubtedly close to flat. As such, together with similar results from the TOCO experiment, our results were named one of *Science* magazine's achievements of 1999.

In April 2000, the results of the BOOMERANG Antarctic Long Duration flight made the front cover of *Nature*. These results provided the first maps of the microwave sky showing real CMB fluctuations. They also provided even stronger confirmation of the flatness of the Universe, while raising interesting questions about its baryon content. Only a few weeks later, in early May 2000, the results of the MAXIMA-1 flight spectacularly confirmed the BOOMERANG results and extended them to even smaller angular scales. These two results mark a qualitatively new level of CMB studies, finally meeting its long-standing promise of precision cosmology. As such, these results were named one of *Science* magazine's achievements of 2000.

In obtaining these results, the MADCAP software has required significant development. As a result we have recently released a completely reworked version 2.0 which features improved portability across different parallel architectures, as well as more generalized data structures to allow for multi-component observations such as those anticipated from the next major challenge—measuring CMB polarization.

This year marked the end of the LDRD effort but not of this work, which continues spectacularly. In December, we held a workshop at Berkeley Lab to train nearly a dozen people how to use MADCAP and related software. Most trainees came from U.S. institutions, but a few came from Europe.

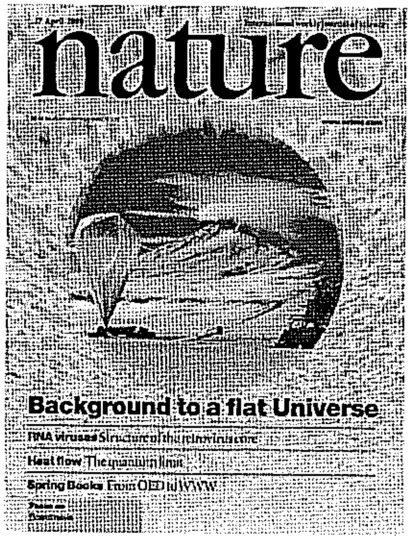

Figure 4.

Publications

J. Borrill, "MADCAP: The Microwave Anisotropy Dataset Computational Analysis Package," in *Proceedings of the 5th European SGI/Cray MPP Workshop* (1999). http://xxx.lanl.gov/abs/astro-ph/9911389

P.D. Mauskopf *et al.*, "Measurement of a Peak in the Cosmic Microwave Background Power Spectrum from the North American test flight of BOOMERANG," *ApJ* **536**, L59 (2000). http://xxx.lanl.gov/abs/astro-ph/9911444

A. Melchiorri, *et al.*, "A Measurement of Omega from the North American test flight of BOOMERANG," *ApJ* **536**, L63 (2000). http://xxx.lanl.gov/abs/astro-ph/9911445

P. de Bernardis, *et al.*, "A Flat Universe from High-Resolution Maps of the Cosmic Microwave Background Radiation," *Nature* **404**, 955 (2000). http://xxx.lanl.gov/abs/astro-ph/0004404

A.E. Lange *et al.*, "First Estimations of Cosmological Parameters From BOOMERANG," submitted to *Phys Rev D* (2000). http://xxx.lanl.gov/abs/astro-ph/0005004

S. Hanany, *et al.*, "MAXIMA-1: A Measurement of the Cosmic Microwave Background Anisotropy on Angular Scales of 10 Arcminutes to 5 Degrees," *ApJ* **545**, L5, (2000). http://xxx.lanl.gov/abs/astro-ph/0005123

A. Balbi, *et al.*, "Constraints on Cosmological Parameters from MAXIMA-1," *ApJ* **545**, L1, (2000). http://xxx.lanl.gov/abs/astro-ph/0005124

A.H. Jaffe *et al.*, "Cosmology from MAXIMA-1, BOOMERANG and COBE/DMR CMB Observations," submitted to *Phys Rev Lett.* (2000). http://xxx.lanl.gov/abs/astro-ph/0007333

J. Borrill, *et al.*, "Cosmic Microwave Background Data Analysis With MADCAP," in *ESO Astrophysics Symposia: Mining The Sky*, ed. A. Banday, Springer-Verlag (2001).

Large Astrophysical Data Sets

Principal Investigators: George Smoot

Project No.: 99040

Project Description

The purpose of this project is to develop an approach to handle the very large, complex astrophysical data sets now being generated by satellites and earth-based detectors. To accomplish this, we must provide a means for filtering these large data sets for events relevant to establishing the underlying astrophysical science and distributing these data sets to larger collaborations. This involves identifying extremely rare and unusual events, determining correlations among parameters in large databases, and coordinating collections of databases. These goals involve issues that are on the forefront of computer science and driving new statistical approaches to data handling.

More specifically, we chose an interesting and exciting astrophysical problem—the study of the supermassive black holes powering and disrupting active galactic nuclei making them visible across the entire universe—which has an appropriate and relevant data set available. We intend to use data generated in the array of sensors that comprise the Antarctic Muon and Neutrino Detector Array (AMANDA) neutrino telescope operating at the South Pole. The detector transmits data now at a rate of ~1 terabyte per year and will increase substantially during further years of operation. This data set and collaboration serve as a pilot project to test: (a) the transmission of large amounts of data from a remote site to the mass storage at the National Energy Research Scientific Computing Center (NERSC), (b) handling and processing of this data, and (c) the distribution of the filtered data sets to the collaboration members and eventually a wider audience.

Accomplishments

We have focused on a number of large astrophysical data sets from AMANDA and for a possible future neutrino telescope located at the South Pole. AMANDA is the current operational telescope with about 6 Tbytes of data from 1996 to 2000 stored in High Performance Storage System (HPSS). We have designed new data handling software. Our goal in the future is to create a seamless data collection and analysis environment to speed publication of scientific results.

We have processed the AMANDA data, from which we have gained expertise with phototube signals, reconstruction of tracks from measurement of the Cerenkov light, and a working knowledge of the collaboration. We have established Berkeley Lab as the expert institution for offline data management within the collaboration.

The 1997 AMANDA data (0.9 Tbytes) was first processed in 1998 on the CRAY using 1600 hours. After the detector was further calibrated, the data was refiltered in 1999 on 24 nodes of the PC Cluster Project belonging to the Future Technologies Group. This second processing included a full reconstruction of particle trajectories, and took 1100 CPU days. This data has been used by the collaboration to produce 10 papers presented at the Salt Lake City Conference, summer 1999. More than three publications are currently in preparation using the Berkeley Lab filtered data.

The 1998 data (1.8 Tbytes) were filtered early this year on the Parallel Distributed Systems Facility (PDSF) cluster. The cumulative processing time was 2800 CPU days. Increased resources were needed to sift through the larger data sample as well as split more complicated data streams. The new filter includes streams for time coincidences with the South Pole Air Shower Experiment (SPASE) array triggers, Burst and Transient Source Experiment (BATSE) triggers, and cascades, in addition to the particle trajectories filtered before.

Filtering of the 1999 data (~1 Tbyte) will commence soon. Filters and scripts are currently being finalized. This will be followed by a second pass over the 1998 data with an improved calibration. The filter scheme is similar to the first pass scheme. The 2000 data (~1 Tbyte) arrived from the South Pole December 1, 2000. It will be transferred to HPSS soon and processed accordingly.

More specifically, we have created a modular Concurrent Versions System (CVS) repository of Perl scripts to organize and automate the AMANDA filtering. Filter scripts can be used independent of the automation, so that users can apply the standard filters to small, simulated samples at their home institutions. A series of scripts has been created for: maintaining the disk cache, job submission, and output file storage. Separating these functions has allowed parallel disk cache maintenance and CPU utilization. A Perl module has been created to apply the standard AMANDA calibration for both the reconstruction and the simulation.

We have also built a web-based data-distribution system. Data (both real and simulated) are now served from HPSS to our international collaboration through a password-protected web page. A Java applet (client/server model) is used to provide read-only file transfer protocol (ftp) functions. The directory structure of HPSS can be scanned and individual files or groups of files scheduled for download. This is a general tool, which can be used by NERSC clients in the future.

We have built a new visualization program. Screen shots of AMANDA and simulated events may be viewed at http://rust.lbl.gov/~jodi/iceCube/vis.html . These have already aided the analysis of very high energy events, as well as helping us with project reviews.

We have begun analyzing the highest energy muons, which were inadvertently removed from the previous AMANDA analysis. This analysis requires that the information for large light depositions be accurately used. Physics algorithms that take into account the statistical deviations in hardware calibrations.

Finally, we have worked on the design of data handling software for a future neutrino telescope called IceCube. We have made progress in understanding data-flow (sources and rates) from the photo-multiplier tubes (PMTs) to the analysis. Calibration and monitor functions make this an interesting problem. Simulations at the new scale are currently rudimentary and we are working to improve our understanding of the detector by developing more sophisticated algorithms. Data-storage is also being studied. Database design is critical to optimizing access for the analysis.

Acronyms and Abbreviations

AECR-U	advanced electron-cyclotron resonance
AFM	atomic force microscopy
AFRD	Accelerator and Fusion Research Division
AIP	American Institute of Physics
ALS	Advanced Light Source
ARPES	angle resolved photoemission spectroscopy
BaBar	B/B-bar Detector (for system of mesons produced at SLAC)
BGO	Bismuth-Germanate
BGS	Berkeley Gas-filled Separator
BNCT	Boron Neutron Capture Therapy
CCD	charge-coupled device
CDMS	charge detection mass spectrometry
CERN	the European Laboratory for Particle Physics near Geneva, Switzerland
CFD	computational fluid dynamics
CI2	Chymotrypsin Inhibitor 2
CMB	cosmic microwave background
CMOS	complementary metal oxide semiconductor
CNS	central nervous system
CPU	central processing unit
CS	Computing Sciences
CSD	Chemical Sciences Division
CTS	cryo-thermochromatographic separator
cw	continuous wave
DFT	density functional theory
DNA	deoxyribonucleic acid
DOE	Department of Energy
DOS	density of states
DSB	double strand break
DSBR	double strand break repair
DSP	digital signal processor
E	energy efficiency transfer
ECR	electron cyclotron resonance
ED	Engineering Division
EETD	Environmental Energy Technologies Division
EM	electron microscopy
EPA	Environmental Protection Agency
ES	embryonic stem
ESD	Earth Sciences Division
EST	expressed sequence tag
EXAFS	extended x-ray absorption fine structure
FEM	finite element methods
FRET	fluorescence-resonance-energy transfer
fs	femtosecond
FY	fiscal year
GCM	general circulation model
GFP	green fluorescent protein
HENP	High Energy and Nuclear Physics
HEP	High Energy Physics
HEPAP	High Energy Physics Advisory Panel
HHMI	Howard Hughes Medical Institute
HL	hepatic lipase
HPSS	high performance storage system
IBAD	ion-beam assisted deposition
IR	infrared
IRMPD	infrared multiphoton dissociation
ISOL	isotope separator on line
ITEX	ion-beam thin film texturing
IVR	vibrational energy
JGI	Joint Genome Institute
JPL	Jet Propulsion Laboratory
LBNL	Ernest Orlando Lawrence Berkeley National Laboratory
LCP	liquid crystalline polymers
LDRD	Laboratory Directed Research and Development

LHC	Large Hadron Collider, CERN
l'OASIS	laser Optics and Acceleration Systems Integrated Studies
Lrp	leucine-responsive regulatory protein
LSD	Life Sciences Division
LSI	latent semantic indexing
MAD	multiwavelength anomalous diffraction
MAS	Mesoscale Atmospheric Simulation
MCF	Macromolecular Crystallography Facility, ALS
MEFS	mouse embryonic fibroblasts
MEMS	microelectromechanical structures
MES	molecular environmental science
MEXH	multi-energy x-ray holography
ML	monolayer
MOSFET	Metal-Oxide Semiconductor Field Effect Transistors
MSD	Materials Sciences Division
μ-XAS	micro x-ray absorption spectroscopy
NASA	National Aeronautics and Space Administration
NCAR	National Center for Atmospheric Research
NCEP	National Center for Environmental Prediction
NERSC	National Energy Research Scientific Computing Center
NIH	National Institutes of Health
NIST	National Institute of Standards and Technology
NLC	Next Linear Collider
NMR	nuclear magnetic resonance
NOAA	National Oceanic Atmospheric Administration
NSAC	Nuclear Science Advisory Committee
NSD	Nuclear Science Division
NSF	National Science Foundation
ODBMS	object-oriented database management system
PBD	Physical Biosciences Division
PCB	printed circuit boards
PCR	polymerase chain reaction
PD	Physics Division
PET	positron emission tomography
PI	Principal Investigator
PIC	particulate inorganic matter
PLD	pulsed laser deposition
POC	particulate organic carbon
ppb	parts-per-billion
PSF	point-spread function
PSL	polystyrene latex
QW	quantum well
QWS	quantum well states
R&D	research and development
RCSMhp	high-performance regional climate system model
rf	radio frequency
RHEED	reflection high energy electron diffraction
RHIC	Relativistic Heavy Ion Collider, Brookhaven National Laboratory
RIA	Rare Isotope Accelerator Facility
r.m.s	root mean square
RNA	ribonucleic acid
RTC	recoil product transfer chamber
S&T	Science and Technology
SASE	self amplification spontaneous emission
SC	Office of Science, DOE
SIM	sensitivity imposition method
SIO	Scripps Institute of Oceanography
SLAC	Stanford Linear Accelerator Center
SMP	symmetric multiprocessor
SOA	secondary organic aerosols
spFRET	single-pair FRET
SS	solid state
ss-DNA	single stranded DNA
SST	sea surface temperature
STAR	Solenoidal Tracker at RHIC
STM	scanning tunneling microscope or microscopy
SVD	singular value decomposition
TBP	TATA Binding Protein

TCR	transcription-coupled repair
UC	University of California
UHV	ultra-high vacuum
UV	ultraviolet
VOC	volatile organic compound
XANES	x-ray absorption near-edge structure spectroscopy
XAS	x-ray absorption spectroscopy
XFH	x-ray fluorescence holography
XPS	x-ray photoelectron spectrum
YBCO	YBa2Cu3O7
YSZ	yttria-stabilized zirconia